Understanding the mechanism of apoptosis regulation involving anti-apoptotic protein HAX1 and pro-apoptotic serine protease HtrA2/Omi

by

Mr. Raja Reddy Kuppili

[LIFE09201004009]

Tata Memorial Centre

Mumbai

A thesis submitted to the Board of Studies in Life Sciences

In partial fulfillment of requirements

For the Degree of

DOCTOR OF PHILOSOPHY
Of
HOMI BHABHA NATIONAL INSTITUTE

April, 2016

Homi Bhabha National Institute

Recommendations of the Viva Voce Board

As members of the Viva Voce Board, we recommend that the dissertation prepared by Raja Reddy Kuppili entitled ***'Understanding the mechanism of apoptosis regulation involving anti-apoptotic protein HAX1 and pro-apoptotic serine protease HtrA2/Omi'*** and recommend that it may be accepted as fulfilling the dissertation requirements for the Degree of Doctor of Philosophy.

---------- Date: 19/04/2016

Chairperson: Dr. Vinay Kumar

---------- Date: 19/04/2016

Guide/ Convener: Dr. Kakoli Bose

---------- Date: 19-4-16.

Member 1: Dr. Prasanna Venkatraman

---------- Date: 19/4/16

Member 2: Dr. Sorab Dalal

---------- Date: 19.4.16

External Examiner: Dr. K. V. R. Chary

Final approval and acceptance of this dissertation is contingent upon the candidate's submission of the final copies of the dissertation to HBNI.

I hereby certify that I have read this dissertation prepared under my direction and recommend that it may be accepted as fulfilling the dissertation requirement.

Date: 19/04/2016

Place: Navi Mumbai

Kakoli Bose, Ph.D.

(Guide)

STATEMENT BY AUTHOR

This dissertation has been submitted in partial fulfillment of requirements for an advanced degree at Homi Bhabha National Institute (HBNI) and is deposited in the Library to be made available to borrowers under rules of the HBNI.

Brief quotations from this dissertation are allowable without special permission, provided that accurate acknowledgement of source is made. Requests for permission for extended quotation from or reproduction of this manuscript in whole or in part may be granted by the Competent Authority of HBNI when in her judgment the proposed use of the material is in the interests of scholarship. In all other instances, however, permission must be obtained from the author.

Date: 19/04/2016

Place: ACTREC, Kharghar

Raja Reddy Kuppili

DECLARATION

I, hereby declare that the investigation presented in the thesis has been carried out by me. The work is original and has not been submitted earlier as a whole or in part for a degree / diploma at this or any other Institution / University.

Date: 19/04/2016

Place: ACTREC, Kharghar

Raja Reddy Kuppili

List of Publications arising from the thesis

Journal

1. Allosteric regulation of serine protease HtrA2 through novel non-canonical substrate binding pocket. ***Kuppili R R***[§]**,** Bejugam P.R[§], Singh N, Gadewal N, Chaganti L K, Sastry M, Bose K*. *Plos One* 2013; 8(2):e55416. doi: 10.1371/journal.pone.0055416. Epub Feb 2013. [§] (Authors with equal contribution).
2. Intricate structural coordination and domain plasticity regulate activity of serine protease HtrA2. Chaganti LK, ***Kuppili RR***, Bose K. *FASEB J*. 2013 Aug; 27(8):3054-66. Epub Apr 22, 2013.
3. The structural basis of mode of activation and functional diversity: A case study with HtrA family of serine proteases. Singh N, ***Kuppili R R***, Bose K* (Review article) *Archives of Biochemistry and Biophysics*. 2011 Dec 15; 516(2):85-96.

Chapters in books and lectures notes

1. Calpains and Granzymes: Non-caspase Proteases in Cell death. ***Kuppili R R***, Bose K Bose. (*Chapter 3, Proteases in Apoptosis: Pathways, Protocols and Translational Advances, Springer Book 2015*, ISBN 978-3-319-19497-4).
2. Proteases in Apoptosis: Protocols and Methods. Acharya S, ***Kuppili R R***, Chaganti LK, Bose K. (*Chapter 5, Proteases in Apoptosis: Pathways, Protocols and Translational Advances, Springer Book 2015*, ISBN 978-3-319-19497-4).

Conferences

1. Presented Poster titled 'Delineating the mechanism of HtrA2 mediated HAX1 regulation in the intrinsic pathway of apoptosis' at the **Keystone Symposia on "Frontiers of Structural Biology".** UT, USA, March 2014.

2. Presented poster titled **"**Allosteric regulation of pro-apoptotic serine protease HtrA2", at the **"International symposium on the Conceptual Advances in cellular homeostasis regulated by proteases and chaperones",** ACTREC, Navi Mumbai, India, Dec 2013.

3. Won 2nd prize for Poster & Oral presentation for **"**Allosteric regulation of pro-apoptotic serine protease HtrA2" at **"Accelerating Biology 2013: The Next Wave"** organized by C-DAC, Pune, India in Feb 2013.

4. Presented Poster at the Conference on **"Recent Advances in Computational Drug Design"**, IISC, Bangalore, India in Sep 2013.

5. Presented Poster at the **Annual meeting of the Indian Biophysical Society (IBS),** held at University of Mumbai, India in Jan 2013.

6. Selected for Oral presentation titled Biophysical characterisation of HAX1, a key player in the intrinsic pathway of apoptosis at the **Annual meeting of the Indian Biophysical Society (IBS),** University of Madras, Jan 2012.

Dedicated

to

Amma

Naana

Acknowledgements

Firstly and deservingly I would like to thank the most important person during my PhD, my guide and mentor Dr. Kakoli Bose. She was the one who helped me steer my ship in rough weather and encouraged me when there was success. She not only provided me diverse opportunities in the form of collaborative projects apart from my main project but also gave the freedom to execute those. That I'm sure is rare among guides. I still distinctly remember how she would literally talk me into taking up different projects and presenting at conferences. When the project hit obstacles those were times her support both technical and moral was all the more invaluable. Thanks Ma'am for everything.

My doctoral committee meetings were something I looked forward to each year as it was an external unbiased view on the status of my research project. I therefore thank my honorable doctoral committee members Dr. Vinay Kumar, Dr. Prasanna Venkatraman, Dr. Sorab Dalal for all their suggestions, encouragement and constructive criticism as it has helped me have a different perspective not only about my project but also to shape my career.

I thank Dr. Chiplunkar, Director, ACTREC for providing the infrastructure, DAE and ACTREC for my fellowship and DBT for funding the project. I would also take this opportunity to thank the staff in ACTREC for taking good care of the facilities.

When I joined the lab there were two senior students Lalith and Nitu who have taught me a lot of things that I still carry in my skill kit. Thank you both for imparting those technical skills in me. Our lab is also fortunate to have capable juniors Saujanya, Ajay and Raghu. They were not just my juniors but great friends too and would like to wish them best of luck for their projects as well as their lives. It was a wonderful lab environment with such good people around. Special thanks to Padale Sir and Snehal for helping maintain the lab.

Now it's the turn to thank my PhD batchmates, the batch of 2010. It was awesome being with them and there was a healthy competition that made us mature both scientifically and otherwise. Special thanks to Rushikesh, Indu, and Saikat for keeping me on my toes.

All the extensive scientific discussions were an integral part of my experience during PhD that will help me find a way in my future endeavors.

- Raja Reddy

Contents

Synopsis

Homi Bhabha National Institute

SYNOPSIS of Ph.D. THESIS

1. Name of the Student: Raja Reddy Kuppili

2. Name of the Constituent Institution: TMC-ACTREC

3. Enrolment No. LIFE09201004009

4. Title of the Thesis: Understanding the mechanism of apoptosis regulation involving anti-apoptotic protein HAX1 and pro-apoptotic serine protease HtrA2/Omi

5. Board of Studies: Life Sciences

Introduction

Apoptosis is executed by a family of cysteine proteases known as caspases, which on activation ultimately lead to cell death [1]. There are two principal pathways of caspase activation in mammalian cells, the extrinsic or receptor-mediated pathway and the intrinsic or mitochondria-dependent pathway. Activated caspases can be inhibited by the inhibitor of apoptosis (IAP) family of proteins, which in turn can be antagonized by mitochondrial pro-apoptotic proteins Smac/DIABLO and HtrA2/Omi [2, 3]. Pro-apoptotic HtrA2/Omi belongs to a family of serine proteases conserved from prokaryotes to humans and is involved in both caspase-dependent and independent pathways. On apoptotic stimuli, mature oligomeric HtrA2 is translocated to the cytosol, where it binds to IAPs, relieves the inhibition of caspases and causes apoptosis [4]. However, the caspase-independent apoptotic function and protease

activity of HtrA2 are poorly characterized. Identification of anti-apoptotic substrates of HtrA2 have suggested that its pro-apoptotic function is also regulated by its protease activities [5]. Most of its cytoplasmic partners and substrates such as IAPs, Pag, Mxi-2 and Pea-15 [6, 7-8] suggest an interaction after being released from the mitochondria. However, subsequent studies have identified a mitochondrial anti-apoptotic protein HAX1 (Hematopoietic cell specific Lyn-substrate 1) as a binding partner cum substrate of HtrA2, which on interaction with the latter degrades and leads to subsequent activation of HtrA2 as an early event in apoptosis [9]. However, details of this interacting complex and mechanism of action are yet to be delineated. Human HAX1 is a 35 kDa protein that interacts with HS-1, a Src kinase substrate and is involved in B cell signal transduction. It is ubiquitously expressed in murine and human tissues [10, 11] and appears to be predominantly localized to mitochondria [12]. Its overexpression resists mitochondrial membrane permeabilization during apoptosis which is correlated to its anti-apoptotic activity. Moreover, its overexpression in several human cancers suggests its role in oncogenesis and metastasis [13, 14].

Although, HtrA2 is primarily a mitochondrial protein there were no reports until recently on its involvement in early stages of apoptosis while it still resides in the mitochondria. Understanding HtrA2-mediated HAX1 cleavage if any, will help devise ways to regulate mitochondrial membrane potential and hence early stages of apoptosis. Here, we studied HtrA2-HAX1 interaction using multidisciplinary tools to decipher the mechanism of HtrA2 activation and its early regulation of apoptosis in the mitochondria. We also have identified and characterized a novel allosteric pocket in HtrA2. Apart from this we developed a PDZ domain database, 'PDZome,' that will be of great value to researchers in this field.

Aims and Objectives:

I. Structural analysis of HAX1 and HtrA2 (X-ray crystallography or similar techniques)

II. To characterize the interaction between pro-apoptotic serine protease HtrA2/Omi and its binding partner cum substrate HAX1 using biochemical and biophysical tools

III. Elucidation of serine protease activity of HtrA2 on HAX1 and characterization of the cleavage sites by proteomic analysis

Results:

Aim I: Structural analysis of HAX1 and HtrA2 (X-ray crystallography or Biophysical techniques)

1. *In silico* model generation of HAX1 protein

HAX1 is a unique anti-apoptotic protein which belongs to the HAX1 family and this protein shares very low query coverage, identity or similarity with the other known proteins as observed from the BLAST search performed. Moreover, no structural or biophysical data is available on this protein. Considering the anti-apoptotic nature of the protein, domain comparisons with Bcl2 family members were performed to identify the Bcl2 homology (BH) domains, but they were absent. *In silico* models of HAX1 were thus generated using different servers namely I-TASSER, QUARK, and Robetta [18-21]. Among the generated models, the best ones were chosen after validation by Procheck, whatcheck, Prosa, verify 3D and SAVS analysis.

2. Cloning and purification of HAX1 and its biophysical characterization

The HAX1 gene was cloned in bacterial expression vector pMALc5E. Purified HAX1 protein was obtained by affinity purification followed by size exclusion chromatography (SEC). The secondary and tertiary structure of HAX1 was determined by Far UV Circular Dichroism (CD) spectroscopy and fluorescence spectroscopy respectively. Overall, these studies showed that protein is well folded with proper secondary and tertiary structural properties. Thermal stability of the protein was also studied by thermal denaturation using Circular dichroism and Fluorescence spectroscopy and the melting temperature (Tm) was found to be about 60ºC.

3. Experimental validation of the protein model

a. Quenching studies for model validation

The 3D model of HAX1 was important to understand its overall structural arrangement and also carry out docking studies with HtrA2 so as to dissect the interacting interface and identify the residues required to mediate the interaction. Spectroscopic approach utilizing intrinsic fluorescence of the protein was used to validate the model where the five tryptophans in HAX1 were utilized as positional markers. Accessibility of fluorophores to water soluble quenchers can determine the fluorophore environment. HAX1 positional mutants were thus generated by site directed mutagenesis to obtain exposed double mutant (W98A, W160A), exposed triple mutant (W98A, W160A, W275A), and buried double mutant (W44A, W173A).

The Far UV CD analysis was carried out for the wild type HAX1 and all mutant proteins and they showed minimal secondary structural changes. Fluorescence emission maxima for each of the mutants with excitation at 295nm for the surface mutants showed blue shift as expected. The accessibility of the tryptophans in WT HAX1 and mutants were studied using non-polar acrylamide and negatively charged potassium iodide (KI) as quenchers. The Ksv (Stern Volmer constant) values that are indicative of the quenching gave us a comprehensive idea of the Tryptophan positions which corroborated very well with that suggested by the Robetta model.

b. Limited proteolysis and N-terminal sequencing:

A second approach that was used to validate the 3D model was limited proteolysis where trypsin was used at very low concentration to cleave HAX1.The resulting peptides were analyzed by N-terminal sequencing to determine the sites of cleavage with time, thus providing us useful information on the accessibility of arginine and lysine residues in the 3D structure of HAX1. An extremely good compliance was observed for the N terminal sequencing results with the *in silico* 3D model obtained from Robetta.

c. X-ray Crystallographic studies of HAX-1:

Crystal trials were set up for MBP-HAX1 at concentrations of 3mg/ml, 5mg/ml and 8mg/ml in Hampton crystal screens as well as in crystallizing conditions for other membrane associated proteins. Either precipitation or clear drops were observed, but none of the conditions showed crystals.

4. Identifying and characterizing allosteric regulation in HtrA2

In HtrA2, C-terminal PDZ domain upon substrate binding regulates its functions through coordinated conformational changes the mechanism of which is yet to be elucidated. Although allostery has been found in some of its homologs, it has not been characterized in HtrA2 so far. Here, with an *in silico* and biochemical approach we have shown that allostery does regulate HtrA2 activity [15].

a. Identification of Selective Binding Pocket (SBP)

The crystal structure of HtrA2 (PDB ID: 1LCY) that lacked flexible loops, linkers and some N-terminal residues was the target protein for our studies. These missing regions were modelled and energy minimised. Among the five possible putative binding sites that were identified by site map, Site2 or SBP that encompasses the groove generated by SPD-PDZ linker, protease and PDZ domains attained the best site score. The site score accounts for the volume, density, solvent exposure, hydrophilic and hydrophobic nature of residues and donor to acceptor ratio.

b. Peptide docking show similar interacting residues

Different techniques were applied in parallel so as to conduct a comprehensive search for a signature pattern of activating peptides that would dock at SBP. Leads from literature and *in silico* structure-guided tools were used for designing signatures. These peptides were docked using Glide module. Analyses of docking results with all these different peptides show interaction with similar residues *viz*. N216, S217, S219, E292 and E296 of SBP. This result suggested that SBP might be the possible binding site and therefore a prospective putative allosteric site.

c. MDS Analyses of HtrA2 and HtrA2– Peptide Complex

Of the docked peptides GSAWFSF, derived from a well-known HtrA2 binding protein pea-15 and a designed peptide GQYYFV were chosen for 30ns Molecular Dynamics Simulation (MDS) studies. Domain wise RMSD analysis of these trajectories provided quantitative output of deviations with respect to time. The trajectory graphs show that along the entire sequence, hinge region (211-226) has RMSD of 2.5 Å for the peptide GSAWFSF and 1.5 Å for GQYYFV from the starting unbound form. In addition to this, binding of peptides led to dynamic movements in many functionally important regions distal to SBP, such as helices α5 and α7 in the PDZ domain.

d. Conformational Transitions in Flexible Regions and at the Active Site

The peptide bound HtrA2 complex show relative movements in the active site triad residues, compared to the unbound form, in a manner promoting a nucleophilic attack. This pattern being consistent with both the peptides suggests that interaction of peptide activator with SBP leads to opening up of the active site cleft. Apart from active site triad, changes were also observed in the orientation of mechanistically important L1, LD and LA loops in the peptide bound complex. Their orientations with respect to the active site determine proper oxyanion hole formation, accessibility of the active site, formation of catalytic triad and hence enzyme activity.

e. In vitro studies to probe the role of SBP in HtrA2 activation

To determine whether critical SBP residues (N216, S219, E292 and E296) and the conserved YIGV residue G230 are important for mediating allosteric propagation in HtrA2, they were mutated to alanine. Moreover, since the protein is found to be active in its trimeric form we also used trimeric and monomeric HtrA2 variants, N-SPD and F16D respectively to understand the role of PDZ in intra and inter-molecular cross-talk.

Enzymology studies with different mutants were done using β-casein, a well-established generic substrate of serine proteases. The catalytic efficiency (kcat/Km) for the double mutant

N216A/S219A and single mutant E292A showed 2.4 fold decrease in enzyme activity, as compared to wild type. Though, Km values for the mutants were not significantly altered there was a marked decrease in Vmax and in substrate turnover (kcat) rates for N216A/ S219A and E292A suggesting presence of a malformed oxyanion hole in the SBP mutants. This demonstrated that these residues of SBP are important for mediating allosteric activation of HtrA2 upon activator binding and was further supported by our isothermal calorimetric studies. Enzymology studies with G230A demonstrated increase in Km value compared to the wild type highlighting the involvement of YIGV in this intricate allosteric mechanism. Interestingly, although catalytic efficiency for N-SPD has been found to be 3.4 fold less as compared to the wild type, its Km value suggests slight increase in substrate affinity for the enzyme. However in N-SPD, kcat was found to be 5 fold less than that of wild type highlighting the role of PDZ in initiating conformational changes near the active site pocket as well as in the oxyanion hole so as to increase overall enzyme stability. However, in the monomeric mutant of HtrA2 (F16D), there is a two fold increase in Km with significant decrease in the catalytic efficiency which emphasizes importance of intermolecular crosstalk between PDZ and protease domains.

The importance of intermolecular interaction between PDZ* and SPD has also been manifested in our MD studies where structural analyses show binding of peptide activator at the SBP alters PDZ orientation and brings $\alpha 5$ helix of PDZ from one subunit in close proximity to the protease domain of the adjacent subunit. The helix movement shifts the orientation of the phenyl ring of F170 which is a part of oxyanion hole towards H65 of the catalytic triad so as to accommodate the loop. These rearrangements result in a more stable and catalytically competent HtrA2 formation with a proper oxyanion hole. Therefore, designing suitable SBP binding peptides or peptidomimetics of HtrA2 might be an excellent approach to modulate HtrA2 functions for devising therapeutic strategies against various diseases it is associated with.

II. To characterize the interaction between pro-apoptotic serine protease HtrA2/Omi and its binding partner cum substrate HAX1 using biochemical and biophysical tools

1. *In silico* interaction studies

Docking studies were performed for preliminary clues of HtrA2-HAX1 interaction using HADDOCK and ClusPro platforms. These studies helped us elucidate the residues that might be critical for interaction. The residues at the interface of the docked complex were used to characterize the interaction.

2. Pull down studies

The HAX1 gene was cloned in pGEX-2T to obtain GST-HAX1 fusion protein which was expressed in *E.coli* pLysS cells and used to determine the minimal binding region. To deduce the domains involved in the interaction the different domains and domain combinations of HtrA2 i.e. N-SPD (N-terminal and serine protease domain), PDZ, SPD-PDZ, were purified by appropriate strategies. These purified domains were then used for pull down studies with GST-HAX1. Similarly truncated versions of HAX1 were generated to deduce its minimal binding region. From these experiments, it was observed that N-SPD is involved in the interaction with HtrA2 whereas PDZ alone was not. Based on the docking analyses for these proteins we narrowed down on putative residues that might be critical for this interaction. Proteins with these residues substituted by SDM were used to understand the critical role of these residues. The mutagenesis and pull down studies along with western blotting confirmed the role of residues P155, Q156, R158, R74, R76 from HtrA2 and P174, D176 from HAX1 in this interaction.

III. Elucidation of serine protease activity of HtrA2 on HAX1 and characterization of the cleavage sites by proteomic analysis

Interestingly, experiments in Mnd2 MEF cells reconstituted with wild-type HtrA2/Omi demonstrated that HtrA2/Omi-mediated degradation of HAX1 correlated with extensive cell death in response to etoposide, cisplatin and H_2O_2 [8]. Due to the existing ambiguities in

this pathway we wanted to elucidate whether HAX1 is a binding partner, activator or substrate of HtrA2.

1. Activation Assay to study the effect of HAX1 on HtrA2 protease activity

To study the effect of HAX1 on HtrA2 protease activity FITC- β–casein, a generic substrate of HtrA2 was used. The activation assay was performed for HtrA2 and N-SPD proteins HAX1 in the presence and absence of HAX1. Increase in fluorescence of unquenched FITC was monitored as a function of time and the initial reaction velocities were. Michaelis-Menten curve was plotted by taking initial velocities on Y-axis and [S] on X-axis. V max and Km values were determined by fitting the Michaelis- Menten curve in Kaleidagraph using the Hill's equation The activation assay shows 3.2 fold increase in the activity of HtrA2 and 1.5 fold increase in the activity of N-SPD in the presence of HAX1. The significant increase in the activity for HtrA2 in the presence of HAX1 proves that the latter is an activator of HtrA2. This is a first such report in the context of these two crucial apoptotic proteins.

2. Cleavage assay

With an aim to understand whether HAX1 is just an interacting partner and activator of HtrA2 or a substrate, both were incubated at different temperatures and concentrations. The observations so made clearly show that there was no cleavage of HAX1 by HtrA2 and therefore the latter might not be a substrate of HtrA2 as observed in some studies [8].

3. Cleavage assay with HAX1 bearing post-translational modifications

With an aim to confirm the cleavage of HAX1 by HtrA2 it was essential to obtain HAX1 with post-translational modifications. This was attained by heterologous expression of HAX1 in yeast *Pichia pastoris.* HAX1 clone was generated in pIB4 vector and transformed in the yeast and the gene intergration confirmed using PCR amplification of the locus followed by sequencing. HAX1 was purified and subsequently used for cleavage assays with HtrA2. Since HAX1 so expressed bears post-translational modifications namely the

N- and O- linked glycosylation, it was used for cleavage assays with HtrA2. No cleavage of HAX1 was observed in these gel based assays emphasizing that it might not be a substrate of HtrA2.

4. Probing the possibility of adapter proteins in HtrA2-HAX1 mediated apoptosis

Based on literature two proteins PARL (Presinilins associated rhomboid like protein) and XIAP can be the probable partners of HtrA2 and HAX1. These proteins have been cloned, expressed and purified for combinational cleavage assays. These combinations can be probed in future studies for the effect of HtrA2 activation by HAX1 on XIAP cleavage. Secondly, understanding the interplay between PARL, HtrA2 and HAX1 that are part of a complex in the mitochondria would usher in fresh perspective on the context dependent maturation of HtrA2 and HAX1 cleavage.

Summary:

The activation assay along with the cleavage assays proves that HAX1 might be an activator of HtrA2 and not a substrate. This changes the equation in the mitochondria and might be significant in understanding of apoptosis in context of these two proteins. Since no HtrA2 mediated cleavage of HAX1 was observed in different conditions the possibility of Mass spectrometric analysis of the cleavage products was ruled out.

5. PDZome: A comprehensive PDZ protein database

HtrA2 is a PDZ domain containing protein with multiple cellular roles. The PDZ domain is of paramount importance in protein-protein interactions and cell signalling. Despite such important roles there is no comprehensive and updated database on this extremely important family of proteins. Considering its significance we have generated a PDZ domain protein database, 'PDZome' that encompasses the complete available information on **42,043** PDZ containing proteins with their known and putative binding partners on one platform. It has a user-friendly web interface that can be easily queried. With unique integration of prominent databases, it provides detailed information on PDZ interactome

apart from the customized BLAST option. Most importantly, this database encompasses manually curated information on the mutations and diseases associated with PDZ containing proteins, thus making it a comprehensive compilation. PDZome is freely available in ACTREC website (http://www.actrec.gov.in:8080/Pdzome1/jsp/index.jsp).

Future directions: Probing the possibility of adapter proteins mediating the cleavage of HAX1, and to understand the other roles of HAX1 apart from being an activator of HtrA2 might be significant findings for all future investigations in this field.

References:

1. Fadeel, B., Orrenius, S., (2005) *J. Intern. Med*. 258, 479–517.
2. Philchenkov, A. (2004) *J. Cell. Mol. Med.* 8(4), 432-444.
3. Suzuki, Y., Imai, Y., Nakayama, H., Takahashi, K., Takio, K., and Takahashi, R. (2001) *Mol.Cell.* 8(3), 613-621.
4. Verhagen AM, Ekert PG, Pakusch M, Silke J, Connolly LM, Reid GE et al. (2000) *Cell* 102, 43–53.
5. Kroemer, G., and Martin, S. (2005) *Nat. Med.* 11(7), 725-730.
6. Hong, SK., Cha, MK., and Kim, IH. (2006) *Free Rad. Biol. and Med.* 40, 275-284.
7. Faccio, L., Fusco, C., Chen, A., Martinotti, S., Bonventre, J., and Zervos, A. (2000) *J. Biol. Chem.*275, 2581-2588.
8. Trencia, A., Fiory, F., Maitan, M., Vito, P., Barbagallo, A., Perfetti, A., Miele, C., Ungaro, P., Oriente, F., Cilenti, L., Zervos, A., Formisano, P., and Beguinot, F. (2004) *J. Biol. Chem.* 279,
46566-46572.
9. Cilenti, L., Soundarapandian, M., Kyriazis, G., Stratico, V., Singh, S., Gupta, S., Bonventre, J., Alnemri, E. and AS., Z. (2004) *J. Biol. Chem.* 279, 50295-50301.
10. Lees, D., Hart, I., Marshall, J.F., (2008) *J. Mol. Biol*. 379, 645–655.
11. Carlsson, G., Van't Hooft, I., Melin, M., et al., (2008) *J. Intern. Med*. 264, 388–400.
12. Suzuki, Y., Demoliere, C., Kitamura, D., Takeshita, H., Deuschle, U., Watanabe, T., (1997) *J. Immunol*. 158, 2736–2744.
13. Ramsay, A., Keppler, M., Jazayeri, M., Thomas, G., Parsons, M., Violette, S., Weinreb, P., Hart, I., and Marshall, J. (2007) *Cancer Res.* 67, 5275-5284.
14. Fadeel, B., and Grzybowska, E. (2009) *Biochim. Biophys. Acta* 1790, 1139-1148.
15. Bejugam, P.R., Kuppili, R.R., Singh, N., Gadewal, N., Chaganti, L.K., Sastry, G.M., and Bose K. (2013) *Plos One.* 8(2):e55416.

Publication in Referred Journal:

a. Published:

1. Allosteric regulation of serine protease HtrA2 through novel non-canonical substrate binding pocket. ***Raja R. Kuppili*** [§]**,** Pruthvi Raj Bejugam [§], Singh N, Gadewal N, Chaganti L K, Sastry M, Bose K*. *Plos One* 2013; 8(2):e55416. doi: 10.1371/journal.pone.0055416. Epub Feb 2013. [§] (Authors with equal contribution)

b. Accepted: NA

c. Communicated:

1. PDZome: A comprehensive PDZ database. ***Raja R. Kuppili,*** Sidddarth Gurdasani, Pallavi Mahajan, Gauri Shende, Pruthviraj Bejugam, Kakoli Bose.

d. Other Publications and Conference proceedings:

1. Intricate structural coordination and domain plasticity regulate activity of serine protease HtrA2. Chaganti LK, *Kuppili RR,* Bose K. FASEB J. 2013 Aug; 27(8):3054-66. Epub 2013 Apr 22.

2. The structural basis of mode of activation and functional diversity: A case study with HtrA family of serine proteases. Singh N, *Raja R. Kuppili,* Bose K* (Review article) Archives of Biochemistry and Biophysics. 2011 Dec 15; 516(2):85-96.

Conference attended / Oral/ poster presentations:

1. Presented poster titled **"Delineating the mechanism of HtrA2 mediated HAX1 regulation in the intrinsic pathway of apoptosis"** at the Keystone Symposia on "Frontiers of Structural Biology". UT, USA, March 2014.

2. Presented poster titled "**Allosteric regulation of pro-apoptotic serine protease HtrA2: a novel mechanism presenting potential therapeutic strategies**" at the International conference on chaperones and proteases, ACTREC, Navi Mumbai, Dec 2013.

Signature of Student

Date: 28/04/15

Doctoral Committee:

S. No.	Name	Designation	Signature	Date
1.	Dr.Vinay Kumar	Chairperson		23/4/2015
2.	Dr. Kakoli Bose	Guide		28/4/15
4.	Dr. Sorab Dalal	Member		28/4/15
5.	Dr. Prasanna Venkatraman	Member		23/4/15

Forwarded through:

28/5/15

Dr. S.V. Chiplunkar
Director ACTREC
Chairperson,
Academic & Training Programme

Dr. S. V. Chiplunkar
Director
Advanced ... Research &
Education ... (ACTREC)
Tata Memorial Centre
Kharghar, Navi Mumbai 410210.

Dr. K. Sharma
Director, Academics
T.M.C.

PROF. K. S. SHARMA
DIRECTOR (ACADEMICS)
TATA MEMORIAL CENTRE,
PAREL, MUMBAI

LIST OF ABBREVIATIONS

APS	Ammonium per sulfate
BME	Beta mercaptoethanol
D/W	Distilled water
DIABLO	Direct IAP binding protein with low pI
EDTA	Ethylene Diamine Tetra Acetic Acid
EtBr	Ethidum Bromide
DNA	Deoxyribonuclieotide Acid
HtrA	High Temperature requirement Protease A
HtrA1	High Temperature requirement Protease A1
HtrA2	High Temperature requirement Protease A2
HtrA3	High Temperature requirement Protease A3
HtrA4	High Temperature requirement Protease A4
PRSP	Pregnancy related Serine Protease
IAP	Inhibitors of Apoptosis
ECM	Extracellular Matrix
TNF	Tumor Necrosis Factor
DD	Death Domain
Cyt c	Cytochrome c
Apaf-1	Apoptotic protease activating factor 1
Smac	Second mitochondrial activator of caspases
Bcl-2	B-cell lymphoma 2
CARDs	Caspase recruitment domains
SP	Serine protease
UPR	Upregulated Protein Response
SV-40	Sivian Virus-40
PDZ	Post Density Protein 95 disc zona occludens
SPD	Serine Protease Domain
IGFBP	Insulin Growth Factor Binding Protein
TGF-β	Tumor Growth factor-β
PCR	Polymerase Chain reaction
FP	Forward Primer
RP	Reverse Primer
dNTPs	Deoxyribonuclieotide triphosphates
$MgCl_2$	Magnesium chloride
bp	Base Pair
MBP	Maltose Binding Protein

IPTG	Isopropyl Thio-Galacto Pyranoside
$CaCl_2$	Calcium Chloride
His	Histidine
SDS	Sodium Dodecyl Sulfate
CBB	Coomassie Brilliant Blue
RT	Room temperature
TFA	Tri-Fluro Acetic Acid
ACN	Acetonitrile
SDM	Site Directed Mutagenesis
TEV	Tobacco Etch Virus
XIAP	X-linked Inhibitor of Apoptosis
Ni	Nickel
Ni-IDA	Nickel-Imino Diacetic Acid
ng	Nanogram
OD	Optical Density
PAGE	Poly Acrylamide Gel Electrophoresis
LB	Luria Broth
UV	Ultra Violet
µl	Microlitre
µg	Microgram
µM	Micromolar
mM	Millimolar
M	Molar
ml	Milliliter
L	Liter
kDa	Kilo Dalton
MDa	Mega Dalton
Kana	Kanamycin
Amp	Ampicillin
Chlor	Choramphinicol

LIST OF FIGURES

LIST OF TABLES

Chapter 1

Introduction

Apoptosis is a tightly regulated process of cell death, necessary for typical growth and development in multicellular organisms. It is considered to be a vital component of various processes including normal cell turnover, proper development and functioning of the immune system, embryonic development and chemical-induced cell death. Apoptosis occurs normally during development and aging and as a homeostatic mechanism to maintain cell population in tissues. It also occurs as a defence mechanism such as in immune reactions or when cells are damaged by disease or noxious agents (*1*). Cancer, a potentially fatal disease arising due to environmental factors and genetic alterations, occurs due to unregulated cell growth and characterized by malignancy. Normal cells on the other hand are destined to programmed cell death after a time prescribed by the cellular network. Therefore, research continues to focus on the elucidation and analysis of the cell cycle machinery and signaling pathways that control cell cycle arrest and apoptosis. A myriad of proteins are involved in the cascade to execute this phenomena. These players are thus recognized for their immense therapeutic potential owing to their ability to modulate the life or death of a cell.

Apoptosis is executed by a family of cysteine proteases known as caspases, which on activation ultimately lead to cell death (*2*). There are two principal pathways of caspase activation in mammalian cells, the extrinsic or receptor-mediated pathway and the intrinsic or mitochondria-dependent pathway. Both pathways converge in the activation of a cascade of caspases, which ultimately leads to the death of cell without damage to surrounding cells and tissues. These two major pathways of apoptosis are regulated by the interaction of pro and anti-apoptotic proteins, which act by promoting death signals and blocking apoptosis by promoting survival signals respectively. Activated caspases

can be inhibited by the inhibitor of apoptosis (IAP) family of proteins, which in turn can be antagonized by mitochondrial pro-apoptotic proteins Smac/DIABLO and HtrA2 (High temperature requirement protein A2) (*3*). Pro-apoptotic HtrA2/Omi belongs to a family of serine proteases conserved from prokaryotes to humans and is involved in both caspase-dependent and independent pathways. This pro-apoptotic serine-protease plays major roles in cellular homeostasis and apoptosis. It is a nuclear encoded protein, localized in the mitochondrial inter membrane space (IMS). In response to various cellular stresses, HtrA2 is released into the cytosol. On apoptotic stimuli, mature oligomeric HtrA2 is translocated to the cytosol, where it binds to IAPs, relieves the inhibition of caspases and causes apoptosis. However, the caspase-independent apoptotic function and protease activity of HtrA2 are poorly characterized (*3*).

HtrA2 has also been implicated in many diseases including neuro-degeneration and cancer thus making it an important therapeutic target. HtrA2 is also known to promote apoptosis by a less understood non classical pathway or the caspase independent pathway. Based on information from literature, this multitasking ability of HtrA2 can be attributed to its serine protease activity which is intricately coordinated by its unique substrate binding process, complex trimeric structure, interdomain networking and conformational plasticity. However, the unbound inactive form of the crystal structure with partially missing active site loops and flexible PDZ protease linker has been unable to clearly determine the role of dynamics and allostery if any in HtrA2 activation and specificity. Therefore, to understand the molecular details of its mechanism of action, probe the possibility of allosteric mechanism regulating the dynamics, characterization of the substrate binding site and active site pocket becomes imperative. As a part of this

study we have been able to identify and characterize one such novel allosteric pocket in HtrA2 which possibly regulates its protease activity on its binding partners.

Identification of anti-apoptotic substrates of HtrA2 have suggested that its pro-apoptotic function is also regulated by its protease activities. Identifying the interacting partners of HtrA2 and their mode of interaction can be an important step forward. These interacting partners might be mitochondrial or cytoplasmic proteins, and their interaction with HtrA2 could be part of the apoptotic process. One such interacting partner that has been identified is the HS1-associated protein X-1 (HAX1) (*4*).

HAX1 protein is an anti-apoptotic factor reported to be involved in cell migration, endocytosis and probably mRNA transport. HAX1 has been recognized as a novel mitochondrial interacting partner of HtrA2 which is proposed to be cleaved by the protease upon apoptotic induction followed by drop in mitochondrial membrane potential. This observation opened up an avenue to investigate the pro-apoptotic role of HtrA2 during early stages of apoptosis while it still resides in the mitochondria. However, details of the complex mechanism of HtrA2-HAX1 interaction are yet to be elucidated (*5*).

Our study here aimed at characterizing the structural and functional aspects of HtrA2-HAX1 interaction. HtrA2's mechanism of caspase activation is attributed to its IAP-inhibiting activity and most of its cytoplasmic partners and substrates such as IAPs, Pag, Mxi-2 and Pea-15 (*5*) suggest an interaction after being released from the mitochondria. However, subsequent studies have identified a mitochondrial anti-apoptotic protein HAX1 (Hematopoietic cell specific Lyn-substrate 1) as a binding

partner cum substrate of HtrA2, which on interaction with the latter degrades and leads to subsequent activation of HtrA2 as an early event in apoptosis. Human HAX1 is a 35 kDa protein that interacts with HS-1, a Src kinase substrate and is involved in B cell signal transduction. It is ubiquitously expressed in murine and human tissues and appears to be predominantly localized to mitochondria. Its overexpression resists mitochondrial membrane permeabilization during apoptosis which is correlated to its anti-apoptotic activity. Moreover, its overexpression in several human cancers suggests its role in oncogenesis and metastasis. Despite establishing proofs of HAX1 being an anti-apoptotic protein, structural details of its interaction with other apoptotic proteins remain to be elucidated. HAX1 lacks Bcl-2 homology (BH) domains and belongs to the unique HAX1 family with structural information unavailable for any of its members. This is one of the reasons for very little information on its interacting modules till date. On the other hand, although, HtrA2 is primarily a mitochondrial protein, there were no reports until recently on its involvement in early stages of apoptosis while it still resides in the mitochondria.

Therefore, based on several literature reports it is understood that characterization of HtrA2-mediated HAX1 cleavage if any, will help devise ways to regulate mitochondrial membrane potential and hence early stages of apoptosis. Here, we studied HtrA2-HAX1 interaction using multidisciplinary tools to decipher the mechanism of HtrA2 activation and its early regulation of apoptosis in the mitochondria. Recombinant HtrA2 has been reported to catalytically cleave IAPs and to inactivate XIAP (X-linked inhibitor of apoptosis) *in vitro* thus leading to activation of caspases (*6*). In this study, it has been hypothesized that in the presence of HAX1, the HtrA2-driven destruction of

XIAP might be augmented as in the case of GRIM 19 (gene associated with retinoic-interferon-induced mortality 19) (*7*). This characterization also involved studying the HtrA2 activity in the presence of a mitochondrial protease PARL (presenilin-associated, rhomboid-like) which has been reported to be involved in the processing of HtrA2 to the active protease localized in the mitochondrial intermembrane space (*8*).

While trying to understand the domain architecture and the roles of different domains in HtrA2, we realized the importance of the PDZ [post synaptic density protein (PSD95), Drosophila disc large tumor suppressor (Dlg1), and zonula occludens-1 protein (zo-1)] domain both in the functional dynamics of the protein as well as protein-protein interactions. But surprisingly there is not a single database with updated information on this important class of PDZ containing proteins and their interacting partners. With an aim at providing updated and comprehensive information on these proteins, we developed a PDZ domain database, 'PDZome,' that comprises details of 42,043 proteins and their interacting partners. This will be of great value to both basic and clinical researchers in this field both for identifying new targets as well as establishing therapeutic strategies.

Aim

HtrA2 is a mitochondrial pro-apoptotic protein with no reports on its involvement in early stages of apoptosis. Its interaction with anti-apoptotic HAX1 might provide clues of its pro-apoptotic function while it still resides in the mitochondria. Thus, our aim was to understand HtrA2-HAX1 interaction and its functional relevance which would in turn help devise ways to regulate mitochondrial membrane potential and hence early stages of apoptosis.

Objectives:

I. Structural analysis of HAX1 and HtrA2

i. *In silico* model generation of the anti-apoptotic protein HAX1

ii. Cloning and purification of HAX1 and its biophysical characterization

iii. Experimental validation of the protein model

iv. Identifying and characterizing allosteric regulation in HtrA2

II. To characterize the interaction between pro-apoptotic serine protease HtrA2/Omi and its binding partner cum substrate HAX1 using biochemical and biophysical tools

i. *In silico* HtrA2-HAX1 interaction studies

ii. *In vitro* pull down studies to characterize the mode of HtrA2-HAX1 interaction

III. Elucidation of serine protease activity of HtrA2 on HAX1 and characterization of the cleavage sites by proteomic analysis

i. Activation Assay to study the effect of HAX1 on HtrA2 protease activity

ii. Cleavage assay to determine if HAX1 is a substrate of HtrA2

IV. PDZome: A comprehensive PDZ protein database

Chapter 2

Review of Literature

2.1 Cancer

Cancer is an umbrella term for diseases characterised by excessive cellular division and proliferation. Cancer may start developing in any of over sixty body organs and is usually named after the affected organ. Each organ consists of different cell types that may be affected by cancer, so several cancer types may affect each organ. There are more than 200 types of cancer having different causes, symptoms and treatments.

Cancer does not develop overnight; instead it often evolves over several years with detectable premalignant lesions portending the development of full-blown malignancy. Factors that contribute to the etiology of the disease may be external or environmental factors as well as internal or cellular factors. The external factors include infectious organisms, exposure to carcinogens that include various chemicals, radiations while the cellular factors include defects in DNA repair, in DNA damage checkpoints or in telomere maintenance leading to genomic instability. This genomic instability causes a normal cell to accumulate sufficient mutations to become cancerous.

Cancerous cells display altered behaviour and these behavioural changes are attributed to the changes in physical properties of cells. Some of the changes have been identified and used to distinguish cancer cells. Tumour cells display a characteristic set of features that distinguish them from normal cells. For example, cancerous cells do not show cell to cell communication like normal cells. Normal cells exhibit contact inhibition, that is, they cease to divide when they come in contact with other cells. Cancer cells lack the property of contact inhibition. During the metastatic cascade, changes in cell-cell and cell-matrix adhesion are of paramount importance. (*9*)

Cancer treatment depends on its type and also the stage of the cancerous state. Uniform treatment modality cannot be devised in case of cancer as it is not a single disease. The primary treatment mode is surgery, wherein, a tumor in benign state is removed. Radiation therapy is another option wherein high energy rays are targeted directly on tumour cells. Radiation therapy is also widely used to control local disease. However, over time it was realized that neither surgery nor radiation or the two in combination could adequately control the metastatic cancer and for the treatment to be effective, therapy needs to reach every organ of the body. Therefore, current efforts to cure cancer have been focusing on targeted therapy. Targeted therapy refers to a new generation of cancer drugs designed to interfere with a specific target protein that is believed to have a critical role in tumour growth or progression (*10*). These new generation of drugs target signals that promote or regulate the cell cycle, growth factors and their receptors, signal transduction pathways and pathways affecting DNA repair and apoptosis (*11*).

2.2 Apoptosis

The demise of cells by programmed cell death is marked by a well-defined sequence of morphological changes, collectively referred to as *apoptosis* (*12*)- a Greek word that means “dropping off” or “falling off” (*13*) as in leaves from a tree. Dying cells shrink and condense and then fragment, releasing small, membrane-bound apoptotic bodies, which generally are phagocytosed by other, cells (Figure 2.1). Importantly, the intracellular constituents are not released into the extracellular milieu as in case of necrosis, where they might have deleterious effects on neighboring cells. The highly stereotyped

observable changes accompanying apoptosis suggested that this type of cell death was under the control of a strict cellular program.

Apoptosis occurs normally during development and acts as a homeostatic mechanism to maintain cell populations in tissues. Apoptosis also occurs as a defense mechanism such as in immune reactions or when cells are damaged by disease or noxious agents.

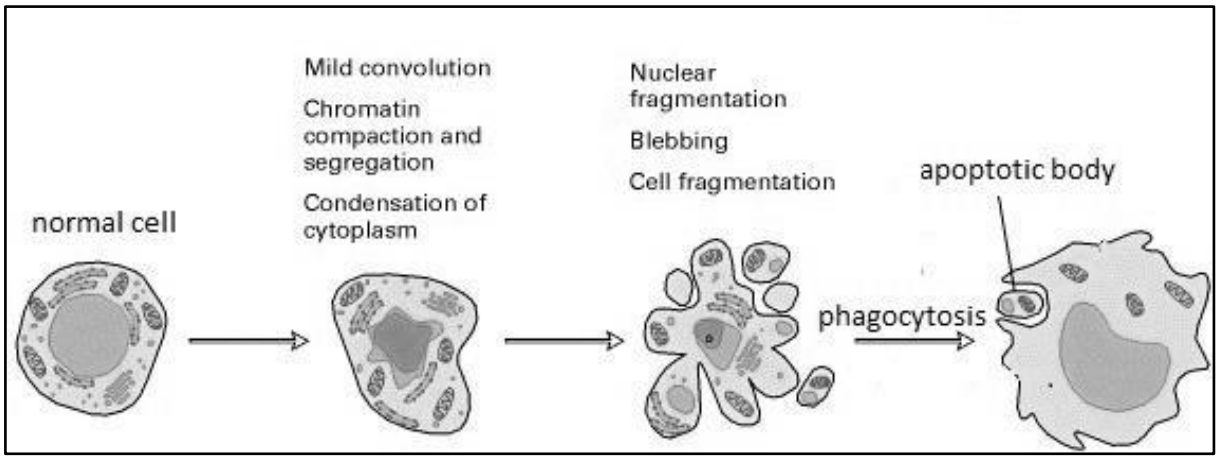

Figure 2.1. Morphological changes during apoptosis. (*12*)

Discerning the mechanism of apoptosis is very crucial since it helps in the understanding of the pathogenesis of the conditions that result from disordered apoptosis. This in turn, may help in the development of drugs that target certain apoptotic genes or pathways.

2.2.1 Caspases: Initiators and executioners

The effector molecules in the apoptotic pathway are a family of enzymes called caspases, so named because they are cysteine proteases that selectively cleave proteins at sites just C-terminal to aspartate residues. These proteases have specific intracellular targets such as proteins of the nuclear lamina and cytoskeleton. Cleavage of these substrates leads to the demise of a cell (*14*).

Caspases are central to the mechanism of apoptosis as they are both the initiators and executioners. There are three pathways by which caspases can be activated. The two commonly known initiation pathways are the intrinsic (or mitochondrial) and extrinsic (or death receptor) pathways of apoptosis (Figure 2. 2). Both pathways eventually lead to a common pathway or the execution phase of apoptosis. A third less well-known initiation pathway is the intrinsic endoplasmic reticulum pathway (*12*).

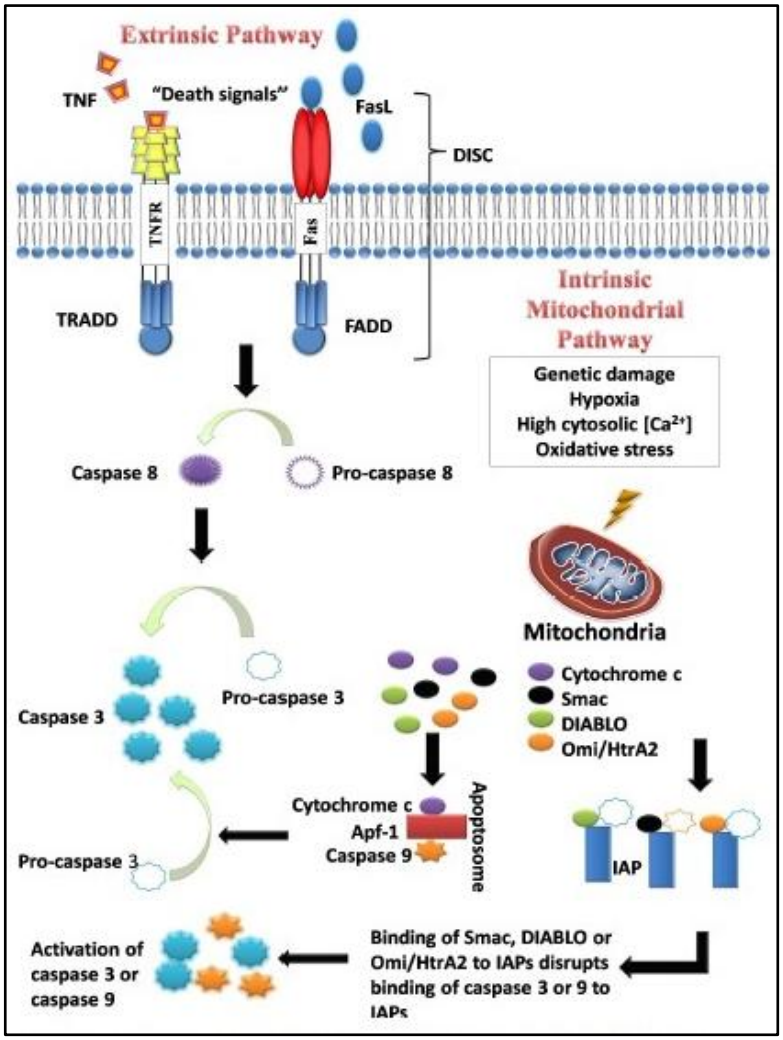

Figure 2.2: Extrinsic and intrinsic pathways and the players involved in apoptosis (*13*)

2.2.2 Extrinsic pathway or death receptor pathway

The extrinsic death receptor pathway, as its name implies, begins when death ligands bind to a death receptor. The best known death receptors is the type 1 TNF receptor (TNFR1) and a related protein called Fas (CD95) and their ligands are called TNF and Fas ligand (FasL) respectively. These death receptors have an intracellular death domain that recruits adapter proteins such as TNF receptor-associated death domain (TRADD) and Fas-associated death domain (FADD), as well as cysteine proteases like caspase 8. Binding of the death ligand to the death receptor results in the formation of a binding site for an adaptor protein and the whole ligand-receptor-adaptor protein complex is known as the death-inducing signalling complex (DISC). DISC then initiates the assembly and activation of pro-caspase 8. The activated form of the enzyme, caspase 8 is an initiator caspase, which initiates apoptosis by cleaving other downstream or executioner caspases (*15*).

2.2.3 Intrinsic or mitochondrial death pathway

The intrinsic pathway is initiated within the cell. Internal stimuli such as irreparable genetic damage, hypoxia, extremely high concentrations of cytosolic Ca^{2+} and severe oxidative stress are some triggers of the initiation of the intrinsic mitochondrial pathway (*16*). Regardless of the stimuli, this pathway is the result of increased mitochondrial permeability and the release of pro-apoptotic molecules such as cytochrome-c into the cytoplasm. This pathway is closely regulated by a group of proteins belonging to the Bcl-2 family, named after the BCL2 gene originally observed at the chromosomal breakpoint of the translocation of chromosome 18 to 14 in follicular non-Hodgkin lymphoma. There

are two main groups of the Bcl-2 proteins, namely the pro-apoptotic proteins (e.g. Bax, Bak, Bad, Bcl-Xs, Bid, Bik, Bim and Hrk) and the anti-apoptotic proteins (e.g. Bcl-2, Bcl-X_L, Bcl-W, Bfl-1 and Mcl-1). While the anti-apoptotic proteins regulate apoptosis by blocking the mitochondrial release of cytochrome-c, the pro-apoptotic proteins act by promoting such release. It is not the absolute quantity but rather the balance between the pro- and anti-apoptotic proteins that determines whether apoptosis would be initiated (*17*). Other apoptotic factors that are released from the mitochondrial inter-membrane space into the cytoplasm include apoptosis inducing factor (AIF), second mitochondria-derived activator of caspase (Smac), direct IAP Binding protein with Low pI (DIABLO) and Omi/high temperature requirement protein A2 (HtrA2) (*17*).

2.2.4. Dysregulation of apoptosis and carcinogenesis

Defective or inefficient apoptosis is a hallmark of cancer cells. The survival of malignant cells mainly relies upon developing resistance towards apoptosis. Evasion of apoptosis by malignant cells can be part of a cellular stress response to ensure the cell's survival upon exposure to stressful stimuli. This acquired resistance to apoptosis may contribute to carcinogenesis, tumour progression, and also treatment resistance (*18*). There are many ways a malignant cell can acquire resistance to apoptosis. Generally, the mechanisms by which evasion of apoptosis occurs can be broadly divided into: 1) disrupted balance of pro-apoptotic and anti-apoptotic proteins 2) reduced caspase function 3) impaired death receptor signalling and 4) Defects in tumour suppressor gene that will facilitate proliferation signals.

There are various proteins exhibiting pro or anti-apoptotic activity within the cell. The ratio of these proteins plays a critical role in regulating cell death. Any case of over or

under-expression of certain genes (hence the resultant regulatory proteins) have been found to contribute to carcinogenesis by reducing apoptosis in cancer cells. Thus, understanding the action of pro and anti-apoptotic proteins will help in gaining valuable insights into carcinogenesis due to apoptotic failure. One of the most promising discoveries in the developmental therapeutics is the identification of agents that effect programmed cell death regulated by Bcl-2 family of proteins (*19*).

IAPs are the proteins belonging to anti-apoptotic family, which halt the apoptosis process by preventing the activation of caspases. Over-expression of IAP proteins has been associated with increased resistance to pro-apoptotic stimuli (*19*). Antagonists of IAP's are the protein molecules released from mitochondria along with cytochrome c in response to apoptotic stimuli. Cytoplasmic release of cytochrome c activates caspase 3 via the formation of a complex known as apoptosome which is made up of cytochrome c, Apaf-1 and caspase 9. On the other hand, Smac/DIABLO or Omi/HtrA2 promotes caspase activation by binding to inhibitor of apoptosis proteins (IAPs) which subsequently leads to disruption in the interaction of IAPs with caspase-3 or -9. HtrA2/Omi is most well characterized human serine protease belonging to the HtrA family.

2.3 The HtrA Family

HtrA proteins belong to a unique family of oligomeric serine proteases (S1, chymotrypsin family) that are conserved from prokaryotes to humans. DegP or HtrA is the first one in the family to be identified in *Escherichia coli* and later its homologs were identified in wide spectrum of organisms that include bacteria, fungi, plants,

frogs, fish and mammals (*20*). Prokaryotic HtrAs are involved in the heat shock response and play important role in quality control of periplasmic proteins. In eukaryotes, HtrA proteins are involved in numerous cellular processes such as extracellular matrix modelling, apoptosis and protein quality control (*21*)

In humans HtrA family consists of four members in: HtrA1 (PRSS11), HtrA2/Omi, HtrA3 (PRSP) and HtrA4. All proteins share a highly conserved chymotrypsin like serine protease domain and one PDZ domain at C-terminus. However, the structure of N-terminus of HtrA1, 3 and 4 is distinct from that of HtrA2. These mammalian serine proteases are involved in several important biological mechanisms such as growth, apoptosis, arthritis, embryogenesis, neurodegenerative and neuromuscular disorder, and cancer.

The expression of HtrA1 gene is down-regulated in many types of cancer and is believed to be a tumor suppressor. HtrA3 resembles HtrA1 structurally and its downregulation has been observed in ovarian and endometrial cancers. Both HtrA1 and HtrA3 function in inhibition of TGF-beta signalling. HtrA4 is the least characterized protein among the HtrA family members.

Of all the four members of human HtrA family, the structure of HtrA2 is well characterized. It serves as a protein quality factor and plays a pivotal role in apoptosis both by caspases-dependent and independent pathways (*22*)

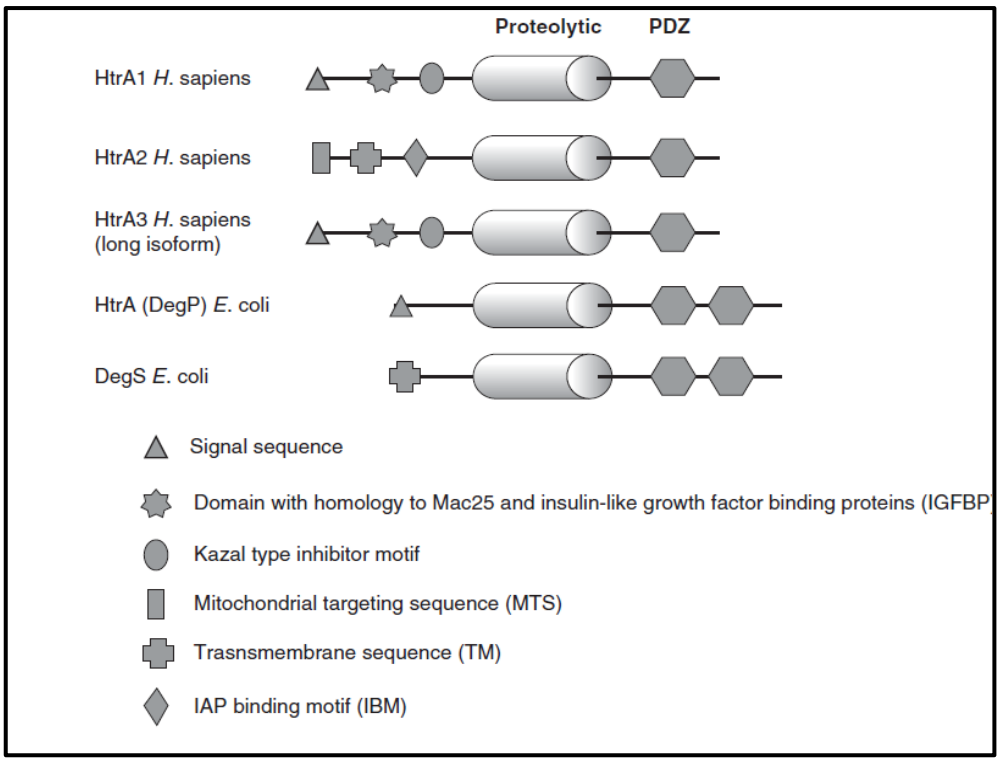

Figure 2.3. Domain organization of human HtrA family members and their homologs from *Escherichia coli* *(23)*

2.4 HtrA2 (High Temperature Requirement protease A2)

HtrA2 is an ATP independent serine protease found in the mitochondria of mammalian cells. The protein is encoded in the second chromosome of human karyotype at position 2p13.1. It has been identified as a promoter of cell death and this is confirmed by several independent research groups (*24*, *25*).

Interestingly, of all the four human HtrA family members, only HtrA2 has a clear intracellular localization. It has also been implicated in maintaining mitochondrial homeostasis through its role as a potential chaperone in the mitochondria (*25*).

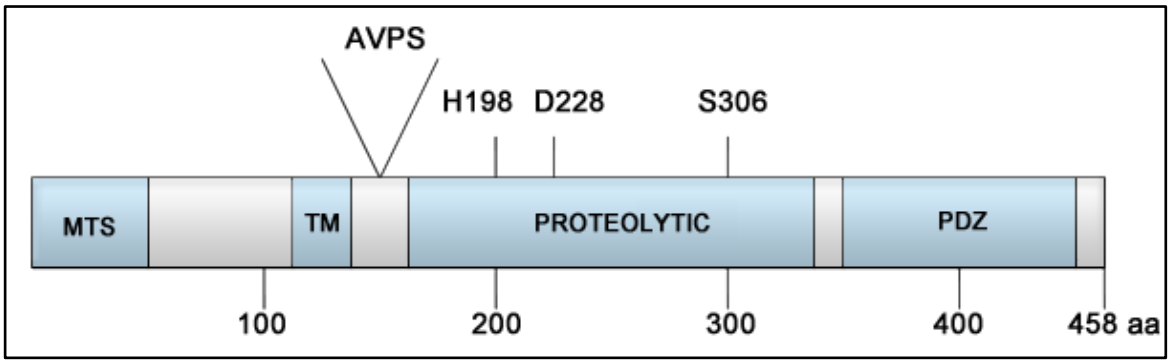

Figure 2.4: Domain organization of human HtrA2 protein. MTS: mitochondrial targeting signal, TM: transmembrane domain, PROTEOLYTIC: trypsin-like domain, PDZ: PDZ domain, AVPS: amino acids of the IAPs binding motif. Amino acid residues of the HtrA2 catalytic triad are marked (numbers indicate the position of the given residue in the polypeptide chain).

The HtrA2 gene encodes a polypeptide of 458 amino acids having a mass of 49 kDa. The full-length HtrA2 contains the N-terminal mitochondrial targeting sequence (1-40 aa), a transmembrane domain (105-125 aa), followed by a serine protease domain (150-343 aa) with the catalytic triad His198-Asp228-Ser306, and one PDZ domain (364-445 aa) at the C-terminal end (Figure 2.4). The transmembrane domain (TM) determines the topology of HtrA2 in the mitochondrial intermembrane space and anchors the proform of the protease in the inner membrane. The protease and the PDZ domains are exposed into the mitochondrial intermembrane space (*26*).

Upon activation HtrA2 undergoes proteolysis generating a 36 kDa mature form of the protease (134-458 aa) with the N-terminal Ala-Val-Pro-Ser motif governing interaction with the Inhibitor of Apoptosis Proteins (IAPs). Following apoptotic stresses the mature

HtrA2 is released from the mitochondria into the cytosol (*25*). An X-ray crystallographic study showed that HtrA2 molecule is a pyramid-shaped homotrimer. The N-terminal IAPs binding motifs of monomers form the top of the trimer and the PDZ domains are located at the bottom of the structure. Formation of the homotrimeric stucture has been confirmed by experimental data (*27, 28*). Oligomerization is mediated by the trimerization motif of the protease domain (146-151 aa) wherein phenylalanine at the residue 149 is suggested to be a major determinant of the trimeric assembly. It was also demonstrated that the formation of the homotrimer is required for the HtrA2 proteolytic activity (*27, 28*)

Trimeric Assembly of HtrA2

The mature form of HtrA2 (134-458 aa) is predicted to be ~36 kDa, while its elution volume from gel filtration corresponds to an apparent molecular mass of ~110 kDa, which suggests the formation of a homotrimer. Trimerization creates pyramid shaped structure, with the N-terminal IAP-binding sequences on top and the PDZ domains at the bottom. The three amino acids namely Tyrosine 15, Phenylalanine 16 and Phenylalanine 123 stack themselves on top of the pyramid forming a hydrophobic cylinder generating a high hydrophobic region in the centre, supporting the trimeric structural stability. This protease comprises 7 α helices and 19 β strands (*27*).

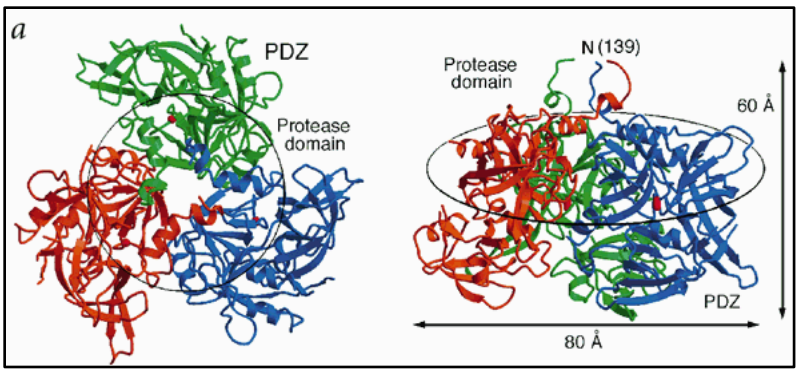

Figure 2.5: Trimeric assembly of HtrA2 (*27*).

Formation of homotrimer is a pre-requisite for the pro-apoptopic function of HtrA2 as in the monomeric form of HtrA2 the PDZ domain may slide over and completely block the access to the active site of SPD. The PDZ domain serves as a sensitive regulator of the serine protease activity in HtrA2 (*27*).

PDZ is a structural domain of 80-90 amino acid residues. Proteolytic activity of proteases is modulated by the relative orientation of the PDZ domain. In an inactive state the PDZ domain traps the active site of the enzyme as well as its own peptide binding site through non- canonical interactions. The PDZ domain is linked to the protease domain via a flexible linker sequence and has a peptide binding groove that contains peptide-recognition motif YIGV (361-364). Upon ligand binding, the PDZ domain would release the flexible L3 loop in the vicinity of the active site, triggering conformational changes and resulting in the formation of a functional and accessible active site. This finding suggests that the proteolytic activity of HtrA2/Omi is augmented in the absence of its PDZ domain (*29*). Thus PDZ plays a very important role in the dynamics of this protease as well as its interactions with other cellular proteins.

Serine proteases cleave peptide bonds in which serine acts as a nucleophilic amino acid at active site. As this site is deeply buried in the core region, the conformation is crucial for activity (*30*). The protease domain of HtrA2/Omi is of chymotrypsin type where the active site consisting of the catalytic triad His198-Asp228-Ser306 is located. The domain contains several loops which are named according to the chymotrypsin nomenclature, LA, L1, L2, L3 and LD and these are important for proteolytic activity and its regulation (*31*). The serine protease domains of HtrA2/Omi favour the aliphatic residues Val, Ile and Met in the P1 position. At the P2 and P3 position Arg is selected most strongly with a secondary preference for other hydrophilic residues (*29*). The PDZ domain restricts the active site of serine protease by packing against it through Van Der Waals contacts. When peptide binds to the hydrophobic groove of PDZ domain it leads to conformational change at the PDZ-Protease interface which removes the inhibitory effect of PDZ from the active site, thus enhancing the activity of HtrA2 (*27*). Bose and co workers elucidated the role of different domains, their combinations, oligomerization, and critical residues in modulating HtrA2 activity and specificity thus developing a model describing its mechanism of action (*32*). Their findings highlight importance of N-terminal region, oligomerization, and intricate intermolecular PDZ-protease interaction in proper active-site formation and enzyme-substrate complex stabilization in HtrA2 enzymatic functions. Their observations redefine the existing activation model (*27*) and showcase a unique example of how precise inter-domain coordination, plasticity, and intermolecular contacts lead to distinct functional properties and provide new insights into HtrA2 structure, function, and dynamics (Figure 2.6).

Temperature induced activation of HtrA2 was either achieved by heat shock induced stress or upon exposure of HtrA2 to temperatures. When temperature increases, HtrA2 structure relaxes and conformational changes are gradual, with changes in the PDZ domain occurring first, which leads to increased accessibility of the peptide binding groove, followed by increased exposure of the active site of the protease domain (*31*, *32*).

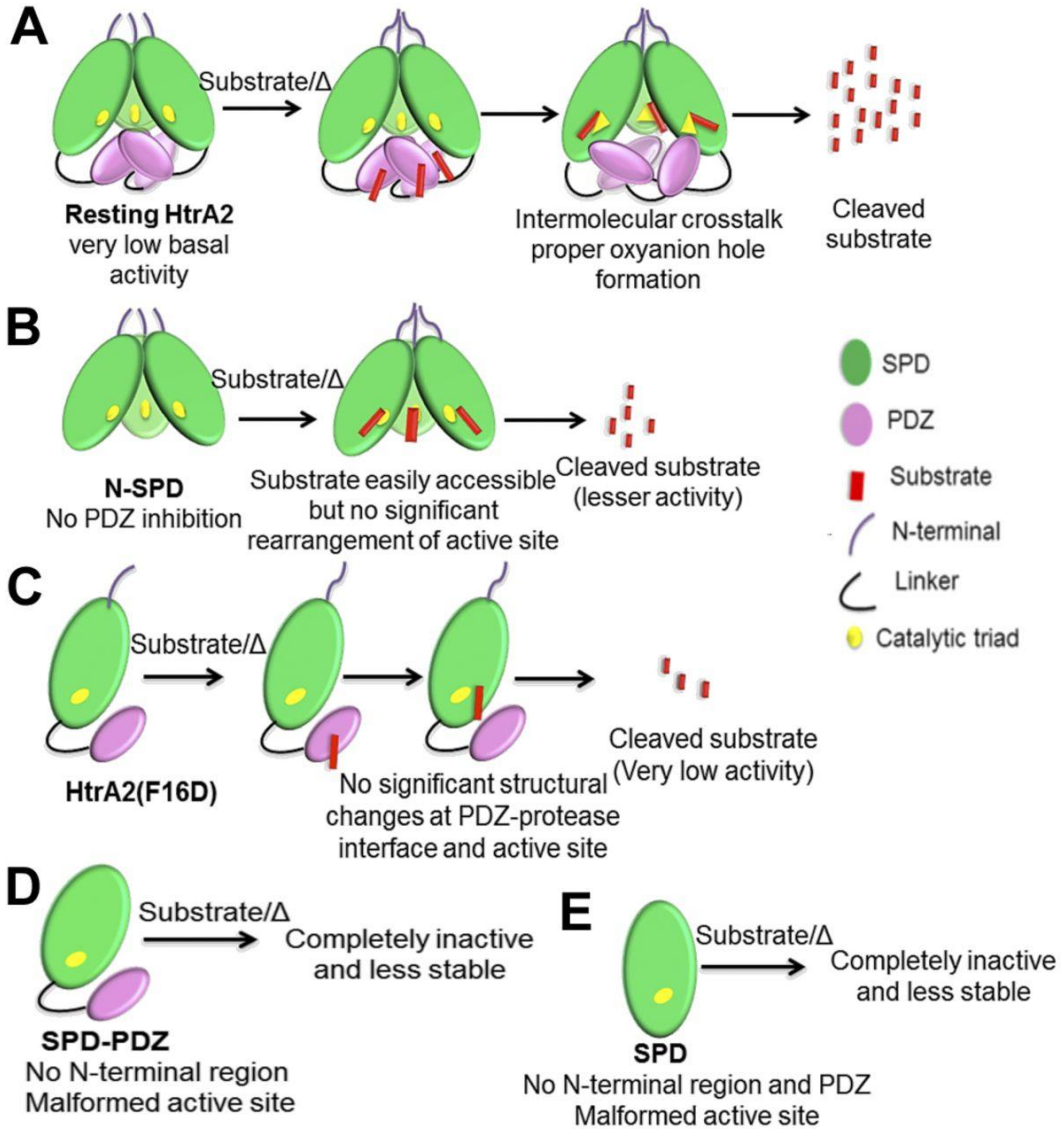

Figure 2.6: Model representing mechanism of HtrA2 activation (*32*).

HtrA2: A multitasking serine protease:

As protein quality factor: In normal physiological conditions it serves as protein quality control factor in mitochondria. Loss of HtrA2 causes an accumulation of unfolded proteins in mitochondria, dysfunction of the mitochondrial respiration, and generation of reactive oxygen species and contributes to cell death.

HtrA2 and apoptosis: Under stressful conditions such as nuclear DNA damage, death receptor activation, treatment with staurosporine, etoposide etc., anti-Fas antibodies or UV exposure HtrA2 may switch from a protector into a pro-apoptopic factor. This causes the translocation of the mature protease into cytosol, where it contributes to apoptosis through both caspase dependant and independent mechanisms.

Caspase dependent mechanism:

HtrA2/Omi unleashes caspase activity by proteolytically removing the natural inhibitors of caspase-3, -7 and -9. The BIR2 and BIR3 domains of cIAP1, cIAP2 and XIAP all bind the IBM motifs in the N terminus of the small catalytic subunits of active caspases-3, -7 and -9, but only XIAP engages a second interaction surface that allows potent inhibition of caspases. Nevertheless, cIAP1 and 2, as well as XIAP, may prevent caspase activation by targeting bound caspases for ubiquitin- mediated proteasomal degradation,71 providing an explanation why HtrA2/Omi targets all three IAP members (*29*).

Caspase independent mechanism:

The protease may also contribute to cell death by degradation of proteins other than IAPs which exhibit anti-apoptopic properties. HtrA2 binds to degrade the cytoplasmic Ped/Pea15 which acts as an anti-apoptopic protein. Additionally, at very early stages of cell death HtrA2 induces apoptosis by degradation of the mitochondrial protein HAX1.

HtrA2 also may contribute to cell death by degradation of several proteins such as components of translation machinery (eIF-4G1, EF-1 a) and cytoskeletal elements tubulin, actin, vimentin (*22*).Also upon induction of apoptosis HtrA2 is translocated to the nucleus where it cleaves p73 which leads to the transcription of the BAX gene whose protein product exhibits proapoptopic function (*33*).

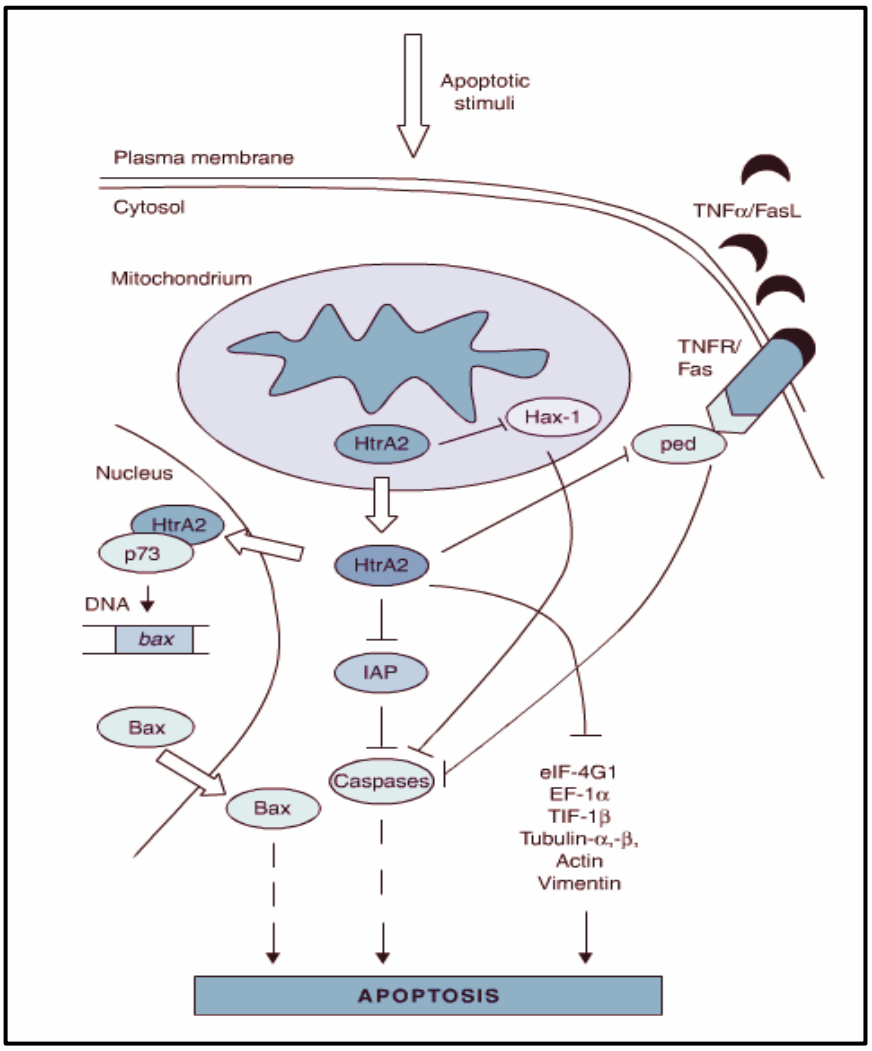

Figure 2.7: Apoptotic mechanisms mediated by HtrA2 (*33*).

HtrA2 as a chaperone protein

HtrA2 prevents the aggregation of amyloid β42, a major element of neurotoxic deposits in brains of alzheimers disease patients, keeping the peptide in the monomeric state. It binds to oligomeric Aβ via its PDZ domain and this interaction attenuates the HtrA2 proapoptopic activity and prevents neuronal death (*34*).

HtrA2 in various diseases

HtrA2 and Cancer:

There is an obvious relation between HtrA2 and cancer development as it plays a crucial role in induction of apoptosis. Dysfunction of apoptosis facilitates neoplastic transformation. Disturbances in the HtrA2 pro-apoptotic activity may also contribute to metastasis. The different types of cancer with which HtrA2 has been linked are gastric cancer, ovarian cancer, prostate cancer, lymphoma and leukaemia (*35*).

HtrA2 and Parkinsons disease:

Two single nucleotide polymorphisms in the HtrA2/Omi gene cause missense mutations (A141S, and G399S) and affect the enzymatic activity of the protease. These have been associated with the development of Parkinson's disease in humans (*29*).

HtrA2 and Alzheimer's disease:

Alzheimer's is a progressive neurodegenerative disorder which is caused due to deposition of extracellular plaques, which consist of amyloid beta peptides which are generated from the COOH-terminal end of amyloid precursor protein (APP). HtrA2

contributes to Alzheimer's disease through its interactions with presenilin, amyloid precursor protein and amyloid beta-peptide (*31*).

2.5 HAX1 - The anti-apoptotic protein

HAX1 (HS-1-Associated-protein-X-1) is a 35 kDa protein that was first identified by its ability to associate with hematopoietic cell-specific Lyn substrate 1 (HS1); which is a component of the B-cell receptor signalling pathway (*36*). HAX1 is ubiquitously expressed in murine and human tissues (*37*). It appears to be predominantly localized to mitochondria; on the inner or outer mitochondrial membranes and exposed to the inter-membrane space.

It is encoded by *HAX1* gene located on chromosome 1 (1q21.3) (*36*). In humans, the expression in liver, heart and testis are observed to be high. The human HAX1 has 8 isoforms generated by alternative splicing (Figure 2.8). Alternative splicing occurs mostly in the 5′ end of the HAX1 transcript, thus modifying the N-terminal part of the protein. The functional significance of each isoform is still not defined. Of all the isoforms, the isoform 1 is more prevalent in tissues suggesting that it has a dominant role (*37, 38*).

Domain organization of HAX1

HAX1 is an anti-apoptotic protein that was initially found to share homology with the BH1 and BH2 domains from the Bcl-2 family proteins. Apart from the two BH domains, it is suggested to have a PEST sequence (a.a 104–117) and a transmembrane domain at the C-terminus. PEST is a peptide sequence rich in proline (P), glutamic acid (E), serine (S), and threonine (T) residues. The proteins that show presence of this

sequence have a short intracellular half-life; hence, it is hypothesized that the PEST sequence acts as a signal peptide for regulated and rapid protein degradation.

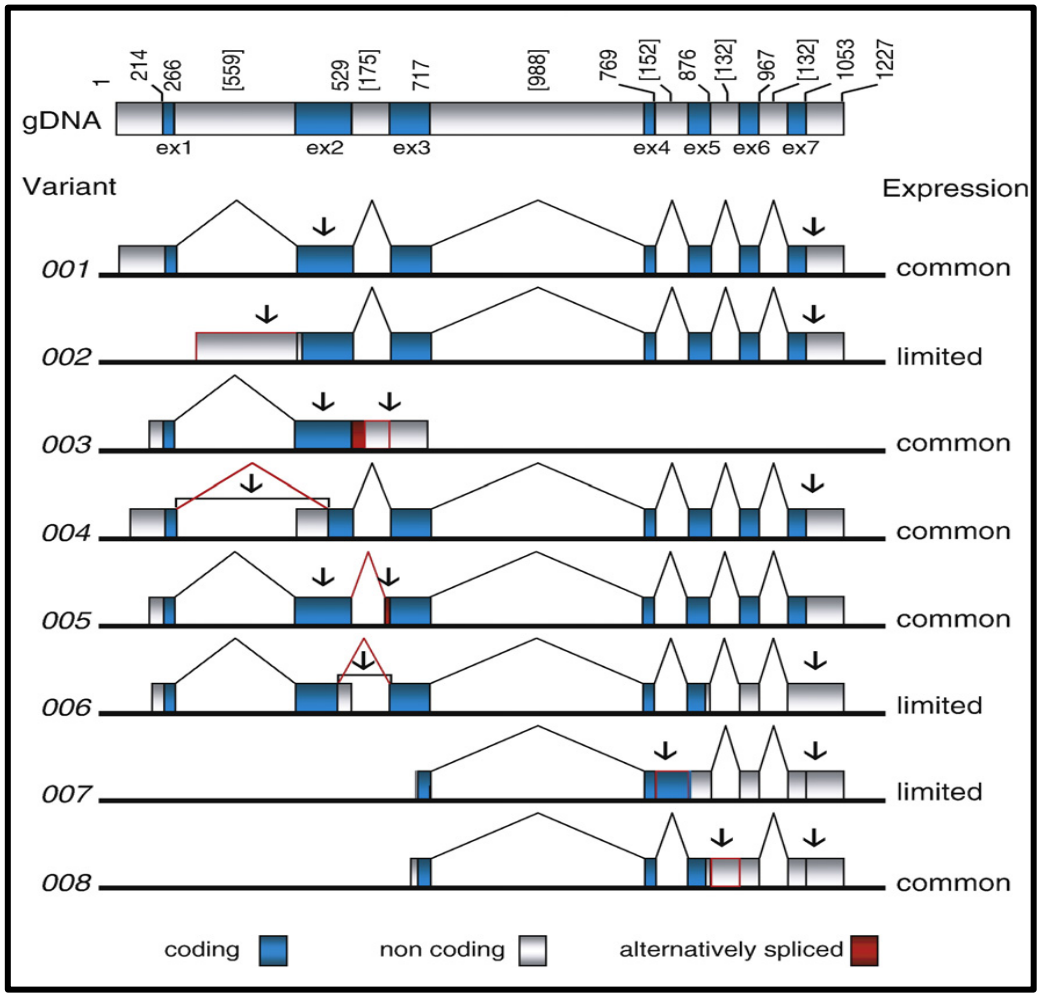

Figure 2.8: Schematic representation of human HAX1 isoforms (*37*)

HAX1 also has an acid box whose function has not yet been deduced. It has been shown that the acid box is rich in glutamic acid and aspartic acid. The C-terminal of the protein is suggested to have binding regions for interactions with various proteins. But recent

comprehensive studies on the domain organization have proven the absence of BH1 and BH2 domains apart from TMD. Thus ambiguity exists in this context.

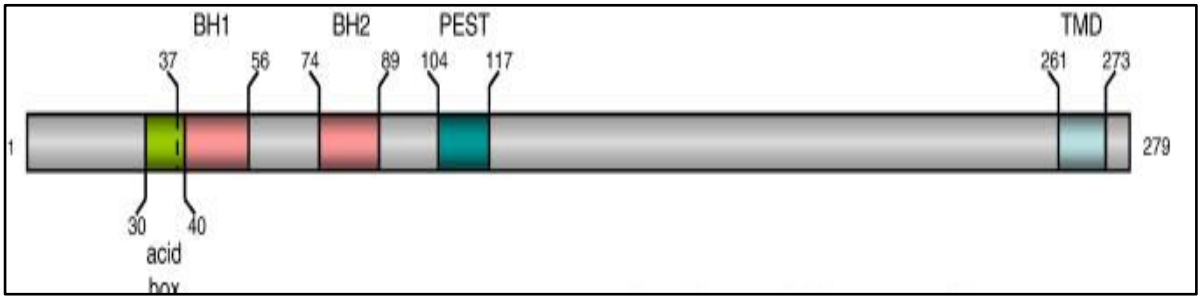

Figure 2.9: Schematic representation of HAX1 domains; all HAX1 domains are not characterized (*38*)

Physiological roles of HAX1

HAX1 was found to interact with a diverse group of proteins including phospholamban, F-actin-binding protein-cortactin, polycystic kidney disease protein PKD2, SERCA2, Epstein–Barr virus nuclear antigen leader protein (EBNA-LP), and K15 protein of Kaposi's sarcoma-associated herpes virus, Omi/HtrA2 serine protease and caspase-9.(*39*). Its multi-functionality and its involvement in processes regulating cell death suggest a role for HAX1 in oncogenesis and metastasis.

The first evidence of HAX1 being an anti-apoptotic protein was provided by Sharp *et al.* In this study they showed that Kaposi's sarcoma-associated herpes virus (KSHV) (or human herpesvirus 8, HHV-8) open reading frame (ORF) K15 interacts with HAX1 through its C-terminal domain. Also HAX1 co-localizes with K15 in endoplasmic reticulum and mitochondria. HAX1 was also reported to block Bax-induced apoptosis in a transient transfection assay in HeLa cervical carcinoma cells. Evidence of role of

HAX1 as an anti-apoptotic protein is also provided by studies on the pathogenesis of severe congenital neutropenia (Kostmann disease). In this syndrome the myelocyte undergo apoptosis due to which there is deficiency of neutrophils leading to immune-deficiency. Also it was found that mutant HAX1 is expressed in this syndrome which is inactive, thus suggesting the anti-apoptotic nature of HAX1 (*38*).

One of the ways by which HAX1 exhibits its anti-apoptotic role is by regulating mitochondrial membrane potential. HAX1 was demonstrated to interact with proteins involved in mitochondrial membrane permeabilization and elements of the mitochondrial mega-channel (*40*)**.** It has been observed that HAX1 overexpression resists mitochondrial membrane permeabilization during apoptosis. This property can be correlated to its anti-apoptotic activity and its overexpression in several human cancers such as oral, breast, lungs and melanoma (*41*). It was reported by Klein *et al*. that there is higher degree of apoptosis, *ex vivo*, of peripheral blood neutrophils derived from HAX1 deficient individuals when compared to cells from normal donors. In addition to this, it was also reported that neutrophils from the patients but not from normal controls displayed loss of mitochondrial membrane potential upon treatment with valincomycin (*42*)

HAX1 is reported to interact with Human Immunodeficiency Virus -1 (HIV-1) encoded proteins. HAX1 has been shown to associate with Vpr, a viral protein. Vpr has been implicated in T cell apoptosis through its activation of caspase-3 and caspase-9 and causing drop in the mitochondrial membrane potential. Overexpression of Vpr in HeLa cells was shown to sequester HAX1 from its normal location in mitochondria with resultant cell death. Also the overexpression of HAX1 suppressed the pro–apoptotic

activity of Vpr. This study thus concluded that HAX1 is immensely important in stabilization of the mitochondria (*43*).

Recent studies have shown that HAX1 associates both with PLN and SERCA2, thus implying a potential role for HAX1 in modulation of Ca^{2+} homeostasis since both SERCA2 and phospholamban have been shown to be involved in Ca^{2+} modulation. This provides a further link between Ca^{2+}homeostasis and cell survival/apoptosis (*44*). In fact, the observation that HAX1 may interact with ER proteins is in accord with the role of HAX1 and members of the Bcl-2 family members, which have been shown to control apoptosis not only at the level of mitochondria but also through direct effects on the ER.

The involvement of HAX1 in inhibition of apoptosis and promotion of cell migration processes crucial to carcinogenesis and metastasis – suggests that overexpression of HAX1 in cancer is likely to occur, as this could promote cell survival and enhance the invasive potential of malignant cells. Moreover, for comparison, numerous previous studies have demonstrated that anti-apoptotic Bcl-2 and related BH domain-containing proteins are overexpressed in human malignancies. ONCOMINE, a cancer cDNA microarray database, thus reveals overexpression in normal versus cancer tissues for hepatoma, lung cancer, lymphoma, melanoma, leukaemia and myeloma. (*41*). HAX1 is overexpressed in several solid tumours including breast cancer Down-regulation of HAX1 using antisense RNA has been shown to induce apoptosis in HaCaT cells. (*45*). Nevertheless, in spite of the large body of data indicating its role in apoptosis, molecular mechanisms of HAX1 mediated cell protection still remain unclear. To gain an understanding of the mechanisms involved, it is essential to study the nature and mode of

interaction between HAX1 and its interacting partners. One of the most important finding in this context is its interaction with the pro-apoptotic serine-protease HtrA2.

2.6 HAX1 and HtrA2 interaction

HtrA2 is identified as a serine protease and acts as a pro-apoptotic factor. It can induce apoptosis by caspase dependent and caspase independent manner. In caspase dependent manner it acts by inhibiting IAPs and subsequently brings about apoptosis. The caspase independent pathway is still to be elucidated. For this, it is imperative to find substrates and interacting partners of HtrA2. This will aid in understanding the caspase independent activity of HtrA2. Various binding partners for HtrA2 have been identified including Pea-15, Mxi-2 and IAPs.

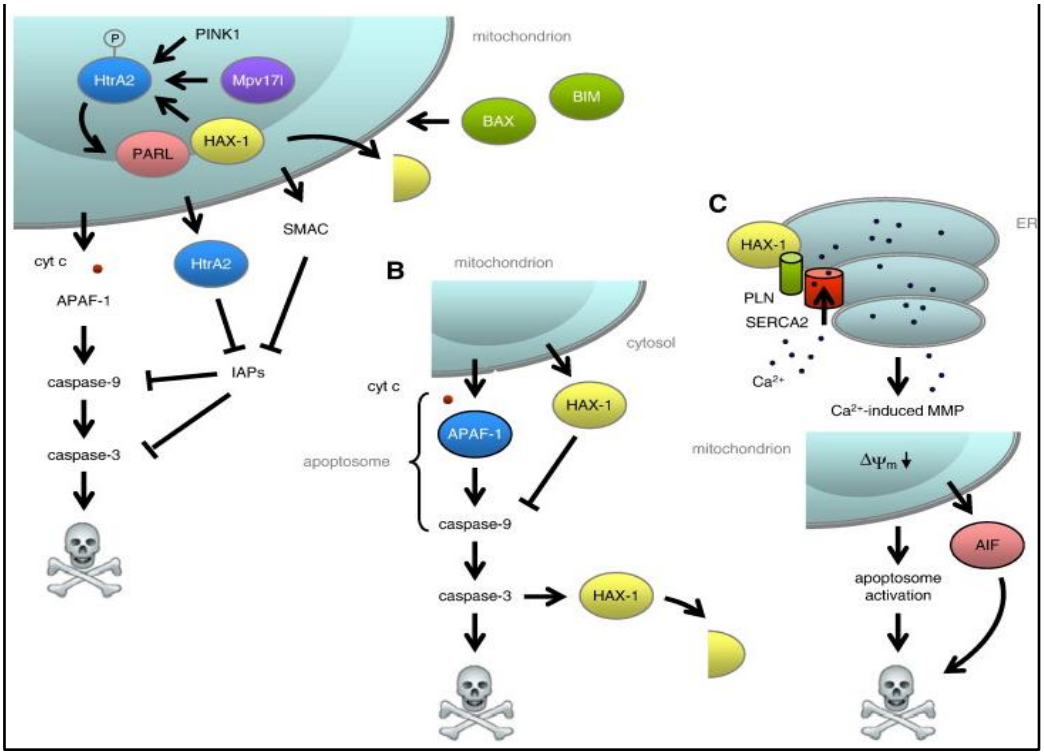

Figure 2.10: Schematic representation of anti-apoptotic function of HAX1 in three putative scenarios: in the mitochondria, in the cytosol, and on the endoplasmic reticulum (*38*).

These are cytosolic proteins and HtrA2 interacts with these entities once it has been released into the cytoplasm after an apoptotic signal. However, Cilenti, *et. al.* found HAX1, a mitochondrial protein is an interacting partner for HtrA2 (*5*). Thus, this interaction is an early event in the apoptotic signaling pathway. The interaction of HtrA2 with HAX1 leads to the decrease in the latter's level. Using a specific inhibitor of HtrA2, HAX1 degradation is prevented and cell death was found to be significantly reduced. Cleavage of HAX1 was not observed in a cell line derived from motor neuron degeneration 2 mice that carry a mutated form of Omi that affects its proteolytic activity (*11*)

The importance of this interaction is highlighted by the fact that HtrA2 interacts with HAX1 while it is still confined in the mitochondria. Understanding the nature of this interaction and subsequent event that ensues will provide leads in caspase independent activity of HtrA2. These can subsequently also lead to therapeutic solutions in cancers and neurodegenerative disease wherein the apoptotic process is not under proper control.

2.7 Other interacting partners of HtrA2 and HAX1 in the mitochondria

Reports suggest that HAX1 is involved in suppression of apoptosis in lymphocytes and neurons. This activity requires the interaction of HAX1 with the mitochondrial proteases PARL (presenilins-associated, rhomboid-like) and HtrA2. These interactions allow HAX1 to present HtrA2 to PARL, and thereby facilitate the processing of HtrA2 to the active protease localized in the mitochondrial inter-membrane space (*8*)**.** But a recent study challenges the conclusions of Chao et al. by showing that HAX1 is not a Bcl-2-family-related protein because it does not contain bonafide BH modules, and that, *in vivo,*

the activity of HAX1 cannot be mechanistically coupled to PARL because the two proteins are confined in different cellular compartments, and their interaction *in vitro* is an artefact. (*46*). Thus, to get a clearer picture of the mechanism of interaction between HtrA2 with HAX1, this study aims to study the interaction in the presence of PARL. To understand the mechanism of action of HtrA2 and other potential roles, it becomes necessary to identify the interacting partners of HtrA2 and their mode of interaction. One such interacting partner that has been identified is the HS1-associated protein X-1 (HAX1, anti-apoptotic protein). Mitochondrial protease PARL (presenilin-associated, rhomboid-like) which has been reported to be involved in the processing of HtrA2 to the active protease localized in the mitochondrial inter-membrane space.

PARL belongs to a subfamily of rhomboid proteins that functions as an intra-membrane serine protease (*47*). The PARL subfamily is composed strictly of mitochondrial localized members. The mammalian *PARL* gene codes for a 379 amino acid PARL protease, which has been shown to reside exclusively in the inner mitochondrial membrane, with its N-terminus facing the matrix and its C-terminus exposed to the IMS (*48*) .Not much is known about PARL substrate specificity and cleavage site determination, since very few substrates have been found with some reports even suggesting its role in HtrA2 processing (*46*).

PARL is a multi-pass transmembrane protease situated in the inner mitochondrial membrane (IMM). This mammalian mitochondrial rhomboid possesses a '1+6' transmembrane structure consisting of an additional transmembrane helix (TMH) at its N-terminus, followed by the 6 TMH core. A catalytic serine (S) and histidine (H) are located approximately a third of the way into the membrane on the matrix side in TMH4

and TMH6, respectively. The interaction between these two catalytic residues is essential for stability of the PARL protein. Three cleavage sites exist in PARL: the most distal α site releases PARL's mitochondrial targeting sequence upon import into the mitochondria; the β site releases the Pβ peptide, the γ site within loop 1 may destabilize PARL when its degradation is required within specific tissues. Phosphorylation of three residues (S65, T69 and S70) within the Pβ domain regulate β-cleavage.

The active sites of PARL are believed to be located towards the matrix side of the mitochondrial membrane and the cleaved fragment of its substrate is released into the intermembrane space. Vertebrate specific phosphorylation and cleavage sites that are important for mitochondrial morphology have been located. In mammalian vertebrates, the phosphorylation state of this site dictates whether or not PARL will be cleaved and subsequently mediates mitochondrial fragmentation. Ultimately, induction of mitochondrial fragmentation triggers apoptosis. The N-terminal domain of human PARL harbors two consecutive cleavage sites. Overall, the N-terminal domain is conserved among vertebrates, particularly between mammals (*49*). Mammalian PARL is constitutively processed between position Gly52 and Phe53 which is the proximal α-cleavage site that removes PARL's mitochondrial targeting signal. Distal to the α-cleavage site is the β-cleavage site between residues Ser77 and Ala78.

β-cleavage of PARL releases a Pβ peptide of 25 amino acids in mammalian PARL that may mediate mitochondria-to-nucleus signaling which appears to be under developmental control and might be linked to neuronal development (*49*). Full-length PARL contains three cleavage sites α, β and γ.

Constitutive α-cleavage removes the mitochondrial targeting sequence (MTS) and is followed by β-cleavage only if PARL undergoes dephosphorylation at three residues: S65, T69 and S70 within the Pβ domain. β-cleavage liberates the approximately 25 amino acid long Pβ peptide which may translocate to the nucleus and be involved in mitochondrial-to-nucleus signaling where it may activate nuclear responses linked to mitochondrial biogenesis (*49*).

In primary cultures of immature rat cortical neurons (undifferentiated neuronal state), PARL is cleaved to liberate the Pβ peptide which is targeted to the nucleus by a nuclear localizing signal (NLS) located near the N-terminal of the Pβ peptide. Once differentiation is complete, as in differentiated neuronal cells, β-cleavage decreases or stops thus Pβ is detected in mitochondria. The destabilization pathway: γ-cleavage destabilizes PARL and may function to negatively regulate PARL activity in mitochondria. The amino acid sequence of this Pβ peptide is vertebrate-specific and contains a nuclear localization signal (NLS). This nuclear localizing signal consists of three closely spaced pairs of positively charged amino acids located within amino acids 54-65. The first two pairs are conserved in vertebrates, while the third is specific to mammals. In primary cultures of immature rat cortical neurons, the Pβ peptide is found primarily in the nucleus, where as in differentiated neurons it is predominantly located in mitochondria. Thus, in the early stages of neuronal differentiation, PARL is α- and β-cleaved generating a Pβ peptide which is shuttled to the nucleus. After differentiation, the generation of the Pβ is halted or considerably reduced, and is detected in the mitochondria but no longer in the nucleus. This suggests that β-cleavage of PARL may be under developmental control and the nuclear targeting of Pβ may play a function in

neuronal development. Since PARL plays a crucial role in induction of apoptosis there is an obvious link with cancer development (*48*). Dysfunction of apoptosis facilitates neoplastic transformation. Also disturbances in the PARL anti-apoptotic activity may also contribute to metastasis. Thus identifying it's in HtrA2 processing, which is a topic of contention, and its utility in HtrA2-HAX1-PARL complex might prove to be a cornerstone in the intrinsic pathway of apoptosis.

HtrA2's mechanism of caspase activation is attributed primarily to its IAP-inhibiting activity. Recombinant Omi/HtrA2 was observed to catalytically cleave IAPs and to inactivate XIAP *in vitro*, suggesting that the protease activity of Omi/HtrA2 might be responsible for its IAP-inhibiting activity. Despite availability of vast literature on this mechanism, the role of the mitochondrial activation of HtrA2 through its interactions and its implication of the XIAP mediated pathway of apoptosis is still elusive.

2.8 PDZ domains

The concept of domains has been one of the core themes in protein studies; one such being PDZ - a ubiquitous 70–90 residue protein–protein interaction module. PDZ helps localization and clustering of membrane receptors by binding primarily to their C-terminus in different pathways that drive life (*50-53*). The specificity of PDZ-domain-based interactions is determined primarily by the sequence of the C-terminus of the proteins they bind, although few exceptions do exist. The only existing database on this domain comprises only about 300 proteins which was last updated way back in 2004 (*54, 55*) thus creating a need for a database on this domain family that would include the

developments of the last decade. With cellular PDZ proteins as common targets of pathogenic viruses emerging as an important new theme in virology, high throughput and wide spectrum studies on this family of proteins is of significant value (*56*).

Chapter 3

Materials and Methods

3.1 MATERIALS

3.1.1 Bacterial strains:

Host/ Strain	Genotype	Origin
E. coli DH5α (Cloning host)	F^-, supE44, ΔlacU169, [Φ80lacZΔM15], hsdR17, recA1, endA1, gyrA96, thi^{-1},(res^-, mod^+), deoR	Invitrogen, Carlsbad, CA, USA
E. coli BL21 (DE3) (Expression host)	F^- ompT hsdSB(rB^- mB^-) gal dcm (DE3)	Novagen, Billerica, MA, USA
E. coli BL21 (DE3 pLysS) (Expression host)	F^- *ompT* $hsdS_B$(r_B^- m_B^-) *gal dcm* (DE3) pLysS (Cam^R)	Novagen

3.1.2. Plasmids used for cloning:

Plasmid / Vector	Tag	Source
pET 20b	C- terminal His_6 tag	Addgene (Cambridge, MA, USA)
pMAL c5E-TEV	N-terminal MBP tag (Maltose binding protein) with TEV protease site	New England Biolabs (NEB), Ipswich, USA
pGEX 2T	N- terminal GST (Glutathione-S-transferase) tag	
pIB 4	N terminal FLAG tag, His tag	Gift from Dr. Dibyendu Bhattacharya

3.1.3. Resins used for protein purification

Resin	Tag	Source
Ni-IDA	His_6 tag	Biotex, Houston, USA
Amylose	MBP tag	NEB
Glutathione-S transferase	GST tag	GE healthcare, Bjorkgatan, Uppsala, Sweden
Superdex 200	For gel filtration	GE healthcare, Bjorkgatan, Uppsala, Sweden

3.1.4. Kits used

Kit	Purpose	Source
Plasmid miniprep kit	Plasmid isolation	Sigma chemicals, St. Louis, MO
Gel extraction kit	DNA extraction from agarose gel	Sigma
pJET 2.1 blunt end cloning kit	Blunt end cloning	Fermentas, Waltham, Massachusetts, USA
Quick change site directed mutagenesis kit	Mutagenesis	Stratagene, Cedar Creek, TX, USA

3.1.5. Specialized instruments

Instrument	Purpose	Source
Jasco J815 CD spectrophotometer	Secondary and tertiary structure of proteins	JASCO, Easton, MD, USA
Fluorolog-3 spectrofluorimeter	Fluorescence emission studies, enzyme kinetics, quenching, FRET	HORIBA scientific,

		Edison, NJ, USA
Mithras multiwell plate reader	Enzyme kinetics	Berthold technologies, Wildbad, Germany
AKTA purifier	Gel filtration	GE Healthcare, Buckinghamshire, United Kingdom

3.2. Buffers and Reagents:

3.2.1. Bacterial culture media

a) Luria-Bertani (LB) medium (for 1 L):

25 g of LB powder (Himedia, Mumbai India) was dissolved in 1 L of Milli Q (MQ) water and autoclaved.

b) LB- Agar Plates (for 1 L):

25 g of LB agar powder (Himedia) was dissolved in 800 ml of MQ water and then made upto 1L with MQ water and autoclaved. It was cooled to about 55 °C and 1 ml of respective antibiotic was added from stock. The media was poured into petri dishes (~25 ml/100 mm plate).

3.2.2 Antibiotics

a) Ampicillin sodium salt (Sigma):

Stock concentration: 100 mg/ml (Filter sterilized using 0.22µ membrane), in water and stored at -20 ^{o}C. Working concentration: 100 µg/ml, stored at -20 ^{o}C

b) Chloramphenicol (MP Biomedical):

Stock concentration: 34 mg/ml (Filter sterilized using 0.22µ membrane), dissolved in ethanol and stored at -20 ^{o}C

Working concentration: 34 µg/ml, stored at -20 ^{o}C

3.2.3. For cloning and site directed mutagenesis

a) Primers:

PCR primers were commercially procured from Sigma in a lyophilized form. The primer pellet was centrifuged at 10,000 rpm for 1 min and then reconstituted in autoclaved deionized water to obtain final concentration of 1µg/µl. A working dilution prepared for further PCR based experiments was 125 ng/µl.

b) Restriction Digestion and Ligation:

Fast Digest DpnI, BamHI, EcoRI, NcoI, NdeI enzymes along with 10X fast digest buffer were obtained from Fermentas. T4 DNA ligase and 10X ligase buffer were supplied from NEB.

c) 0.5 M EDTA, pH 8 (for 1 L):

To 148 g of EDTA ~30-40 g of NaOH was added, pH was adjusted to 8 and volume was made to 1L.

d) Tris-EDTA (TE) Buffer (for 50 ml):

Tris	60.66 mg (10 mM)
EDTA	14.62 (1 mM)

pH was adjusted to 7.5 with 10 N NaOH and autoclaved.

e) Tris Acetate EDTA (TAE) running buffer for agarose gel electrophoresis (for 1 L)

Stock concentration: 50X TAE (2 M Trisacetate, 50 mM EDTA, pH 8)

Working concentration: 1X TAE (0.04M Trisacetate, 1mM EDTA, pH 8)

Tris base	242 g
Glacial acetic acid	57.1ml
0.5 M EDTA (pH 8.0)	100 ml

f) 6X Gel Loading Buffer for DNA (for 100 ml)

(0.25% Xylenecynol, 0.25% bromophenol blue, 30% glycerol)

Xylene Cyanol FF	0.25 g (migrates at 4160 bp with TAE)
Bromophenol blue	0.25 g (migrates at 370 bp with TAE)
Glycerol	30 ml
Autoclaved Milli Q	70 ml

g) Ethidium Bromide (EtBr)

Stock concentration: 10 mg/ml (20000X)

Working concentration: 0.5 µg/ml

3.2.4. Buffers for protein expression and purification

a) 1M Isopropyl-β-D-thiogalactopyranoside (IPTG) (for 5ml)

IPTG 1.19 g

Autoclaved Milli Q 5 ml

Filter sterilized (0.2µ) and stored at -20 ^{o}C.

b) Phosphate buffer, pH 8*:*

Components:

Monobasic or monosodium phosphate (NaH_2PO_4) 59.99 g for 500ml (1M)

Dibasic or disodium phosphate (Na_2HPO_4) 70.98g for 500ml (1M)

NaCl 35.6 g for 1lit (1M)

Stock concentration: 10X (200mM NaH_2PO_4/Na_2HPO_4, 1000mM NaCl, pH 8)

Working concentration: 1X (20mM NaH_2PO_4/Na_2HPO_4, 100mM NaCl, pH 8)

To 200ml of 1M dibasic solution, 1M monobasic solution was added and pH was adjusted to 8. Later 1M NaCl was added, volume was made to 1L using Milli Q. Buffer was filtered using 0.2µm filter and autoclaved.

3.2.4.1. Ni -IDA Column Purification buffers:

For HtrA2 and its mutants:

a) Lysis buffer (for 1 L): (20mM NaH_2PO_4/Na_2HPO_4, 100mM NaCl, pH 8, 0.1% triton X 100)

10X Phosphate buffer pH 8 10 ml (1X)

1M Imidazole 10ml (10 mM, reduces non-specific binding of proteins)

TritonX-100 10ml (0.1%)

10X Protease inhibitor 1X

BME (14.3 M) 0.34 ml (5 mM)

b) Ni-IDA Binding/Washing Buffer (for 1 L):

(20mM NaH_2PO_4/Na_2HPO_4, 100mM NaCl, 10mM Imidazole, pH 8)

10X stock Phosphate buffer pH 8 10 ml (1X)

1M Imidazole stock 10ml (10 mM, reduces non-specific binding of proteins)

14.3M BME stock 0.14ml (2 mM)

pH was adjusted to 8 , filtered (0.22µm) and autoclaved

c) Ni-IDA Elution Buffer (for 100ml):

(20 mM NaH_2PO_4/Na_2HPO_4, 100 mM NaCl, 20-250 mM Immidazole, pH 8, 2mM BME)

10X stock Phosphate buffer pH 8 10 ml (1X)

1M Imidazole stock 2 ml (20 mM), 10ml (100 mM), 25 ml (250 mM)

BME (14.3 M) 0.14 ml (2 mM)

pH was adjusted to 8, total volume was made to 100 ml, filtered (0.22µm) and autoclaved.

3.2.4.2. Amylose column purification buffers:

For HAX1 and its mutants

a) 1X HEPES buffer

HEPES (pH 7.5) 10mM

NaCl 250mM

Glycerol 5%

10X Protease inhibitor 1X

b) Lysis buffer

0.1% Triton-X in 1X HEPES buffer

c) Binding buffer or column equilibration buffer:

1X HEPES buffer - 10mM HEPES, 250mM NaCl, pH 7.5

d) Elution buffer for 100 ml

(10mM HEPES, 250mM NaCl, pH 7.5, 10mM maltose, 2mM BME)

10X Stock HEPES buffer pH 7.5 10 ml

0.5M Maltose (stock) 2ml (10mM)

Milli Q	88 ml
Total Volume	100ml

Note: filtered using 0.22 µm

3.2.4.3 GST fusion protein purification buffers:

a. Glutathione sepharose resin

b. Lysis buffer same as 3.2.4.2

c. Elution buffer same as 3.2.4.2 with 20mM reduced Glutathione instead of maltose

3.2.4.4. 5X SDS sample loading buffer (10ml):

(250mM tris-HCl pH 6.8, 10% SDS, 0.5%BME, 30% glycerol)

1M Tris-HCl pH 6.8	2.5 ml from stock 1M
SDS	10g
Glycerol	3ml
BME	0.5ml from stock 14.3M
Bromophenol blue	0.02g
Milli Q	4ml

3.2.4.5. 30% acrylamide: (29.2% Acrylamide, 0.8 % N'N'-bis-methylene-acrylamide)

Acrylamide	29.2 g (29.2%)

N’N’-bis-methylene-acrylamide 0.8 g (0.8%)

Milli Q Volume made upto 100 ml

3.2.4.6. SDS-PAGE Running Buffer (for 1 L):

(25mM Tris, 192mM glycine, pH 8.3, 1% SDS)

Tris Base 3.02 g (25mM)

Glycine 14.4 g (192mM)

Miili Q 1 L

No need to adjust pH

3.2.4.7. Staining / Destaining solution (for 1L):

(50% water, 40% methanol, 10% acetic acid, 0.1% Coomassie blue R-250)

Methanol 400 ml

Acetic Acid (glacial) 100 ml

Milli Q 500ml

Coomassie blue R-250 1g

Destaining solution is the same, minus Coomassie blue.

3.2.4.8. 1X Transfer Buffer (for 1 L)

(25mM Tris, 192mM glycine, pH 8.3, 20% methanol)

Glycine	14.4 g (192mM)
Tris Base	3.02 g (25mM)
Milli-Q	0.8 L
Methanol	200 ml (20%)

Note: No need to adjust pH

3.3 General Methods

3.3.1. Sterilization

Bacterial culture media and reagents were sterilized by autoclaving at 120 °C with a pressure of 120 lbs for 20 min. Heat sensitive solutions were sterile filtered with a 0.22 µ filter.

3.3.2. Growth conditions

All recombinant proteins were expressed either in *E. coli* BL21 (DE3) or pLysS cells in LB-medium with appropriate antibiotic at 37°C until they reached OD 0.6 at 600 nm. Cells were induced with IPTG concentrations ranging from 0.1mM to 0.3mM and grown for 16 hrs at 18 °C.

3.3.3. Primer Reconstitution

All the primers used were synthesized from Sigma and were received as a lyophilized nucleic acid pellets (not visible with naked eyes). The primer pellet was centrifuged at 10,000 rpm for 1 min. Primers were suspended in 10 mM Tris, pH 7.5 or autoclaved Milli

Q water, pH 7 to obtain stock concentration of 1 µg/µl. Reconstituted primers were stored at - 20° C. The working concentration of 125ng/µl was prepared. Detailed list of primers used in this thesis are mentioned in Table 3.1.

Table 3.1 List of primers

HtrA2 mutants	
G230A	GTC CCA GCG GCG CTACATTGC GGT GAT GATG
N216A, S219A (F)	GGAAAAGAAGGCTTCCTCCGCCGGAATCAG
E296A (F)	CTGAAGATGTTTATGCAGCTGTTCGAACC
E292A(F)	GTACAAAATGCTGCAGATGTTTATG
E292A(R)	CATAAACATCTGCAGCATTTTGTAC
D69A/R70A (F)	GTGGTGGCTGCTGCGCGCAGAGT
D69A/R70A(R)	ACTCTGCGCGCAGCAGCCACCAC
R74A/R76A (F)	GCGCAGAGTCGCTGTGGCACTGCTAA
R74A/R76A (R)	TTAGCAGTGCCACAGCGACTCTGCGC
HAX1 cloning	
HAX1(F)	AGCTGGATCCATGAGCCTCTTTGATCTC
HAX1(R)	AGAATTCCTACCGGGACCGGAACC
Nde I Hax (F)	AGCTCATATGAGCCTCTTTGATCTCTTC
HAX1 (R)	AGGTCATCAAAGCCGAAGTTATCG
PARL cloning	
PARL full length (FP)	ATATGGATCCATGGCGTGGCGAGGCTGGG
PARL full length (RP)	GCGAATTCTTACTTAGAGCCACCTCCTTTTTTGGG
HAX1 mutants	
E106A (F)	CCATCCTCCTGCACTTCCAGGT
E106A (R)	ACCTGGAAGTGCAGGAGGATGG
H136A,Q137A (F)	CCAGATAGTGCCGCGCCCAGGATCTT
H136A,Q137A (R)	AAGATCCTGGGCGCGGCACTATCTGG
P174A/D176A (F)	GATGATGTATGGGCTATGGCCCCCCATCCTAGAA
P174A/D176A (R)	TTCTAGGATGGGGGGCCATAGCCCATACATCATC

187 TO 190A(F)	GAGAGGACAATGATCTTGATTCCCAGGTTTCCCAGGAGGGTC
187 TO 190A(R)	GACCCTCCTGGGAAACCTGGGAATCAAGACATTGTCCTCTC
192 TO 195A(F)	CTTGATTCCCAGGTTGCCGCGGCGGCTCTTGGCCCGGTTG
198 TO 201 A(F)	CAGGAGGGTCTTGGCGCGGCTGCAGCGCCCCAGCCCAAAT
181.184.185 A (F)	CCCCATCCTAGAGCCAGAGAGGCCGCTGATCTTGATTCCCA
202.203.204.206 A(F)	CCGGTTGTACAGGCCGCGGCCAAAGCCTATTTCAAGAGCAT
117 STOP (F)	CCAGAGACACCTGGTTAGAGACTACGGGA
180 STOP (F)	GGACCCCCATCCTTGAACCAGAGAGGACAA
F276A, R277A	GGACGTTGGGCCGCGTCCCGGTAG
D170A, D171A, V172A (F)	CATAGGTTTGATGATGTATGGCCTATGG
HAX TEV (F)	CGATGGATCCGAGAACCTGTACTTTCAGGGTATGAGCCTCTTTGATCTCTT
D246A (F)	CGACACGAAGCAGCTAGCAGTCCTA
F208A (F)	CCCAAATCCTATGCCAAGAGCATCTCTGT
Q244A (F)	GTAACCCGACACGCAGCAGATAGCAGT
W275 (F)	CCTGGGACGTTATTTCCGGTC
W44A (F)	GAAGAAGGGGGCTCAGCGGGCCGTGGGAA
W173A (F)	GGTTTGATGATGTAGCGCCTATGGA
W275A (F)	CTGGGACGTGCGTTCCGGTC
W160A	CAACCAGCACCAGACGCGGGCTCCCAGA
R44A, W45A E2 (F)	GGCAACTAATAGCTGCGGAAAATGCAATATT
DEL_HAX_TMD 261-273 (F)	CAAGACCTCCAGCCTGATAGCTGGATGATGC
DEL TMD R	AGAATTCTATCAGGCTGGAGGTCTTGG
R44A (F)	GCAACTAATAGCTTGGGAAAATG
W45A (F)	CAACTAATACGTGCGGAAAATGCA
W98A (F)	CGATATGGGGGCCGCGACCTTGCCTTC
SEQUENCING PRIMERS	
CMV promoter	CGCAAATGGGCGGTAGGCGTG
T7 promoter	TAATACGACTCACTATAGG
T7 terminal	GCTAGTTATTGCTCAGCG
MBP	GGCCCAGTCTTTCGACTGG

forward	
MBP reverse	GATGAAGCCCTGAAAGACGCGCG

3.3.4. Determination of DNA concentration

The concentrations of the template DNA as well as the primers were ascertained based on their absorbance at 260 nm. This was measured with a micro-volume UV-Vis spectrophotometer (NanoDrop, Model - ND 1000) and the concentration was calculated according to the Lambert Beer Law. The ratio of absorptions at 260 nm versus 280 nm was used to assess the purity of the sample with respect to protein contamination. For a pure nucleic acid sample, the 260:280 ratios should be around 1.8-2. The absorbance for primers were measured at 260 nm using the single stranded DNA module of NanoDrop.

3.3.5. Polymerase chain reaction (PCR)

All PCR amplifications were done using Pfu turbo polymerase (Stratgene kit) with proofreading activity. For sub cloning, the gene of interest was PCR amplified using gene specific forward and reverse primers. For site directed mutagenesis (SDM) plasmid with gene of interest was amplified using the forward and reverse primer with desired mutation. In all SDMs, the sequence of the reverse primer is complementary sequence of the forward primer (Table 3.1). The primers were designed using primer-X software and oligoanalyser tools. The parameters taken under consideration for designing primers are primer length: 18-24 nucleotides, GC content: 40-60%, Tm: 50-65 °C. A typical PCR reaction composition is shown below:

Reagents	Volume (µl)
Autoclaved Milli Q water, pH 7	15.5
10 X Pfu buffer	2
10mM dNTPs	0.5
Template DNA (60ng)	1
Forward primer (125ng/µl)	0.5
Forward primer (125ng/µl)	0.5
Pfu enzyme (1unit)	0.5
Total Volume	20

Typical cycling steps for the PCR are

Initial denaturation	95 °C, 5 min
Denaturation	95 °C, 30 sec
Annealing temperature	53 °C, 55 sec
Elongation	72 °C, 10 min (elongation time depends on size of the DNA and polymerase used)
Final extension	72 °C, 10 min
Repeat step 2 to 4 for 25 cycles	for gene specific amplification 25 cycles and for SDMs 20 cycles

For SDM, amplified PCR products were treated with DpnI enzyme (Fermentas) at 37 °C to degrade the parental template. DpnI is an endonuclease which would specifically target

the methylated parental DNA strands. The digested PCR product was then transformed in *E. coli* DH5α cells. Plasmids were isolated from colonies and sequence of the desired mutation was confirmed using the DNA sequencing facility at ACTREC.

3.3.6. Agarose gel electrophoresis of DNA

0.8 – 1 % agarose was prepared in 1X TAE and boiled using microwave oven. Solution was allowed to cool to ~50-60 ^{o}C and ethidium bromide (0.5 µg/ml) was added to enable fluorescent visualization of the DNA fragments under UV light. The agarose solution was mixed thoroughly and poured in a gel casting tray with comb. The gel was allowed to polymerize for 20-30 mins. The DNA samples as well as DNA size-ladder in the range of 250–10,000 bp (Fermentas) were loaded along with the 1X DNA loading dye. The samples were resolved at 100 volts for 30-50 min. The DNA bands intercalated with EtBr were analyzed under UV 365 nm and gel was then documented (UVP, Bioimaging Systems) and viewed using LaunchVision Works LS software.

3.3.7. Restriction digestion reaction

Restriction digestion was performed using desired enzymes to prepare the vectors and inserts for cloning. All restriction digestion reactions were carried out at 37° C for 1-4 hours using the supplied buffers (Fermentas). After successful restriction digestion of the insert and the vector, both were purified by gel extraction (Gel Extraction Kit, Sigma). A typical restriction digestion reaction conditions are

10X buffer (Tango/FD)	2 µl (1X)
DNA template	10 µl (2-4 µg)

Restriction enzyme 1 unit	1 µl
Autoclaved MQ water variable	7 µl
Final Reaction Volume	20 µl

3.3.8. Cloning/Ligation

Ligation was set up using T4 DNA ligase supplied with 10X ligation buffer (Fermentas). For cloning blunt end PCR products, pJET cloning kit (Fermentas) was used and ligation was carried out according to the manufacture's protocol. The vector and PCR product were mixed in 1:3 molar ratios and ligated at 22 °C for 30min. For cohesive end cloning, restriction digested vector and insert were gel eluted and mixed in a molar ratios of 1:3 or 1:6 and ligated using T4 DNA ligase 22 °C for 3 hrs or 16 °C for 12 hrs.

Vector to insert molar ratio was calculated suing formula:

$$\frac{\text{Vector concentration (ng)}}{\text{Vector size (bp)}} = \frac{\text{Insert concentration (ng)}}{\text{Insert size (bp)}}$$

$$\text{Insert concetration (ng)} = \frac{\text{Vector concentration (ng) X Insert size (bp)}}{\text{Vector size (bp)}}$$

The above equation is for 1:1 molar ratio of vector: insert concentration. For 1:3 molar ratio 3 times the insert concentration was taken.

Composition for the ligation reaction as follows

Vector DNA concentration	60-80 ng
Insert concentration	Calculated from the above formula
10X T4 DNA ligase buffer	2µl

T4 DNA ligase	1µl
Autoclaved water	---µl
Total Volume	20 µl

3.3.9. Plasmid construction

a) HtrA2 constructs:

Clone for mature HtrA2 construct (Δ133) comprising residues 134-458 in bacterial expression vector (pET-20b) with a C-terminal His_6-tag was obtained from Addgene. Different HtrA2 domains, such as serine protease domain (SPD, residues 19–210), serine protease + PDZ domain (SPD-PDZ, residues 19–210) and PDZ (residues 226-325) domain were sub-cloned between Nde-1 and Xho-1 restriction sites of pET-20b vector. N-SPD, comprising N-terminal and serine protease domains (residues 1–210) of HtrA2 was sub cloned between Nde-1 and EcoR1 site of pMAL-c5E-TEV vector (NEB). For the ease of purification, His_6 was introduced into the C-terminal of pMAL-c5E-TEV-(N-SPD) clone using site-directed mutagenesis. Several mutants of HtrA2 (S174A, R74A, R76A, N216A, S219A, E292A, E296A and F16D) were generated using site-directed mutagenesis. Sequences of all HtrA2 variants were confirmed by automated DNA sequencing facility at ACTREC.

b) HAX1 constructs:

Full length HAX1 (1-279 amino acids) was sub cloned from pGEX 2T in pMALc5E-TEV vector using the BamH1 and EcoR1 restrictions sites. Different deletion constructs of HAX1 were generated with the Quick change site-directed mutagenesis kit

(Stratagene). Several mutants of HAX1 (W98A, W160A, W173A, W275A, F208 stop, R180 stop, H136A, Q137A, P174A, D176A) were generated using site-directed mutagenesis. The resulting mutations were confirmed by DNA sequencing.

3.3.10. Transformation

The ultra-competent *E. coli* DH5α cells from -80 °C were thawed on ice. 10 µl of the ligation mixture or 5 ng of plasmid DNA was added to an aliquot of competent cells and incubated in ice for 30 min. The cells were given heat shock at 42 °C for 90 sec and incubated immediately in ice for 2-3 min. After heat shock, 750 µl of LB medium was added to the tube and incubated at 37 °C for 45 min with vigorous shaking (200-250 rpm). After 45 min cells were centrifuged at 5000 rpm for 3 min. The supernatant was discarded and 100 µl of fresh LB was added to the tube. Pellet was re-suspended and plated on LB plate with appropriate antibiotic and incubated overnight (16 hrs) at 37 °C.

3.3.11. Bacterial protein expression and purification:

a) Sterilization

Bacterial culture media and solutions were sterilized by autoclaving by heating at heating at 120 °C with a pressure of 120 lbs for 20 min. Heat sensitive solutions were sterile filtered with a 0.22 µm filter.

b) Growth conditions

All recombinant proteins were expressed either in *E. coli* BL21 (DE3) or BL21 (DE3) pLysS. These strains lacks the Lon and OmpT proteases and carries a chromosomal copy of the T_7 RNA polymerase under the control of lacUV5 promoter (inducible by IPTG)

and therefore can conveniently express genes driven by the T7 promoter. Additionally, BL21 (DE3) pLysS was used for expression of toxic genes. The strain contains a chloramphenicol resistant pLysS plasmid which encodes for T7 lysozyme to prevent basal or leaky expression.

A single, transformed, isolated colony of expression host was inoculated in 10 ml LB medium and grown overnight at 37 °C with constant shaking at 200-250 rpm. 10 ml inoculum was further inoculated in 1 litre LB broth in a ratio of 1:100. The culture was grown till the $O.D_{600}$ reached 0.6-0.8. Cells were then induced with 0.3 mM isopropyl-D-thiogalactoside (IPTG) and incubated at 18 °C for 16 hrs. Culture was harvested by centrifugation at 5,000 rpm for 10 min at 4 °C. The bacterial pellets were stored at -80 °C until further use.

c) Ni-IDA agarose affinity chromatography:

Ni–IDA affinity purification method was used to purify His_6 tagged proteins. Ni–IDA agarose beads (Biotex) of 2 ml was taken in 1X 10 cm econo column (Millipore). Beads were washed with 1X washing/equilibration buffer with at least three column volumes under native conditions. Equilibrated Ni-IDA beads were then incubated with protein lysate at room temperature (22 °C) for about 30 min. After incubation unbound lysate (flow through) was collected separately. Beads were washed with 3 column volumes of washing buffer. His_6 tagged proteins were eluted with elution buffer containing imidazole gradient (20-500 mM).

d) Amylose affinity chromatography:

Amylose affinity purification method was used to purify the protein tagged with MBP. 2 ml of amylose beads (Novagen) were taken in 1X 10 cm econo column (Millipore). Beads were washed with 3 column volumes of 1X washing/column equilibration buffer. Equilibrated Amylose beads were incubated with protein lysate at room temperature (22 °C) for about 30 min on rocker with gentle agitation. After 30 min, flow through was collected and beads were washed with 3 column volumes of wash buffer. Bound proteins were eluted using elution buffer containing 10 mM maltose.

3.3.12. General protocol for protein purification:

a) Purification of HtrA2 variants:

Production of Recombinant HtrA2 Wild Type, its Mutants and Domains Mature (D133 HtrA2) with C-terminal his6-tag in pET-20b (Addgene, Cambridge, MA) was expressed in *E. coli* strain BL21 (DE3) pLysS. N-SPD, comprising N-terminal and serine protease domains (residues 1–210) of HtrA2 was sub cloned into pMALc5E-TEV using appropriate primers. Point mutations were introduced into pET-20b HtrA2 by PCR using primer sets that included mutations for residues N216A, S219A, E292A, E296A and F16D. N-SPD clone and these mutants were confirmed by DNA sequencing. Protein expression was induced by culturing cells at 18 °C for 20 h in presence of 0.2 mM isopropyl-1-thio-D-galactopyranoside. Cells were lysed by sonication and the centrifuged supernatants for HtrA2 and its mutants were incubated with pre-equilibrated nickel-IDA beads for 1 h at room temperature. Protein purification was done using Ni-affinity chromatography as described earlier. Eluted protein was further purified using gel permeation chromatography. N-SPD was purified using amylose resin where the bound

protein was eluted using 10 mM maltose and was subjected to TEV protease cleavage to remove maltose binding protein (MBP). N-SPD was further separated from MBP by gel filtration using Superdex 200 column. All purified proteins were analyzed by SDS-PAGE for purity. The fractions with 95% purity were stored in aliquots at -80 °C until use.

b) Purification of HAX1:

HAX1 with N-terminal MBP and C-terminal His_6-tags in pMALc5E- TEV vector was expressed in *E. coli* strain BL21 (DE3) pLysS. Protein expression was induced by culturing cells at 18 °C for 20 hr in presence of 0.3 mM isopropyl-1-thio-D-galactopyranoside. Cells were lysed by sonication and centrifuged at 18,000 rpm for 30 min. Supernatant was then incubated with pre-equilibrated amylose resin at 4 °C for 1hr. Beads were washed with 3 column volumes of wash buffer. Elution was performed using 10 mM maltose and was subjected to TEV protease cleavage for removal of MBP. HAX1 was further separated from MBP using gel filtration chromatography. All purified proteins were analyzed by SDS-PAGE for purity.

c) Gel filtration chromatography for HtrA2 and its variants:

Gel filtration or size exclusion chromatography is a separation technique based on size and volume of macromolecules. Relatively small molecules can diffuse into the pores of column matrix whereas large molecules will be prevented by their size from diffusing into the pores thus migrate faster. Gel filtration displays a method that can be applied to purify proteins and also to determine the molecular mass of proteins.

Molecular weights of HtrA2 variants were estimated by size exclusion chromatography. 1 ml aliquots of protein samples (2-3mg) were run on a Superdex 200 10/300 HR column

(GE Healthcare) pre-equilibrated with HEPES buffer. Proteins were eluted with the same buffer at a flow rate of 0.5 ml/min. The standards used for calibration were Alcohol dehydrogenase (ADH), Bovine serum albumin (BSA), Lysozyme and Maltose binding protein (MBP). All standards except for MBP that was lab purified were purchased from Sigma. Elution volume (Ve) / void volume (V_0) versus log of molecular weights of standards were plotted to generate the calibration curve from which molecular weights of HtrA2 variants were calculated.

3.3.13. Determination of Protein concentration:

Two distinct methods have been used to measure the protein concentration of a given sample.

a) Bradford protein assay:

The Bradford protein assay is a spectroscopic analytical procedure used to measure the concentration of protein in a solution (*57*). The assay is based on the observation that the absorbance maximum for an acidic solution of Coomassie brilliant blue G-250 shifts from 465 nm to 595 nm when binding to protein occurs. 5 µl of the BSA standards (1, 0.5, 0.25, and 0.125 mg/ml) were mixed with 200 µl of Bradford reagent (1:4 diluted, Bio-Rad) in triplicates in a 96-well plate. Readings were taken with ELISA plate reader (Spectra Max 790) at 595 nm using SoftMaxPro 4.6 software. Standard graph was plotted by taking absorbance on Y-axis and concentration of protein on X-axis. Protein concentration for unknown was determined by from standard curve.

b) Absorbance at 280 nm:

The absorbance of a protein sample at 280 nm was measured with a Nanodrop. The concentration was calculated according to the Beer-Lambert law: $A = \varepsilon \times c \times l$, where A

is the absorption at 280 nm, ε is the molar absorbance coefficient, c the molar concentration of the protein solution and l is the cell length of the cuvette. Molar extinction of proteins was calculated according to the Edelhoch method (*58*). The equations to calculate the protein concentration are

Protein concentration (mg/ml) = Absorbance $_{280}$/ ε X Molecular weight of protein (Daltons)

Protein concentration (μM) = Absorbance $_{280}$/ ε X 1000000

3.3.14. SDS polyacrylamide gel electrophoresis (SDS-PAGE)

SDS-PAGE was used for the electrophoretic separation of proteins according to the Laemmli method. The stacking and the resolving gel phase were prepared as described previously. The protein samples were mixed with 5x sample buffer, boiled for 5 min and loaded onto the gel. The electrophoresis was performed at 100 V for about 60 min. The gel was stained with Coomassie brilliant blue for 10-15 min. The gel was then destained for an hour and finally preserved in 10% acetic acid and documented.

3.4. Biophysical studies

Biophysical techniques used in this thesis to structurally characterize a given protein are:

a) Circular Dichroism (CD) spectroscopy

CD spectroscopy is used to determine the secondary and tertiary structural properties of biomolecules. Circular dichroism is the property of chiral molecules to absorb the right and left components of circularly polarized light to a different extent. Far UV CD spectra in the range (260-190 nm) was used to analyze different secondary structural

components of the protein such as alpha helix, parallel and antiparallel beta sheet, turn, and others. Absorption minima at λ 208 nm and 222 nm indicate α-helical structure, whereas a minimum at λ 218 nm is a characteristic of β-sheets. The disordered secondary structural elements or random coil protein are characterized by a low ellipticity at 210 nm and negative band near λ 195 nm.

Far-UV CD scans of HtrA2 variants were acquired using a JASCO J 815 spectropolarimeter (Jasco) using a quartz cell with 1-mm path length. Far-UV CD spectrum (260-190 nm) was recorded using a bandwidth of 1 nm and an integration time of 1s, with proteins of 10 μM concentrations. Each spectrum was an average of 5 scans, with a scan rate of 20 nm/min. Thermal stability of proteins were assessed by monitoring the CD spectrum with increasing temperature. A Far-UV CD spectrum was collected in a temperature range of 20 ºC to 100 ºC with an increment of 2 ºC/min. At each data point, the sample was equilibrated for 3 mins. Elipticity corresponding to 222 nm at different temperatures was obtained for calculation of melting temperature (Tm).

b) Fluorescence spectroscopy

Fluorescence is a phenomenon in which a molecule absorbs a lower wavelength photon, undergoes electronic excitation, and then emits longer wavelength. Fluorescence spectroscopy is used for studying dynamics, protein unfolding and biomolecular interactions. The intrinsic fluorescence of a folded protein is a combination of the signal from individual aromatic residues (Phe, Tyr, Trp) with the major contribution from tryptophan residue.

Fluorescence emission of HtrA2 and HAX1 variants were measured with protein solutions (2 μM) in using a Fluorolog-3 spectrofluorometer (Horiba Scientific) using a

quartz cell with 3 mm path length cuvette. Fluorescence spectra of 2 μM protein solutions were recorded with 295 nm excitation followed by emission between 310-400 nm using a 5 nm excitation and emission slit widths with an integration time of 0.1s.

c) KI quenching:

Fluorescence quenching is a process which decreases the intensity of the fluorescence emission. The accessibility of fluorophores in a protein molecule can be measured by extent of quenching. Fluorescence quenching methods are useful to obtain information about the conformational and dynamic changes of proteins. The quencher used for these studies was Potassium Iodide (KI).

The fluorescence quenching measurements were carried out using a Fluorolog-3 spectrofluorometer connected to a water bath. Fluorescence quenching experiments were performed at different quencher concentrations 0–280 mM. The fluorescence emission scans were taken after addition of quencher with excitation at 295 nm. The values of fluorescence were corrected for dilution effects, residual emission, Raman scattering, and absorption of light by KI.

Data analysis

Fluorescence emission maxima of respective proteins were used for data analysis. Data were then analysed using the Stern–Volmer relationship as shown in equation 1.

$F_0 / F = 1 + K_{SV} [Q]$,

For graph with upward curvature, modified Stern–Volmer relationship was used:

$F_0/F = (1+K_D[Q]) \exp([Q]VN/1000)$

where, F_0 and F are fluorescence intensities in absence and presence of quencher respectively, [Q] is concentration of quencher (molar), K_{SV} is the Stern–Volmer quenching constant, K_D is dynamic quenching constant, V is volume of sphere and N is the Avogadros number.

The procedure to fit these equations in Kaleidgraph is to plot the graph and then by going to the curve fit and type the following formula was used.

For linear equation

(1 + m1 * m0); m1=10 (m1=any variable form 1-1000)

m1= K_{SV} value for dynamic quenching constant

(1 + m1 * m0) * exp(m0 * m2 * 25.2 *10 ^ 20); m1 = 1000; m2 = 10 ^ -30

m1= K_{SV} value for dynamic quenching

m2= K_{SV} value for static quenching

3.5. Biochemical studies:

a) Affinity pull down studies

Affinity pull down studies help to understand protein-protein interaction in *in vitro* and *in vivo*. Recombinant GST and MBP-fused HAX1 (wild type and mutants) were lysed in a lysis buffer containing (10 mM , 250 mM NaCl, pH 7.5, 0.1% Triton X100). 10 µg of HAX1 lysate was incubated with 10 µl of amylose beads (Invitrogen) for 1hr at 4 °C. Beads were then washed extensively with the HEPES buffer. After these washes, 100 µg of purified recombinant HtrA2 variants and mutants were incubated with GST fusion HAX1 protein (~10 µg) bound to glutathione beads, in a final volume of 200 µl in wash

buffer. After overnight incubation under agitation at 4 °C, beads were extensively washed for four times with wash buffer and boiled in 30 µl Laemmli buffer. Samples were then analyzed by 12% and 15% SDS-PAGE and coomassie blue staining.

b) *In silico* docking studies

In silico docking studies are computer assisted program used to predict the binding interface in protein–protein interactions. Docking studies between the HtrA2 (receptor) and HAX1 (ligand) were performed using the HADDOCK and *ClusPro* 2.0, fully automated web servers for the prediction of protein–protein interactions (*59, 60*). First, it runs PIPER, a rigid body docking program, based on a novel Fast Fourier Transform (FFT) docking method with pair wise potentials. Second, by using a clustering technique for the detection of near native conformations and by eliminating some of the non-native clusters, the 1000 best energy conformations are clustered, and the 30 largest clusters are retained for refinement. Third, by short Monte Carlo simulations, stability of these clusters is analyzed, and by the medium-range optimization method SDU (Semi-Definite programming based Underestimation), the structures are refined. Total 40 docked models based on a) electrostatic, b) hydrophobic, c) van der Waal-electrostatic and d) balanced interactions were generated (10 docked conformations for each type of interaction). The structures based on the balanced type of interaction were studied, as it favored electrostatic, hydrophobic and electrostatic interactions which were preferred for docking. The interactions observed in these docked conformations were visually examined using the software *PyMol*. The binding interface residues were evaluated using the PDBsum generate server with the default cut-offs.

c) Protease assays with β-casein as substrate

Protease activity of different HtrA2 constructs was determined using substrate β-casein (Sigma), a generic substrate of serine proteases. For each 30µl reaction mixture, 2µg of respective protein was incubated with 6µg of β-casein in assay buffer (20 mM Na_2HPO_4/NaH_2PO_4, pH 8.0, 100 mM NaCl, 0.1 mM DTT) at 37 °C for 2.5 hrs and results were analyzed by SDS-PAGE. For all quantitative studies, FITC (fluorescein isothiocyanate) labelled β-casein (Sigma) was used. Fluorescent substrate cleavage was determined by incubating 200 nm of enzymes with increasing concentration (0–25 µM) of β-casein at 37 °C in assay buffer. Proteolytic cleavage was assessed by monitoring increase in fluorescence intensity of unquenched FITC β-casein in a multi-well plate reader (Berthold Technologies) with excitation and 535 nm emission 485 nm wavelengths.

Prior to the addition of substrate enzyme was pre-incubated with activator for the HtrA2-HAX1 activation assay at room temperature for 15 mins and proteolytic cleavage was monitored with excitation at 485 nm followed by 535 nm emission. Initial velocities were calculated at each respective temperature using linear regression analysis. Assays are representative of at least three independent experiments done in triplicate.

Data analysis

Graph was plotted by taking time (min) on X-axis and increase in fluorescence intensity on Y-axis. Slope value for each substrate concentration was determined using linear regression analysis. Reaction rates v_0 (µM/min) of unquenched FITC at respective substrate concentration were determined by dividing the slope with 19422 (slope of free FITC standard curve). The steady-state kinetic parameters were obtained from the

reaction rates by fitting data to Michaelis-Menten equation using nonlinear least squares subroutine in KaleidaGraph program (Synergy software).

d) Isothermal Calorimetry (ITC) studies

ITC studies for activating peptide with HtrA2 and the SBP double mutant. The peptide used was 13mer SEHRRHFPNCFFV, which has similar consensus sequence as defined for PDZ peptide groove binding substrate. The peptide was better in terms of solubility as compared to other activating peptides and binding studies were done using Isothermal titration calorimetry. The titrations were carried out using Micro Cal ITC200 (GE Healthcare) with the calorimetry cell containing 200 µL of wild type or N216A/S219A mutant HtrA2 in 20 mM Na2HPO4/NaH2PO4 buffer, 100 mM NaCl, pH 7.8. The concentration of protein was in range from 20 to 50 mM and was titrated with 1.5 ml injections of a solution containing 0.4 mM activator peptide reconstituted in the same buffer. To correct the effect of heat of dilution, a blank injection was made under identical conditions. All experiments were performed at 25°C and the data was analyzed using the manufacture provided MicroCal software with the integrated heat peaks fitted to a one site-binding model.

e) Protease assays with HAX1 as substrate

HtrA2 protease activity was assayed by incubating 4 µg of recombinant HtrA2 variants with 2µg of recombinant HAX1 constructs in an assay buffer (20 mM Na_2HPO_4/NaH_2PO_4, pH 8, 100 mM NaCl, 0.1 mM DTT) for 0-8 hrs at 37-55 °C. The reactions were stopped with SDS-sample buffer and boiled after 2hrs. The reaction products were analyzed by SDS-PAGE at a constant voltage of 90 V followed by coomassie Blue staining.

f) Limited proteolysis and N-terminal sequencing

The protein HAX1 was incubated with limited trypsin concentrations (10ng/µl) for 0-60 mins at 37 °C. The proteolytically cleaved HAX1 bands were transferred electrophoretically onto a polyvinylidene difluoride (PVDF) membrane (pore size 0.45 µm, Millipore Corporation, Billerica, MA, US) using wet transfer apparatus in 1X transfer buffer at a constant voltage of 20V for 10hrs. Transferred proteins were stained with 0.2% amido black in 50% methanol, destained in 50% methanol. The stained fragments were excised from the membrane and were air dried. The N-terminal five amino acid residues of each fragment were identified using ABI 494 Protein sequencer, Tufts university core facility, Boston.

3.6 Molecular dynamics simulation and analysis: HtrA2 and activating peptides

After analyzing the docking results, best HtrA2-peptide complexes based on Glide XP score and E-model value were used for Molecular Dynamic Simulation which was performed using Desmond 2010 [22] software package. Optimized Potentials for Liquid Simulations (OPLS) [41] all-atom force field was used to analyze model stability. The protein structures were solvated with Monte Carlo simulated TIP3P [42] water model with a 10 Å buffer space from the protein edges in an orthorhombic box and the system was then neutralized by replacing water molecules with sodium and chloride counter ions. Similarly, unbound HtrA2 system was also developed as a control. Neutralization of systems was done by adding 2 Na+ ions in unbound HtrA2 and 4 Na+ions for peptide bound complexes. The particle-mesh Ewald method (PME) [43] was used to calculate long-range electrostatic interactions with a grid spacing of 0.8 Å . Van der Waals and

short range electrostatic interactions were smoothly truncated at 9.0 Å. Nose–Hoover thermostats were utilized to maintain the constant simulation temperature and the Martina–Tobias–Klein method was used to control the pressure [44].

The equations of motion were integrated using the multistep RESPA integrator [45] with an inner time step of 2.0 fs for bonded interactions and nonbonded interactions within the short range cut-off. An outer time step of 6.0 fs was used for non-bonded interactions beyond the cutoff.

These periodic boundary conditions were applied throughout the system. These prepared systems were equilibrated with the default Desmond protocol that comprises a series of restrained minimizations and MDS. Two rounds of steepest descent minimization were performed with a maximum of 2000 steps and a harmonic restraint of 50 kcal/mol/per Å, 2 on all solute atoms, followed by a series of four MDS. The first simulation was run for 12 ps at a temperature of 10 K in the NVT (constant number of particles, volume, and temperature) ensemble with solute heavy atoms restrained with force constant of 50 kcal/mol/ Å .

The second simulation was similar to the first except it was run in the NPT (constant number of particles, pressure, and temperature) ensemble. A 24 ps simulation followed with the temperature raised to 300 K in the NPT ensemble and with the force constant retained. The last one was a 24 ps simulation at 300 K in the NPT ensemble with all restraints removed. This default equilibration was followed by a 5000 ps NPT simulation to equilibrate the system. A 30 ns NPT production simulation was then run and coordinates were saved in every 2 ps of time intervals.

The total trajectory of MD simulation was 30 ns. MD Simulation was analyzed using the analytical tools in the Desmond package. In MD quality analysis, potential energy of the protein as well as total energy of the entire system was calculated. The lowest potential energy conformations were then used for comparative analysis of peptide bound and unbound structures. Trajectories of peptide bound complexes and unbound HtrA2 were then compared based on their overall calculated RMSD (root mean square deviation), domain wise RMSD and RMSF (root mean square fluctuation) values and were plotted using GraphPad Prism 5.0 (GraphPad Software, San Diego, CA, USA).

Chapter 4

Allosteric Regulation in HtrA2 through a novel non-canonical pocket

4.1 Introduction

Multidomain proteins due to their structural complexity require different levels of regulatory mechanisms for executing cellular functions efficiently within a specified time period. Allosteric modulation of conformations is one such mechanism which often helps a protein to regulate a functional behaviour such as for an enzyme to attain an active functional state upon ligand or substrate binding. In allostery, sometimes there are large conformational changes that require significant rotations and translations of individual domains at the timescales of microsecond to millisecond. While in some other cases, minimal structural perturbation helps in propagation of the signal in an energy efficient way to the functional domain where movement is mainly restricted to the side chains, loops and linker regions and which occur within picosecond to nanosecond timescales (*61*). PDZ (postsynaptic density-95/discs large/zonula occludens-1) domains that are involved in myriads of protein-protein interactions (*62, 63*) exhibit minimal structural changes during allosteric propagation.

These domains have multiple ligand docking sites and are known to possess unique dynamics that regulate conformation of the functional site from a distal region. HtrA2 (High temperature requirement protease A2), a PDZ bearing protein, is a mitochondrial trimeric pyramidal proapoptotic serine protease with complex domain architecture whose activity is likely regulated by interdomain crosstalk and structural plasticity (*64*). Mature HtrA2 comprises 325 amino acids with residues S173, D95 and H65 forming the catalytic triad which is buried 25 Å above the base of the pyramid suggesting requirement of conformational changes for its activation. Apart from PDZ, this multidomain protein has a short N-terminal region, a serine protease domain and a non-conserved flexible linker at

the PDZ protease interface (*64*). HtrA2 is involved in both caspase dependent as well as caspase independent apoptotic pathways (*65-67*). Literature suggests it might have chaperoning functions as well and recently has been found to be associated with several neurodegenerative disorders (*68-70*). Based on information from literature (*64, 71*), this multitasking ability of HtrA2 can be attributed to its serine protease activity which is intricately coordinated by its unique substrate binding process, complex trimeric structure, interdomain networking and conformational plasticity. However, the unbound inactive form of the crystal structure with partially missing active site loops and flexible PDZ protease linker has been unable to unambiguously determine the role of dynamics and allostery if any in HtrA2 activation and specificity. Therefore, to understand the molecular details of its mechanism of action, dynamics study at the substrate binding site and active site pocket becomes imperative.

HtrA2 belongs to a serine protease family that is conserved from prokaryotes to humans (*72*) where allostery is a common mechanism for protease activation in some of its homologs. DegS, a bacterial counterpart of HtrA2, allosterically stabilizes the active site pocket upon substrate binding at the distal PDZ domain (*73*). DegP, the most extensively studied protein of the family, has a cage-like hexameric structure whose activation is regulated by allostery and oligomerization. Peptide binding to distal PDZ1 domain leads to rearrangement of the catalytic pocket into enzymatically competent form that readily oligomerizes and renders stability to the active conformation (*73*).

With an aim at understanding the conformational changes and structural plasticity that govern HtrA2 activity and specificity, we took an *in silico* approach to study the movements of flexible regions of the protein upon ligand binding. The PDZ domain of

HtrA2 has a known hydrophobic substrate binding YIGV pocket (similar to GLGF motif) which is deeply embedded within the trimeric protein structure with P225 and V226 from the serine protease domain occupying the groove (*64*, *74*). This structural arrangement makes it impossible for substrate protein to bind without significant conformational changes. Thus, to examine whether allosteric modulation through an alternative site is involved in substrate binding and catalysis of HtrA2, molecular dynamics simulation (MDS) approach with a bound peptide activator was used to look into the structural rearrangements that occur in nanosecond time scale.

Although the information usually obtained from MDS is restricted primarily to movements in the accessible and flexible regions of a protein, it nonetheless contributes significantly towards understanding of the overall structural rearrangement and dynamics during its allosteric activation. In our study, we modelled the entire mature protease by filling in the missing regions using Prime 3.0 (*75*), followed by energy minimization with GRoningen MAchine for Chemical Simulation or GROMACS (*75*). Identification of the putative binding site(s) on HtrA2 was done using SiteMap 2.5 (*76*) and the selective binding pocket (SBP) for the ligand was chosen based on optimum energy parameters.

Peptides at SBP were docked from our peptide library that was generated based on available literature reports (*77-79*) and structural complementarities. MDS of the docked structures was done using Desmond 2010 (*80*) which provided critical information on loop and linker movements in HtrA2. These results combined with mutational and enzymology studies show that upon activator binding at the novel allosteric pocket, SBP, the linker at the PDZ-protease interface and loops L1, LA and LD around the catalytic groove undergo rearrangements in a coordinated manner so as to form an efficient active

site pocket. Moreover, the PDZ domains mediate intersubunit interactions which stabilize the oxyanion hole. These observations highlight the importance of allostery which might be an important prerequisite for an active conformation of the trimeric protease.

4.2 Results

4.2.1 Identification of Selective Binding Pocket (SBP)

The high resolution crystal structure of HtrA2 (*64*)(Figure 4.1a) that lacked flexible loops, linkers and some N-terminal residues was the target protein for our studies. These regions were modelled and energy minimised as described under Methods section. Comparison of refined model with unrefined structure showed significant movements of the loops defining new binding sites on the protein surface. The linker at SPD-PDZ interface moved towards α7 of PDZ domain whereas the linker in the protease domain moved closer to the SPD-PDZ linker so as to form a groove (Figure 4.1b).

Among the five possible putative binding sites that were identified, Site 2 or SBP (Figure 4.1c) that encompasses the groove generated by SPD-PDZ linker, protease and PDZ domains attained the best score (Table 4.1). The site score takes into account parameters such as volume, density, solvent exposure, hydrophilic and hydrophobic nature of residues and donor to acceptor ratio and hence is a comprehensive representation of the possibility of it being a binding site. SBP has optimum volume and contacts available including maximum hydrogen donor and acceptor groups that are crucial for interacting with peptides. The size of the site is very important since the binding peptides have 6–7 residues and the site needs to be large enough to accommodate them. It also has highest hydrophobicity which makes it the best interaction site and hence used in our studies.

Although sites 1 and 3 have scores closer to that of SBP, taking into account all the above-mentioned parameters, SBP was chosen for further docking and MDS studies.

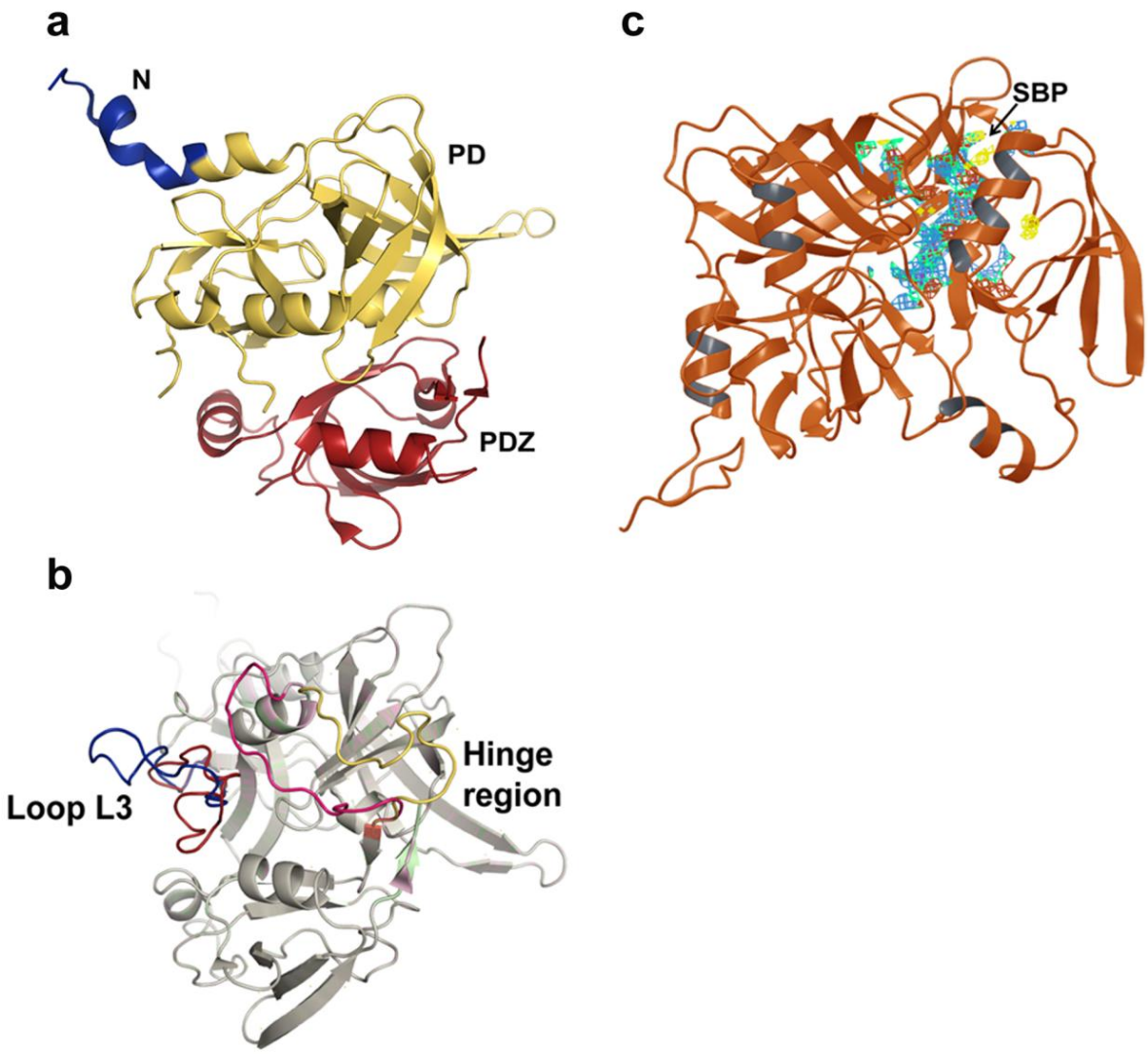

Figure 4.1. Ribbon model of HtrA2 structures (PDB ID: 1LCY). a. Domain organization of HtrA2 protease which comprises N-terminal region (blue), protease domain denoted as PD (yellow) and PDZ domain (red) at C-terminal end. b. Structural

alignment of loop refined (light magenta) and unrefined (light green) structures of HtrA2 protein with modelled N-terminal AVPS, loop L3 (residues 142–162) and hinge region (residues 211–225) built with Prime (Schrödinger LLC, New York, 2011). On refinement, loop L3 and hinge region are reorganized so as to define new regions at the protease and PDZ domain interface. c. Selective binding pocket (SBP) on HtrA2. The energy minimised structure of HtrA2 after modelling flexible regions in the protein is represented as a ribbon model. The binding site designated as SBP, selected on the basis of the Sitemap score and residue analyses, is located at the interface of PDZ and protease domain and shown as a multi-coloured mesh.

Table 4.1. Putative binding sites in HtrA2 identified by SiteMap tool.

Site number from SiteMap	**Residues present in the site**	**Site score**
Site 2	K214, K215, N216, S217, S219, R226, R227, Y228, I229, G230, V231, M232, M233, L234, T235, L236, S237, S239, I240, E243, H256, K262, I264, Q289, N290, A291, E292, Y295, E296, R299, S302	1.092716
Site 1	H65, D69, R71, A89, V90, P92, D95, T324	0.957142
Site 3	N48, H65, D169, S173, K191, M232, H261, L265	0.936056
Site 4	V192, F251	0.807891
Site 5	I33, L34, D35, R36, V73, R74	0.673032

Table 4.2. Docking analysis of replica fragments with HtrA2. The fragments have been arranged based on the docking scores

Fragment Designed	Residue interactions	Glide score
methylammonium - methanol :: acetate_ion – methanol	G230, V231, I229, D95, P92, Y295	-7.092
methylammonium - methanol :: acetate_ion – methanol	D95, V231	-6.427
methylammonium - acetate ion :: methanol – methanol	P92, A64, G230, V231	-6.329
N-methylacetamide - methanol :: methanol – methanol	D95, R226, V231	-6.108
methylammonium - methylammonium :: methanol – methanol	D95, R226, V231	-5.870
methylguanidinium - methanol :: methanol – methanol	D95, Y295, V231	-5.850
N-methylacetamide - methanol :: methanol – methanol	Y295, V231, R227, R226, D95	-5.627
methylguanidinium - methanol :: methanol – methanol	D95, Y295, V231	-4.629
methylammonium :: N-methylacetamide :: methanol – methanol	D95, R226, G230, V231	-2.581
methylammonium :: methanol :: methylguanidinium – methanol	D95, R226, G230, V231	-1.804
N-methylacetamide – methylammonium :: methanol – methanol	D95, V231	-1.071

4.2.2 Peptide Docking Show Similar Interacting Residues

Here, we have used a holistic approach in designing activator peptides where different techniques were applied in parallel so as to conduct a comprehensive search for a

signature pattern that would dock at SBP. In one method, replicas for functional groups were chosen based on sequence and structural complementarities with hydrophobic SBP which were used for generating small molecular fragments. Scores obtained from docking these small molecules (Table 4.2) provided the framework for designing different combinations of tetrapeptides as shown in Table 4.3. With leads from literature and *in silico* structure-guided design, Gly and Val residues were added at N- and C-termini respectively of some peptides which subsequently increased the docking scores from 26 to 210 kcal/mol.

Table 4.3. Designed peptide fragments. Fragments of peptide combinations generated based on functional group studies have been enlisted

Fragment 1 combinations:
Lys-Ser-Glu-Ser
Lys-Ser-Glu-Thr
Lys-Ser-Asp-Ser
Lys-Ser-Asp-Thr
Lys-Thr-Glu-Ser
Lys-Thr-Asp-Ser
Lys-Thr-Glu-Thr
Lys-Thr-Asp-Thr

Fragment 2 combinations :
Arg-Ser-Glu-Ser
Arg -Ser-Glu-Thr
Arg -Ser-Asp-Ser
Arg -Ser-Asp-Thr
Arg -Thr-Glu-Ser
Arg -Thr-Asp-Ser
Arg -Thr-Glu-Thr
Arg -Thr-Asp-Thr

Fragment3 combinations:
Lys-Glu-Ser-Ser
Lys-Glu-Ser-Thr
Lys-Glu-Thr-Ser
Lys-Glu-Thr-Thr
Lys-Asp-Ser-Ser
Lys-Asp-Ser-Thr

Lys-Asp-Thr-Ser
Lys-Asp-Thr-Thr
Arg-Glu-Ser-Ser
Arg -Glu-Ser-Thr
Arg -Glu-Thr-Ser
Arg -Glu-Thr-Thr
Arg -Asp-Ser-Ser
Arg -Asp-Ser-Thr
Arg -Asp-Thr-Ser
Arg -Asp-Thr-Thr

Fragment4 combinations:
Gln-Ser-Ser-Ser
Gln-Thr-Ser-Ser
Gln-Ser-Thr-Ser
Gln-Ser-Ser-Thr
Gln-Thr-Thr-Thr
Asn-Ser-Ser-Ser
Asn-Thr-Ser-Ser
Asn-Ser-Thr-Ser
Asn-Ser-Ser-Thr
Asn-Thr-Thr-Thr

Fragment 5 combinations:
Lys-Lys-Ser-Ser
Lys-Lys-Thr-Ser
Lys-Lys-Ser-Thr
Lys-Lys-Thr-Thr

Fragment 6 combinations:
Arg-Ser-Ser-Ser
Arg -Thr-Ser-Ser
Arg -Ser-Thr-Ser
Arg -Ser-Ser-Thr
Arg -Thr-Thr-Thr

Fragment 7 combinations:
Gln-Ser-Ser-Ser
Gln-Thr-Ser-Ser
Gln-Ser-Thr-Ser
Gln-Ser-Ser-Thr
Gln-Thr-Thr-Thr
Asn-Ser-Ser-Ser
Asn-Thr-Ser-Ser
Asn-Ser-Thr-Ser
Asn-Ser-Ser-Thr
Asn-Thr-Thr-Thr

Fragment 9 combinations:
Lys-Asn-Ser-Ser
Lys-Asn-Thr-Ser
Lys-Asn-Ser-Thr
Lys-Gln-Thr-Ser
Lys-Gln-Ser-Thr
Lys-Gln-Thr -Thr

Fragment 10 combinations:
Lys -Ser- Arg-Ser
Lys -Thr- Arg-Ser
Lys -Ser- Arg-Thr
Lys -Thr- Arg-Thr
Arg -Ser- Arg-Ser
Arg -Thr- Arg-Ser
Arg -Ser- Arg-Thr
Arg -Thr- Arg-Thr

Similarly, two peptides previously reported in the literature as well peptides designed from the putative binding sites in pea-15 and HAX1 also interacted well with SBP. Analysis of docking results with all these different peptides show interaction with similar residues of SBP as observed in ligplot (Figure 4.2).

However, the control peptide KNNPNNAHQN, which has quite a few asparagine residues, is an ideal sequence to act as negative peptide for the pocket due to its stereochemical properties (*77*), did not bind to SBP demonstrating the specificity of designed peptides.

From the above extensive docking analysis, N216, S217, S219, E292 and E296 in SBP were found to be common for most of the peptide interactions (Figures 4.3 a–b). Of these residues, N216, S217, S219 belong to the linker region while E292 and E296 to the PDZ domain that were either involved in hydrogen bond formation or Van der Waals

interaction with the peptides. This result suggests that SBP might be the possible binding site and therefore a prospective putative allosteric site.

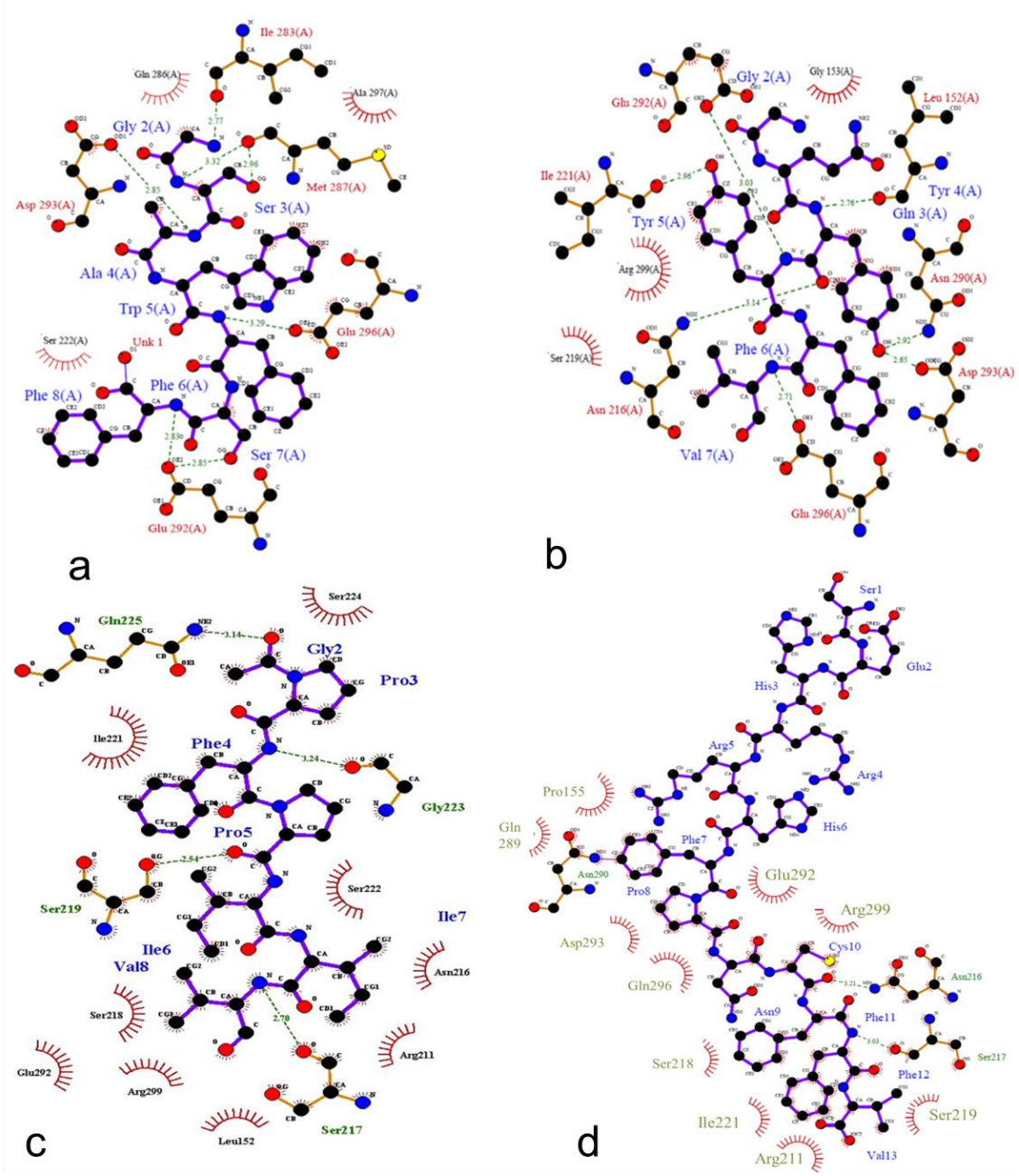

Figure 4.2. Interaction of peptides with HtrA2. a. Ligplot for GSAWFSF with HtrA2 which represents residues involved and the nature of interactions. b. Ligplot for GQYYFV interaction

pattern with HtrA2. c. Ligplot for GPFPIIV with HtrA2 which represents residues involved and the nature of interactions. d. Ligplot for SEHRRHFPNCFFV peptide with HtrA2 which represents residues involved and the nature of interactions. The residues of peptides and HtrA2 involved in interaction are shown in blue and red respectively.

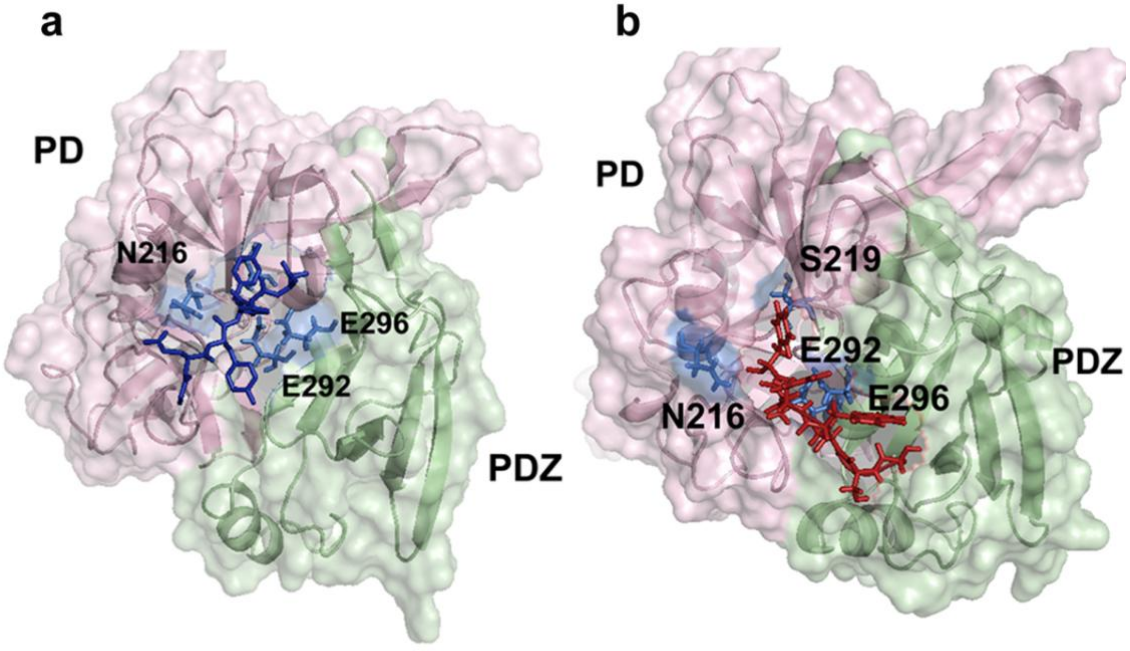

Figure 4.3. Representative surface structures of peptide activator docked HtrA2. a. Peptide GSAWFSF -HtrA2 complex and b. Peptide GQYYFV-HtrA2 complex. The former peptide represents putative SBP binding peptide in Pea-15 and the latter is a peptide obtained from the literature. The common interacting residues from SBP for both the peptides are labelled and are shown as blue sticks. PD denotes serine protease domain in both the Figures.

The role of some of these important residues in allostery if and its subsequent effect on catalytic activity and substrate turnover was further probed by enzymology studies as

described later in the text. MDS Analyses of HtrA2 and HtrA2– Peptide Complexes The peptides GSAWFSF was chosen for MDS studies as it gave the best XP and E-model scores (Table 4.4). GQYYFV has been reported to be a well known activator of HtrA2 (*77*) and hence used as another representative peptide for simulation studies. Moreover, the two peptides were chosen such that one is a designed peptide (GQYYFV) while the other is a part of a well-known HtrA2 binding protein Pea-15 (GSAWFSF). In addition to this, GQYYFV with docking score lesser than GSAWFSF was chosen for MDS analysis to understand whether different affinity for the substrate results in similar movements in the protease.

Peptides Used in Our study	Interacting Residues		Glide score in Kcal.mole^{-1}
	H bond Interactions	Vdw Interactions	
PEA 15 (GSAWFSF)	Glu 292, Glu 296, Asp 293, Ile 283, Met 287	Gln 286, Ala 297, Ser 222	−10.564
Designed (VKSDSG)	Asn 216, Leu 152,Glu 296, Glu 292	Ala 89, Ile 221, ser 218,	−10.394
Designed (GRTDSV)	Glu 296, Glu 292, Asn 216, Ser 217	Asp 293	−10.037
Designed (GRDTSV)	Ser 219, Glu 292	Ser 239,Gln 286	−9.57
Designed (GRDTYV)	Asp 293, Asn 216, Ser 217, Ser 219	Glu 296, Arg 299,	−9.54
Phosphatase (PAEWTRY)	Asp 117, Ala 149, Arg 150, Lys 215, Gln 146	Pro 148, Leu 152, Lys 214, Gln 156, Val 159, Ser 239	−9.481
HAX-1 (TKPDIGV)	Glu 292, Glu 296, Ser 219, Ile 221, Arg 299	Asn 216, Ser 222	−8.486
Connexin (ARKSEWV)	Asp 293/426, Asn 290/423, Gln 156/289	Glu 292, Pro 155, Gln 289, Met 287, His 256, Glu 255, pro 238	−8.165
Presenilin (AFHQFYI)	Leu 152, Asn 216, Ser 217, Glu 292, Glu 296	Pro 155, Arg 211, ser 218, Ser 219	−8.063
IL-EBF (AGYTGFV)	Asn 216, Ser 217, Glu 292, Arg 150/, Leu 152	Ser 219, Gly 153, pro 155	−7.903
Yes Protein (ESFLTWL)	Asn 216, Leu 152, Glu 296, Asp 293, Gln 289, Ser 237	Gln 156, Pro 238, Pro 155, Ser 218, Glu 292, Gln 286	−7.722
Cathepsin SVSSIFV	Glu 296, Asn 216, Ile 283/416,	Glu 292, Leu 152,Gly 153,Ala 297	−7.524
Warts Protein Kinase (NRDLVYV)	Lys 214, Lys215, Ala 149,Glu 207, Arg150, Gln 146	Leu 152, Gln 156, Val 159	−7.321
GQYYFV[6]	Glu 292, Glu 296, Asn 216, Ile 221,Leu 152	Ser 219,Gly 153, Arg 299	−7.163
GGIRRV[6]	Glu 292, Glu 296, Asn 216,Ser 217, Ser 219	Arg 211, Gly 153	−6.785
Tuberin (EDFTEFV)	Arg 211, Asn 216, Ser 219	Ala 89, Ile 221, ser 218, Arg 299, Glu 296, Glu 292, Gly 153	−1.883
Control Peptide (KNNPNNAHQN)		Did not dock with HtrA2	

Table 4.4. Peptide docking of HtrA2 and identification of interacting residues.

MDS analyses of HtrA2-GQYYFV and HtrA2- GSAWFSF complexes demonstrated significant difference in conformation as well as dynamics when compared with unbound HtrA2. Visual inspection of the domain wise movements in peptide bound HtrA2 indicated large fluctuations in hinge/linker region (211–226) as shown in Figures 4.4 a and b. Although these movements were larger for GSAWFSF than GQYYFV bound complex, the movement pattern remained similar in these two peptides. Enhanced dynamic movement in the former complex could be attributed to the peptide length (heptameric as compared to hexameric in the latter). Domain wise RMSD analysis of these trajectories provided quantitative output of deviations with respect to time. The

trajectory graphs (Figures 4.4 c–e) show that along the entire sequence, hinge region (211 2226) has RMSD of 2.5 Å for the peptide GSAWFSF and 1.5 Å for GQYYFV from the starting unbound form.

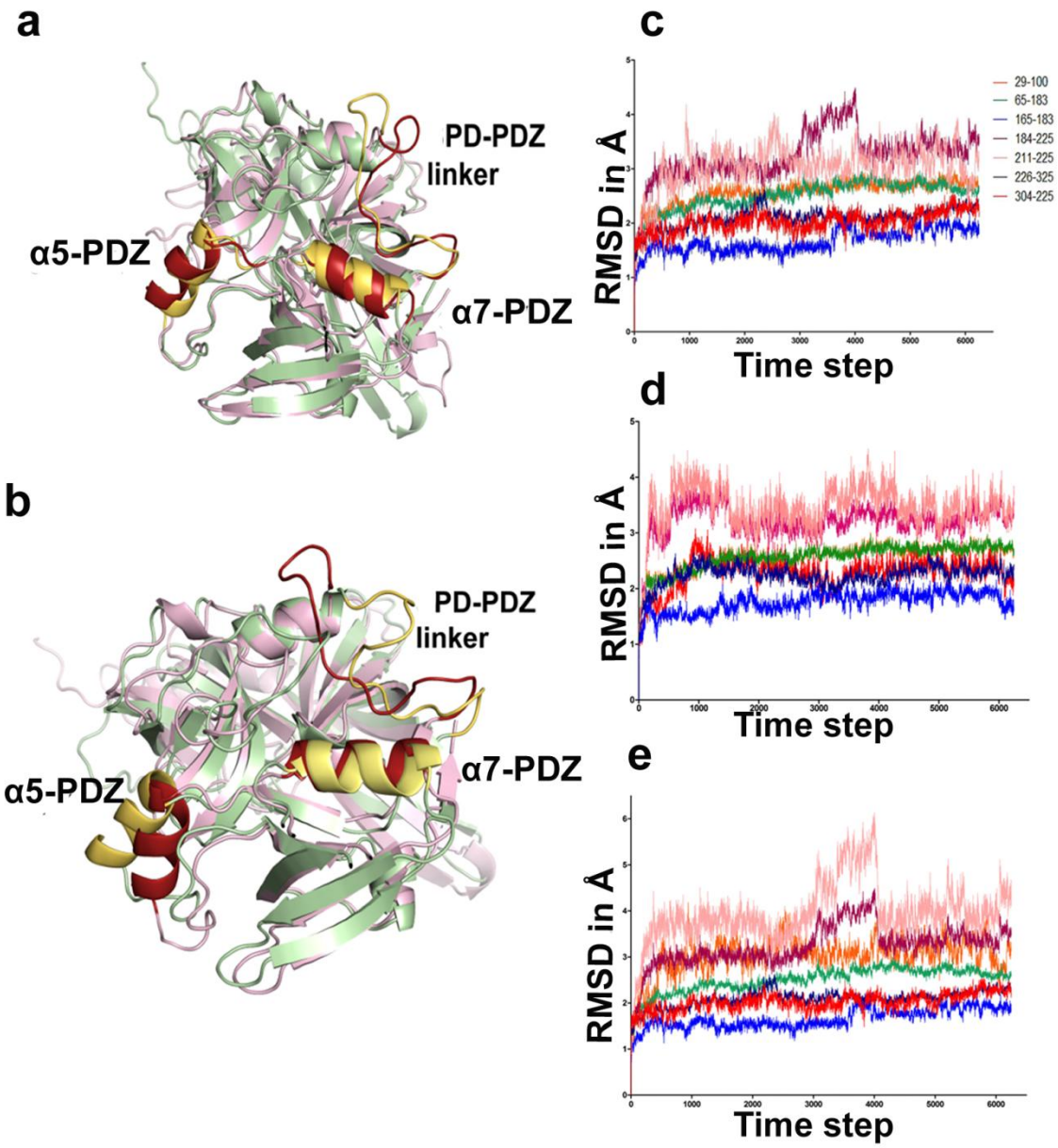

Figure 4.4. Domain wise conformational changes induced on peptide binding at SBP. a. The structural alignment of minimum energy structure of the peptide bound GQYYFV-HtrA2 complex (light pink) and unbound structure (green) displays orientation of the movement of the hinge region and the α-helices of PDZ. b. The structural alignment of GSAWFSF-HtrA2 complex (light pink) and unbound structure (green). Graphical representations of the RMSD for the 30 ns MDS trajectory of the following: c. HtrA2–GQYYFV complex. d. unbound HtrA2 (negative control). e. HtrA2– GSAWFSF complex. The stretch of residues selected for each set of RMSD calculations are shown on the right of panel c.

The RMSF of these trajectories were comparable with rmsd values showing higher relative fluctuations in and around the hinge region. Representative RMSF plots for GQYYFV and GSAWFSF bound HtrA2 complexes depict these large fluctuations for residues 190–225 as shown in Figures 4.5b and C respectively. All structural alignment comparisons and relative fluctuation analyses post MDS emphasize distinct significant conformational change in the hinge (211–226) region upon peptide binding. In addition to this, binding of peptides led to dynamic movements in many functionally important regions distal to SBP such as helices α5 and α7 in PDZ domain.

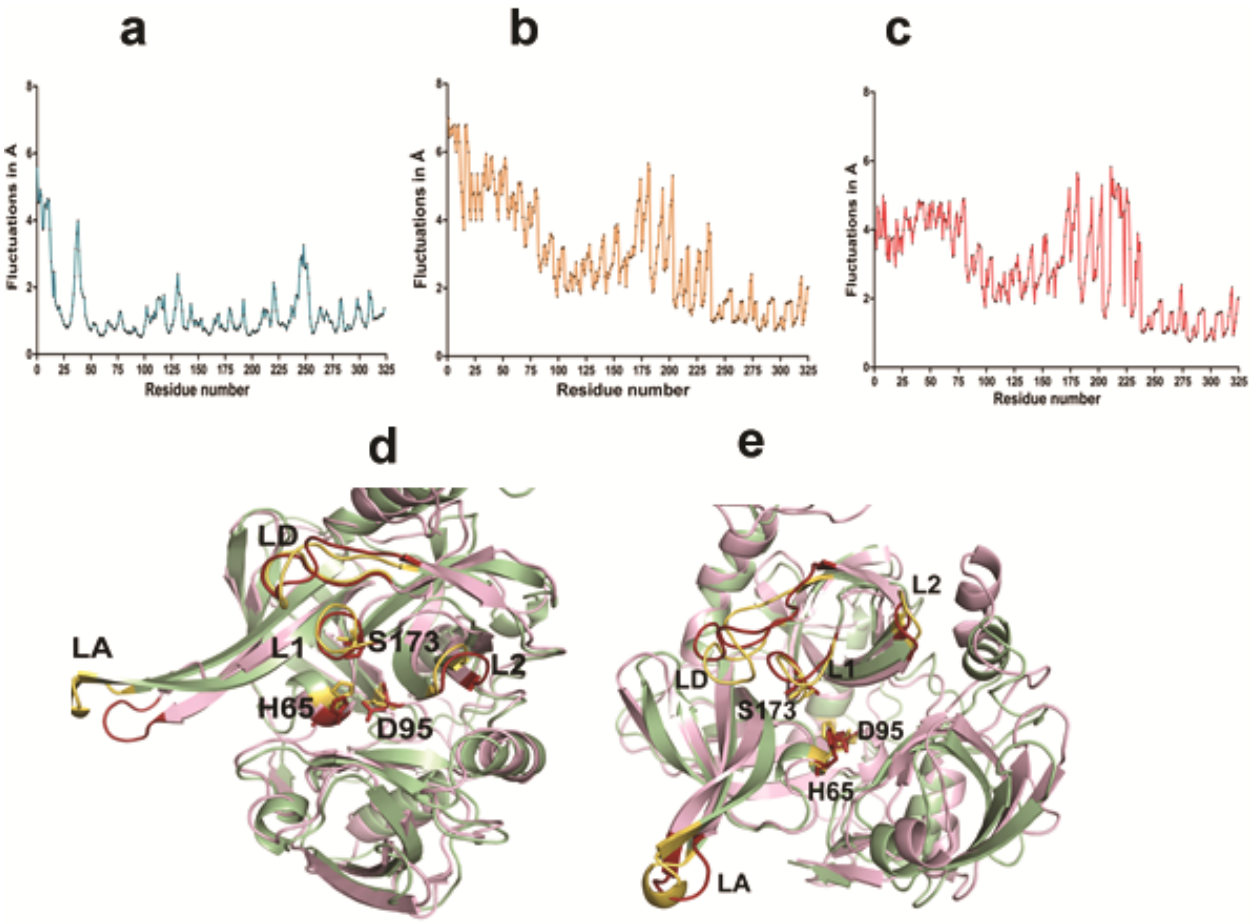

Figure 4.5. Graphical representation of root mean square fluctuation (RMSF) and loop movements upon peptide binding. a. MD simulation trajectory for unbound HtrA2. b. RMSF graph for GQYYFV bound HtrA2. c. RMSF graph for GSAWFSF bound HtrA2. d. Comparison of fluctuations in loops LA, L1, L2 and LD in the GQYYFV peptide bound (pink) and unbound structure (green). The loops in the bound and unbound forms are displayed in red and yellow respectively. e. Comparison of fluctuations in loops LA, L1, L2 and LD in the GSAWFSF peptide bound (pink) and unbound structure (green). The loops in the bound and unbound forms are displayed in

red and yellow respectively. The catalytic triad residues are shown in both panels d. and e.

4.2.3 Conformational Transitions in Flexible Regions and at the Active Site

Further detailed analyses of the effect that local subtle structural changes at SBP had on distal regions of the protease especially at the active site and its vicinity revealed the possibility of SBP being a putative allosteric site. Functional active site formation and its accessibility along with a well formed oxyanion hole are important prerequisites for the activity of an enzyme. Structural comparison of the MD simulated peptide bound structure of HtrA2 with the unbound form show movements indifferent domains and linker regions. The PDZ-protease linker that covers the peptide binding groove in the PDZ domain moves away from it thus increasing it accessibility.

The peptide bound HtrA2 complex show relative movements in the active site triad residues compared to the unbound form. Atomic distance analysis of both the forms revealed that distances between nitrogen (e) atom of H65 and oxygen (c) atom of S173 increased in peptide bound complexes while that between nitrogen (d) atom of H65 and oxygen (d) of D95 decreased when compared with the unbound HtrA2 structure (Table 4.5). This pattern being consistent with both the peptides suggests that interaction of peptide activator with SBP leads to opening up of the active site cleft.

Apart from active site triad, changes were also observed in the orientation of mechanistically important L1, LD and LA loops in the peptide bound complex (Figures 4.5d–e). Their orientations with respect to the active site determine proper oxyanion hole formation, accessibility of the active site, formation of catalytic triad and hence enzyme

activity. MDS analyses for these regions showed significant deviations upon peptide binding.

Table 4.5. Comparison of distances between atoms of the catalytic triad in the peptide bound and unbound forms of HtrA2.

Protein Complex	NE2 (His) – OG (Ser)		ND1 (His) – OD1(Asp)	
	Bound	Unbound	Bound	Unbound
HtrA2 (GSAWFSF)	5.2	4.1	2.6	2.9
HtrA2 (GQYYFV)	5.5	4.1	2.7	2.9

Structural alignment of GSAWFSF bound HtrA2 complex with the unbound form demonstrated breaking of Van der Waals contacts between loop LD and β2 strand of protease domain which facilitates LD movement towards α1 of protease domain and bringing P130 of the former in proximity to A25 of the latter. Similarly, S50 in β2 of protease domain establishes interactions with G171 of L1(oxyanion hole residue) while breaking contacts with A132 of LD loop due to movement or tilt in the L1 loop. As a result of this reorganization, LD which was closer to L1 in the unbound HtrA2 moves sharply away from it upon peptide binding. These positional rearrangements also lead to disruption of interaction between D165 of L1 and G195 of L2 loops. All these movements coordinate to bring LD closer to the proximal region of protease domain thereby opening up the catalytic site. For GQYYFV peptide, movements of all these

loops were subtle as compared to that for GSAWFSF except for the LA loop which exhibited larger deviation in the former.

The other significant flexible region movement is in loop L3 which, in concert with linker region, assists in accommodating the peptide at SBP. The relative reorientation of these loops along with catalytic triad residues seems to be assisting formation of a more open structure near the active site. However, loop L2 that harbors the specificity pocket remains mostly unchanged suggesting presence of a well formed binding pocket in the unbound form whose accessibility is limited compared to the substrate bound form. In context with trimeric HtrA2, more open conformation might be significant as it enhances the accessibility of the substrate and thereby might contribute positively toward the rate of enzyme catalysis.

4.2.4 Influence of SBP on HtrA2 Activity and Role of PDZ Domain

To determine whether critical SBP residues (N216, S219, E292 and E296) are important for mediating allosteric propagation in HtrA2, site directed mutagenesis to alanine were done. Mutation of a conserved YIGV residue (G230A) was also done to understand the role of canonical YIGV groove in this complex signal propagation pathway. Moreover, since the protein is found to be active in its trimeric form (*64*) and also that SBP encompasses a major part of PDZ, we used trimeric and monomeric HtrA2 variants, N-SPD and F16D respectively to understand the role of PDZ in intra and inter-molecular cross-talk.

To negate the role of overall conformational changes if any due to these mutations, MDS and secondary structural analyses were done on the mutant proteins. Similar active site

conformations were observed in both the wild type and mutants. Moreover, the overall secondary structure and thermal stability remained unperturbed due to the mutations.

Enzymology studies with different SBP mutants were done using β-casein, a well-established generic substrate of serine proteases (*81*). β-casein has a putative SBP binding site (GPFPIIV) which has been found to interact with the similar residues at SBP by our docking studies (Table 4.2) and hence expected to mimic the allosteric modulation mediated by SBP binding if any.

The kinetic parameters for wild type, N-SPD domain, F16D and other mutants were determined using fluorescent β-casein (Figure 4.6). The catalytic efficiency (kcat/Km) for the double mutant N216A/ S219A and single mutant E292A showed, 2.4 fold decrease in enzyme activity as compared to wild type whereas enzymatic parameters remained mostly unchanged for E296A. Km values for the mutants were not significantly higher compared to the wild type, suggesting that the specificity pocket might be mostly intact with some subtle alterations. However, there was a marked decrease in *Vmax* and in substrate turnover (kcat) rates for N216A/ S219A and E292A suggesting presence of a malformed oxyanion hole in the SBP mutants.

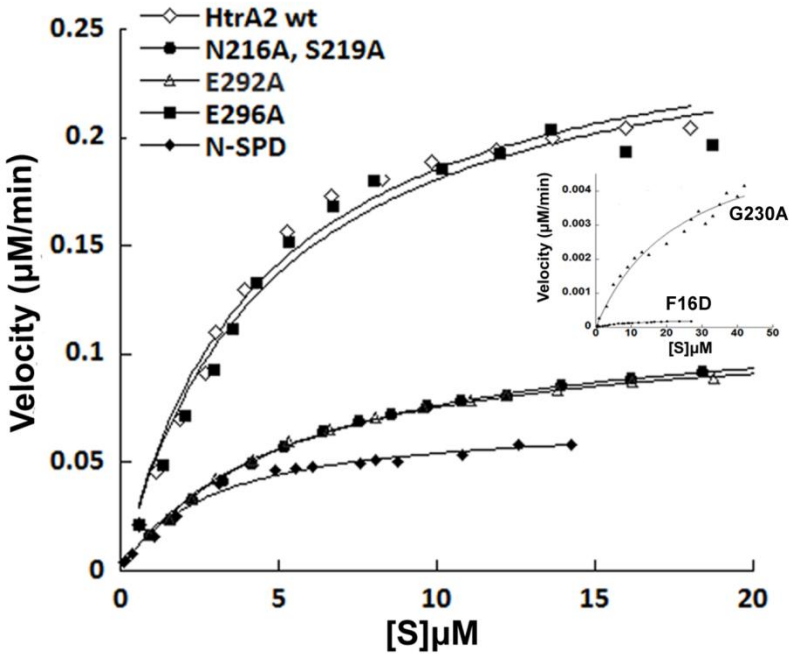

Figure 4.6. Steady state kinetic parameters of HtrA2. Graph representing relative activity of wild type HtrA2 and its mutants and variants with FITC labelled β-casein as the substrate. The graph for two mutants (F16D and G230A) is shown in inset.

These results demonstrate that N216/ S219 and E292 of SBP are important for mediating allosteric activation of HtrA2 upon activator binding. This is strengthened by the observation that SBP mutants did not interact with the activating peptides as seen by isothermal calorimetric studies shown in Figure 4.7. In addition, the ligplot of the peptide showing the detailed interaction with HtrA2 is also depicted in Figure 2.

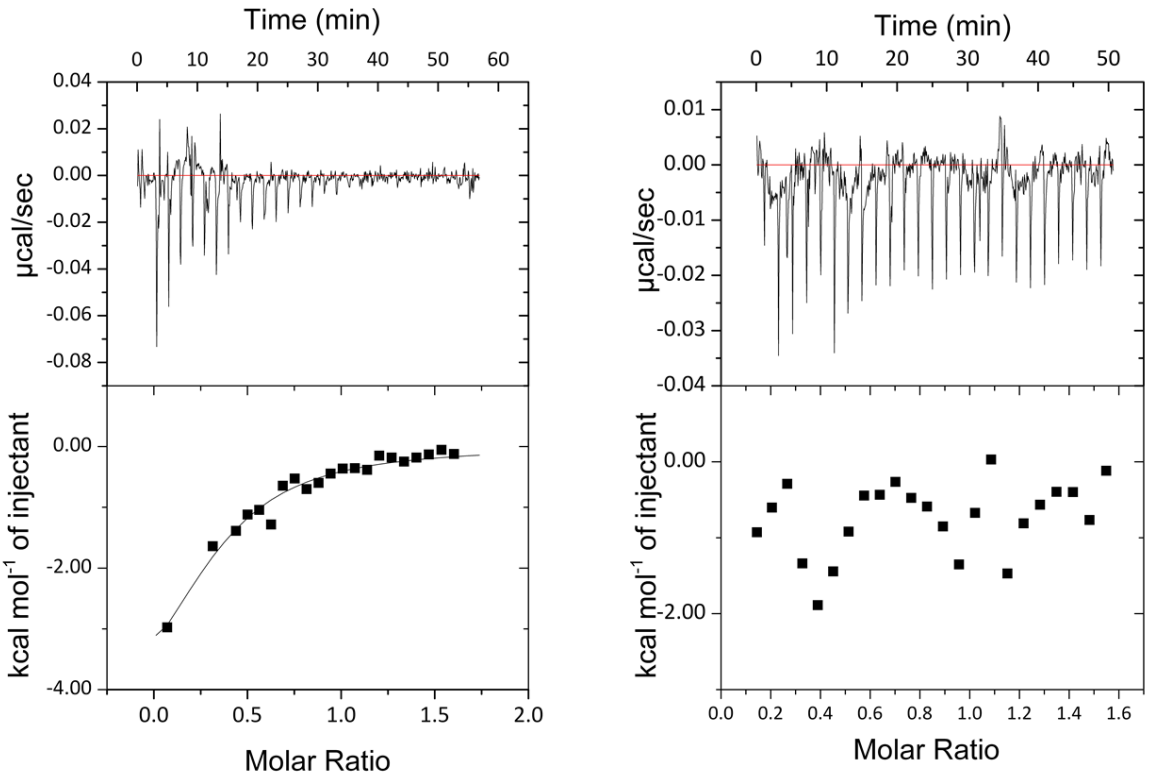

Figure 4.7. ITC studies for activating peptide with HtrA2 and the SBP double mutant. The peptide used was 13mer SEHRRHFPNCFFV, which has similar consensus sequence as defined for PDZ peptide groove binding substrate. The peptide was better in terms of solubility as compared to other activating peptides and binding studies were done using Isothermal titration calorimetry. The titrations were carried out using Micro Cal ITC200 (GE Healthcare) with the calorimetry cell containing 200 µL of wild type or N216A/S219A mutant HtrA2 in 20 mM Na2HPO4/NaH2PO4 buffer, 100 mM NaCl, pH 7.8. The concentration of protein was in range from 20 to 50 mM and was titrated with 1.5 ml injections of a solution containing 0.4 mM activator peptide reconstituted in the same buffer. To correct the effect of heat of dilution, a blank injection was made under identical conditions. All experiments were performed at 25 °C and the data was analyzed

using the manufacture provided MicroCal software with the integrated heat peaks fitted to a one site-binding model. Simulated ITC raw data for the protein with the activating peptide is represented in the upper panel and the integrated data in the lower panel. The dissociation constant was calculated to be 7.5 μM for wild type (left panel) and no significant heat change was observed for the SBP double mutant (right panel).

In our *in silico* studies, YIGV has been found to be a part of the greater SBP mesh (Table 4.1) and since docking with small molecular fragments (~ 35–100 Da) showed direct binding with YIGV residues (Table 4.2), we wanted to understand the effect of YIGV mutation on HtrA2 activity as well. Enzymology studies with G230A demonstrated increase in Km value compared to the wild type highlighting the involvement of YIGV in this intricate allosteric mechanism. Protein turnover rate was also much lower in G230A as compared to the wild type reiterating the importance of oxyanion hole formation upon activator binding at SBP.

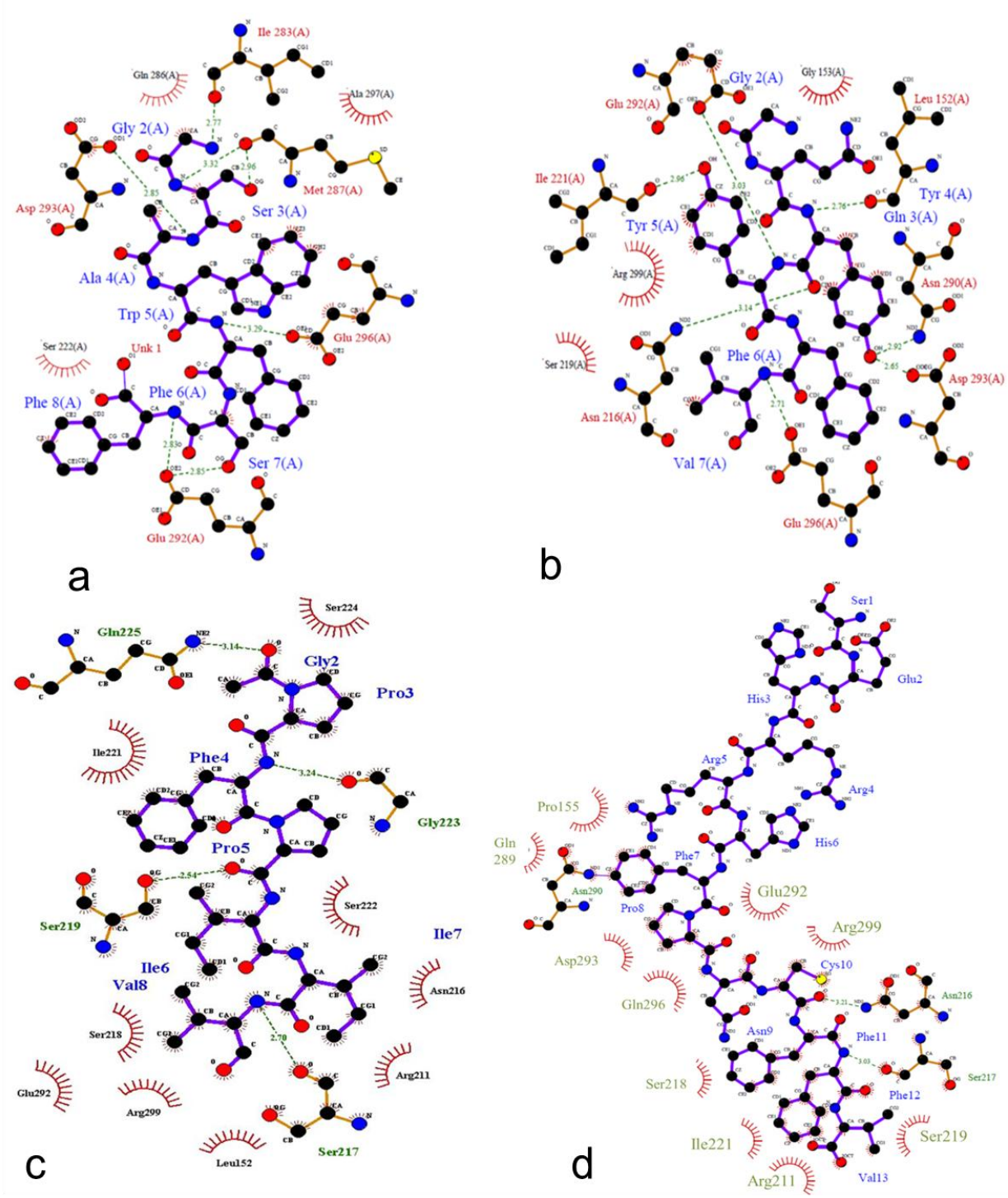

Figure 4.8. Interaction of peptides with HtrA2. a. Ligplot for GSAWFSF with HtrA2 which represents residues involved and the nature of interactions. b. Ligplot for

GQYYFV interaction pattern with HtrA2. c. Ligplot for GPFPIIV with HtrA2 which represents residues involved and the nature of interactions. d. Ligplot for SEHRRHFPNCFFV peptide with HtrA2 which represents residues involved and the nature of interactions. The residues of peptides and HtrA2 involved in interaction are shown in blue and red respectively.

Thus, inaccessibility of the canonical PDZ binding pocket YIGV, in the trimeric protease structure might have adjured presence of exposed SBP which is dynamically coupled to YIGV groove for efficient allosteric signal propagation to the distal active site. Direct binding of small molecules at YIGV supports this hypothesis as they could be accommodated in the classical binding groove without requirement of any initial conformational change as it might be with the larger peptide activators.

Interestingly, although catalytic efficiency for N-SPD has been found to be 3.4 fold less as compared to the wildtype, its Km value suggests slight increase in substrate affinity for the enzyme (Table 4.6). This increase in substrate affinity might be due to absence of PDZ surrounding the active site region resulting in greater substrate accessibility. However in N-SPD, kcat was found to be 5 fold less than that of wild type highlighting the role of PDZ in initiating conformational changes near the active site pocket as well as in the oxyanion hole so as to increase overall enzyme stability. However, in the full length monomeric mutant of HtrA2

(F16D), there is a two fold increase in Km with significant decrease in turnover rate and hence catalytic efficiency (Table 4.6) which emphasizes importance of intermolecular crosstalk between PDZ and protease domains in trimeric HtrA2 structure.

HtrA2 Proteins	K_m (μM)	V_{max} (M/s)	k_{cat} (1/s)	k_{cat}/K_m (1/M.s)
Wild type	4.59	4.083×10^{-9}	0.02041	4.452×10^{3}
N216A, S219A	5.43	1.937×10^{-9}	0.00968	1.788×10^{3}
E292A	5.15	1.903×10^{-9}	0.00951	1.849×10^{3}
E296A	4.68	3.734×10^{-9}	0.01868	3.995×10^{3}
N-SPD	3.02	0.7851×10^{-9}	0.0039	1.29×10^{3}
F16D	9.3	4.08×10^{-12}	0.000025	0.0026×10^{3}
G230A	9.32	1.03×10^{-9}	0.0051	0.54×10^{3}

Table 4.6 Steady state kinetic parameters for HtrA2 wild type, variants and mutants with β-casein as the substrate.

The importance of intermolecular interaction between PDZ* and SPD has also been manifested in our MD studies where structural analyses show binding of peptide activator (GQYYFV) at the SBP alters PDZ orientation and brings α5 helix of PDZ from one subunit in close proximity to the protease domain of the adjacent subunit. The helix moves towards LD loop of the protease domain, thereby shifting the orientation of the phenyl ring of F170 which is a part of oxyanion hole towards H65 of the catalytic triad (Figure 4.9a) so as to accommodate the loop.

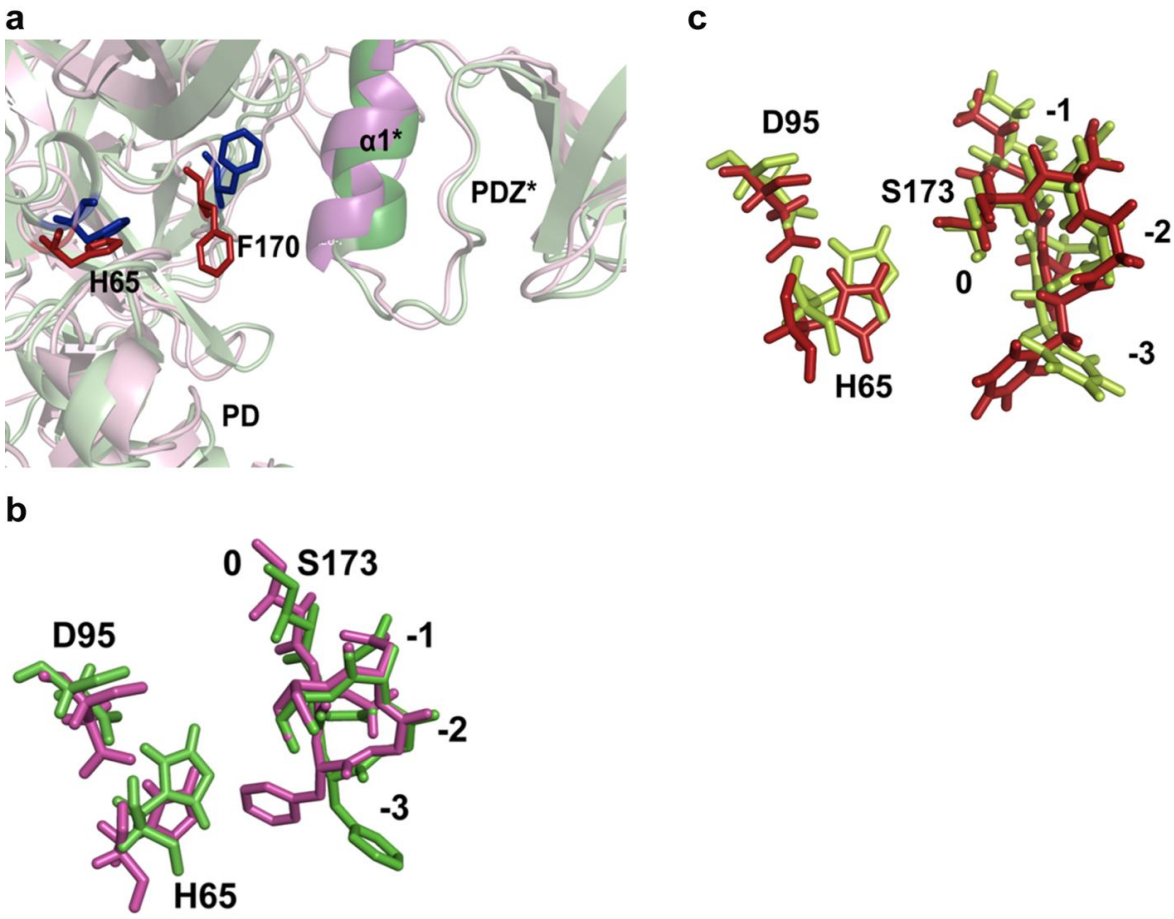

Figure 4.9. Structural changes at the oxyanion hole and YIGV groove upon peptide binding. a. Overlay of the oxyanion hole and catalytic triad residues represented as sticks for peptide GQYYFV bound (magenta) and unbound (green) structures. PD denotes serine protease domain of HtrA2. b. Overlay of the oxyanion hole and catalytic triad residues represented as sticks for peptide GSAWFSF bound (red) and unbound (limon green) structures. c. Role of PDZ in the formation of proper active site formation. The structural superposition of GQYYFV bound (pink) and unbound (green) structures shows α5 helix of PDZ of one subunit moves towards the LD loop and oxyanion hole of the adjacent subunit. The positions of the residues in the oxyanion hole are denoted as 0, -1,-2 and -3. These rearrangements result in a more stable and catalytically competent HtrA2

formation with a proper oxyanion hole. Thus the full length trimeric HtrA2 is more active than trimeric N-SPD, where the activation pocket is not stable in absence of PDZ.

4.3 Discussion

Our aim was to understand the structural dynamics that regulates activation and specificity of HtrA2. This multidomain trimeric protease has unique proapoptotic properties as it is associated with both caspase-dependent and independent cell death pathways through its serine protease activity.

Association of HtrA2 with cancer and neurodegenerative disorders makes it a promising therapeutic target. For example, overexpression of HtrA2 substrates such as IAPs and the Wilms's tumor suppressor protein WT1 in several cancers suggests modulation of HtrA2 protease activity can effectively regulate their relative levels in the cells (*82-85*). Out of several approaches that can be used to regulate HtrA2 activity, allosteric modulation is one of the simplest and most efficient ways. However, modulating HtrA2 functions with desired characteristics for disease intervention will require a detailed understanding of its mode of activation and the underlying conformational plasticity that controls it. Peptide design using site complementarity followed by MDS of the docked peptide-macromolecular complex is an extremely useful tool to study subtle conformational changes and protein dynamics. HtrA2 has a complex network of flexible loops surrounding the active site pocket and a linker at the PDZ protease interface whose relative orientations and crosstalk with different domains might be critical in defining HtrA2 functions. With partially missing loops and the flexible linker region, the solved structure of HtrA2 (*64*) could not fully explain the dynamics and allostery that regulate its

activity and specificity. Here, with an *in silico* and biochemical approach, we have shown that like few other HtrA family proteins, allosteric propagation does regulate HtrA2 activity.

In this study, peptide binding to SBP showed conformational changes in the distal flexible regions of HtrA2 such as the PDZ-protease interface, loops L1, LD and LA that rearrange to form a more catalytically efficient active site thus establishing the role of SBP as an allosteric site in HtrA2. A close look at and around the active site pocket shows that in the bound form, the N atom of Gly (22 position) faces the oxyanion hole to form an H-bond whereas in the unbound form it flips in the opposite direction to form a malformed oxyanion hole (*72, 86*). Moreover, keeping in trend with other HtrA proteases, the phenylalanine ring of 23 position moves closer to the imidazole ring of His 65 while in the unbound form, it moves outward as observed from decrease in catalytic efficiency in SBP mutants. This observation suggests interaction of substrate protein with SBP brings about rearrangement around the active site of the enzyme by positively influencing its activity thus behaving as an allosteric regulator.

The SBP mutants (N216A/S219A and E292A) show apparent decrease in Vmax without significantly altering the apparent Km (with L2 specificity pocket mostly unaltered) and hence follow the 'V system' of allosteric modulation (*87*). In this system, both the relaxed (R) and the tensed (T) states bind the substrate at the active site with similar affinity while the peptide (activator) at SBP binds the R and T states with different affinity. This differential affinity of the peptide towards SBP along with R state stabilization shifts the equilibrium towards R state thus positively influencing its turnover rate and hence catalytic efficiency which has been observed in case of HtrA2.

In N-SPD, where the PDZ domain is absent, apparent decrease in Km can be attributed to greater accessibility of the substrate to the active site. However, since the change in binding affinity is not large, the specificity pocket might be mostly unaltered compared to the wild type which is confirmed through our MD studies where the loop L2 remains mostly unaltered. Interestingly, kcat value in N-SPD has been found to decrease significantly which is suggestive of either a malformed oxyanion hole and/or decrease in overall protein stability which might be due to absence of supporting PDZ domain. However, similar studies with F16D (monomeric full length HtrA2 mutant) also show significant decrease in turnover rate and catalytic efficiency which accentuates the importance of intermolecular and not intramolecular PDZ-protease crosstalk in trimeric HtrA2. Our MDS supports this observation by demonstrating that in the peptide bound form of HtrA2, α5* of PDZ* moves towards LD loop of protease domain of adjacent subunit thus pushing phenyl ring of F170 of the oxyanion hole towards H65 of the catalytic triad (Figure 4.9a). This reorientation in the oxyanion hole makes the protease poised for catalysis as seen in other HtrA family members as well (*72*) thus significantly enhancing the turnover rate. Therefore, intermolecular crosstalk establishes the requirement of complex trimeric architecture of the protease.

The GLGF motif (YIGV in HtrA2) is the canonical peptide binding site (*62*) in PDZ domains. However, in HtrA2, it is deeply embedded within a hydrophobic groove where the residues are intertwined with each other through several intramolecular interactions making the site highly inaccessible to the binding of peptide (*64*). Thus, peptide binding to YIGV is only possible upon certain structural rearrangements at that site. Given the property of PDZ domains of having multiple docking sites and the fact that HtrA2

requires huge conformational changes for proper active site formation, we hypothesized presence of a relatively exposed pocket where peptide binding occurs prior to interaction with the buried YIGV groove. In our studies, we have found a novel surface exposed region (SBP) around PDZ domain which is easily accessible to the peptide. With an aim at understanding the allosteric mechanism in HtrA2 and whether the binding site is structurally conserved, we did a side-by-side comparison with the peptide-bound PDZ structure of its bacterial counterpart DegS that is known to exhibit allostery (*88*). The structural overlay of peptide bound forms of these two proteins show striking structural similarity in the regions of binding (Figure 4.10a) with the GLGF groove (YIGV in HtrA2 and YIGI in DegS) oriented differently. Since the YIGV motif is buried in HtrA2 structure, its inaccessibility might be the reason for the peptide to initially bind to another relatively accessible region with similar hydrophobic milieu. However, in DegS, the YIGI groove is already exposed to accommodate the peptide easily and hence this kind of initial interaction is not required.

Our MDS studies show that peptide binding at SBP leads to subtle structural changes in the region adjoining YIGV leading to opening up of the pocket. The last β strand of PDZ domain which lies on one side of YIGV groove moves away from it. The YIGV and the loop spanning residues 67–73 move away from each other while the loop comprising residues 263–277 of the b-a-b motif also drifts at an angle away from the YIGV making it more solvent exposed (Figure 4.10b). Therefore, upon SBP binding, the relative movements of the loops in vicinity of the hydrophobic YIGV pocket might confer it with the kind of exposure that is required for interaction with peptides. Our MDS studies show that peptide binding at SBP leads to subtle structural changes in the region adjoining

YIGV leading to opening up of the pocket. The last β strand of PDZ domain which lies on one side of YIGV groove moves away from it. The YIGV and the loop spanning residues 67–73 move away from each other while the loop comprising residues 263–277 of the b-a-b motif also drifts at an angle away from the YIGV making it more solvent exposed (Figure 4.10b). Therefore, upon SBP binding, the relative movements of the loops in vicinity of the hydrophobic YIGV pocket might confer it with the kind of exposure that is required for interaction with peptides.

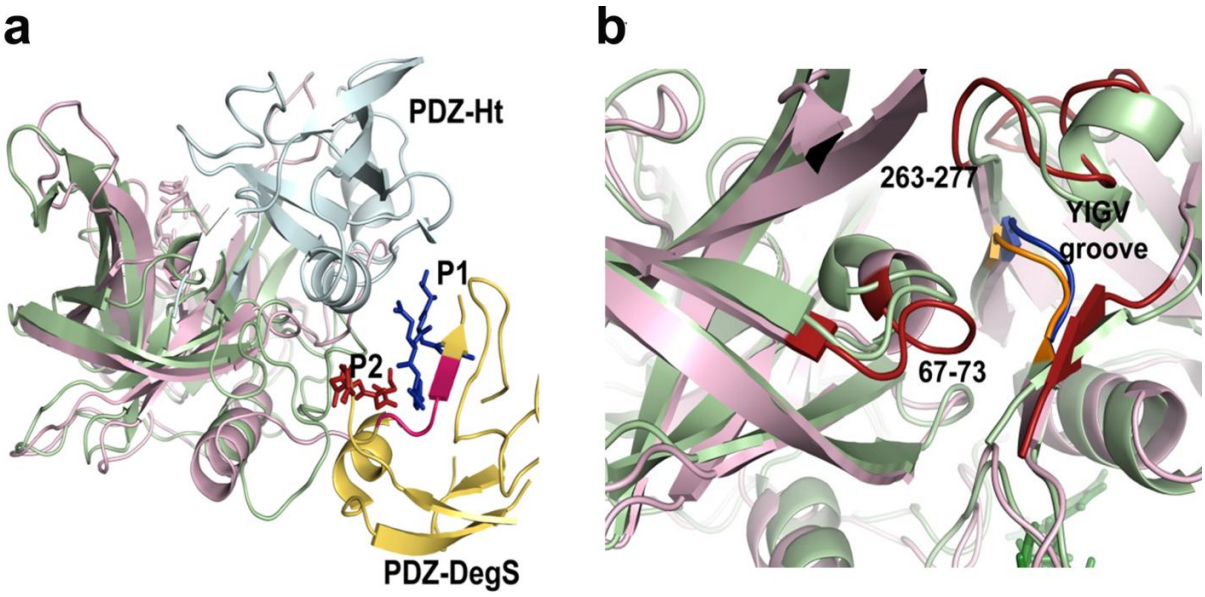

Figure 4.10. Structural comparison of PDZ domain orientation. a. Structural alignment of E. coli DegS (PDB ID: 1SOZ) and the peptide bound HtrA2 showing PDZ domains for both the proteins (represented in blue and yellow respectively) are oriented differently but the peptides, P1 (blue) and P2 (pink) represented as sticks for the respective proteins seem to bind to a structurally similar region. The GLGF substrate binding motif is exposed for DegS while buried for HtrA2 as shown in pink and blue

respectively. b. Alignment of the peptide bound (pink) and unbound (green) structures at the region around the YIGV groove shows outward movement of the loops spanning residues 67–73 and 263–277 shown in red for the bound structures which leads to opening up of the YIGV groove.

These observations along with our enzymology studies with SBP and YIGV mutants, led to defining a model (Figure 4.11) for allosteric propagation in HtrA2. The model suggests that initial binding of the peptide activator at SBP leads to structural fluctuations which result in subtle rearrangement at and around the YIGV groove (a part of greater SBP mesh as identified by Sitemap) thus exposing it. Opening up of the deeply embedded YIGV pocket makes it accessible to the substrate molecule which consequently leads to allosteric signal propagation at the active site in the serine protease domain.

This alternative non-canonical PDZ binding site though novel in HtrA family of proteins, is not unprecedented in literature. It has been observed that PDZ7 of the scaffold protein Glutamate receptor interacting protein 1 (GRIP1) has an alternative exposed hydrophobic pocket that binds its substrate GRASP-1 since the canonical binding site is deeply embedded within the protein (*89*). Overlay of the PDZ from HtrA2 and PDZ7 of GRIP1 show striking structural similarity including the classical peptide binding groove and the novel non-canonical pocket (Figure 4.12).

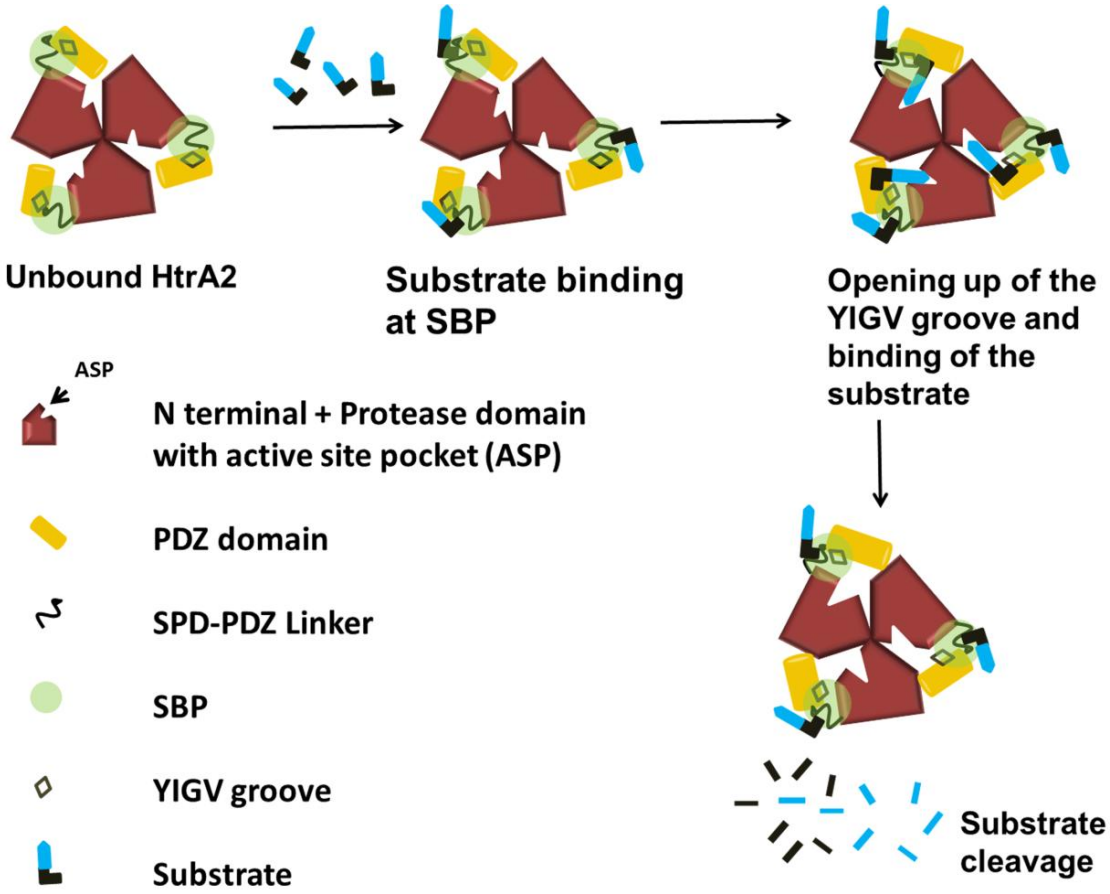

Figure 4.11. Allosteric model for HtrA2 protease activity. The substrate protein binds to relatively exposed part of SBP due to inaccessibility of the YIGV groove which triggers opening up of the PDZ domain. This reorientation makes the YIGV groove accessible for substrate interaction and the PDZ of a subunit moves closer to the protease domain of the adjacent subunit leading to formation of a proper active site and oxyanion hole. This complex allosteric signal propagation leads to subsequent substrate binding and catalysis at the active site pocket. Thus structural perturbations at these two distant sites (SBP and catalytic pocket) might be dynamically coupled to the canonical peptide binding groove through a complex allosteric mechanism.

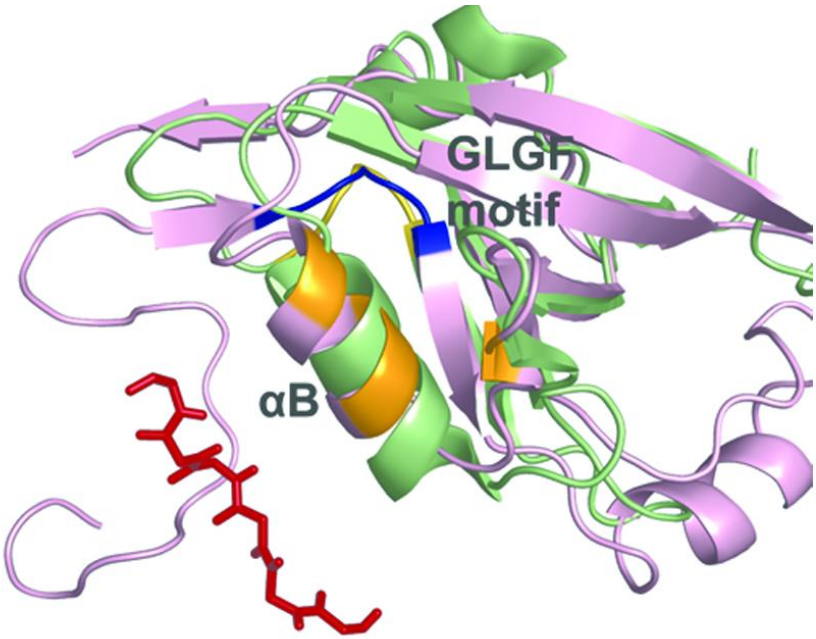

Figure 4.12 Comparison of SBP and allosteric pocket of GRIP-1 protein. Structural overlay of the protein GRIP- 1(green) bearing PDB ID 1M5Z and GQYYFV bound HtrA2 (pink) shows striking resemblance of the orientation of buried GLGF motif shown in yellow and blue respectively. The α helix denoted as αB (green) for GRIP-1, known to be involved in formation of allosteric pocket overlays very well with the one involved in SBP formation (orange) in GQYYFV (red sticks) - HtrA2 complex.

Thus, in these two proteins, perturbations at the alternative distal binding sites might be coupled dynamically to the classical binding groove by a complex mechanism that includes fast (ps–ns) timescale dynamics which consequently leads to allosteric signal propagation to the active site. In the recent past, allosteric modulators have evolved into important drug targets due to several advantages they have over orthosteric ligands that include more diversity, less toxicity and absolute subtype selectivity (*90, 91*). Therefore,

designing suitable SBP binding peptides or peptidomimetics of HtrA2 might be an excellent approach to modulate HtrA2 functions for devising therapeutic strategies against various diseases it is associated with.

Chapter 5

Structural and functional characterization of HtrA2-HAX1 interaction

5.1 Introduction

Despite several reports establishing that the HtrA-HAX1 interplay is detrimental for the fate of the cell, the structural mode of interaction and the mechanism of its functional manifestation is largely unknown. It has been reported that HAX1 suppresses apoptosis in lymphocytes and neurons. This activity requires the interaction of HAX1 with the mitochondrial proteases PARL (presenilins-associated, rhomboid-like) and HtrA2. These interactions allow HAX1 to present HtrA2 to PARL, and thereby facilitate the processing of HtrA2 to an active protease localized in the mitochondrial intermembrane space (*8*). But a recent study challenges these conclusions of Chao et al. by showing that firstly, HAX1 is not a Bcl-2-family-related protein because it does not contain bonafide BH modules, secondly, *in vivo*, the activity of HAX1 cannot be mechanistically coupled to PARL because the two proteins are confined in different cellular compartments thus suggesting their interaction *in vitro* is an artifact (*46*). Therefore, to get a clearer picture of the mechanism of interaction between HtrA2 with HAX1, this study also aimed to study this in presence and absence of PARL.

HtrA2's mechanism of caspase activation is attributed to its IAP-inhibiting activity. Recombinant Omi/HtrA2 was observed to catalytically cleave IAPs and to inactivate XIAP *in vitro*, suggesting that the protease activity of Omi/HtrA2 might be responsible for its IAP-inhibiting activity. Extra-mitochondrial expression of Omi/HtrA2 indirectly induced permeabilization of the outer mitochondrial membrane and subsequent Cyt c-dependent caspase activation in HeLa cells. These results indicate that protease activity of Omi/HtrA2 promotes caspase activation through multiple pathways (*6*). From our studies it has been proven that HAX1 is an activator of HtrA2. On the basis of this

finding it has been hypothesized that in the presence of HAX1, the HtrA2-driven cleavage of XIAP would be augmented as in the case of another mitochondrial protein GRIM 19 (gene associated with retinoic-interferon-induced mortality 19) (*7*).

Aim I: Structural analysis of HAX1 and HtrA2 (X-ray crystallography or Biophysical techniques)

HAX1 is a unique anti-apoptotic protein which belongs to HAX1 family. The other proteins in this family are its counterparts in murine and other mammals. Hence this protein shares very low identity or similarity with any known proteins so much so that even the domains for this protein could not be defined. Moreover, no structural or biophysical data are available on this protein. The pro-apoptotic partner HtrA2 on the other hand has been structurally well defined and the structure of the inactive protein has been solved (*64*). Therefore, with the intent to understand HAX1 structure and its interaction with HtrA2 we carried out the following studies.

5.2 Results

5.2.1 *In silico* model generation of HAX1 protein

HAX1 is a unique anti-apoptotic protein, which belongs to the HAX1 family and this protein shares very low query coverage, identity or similarity with the other known proteins as observed from the BLAST search performed (Figure 5.1). Moreover, no structural or biophysical data is available on this protein. Considering the anti-apoptotic nature of the protein, domain comparisons with Bcl-2 family members were performed to identify the Bcl-2 homology (BH) domains, but they were absent. *In silico* models of

HAX1 were thus generated using different servers namely I-TASSER, QUARK, and Robetta. Among the generated models, the best ones were chosen after validation by Procheck, what check, Prosa, verify 3D and SAVES analysis. The models which showed the best scores for all these parameters and all the residues in allowed region in the Ramachandran plot were the Robetta server generated models (Figure 5.2).

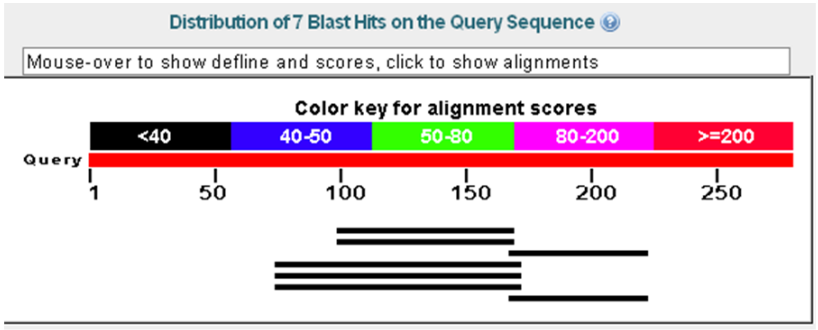

Sequences producing significant alignments:

Accession	Description	Max score	Total score	Query coverage	E value
2EEX_A	Chain A, Crystal Structure Of Cel44a, Gh Family 44 Endoglucanase Fr	29.3	29.3	25%	1.9
2E0P_A	Chain A, The Crystal Structure Of Cel44a >pdb|2E4T|A Chain A, Crys	29.3	29.3	25%	1.9
2PQT_A	Chain A, Human N-Acetyltransferase 1	28.9	28.9	19%	2.9
1B80_A	Chain A, Rec. Lignin Peroxidase H8 Oxidatively Processed >pdb|1B80|	27.3	27.3	35%	7.7
1B82_A	Chain A, Pristine Recomb. Lignin Peroxidase H8 >pdb|1B82|B Chain B,	27.3	27.3	35%	7.8
1B85_A	Chain A, Lignin Peroxidase >pdb|1B85|B Chain B, Lignin Peroxidase	27.3	27.3	35%	7.9
2IJA_A	Chain A, Human N-Acetyltransferase 1 F125s Mutant	26.9	26.9	19%	8.9

Figure 5.1: BLAST analysis for HAX1. It was observed that HAX1 shares query coverage of 25% with the known proteins.

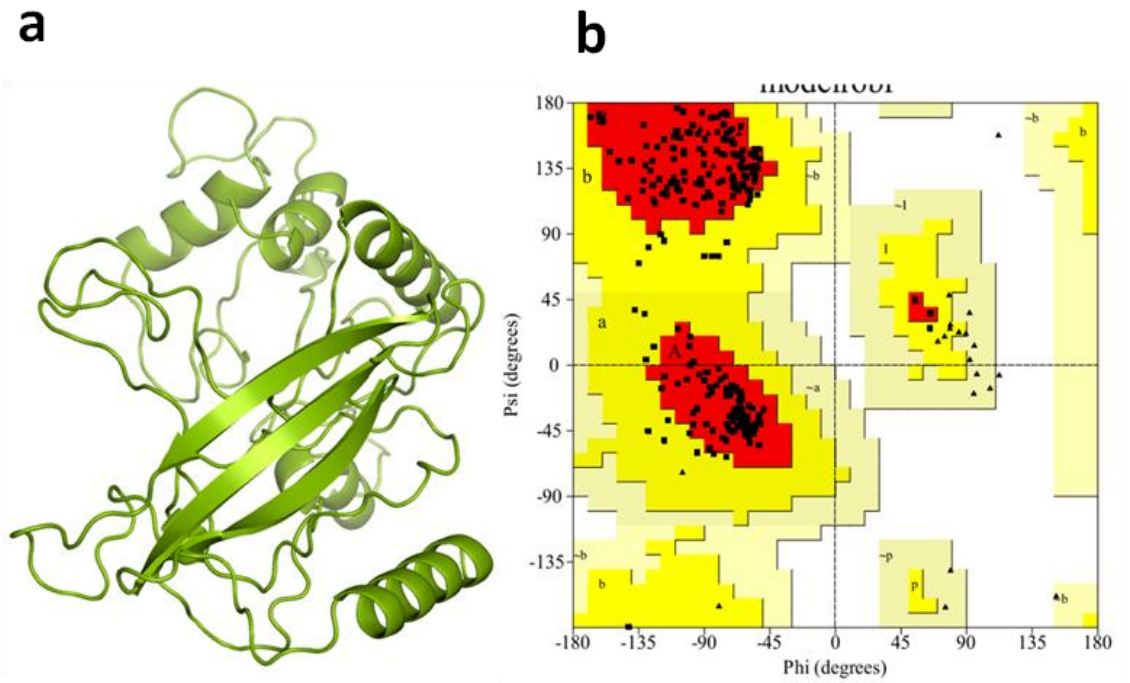

Figure 5.2 Model generated by Robetta server. a. The model with the best score by Robetta server. b. The Ramachandran plot for this Robetta model generated shows no residues in the disallowed region.

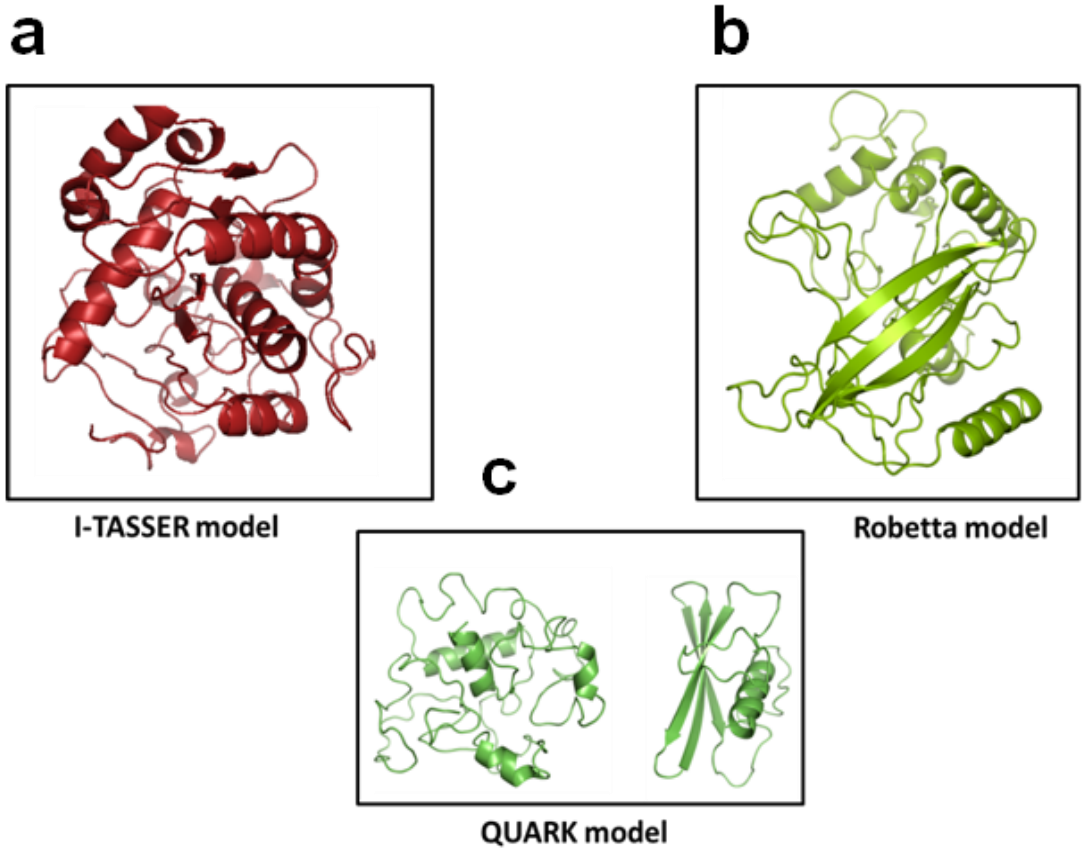

Figure 5.3: *In silico* models for HAX1. Representative models of HAX1 generated using a. I-TASSER b. Robetta and c. Quark servers display slight dissimilarity.

5.2.2 Cloning and purification of HAX1 and its biophysical characterization

HAX1 gene was cloned in several pET and pRSET-a vectors for heterologous expression and purification. HAX1 gene was cloned in pRSETA vector using BamHI and EcoRI sites. The expression studies showed no expression for HAX1 in pRSETA and therefore subcloning was done in pET-28a, pMALc5E and pGEX2T vector. pET-28a showed no expression whereas pMALc5E showed robust expression. The HAX1 protein was thereby purified as a MBP fusion protein.

Purified HAX1 protein was obtained by affinity purification followed by size exclusion chromatography (SEC). Separation of the MBP tag was carried out by TEV cleavage. The cleaved product was subsequently subjected to size exclusion chromatography (SEC) by Superdex 200 column. The pure fractions obtained were used for all biophysical analysis. The secondary and tertiary structure of HAX1 was determined by Far UV Circular Dichroism (CD) spectroscopy and fluorescence spectroscopy respectively. Overall, these studies showed that protein is well folded with proper secondary and tertiary structural properties. The protein was found to be comprised of ~35 % α helices and 19% β sheet. Thermal stability of the protein was also studied by thermal denaturation using Fluorescence spectroscopy and the melting temperature (Tm) was found to be about 60 ºC.

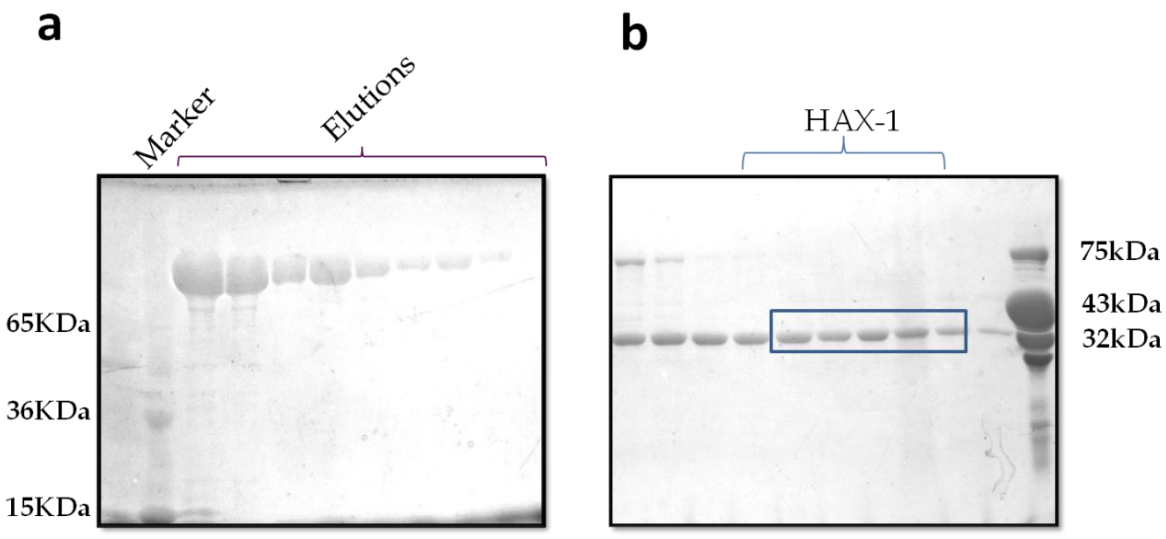

Figure 5.4. SDS gels representing the two step purification of HAX1. SDS-PAGE gels representing the a. purification of MBP-HAX1 using Amylose resin. b. purification of HAX1 by gel filtration following TEV cleavage.

Sequence data:

HCLS1-associated protein X-1 OS=Homo sapiens GN=HAX1 PE=1 SV=2 HAX1_HUMAN

Intensity Coverage:	58.9 % (93622 cnts)	Sequence Coverage MS:	44.4%
Sequence Coverage MS/MS:	0.0%	pI (isoelectric point):	4.6

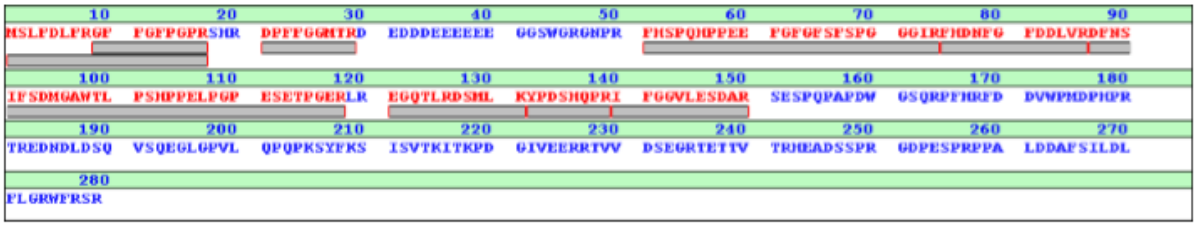

Display Parameter:

Sequence Name:	HCLS1-associated protein X-1 OS=Homo sapiens GN=HAX1 PE=1 SV=2 HAX1_HUMAN		
MH+ (mono):	1.0078	MH+ (avg):	1.0079
Threshold (a.i.):	0.0000	Tolerance (Da):	0.5000
Number of Peaks:	45		

PeakList:

Peak	Mass	Intensity	Peak	Mass	Intensity	Peak	Mass	Intensity
1	804.2262	1506.4466	2	845.0396	343.6209	3	861.0233	457.6692
4	876.9974	377.1500	5	881.2099	222.5348	6	981.4508	20116.6417
7	999.4247	623.6551	8	1003.4251	264.9379	9	1027.4255	602.7431
10	1094.5166	111.0840	11	1163.5548	157.4370	12	1277.6656	218.6168
13	1309.5618	1094.8434	14	1310.0635	1503.0647	15	1460.6542	326.6492
16	1481.6292	4118.4553	17	1516.7514	4935.6597	18	1566.7592	5166.0958
19	1588.7481	601.8184	20	1759.6964	558.9889	21	1785.7578	7079.9994
22	1923.7618	325.3116	23	1993.8250	130.1428	24	2000.7897	72.8025
25	2006.8159	227.3492	26	2008.7351	74.6879	27	2023.8617	29375.8271
28	2039.8223	432.5578	29	2045.8264	193.3300	30	2049.8500	77.3774
31	2229.0041	478.3448	32	2269.0095	1931.4413	33	2326.0126	4724.6297
34	2348.0015	61.3393	35	2357.0823	644.8677	36	2591.3383	75.8709
37	2602.9987	762.5999	38	2610.0416	87.2808	39	2618.0862	67340.5026
40	2634.0706	221.5204	41	2640.0495	327.4621	42	2645.0745	54.5126
43	2675.0934	113.0210	44	2812.1510	658.8871	45	3497.3371	216.3632

Figure 5.5. Mascot analysis output for confirmation of protein identity. The identity of the protein HAX1 was confirmed by mass spectrometric studies on the in-gel digested peptides.

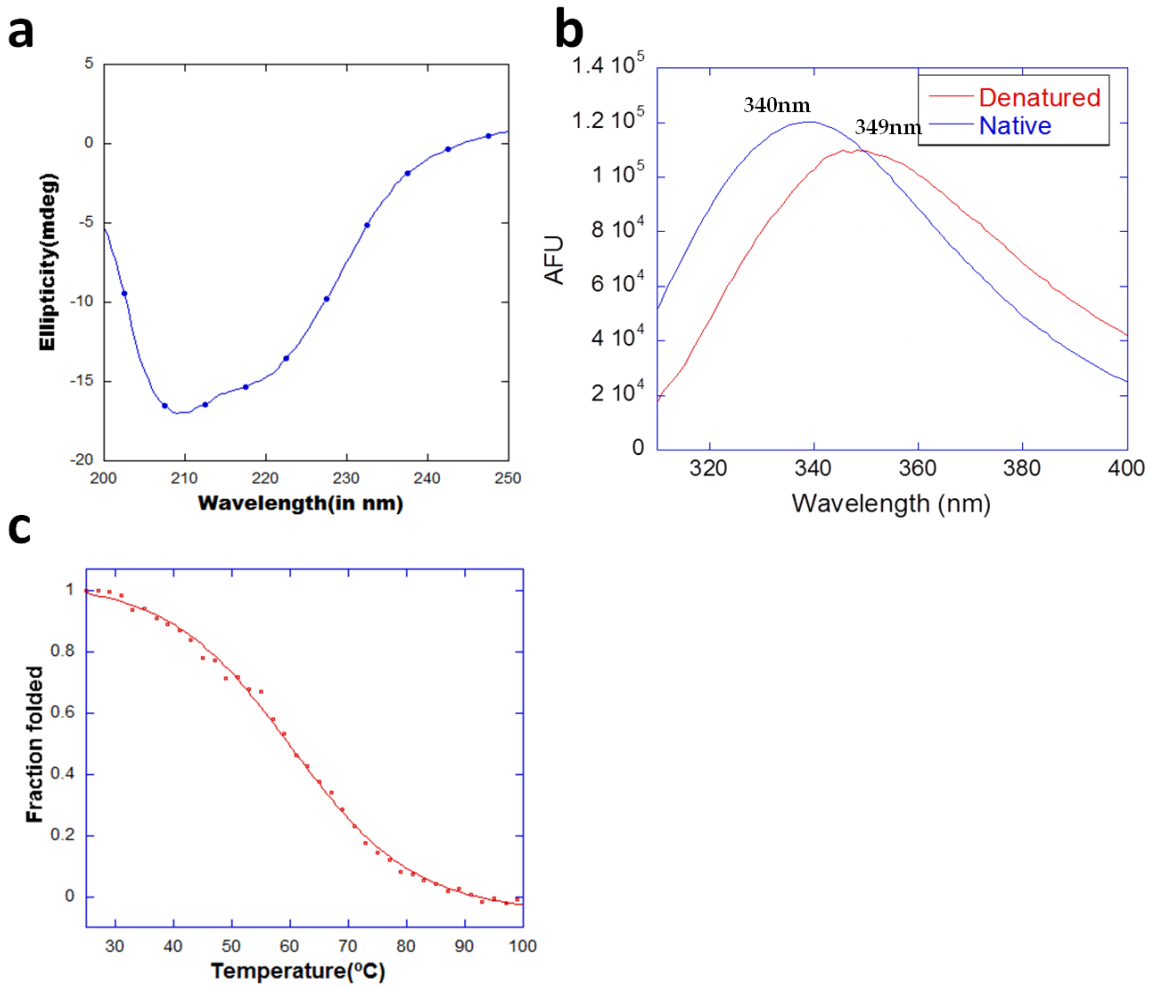

Figure 5.6. Biophysical characterization of HAX1. a. Representation of the CD analysis that shows HAX1 has a well-folded secondary structure with both α helix and β sheet characteristics. b. Fluorescence analysis showing HAX1 with a well folded tertiary structure with emission maxima at 340nm. c. The melting temperature (Tm) of HAX1 determined by Fluorescence spectroscopy was found to be ~ 60 °C.

5.3. Experimental validation of the protein model

5.3.1 Quenching studies for model validation

The 3D model of HAX1 was important to understand its overall structural arrangement and also carry out docking studies with HtrA2 so as to dissect the interacting interface and identify the residues required to mediate the interaction. Spectroscopic approach utilizing intrinsic fluorescence of the protein was used to validate the model where the five tryptophans in HAX1 were utilized as positional markers. Accessibility of fluorophores to water soluble quenchers can determine the fluorophore environment. HAX1 positional mutants were thus generated by site-directed mutagenesis to obtain exposed double mutant (W98A, W160A), exposed triple mutant (W98A, W160A, W173A), and buried double mutant (W44A, W275A).

Protein	Type
WT-HAX1	Wild Type
W98A,W160A	Exposed double mutant
W98A,W160A,W173A	Exposed triple mutant
W44A,W275A	Buried double mutant

Table 5.1 Combinations of tryptophan positional mutants in HAX1

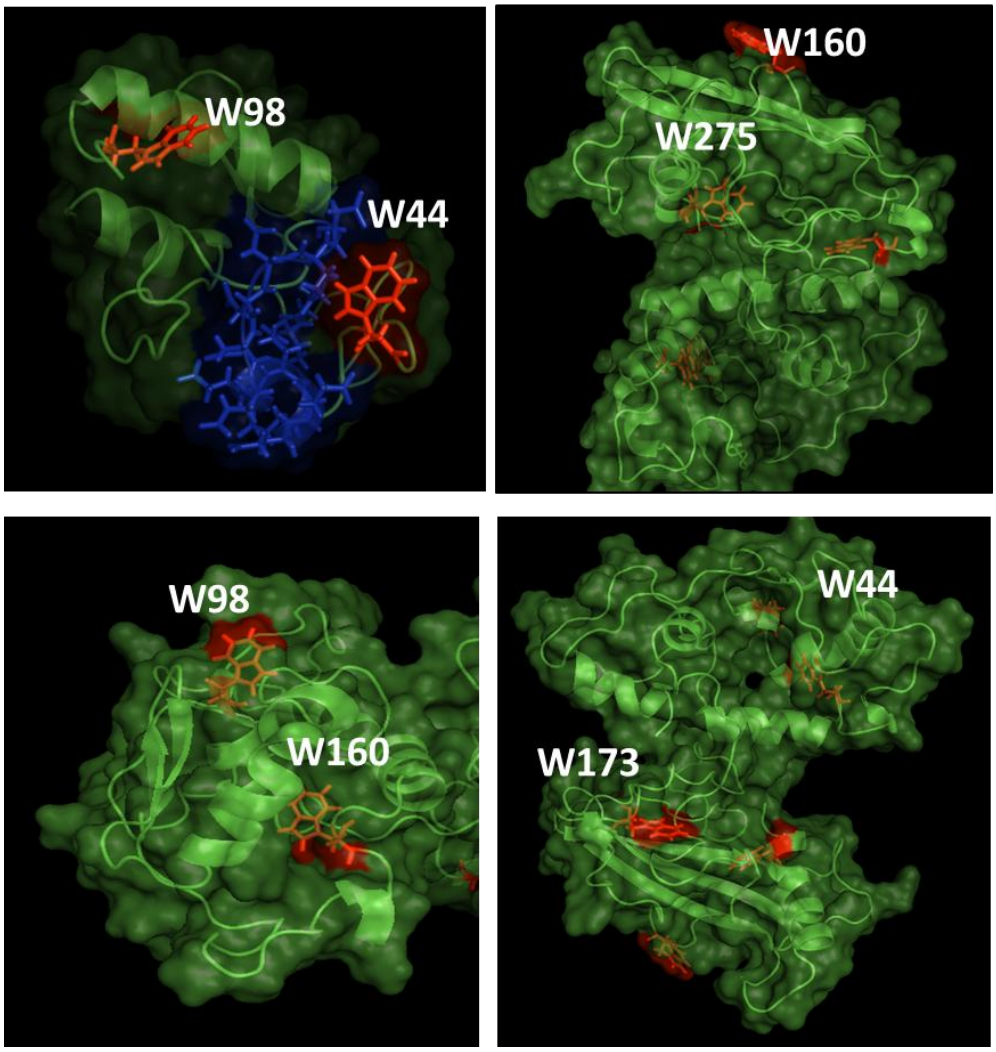

Figure 5.7 Cartoon representations of tryptophan positions in HAX1 model structure. The tryptophan residues are shown as red sticks and the relative solvent exposure of each of these can be observed. The residues shown as blue sticks around W44 indicate the acidic environment.

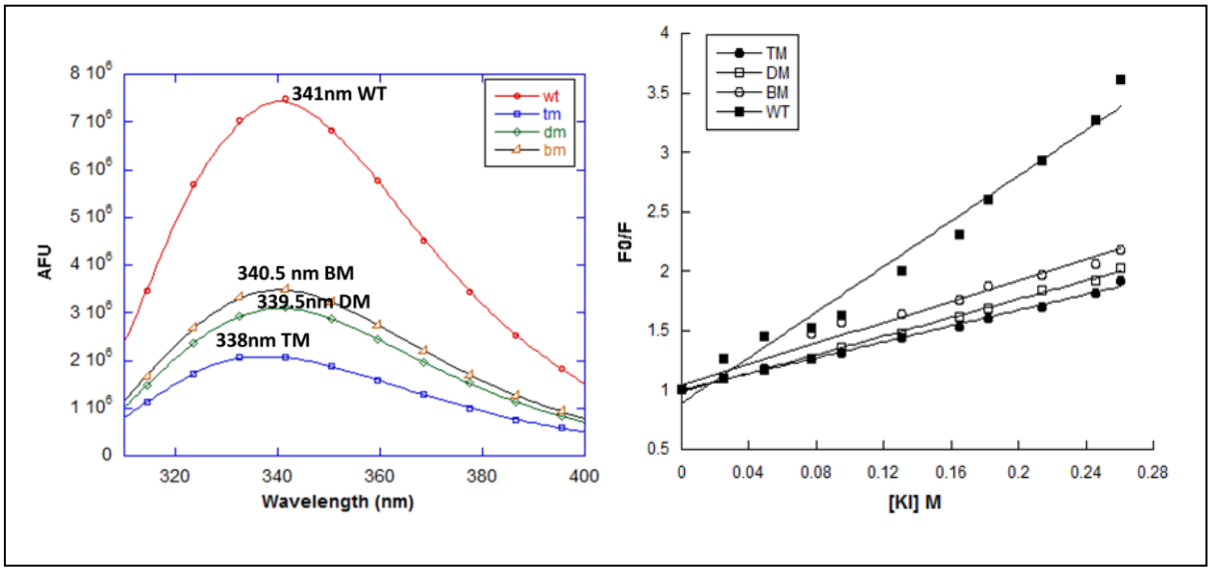

Figure 5.8. Graphical representation of the λ*max* and quenching analysis. a. The emission maxima for HAX1 and its tryptophan positional mutants clearly show a decrease in the emission maxima in the mutants compared to the wild type. b. The plots for KI quenching (F0/F against concentration of quencher) for WT-HAX1 and its tryptophan positional mutants are represented. for WT-HAX1 and its different mutants.

Site directed mutagenesis was used to carry out these substitution mutations. After generating a single mutation, it was subsequently used as a template to inculcate the second mutation. This strategy was followed to generate the combinations mentioned in Table 5.1. All the mutants of HAX1 were purified as described for the WT-HAX1 by amylose resin followed by SEC Superdex200 after tag cleavage. The Far UV CD analysis was carried out for all the mutants and they showed minimal secondary structural changes. Fluorescence emission maxima for each of the mutants with excitation at 295 nm were performed and the surface mutants showed blue shift as expected.

Accessibility of fluorophores to water soluble quenchers can determine the fluorophore environment. The accessibility of the tryptophans in WT HAX1 and its tryptophan mutants mentioned above was studied using negatively charged potassium iodide (KI) as quenchers. KI quenches surface tryptophans to relatively greater extent. The quenching results shown in Table 5.2 gave us a comprehensive idea of the Tryptophan positions which corroborate very well with that suggested by the Robetta model.

Protein	Position	K_{SV} for KI	Fractional accessibility
WT-HAX1	**WT**	**5.05**	**0.64**
W98A,W160A(DM)	**Exposed double mutant (DM)**	**3.81**	**0.47**
W98A,W160A,W173A(TM)	**Exposed triple mutant (TM)**	**3.23**	**0.31**
W44A,W275A(BM)	**Buried double mutant (BM)**	**4.57**	**0.57**

Table 5.2 Comparative representation of the quenching analysis for the tryptophan mutants and WT-HAX1

The decrease in the K_{SV} values were indicative of the removal of the surface tryptophans as in the case of DM and TM, on the other hand this decrease was not so prominent in the case of BM. This clearly shows that tryptophan residues in the combination are indeed their authentic positions as predicted by the modeled structure (Table 5.2).

5.3.2. Limited proteolysis and N-terminal sequencing

A second approach that was used to validate the 3D model was limited proteolysis where trypsin was used at very low concentration to cleave HAX1 (Figure 5.9).The resulting peptides were analyzed by N-terminal sequencing to determine the sites of cleavage with time, thus providing us useful information on the accessibility of arginine and lysine residues in the 3D structure of HAX1 (Figure 5.10). The first trypsin digestion was after the most exposed R139 residue followed by K205 leading to LP1 and LP3 respectively (Figure 5.9). An extremely good corroboration was observed for the N terminal sequencing results with the *in silico* 3D model obtained from Robetta as represented in the cartoon in Figure 5.10.

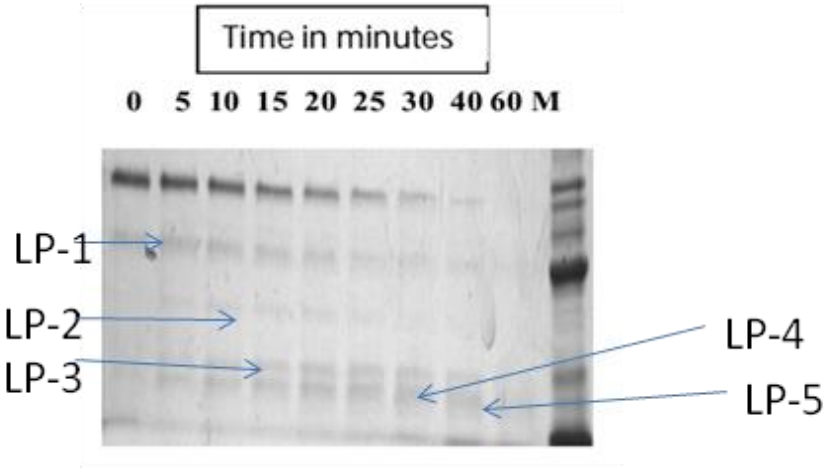

Figure 5.9. Limited proteolysis of HAX1: The protein HAX1 was subjected to limited proteolysis by trypsin. The products of limited proteolysis (LP-1 to 5) were transferred on a PVDF membrane and the peptides of interest were processed for N-terminal sequencing.

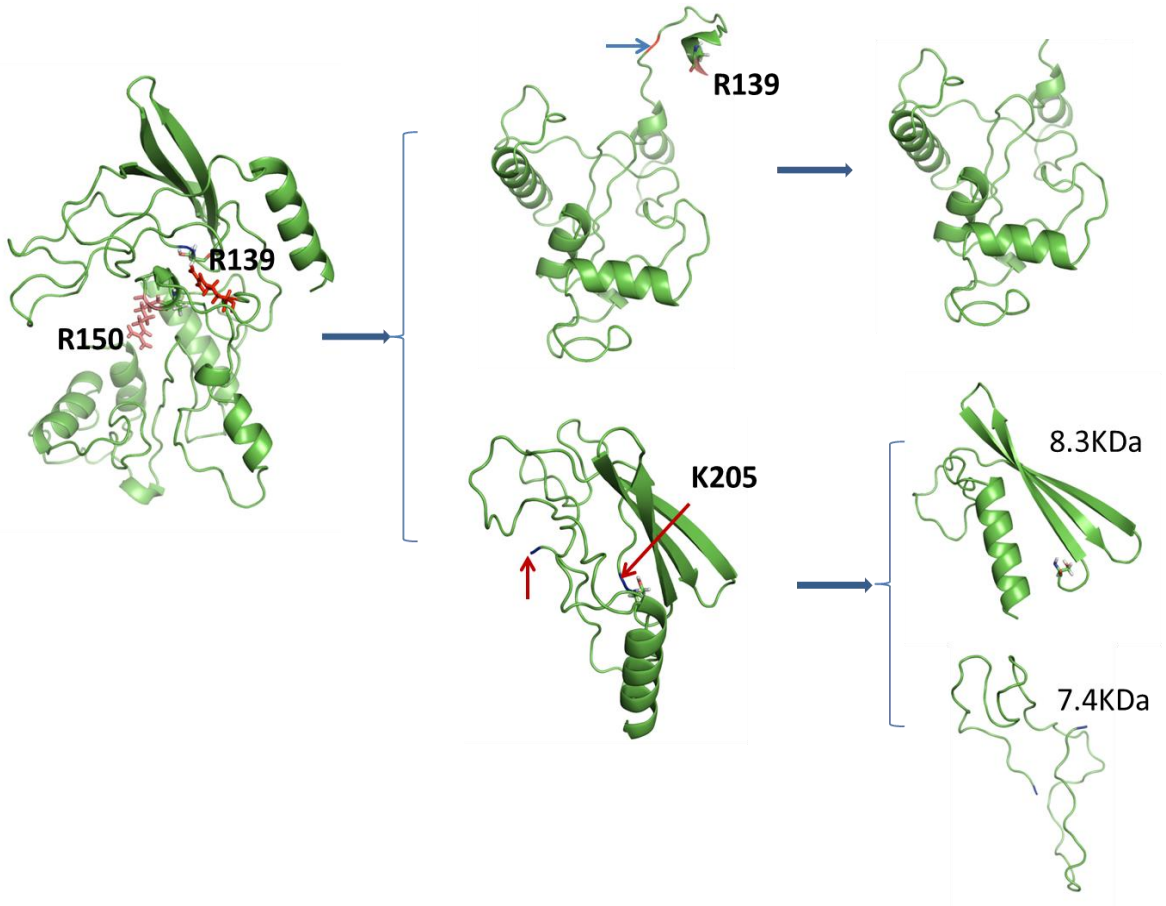

Figure 5.10. Diagrammatic representation of the pattern of HAX1 cleavage by trypsin. Based on the N-terminal sequencing results, the first polypeptide generated begun with residue number 140 in HAX1 indicating the most accessible trypsin cleavage site in HAX1. Similarly based on the other N-terminal sequencing results the possible pattern of cleavage by trypsin has been represented.

5.3.3. X-ray Crystallographic studies of HAX1

Gaining insights into the structure of HAX1 could provide means to understand the mechanism of interaction with various interacting partners. Protein crystallization is

predominantly used for structural biology to study the molecular structure of the protein, most notably for study by X-ray crystallography studies**.**

Like many other types of molecules, proteins can be prompted to form crystals when the solution in which they are dissolved becomes supersaturated. Protein crystallization is subjected to various challenges such as restrictions of the aqueous environment, difficulties in obtaining high-quality protein samples, as well as sensitivity of protein samples to temperature, pH, and ionic strength. In the present study, we attempted to obtain crystals of HAX1 along with MBP fusion tag using Hampton Research Crystal screens 1 and 2 and on the basis of crystallization conditions reported for MBP fusion proteins. Crystal trials were set up for MBP-HAX1 at concentrations of 3mg/ml, 5mg/ml and 8mg/ml in Hampton crystal screens as well as in crystallization conditions for other membrane associated proteins.

Despite these attempts we did not get promising leads for any of the conditions in our trials. Either precipitation or clear drops were observed, but none of the conditions showed crystals. The reasons for this might be the tendency of the protein to precipitate at higher concentration and the membrane associated nature of HAX1. Since one of our major objectives was to determine the interacting modules of HtrA2 and HAX1 we proceeded with the *in silico* model of HAX1 verified by *in vitro* approach for our further detailed interaction studies.

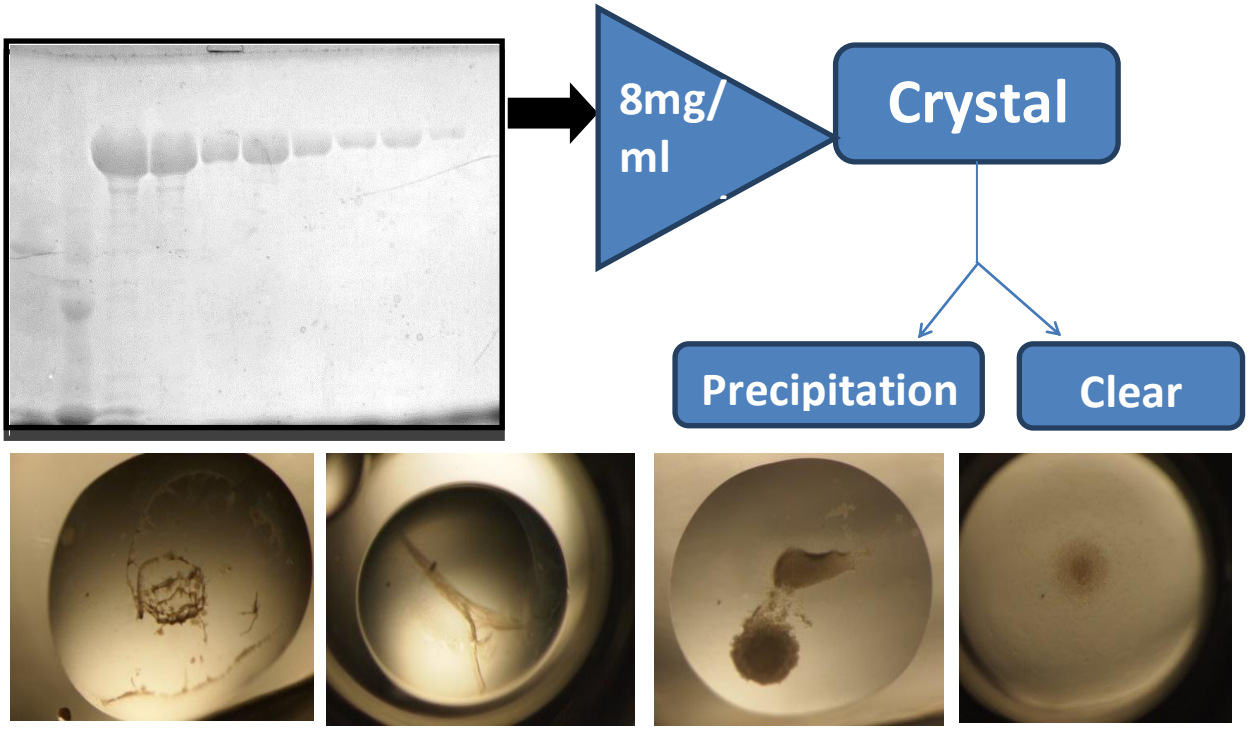

Figure 5.11. Representative images for HAX1 crystal trials showing precipitates.

II. To characterize the interaction between pro-apoptotic serine protease HtrA2/Omi and its binding partner HAX1 using biochemical and biophysical tools

5.4.1. *In vitro* pull down studies

The HAX1 gene was cloned in pGEX-2T to obtain GST-HAX1 fusion protein which was expressed in *E.coli* pLysS cells and used to determine the minimal binding region. To deduce the domains involved in the interaction, the different domains and domain combinations of HtrA2 i.e. N-SPD (N-terminal and serine protease domain), PDZ were purified by appropriate strategies (Figure 5.12). These purified domains were then used for pull down studies with GST-HAX1. Similarly, truncated versions of HAX1 were generated to deduce its minimal binding region. From these *in vitro* pull down experiments, it was observed that N-SPD is involved in the interaction with HtrA2

whereas PDZ alone was not sufficient for interaction (Figure 5.13). These findings were further confirmed by western blotting analysis, and it can be concluded from these domain-wise pull down studies that SPD or the protease domain of HtrA2 might be involved in interaction with HAX1 and not the canonical protein-protein interaction domain PDZ.

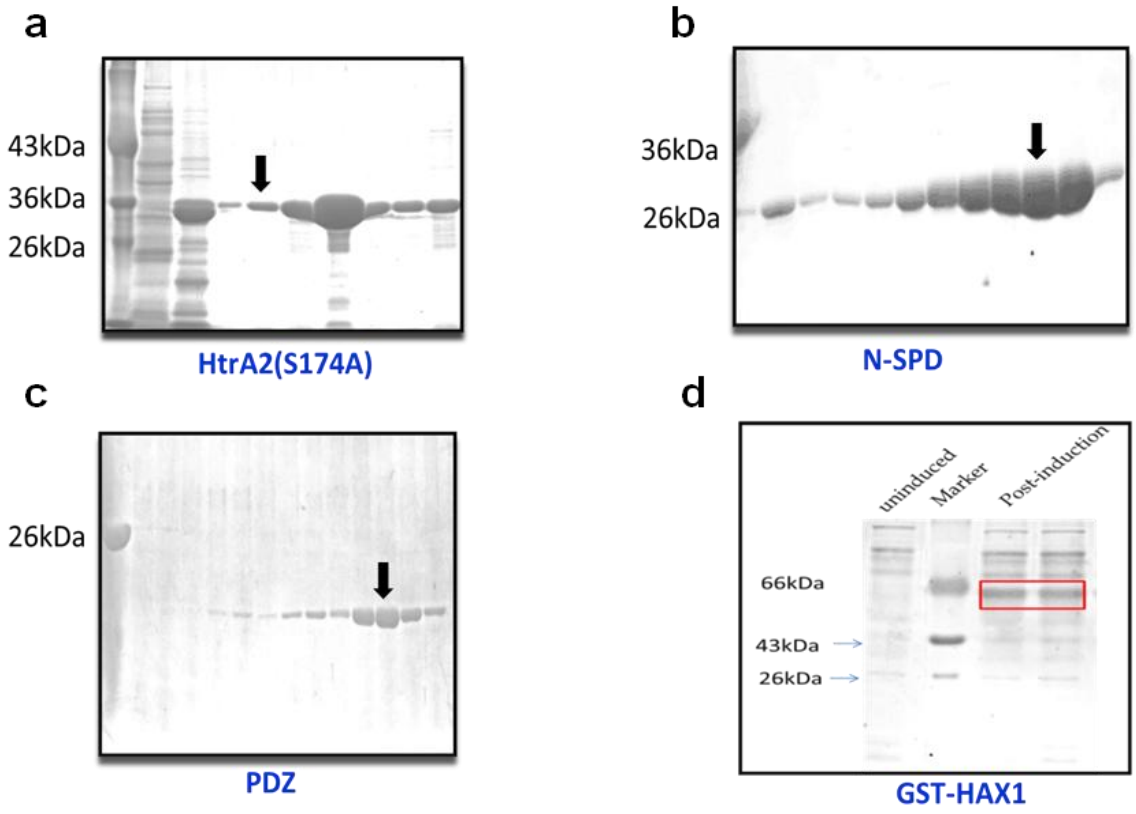

Figure 5.12. SDS-PAGE gels representing purified proteins for HtrA2-HAX1 domain-wise pull down assay. Purification of HtrA2 variants a. Full length HtrA2 (S174A). b. N-SPD c. PDZ by Ni-IDA affinity chromatography d. Gel showing GST-HAX1 expression.

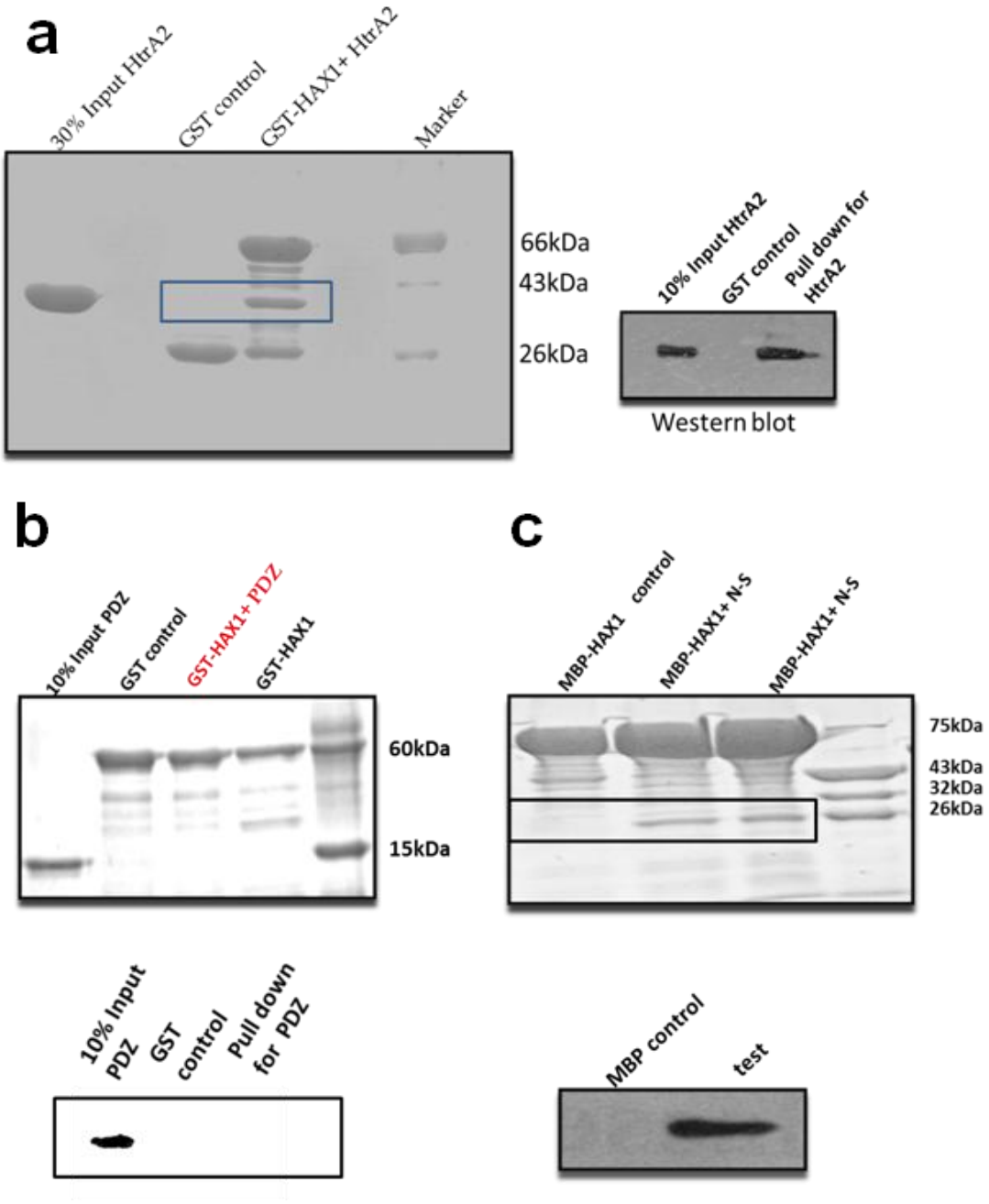

Figure 5.13: ***In vitro*** **pull down studies for HtrA2 and HAX1:** a. GST pull down assay of HAX1 with HtrA2 showing the presence of HtrA2 interaction with HAX1 (3rd lane) confirmed by Western blotting (right panel). b. GST pull down assay showing no interaction of PDZ with HAX1. c. MBP pull down assay displaying the interaction of N-

SPD domain of HtrA2 with HAX1. The lower panels show the confirmation for the same by western blotting.

5.4. 2. *In silico* interaction studies

Docking studies were performed for preliminary clues of HtrA2-HAX1 interaction using HADDOCK and ClusPro platforms. These studies helped us elucidate the residues that might be critical for interaction. The residues at the interface of the docked complex were used to characterize the interaction.

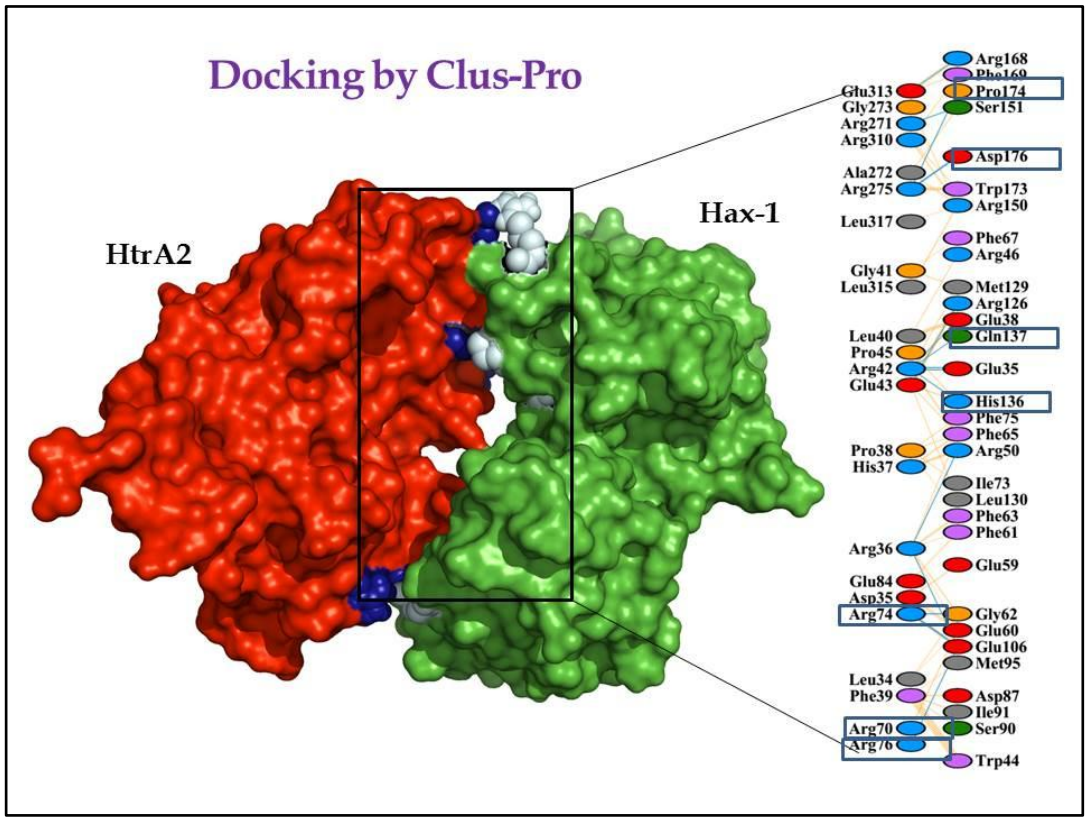

Figure 5.14: Cartoon representation of the *in silico* docking studies by ClusPro 2.0.

From the docking studies P155, Q156, R158, R74, R76 from HtrA2 and P174, D176 from HAX1 were identified as putative residues critical for interaction between HtrA2 and HAX1.

Based on the docking analyses for these proteins, we narrowed down on putative residues that might be critical for this interaction. Proteins with these residues substituted by SDM were used to understand the critical role of these residues. The mutagenesis and pull down studies along with western blotting confirmed the role of residues P155, Q156, R158, R74, R76 from HtrA2 and P174, D176 from HAX1 in this interaction.

5.4.3. Mapping the minimal binding region of HAX1 for HtrA2

After determining the domains of HtrA2 involved in interaction with HAX1 we also sought to determine the region of HAX1 responsible for the interaction with HtrA2. We further generated pGEX 2T plasmids encoding the full length HAX1 (amino acids 1–279), ΔTMD HAX1 (amino acids 1-261), HAX1 208 stop (amino acids 1-208), and HAX1 180 stop (amino acids 1-180). We then compared the ability of HtrA2 to interact with the full-length, and the different truncated variants of HAX1. Site directed mutagenesis PCR was carried out to generate truncated mutant of HAX1 (HAX1 F208stop). The authenticity of mutation was determined by sequencing (Figure 5.15).

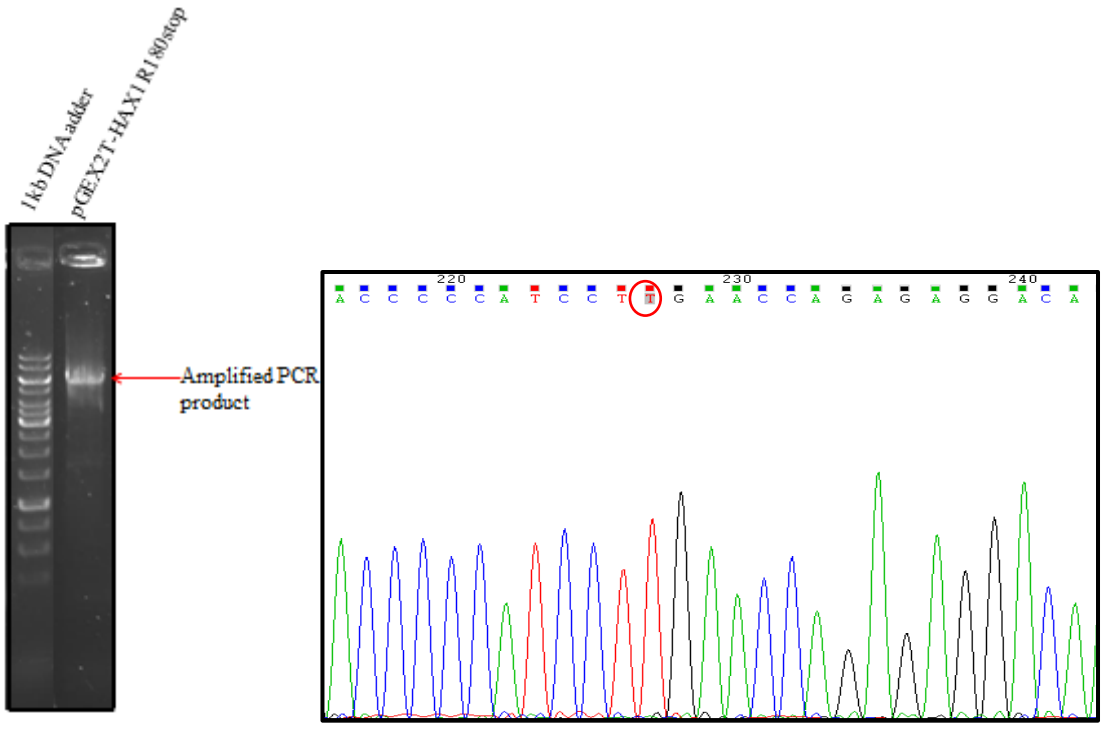

Figure 5.15. Agarose gel representation of Site Directed Mutagenesis PCR for HAX1 (180 stop). Sequencing results showed the introduction of stop codon after residue 180 of HAX1 (mutation introducing stop codon is encircled in the chromatogram).

The plasmid pGEX2T bearing the gene for HAX1 was expressed in BL21 (DE3) pLysS cells for protein expression. The expression of wild type HAX1 tagged with GST was checked by inducing the cells at different IPTG concentrations.

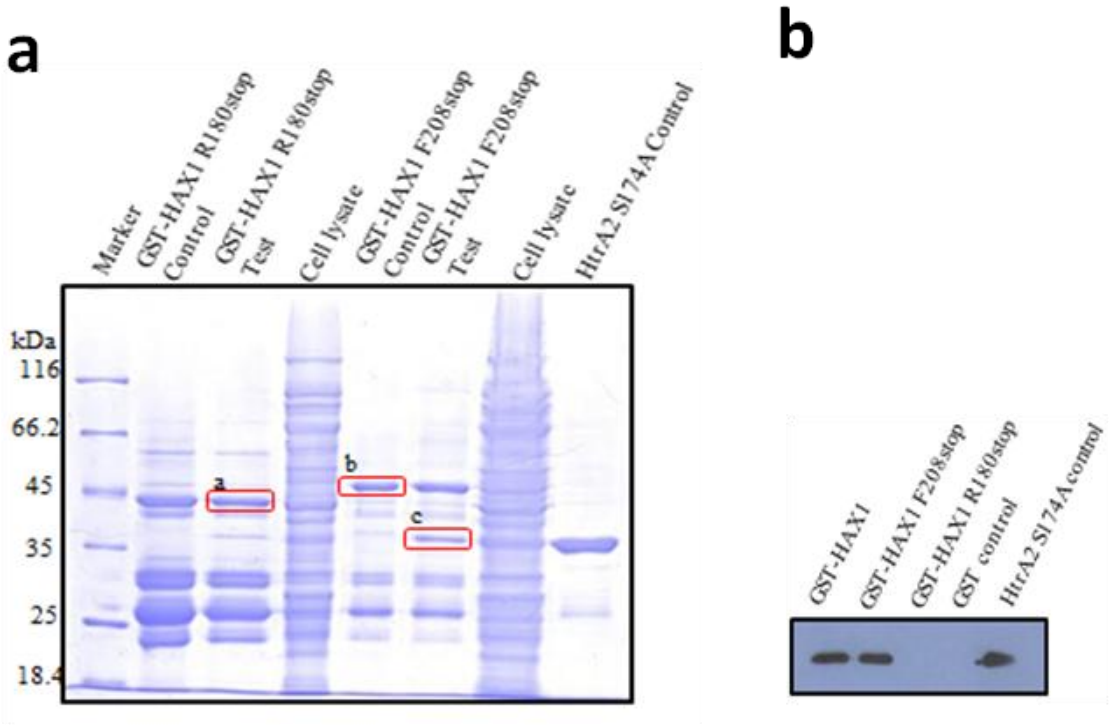

Figure 5.16. Pull down assay for mapping the minimal binding region in HAX1. a. SDS Gel representation of the pull down studies of HtrA2 with different truncated variants of HAX1 shows that the removal of region spanning 180-208 of HAX1 led to abrogation of interaction. b. Western blot for the pull down assay confirms the role of 180-208 residues in interaction.

Pull down assay was performed using glutathione beads and GST-HAX1 F208stop and GST-HAX1 R180stop as bait proteins and HtrA2 S174A as prey protein. After the pull down, the samples were analysed on 12% SDS-PAGE. For pull down assay with GST-HAX1 F208 stop, the test sample showed the presence of HtrA2 that confirms the interaction (Figure 5.16). It was seen that GST-HAX1 F208stop interacts with HtrA2 S174A, but GST-HAX1 R180stop shows negligible to no interaction (Figure 5.16). These observations were also verified by performing western blot analysis for the same

samples, where HtrA2 was probed. From the western blot results, it can be said that there is no difference in the interaction of GST-HAX1 and GST-HAX1 F208stop with HtrA2. However, there was weak or no interaction between GST-HAX1 R180stop and HtrA2 indicating that the regions spanning residues 180-208 in HAX1 might be critical for interaction with HtrA2.

5.4.4 Identifying the residues critical for HtrA2-HAX1 interaction

The residues identified by Clus-Pro as critical were modified by site-directed mutagenesis (SDM). It was done using PCR. The product obtained was checked by agarose gel electrophoresis. The sequences were verified by multiple sequence alignment using ClustalW. The residues predicted to be critical for HtrA2 HAX1 interaction were substiuted successfully with alanine. These mutants of HtrA2 and HAX1 were further expressed and purified as described in chapter 3.

5.4.4.1 Purification of HtrA2 (S174A) and HtrA2 interface mutants

The mutants of HtrA2 generated by SDM PCR were a part of the pET20b vector, hence consisted of a histidine tag at the C-terminal. These proteins were purified by affinity purification using Ni-IDA column and the protein of interest eluted at imidazole concentration of 250mM and resolved at 36 kDa on SDS-PAGE. For interaction studies with HAX1 mutants, inactive mutant of HtrA2 (HtrA2 S174A), was purified and used in further experiments.

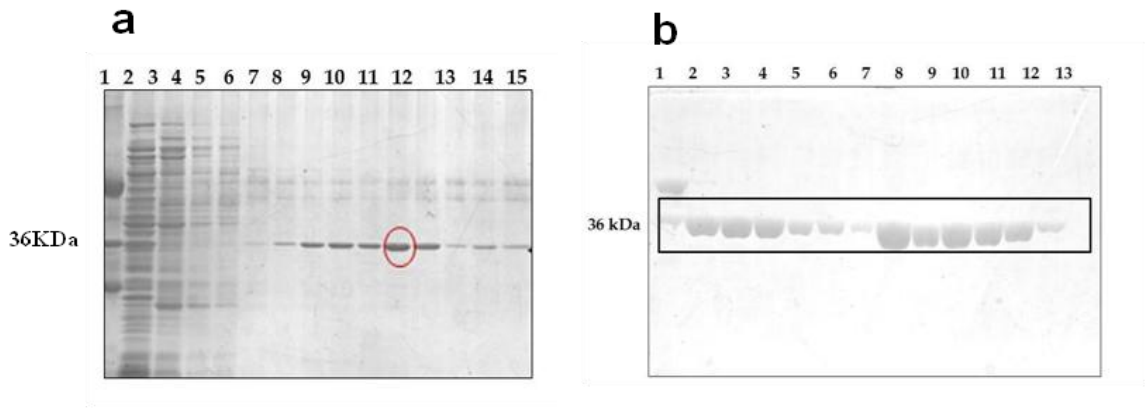

Figure 5.17. SDS-PAGE gels representing purification of HtrA2 mutants. a. Lanes 9-13 of the gel represent purified inactive variant of HtrA2 (S174A) b. Gel representing purified HtrA2 (D69A, R70A) [lanes 2-6] and HtrA2 (R74A, R76A) [lanes 7-12] using Ni-IDA column chromatography.

5.4.4.2 GST-Pull down assay

Pull down assay was performed using GST fusion HAX1 and its mutants to understand the residues critical for the HtrA2-HAX1 interaction. In the gel for pull-down assay represented in Figure 5.18, the bands for HtrA2 (R74A, R76A) and HAX1 (P174A D176A) disappeared which indicates an abrogation of interaction between HtrA2 and HAX1. This was confirmed by western blotting using anti-His antibody. This confirms that these residues identified by Clus-Pro are critical for the interaction.

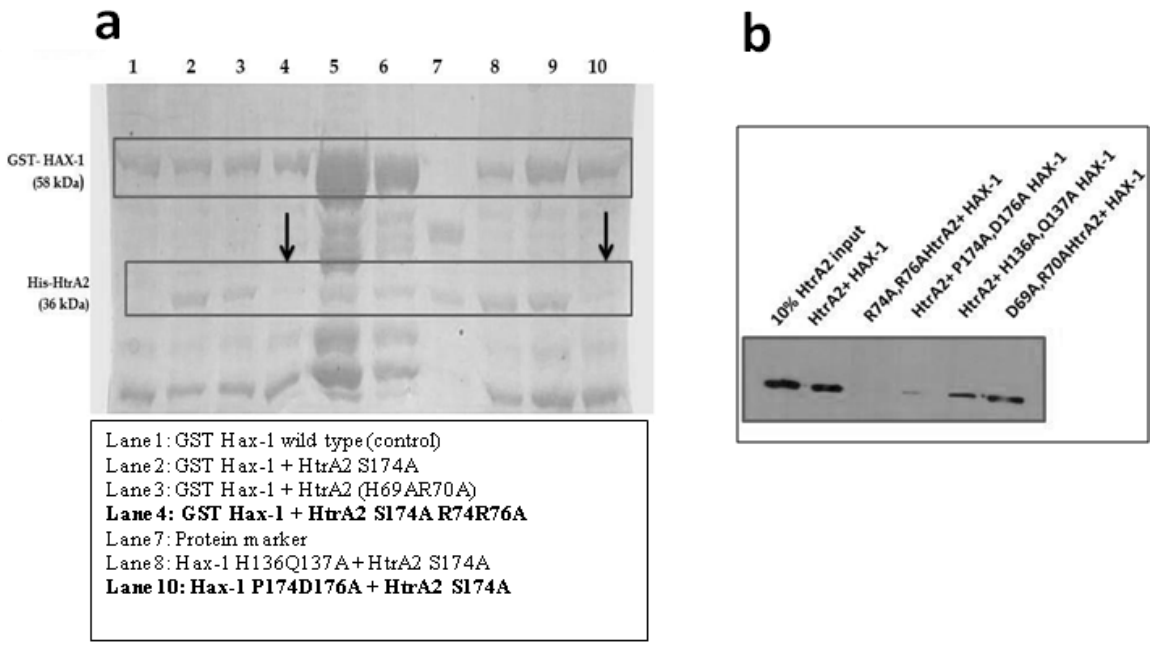

Figure 5.18. Pull down Assay for residues critical for HtrA2-HAX1 interaction. a. From the pull down studies of HtrA2 with different interface muatnts of HAX1 it was observed that there is absence of HtrA2 bands in HAX1 (P174A, D176A) and HtrA2 (R74A, R76A) lanes. b. Western blot for the pull down assay shows there is absence of HtrA2 bands in the HAX1 (P174A, D176A) and HtrA2 (R74A, R76A) lanes.

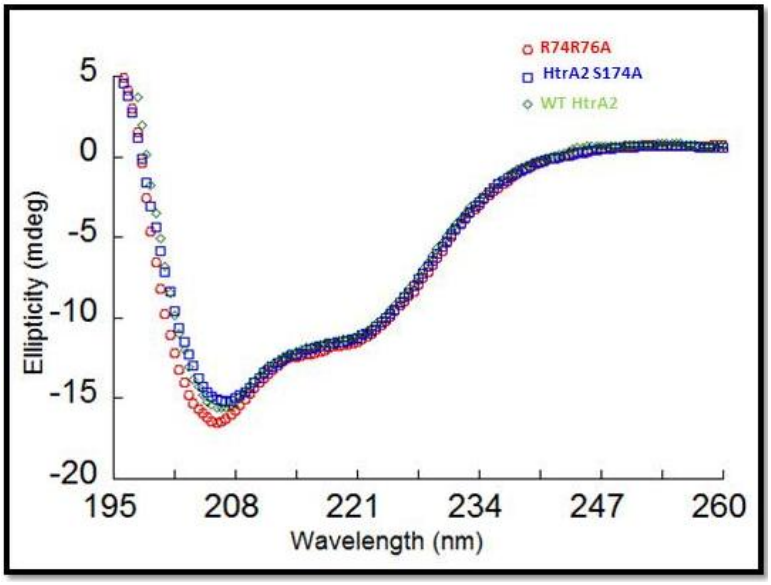

Figure 5.19. Comparative CD Spectra of the HtrA2 and its mutants. wild type, inactive mutant (HtrA2-S174A) and interface mutants HtrA2 (R74, R76A). The graph indicates that the secondary structure of the HtrA2 (R74, R76A) is well-folded and similar to that of HtrA2 S174A and wild type protein.

From the pull-down studies, it was found that, when the Arginine (R) at 74th and 76th position in HtrA2 S174A were mutated to Alanine (A), it failed to interact with HAX1. To confirm this abrogation in the interaction is solely due to the mutation at these residues and not due to any structural or conformational changes, the secondary structure of the mutant was compared with HtrA2 (S174A) and that of wild type HtrA2 by CD spectroscopy. The CD graphs representing ellipticity versus wavelength in Figure 5.19 clearly shows that the HtrA2-HAX1 interface substitution mutant HtrA2 (R74A, R76A) had no effect on the overall secondary structure of the protein. This observation further

confirms the loss of interaction in this mutant is due to the significance of the residues and not due to the loss of conformation in HtrA2 due to the mutation.

III. Elucidation of serine protease activity of HtrA2 on HAX1 and characterization of the cleavage sites by proteomic analysis

Interestingly, experiments in Mnd2 MEF cells reconstituted with wild-type HtrA2/Omi demonstrated that HtrA2/Omi-mediated degradation of HAX1 correlated with extensive cell death in response to etoposide, cisplatin and H_2O_2 . Due to the existing ambiguities in this pathway we wanted to elucidate whether HAX1 is a binding partner, activator or substrate of HtrA2.

5.5. Functional relevance of HAX1–HtrA2 interaction

Both HAX1 and HtrA2 are located in the mitochondrion and since HAX1 promotes HtrA2- dependent cell death, we tested the effect of HtrA2–HAX1 interactions on HtrA2 activity.

5.5.1. Activation Assay to study the effect of HAX1 on HtrA2 protease activity

In order to identify whether HAX1 acts as an activator of HtrA2, the activation assay was performed as described in Chapter 3**.** The activity of HtrA2 was monitored after pre-incubation with HAX1. To determine the steady-state kinetic parameters, we measured the initial rates of substrate cleavage for different β-casein concentrations with or without saturating concentrations of HAX1 proteins (Figure 5.20). It was observed that HtrA2 cleavage of β-casein follows a sigmoidal curve with a Hill constant of ~ 2.4 (Figure

5.21a). Therefore, the positive cooperativity upon substrate cleavage suggests that binding of one substrate (β-casein) molecule to one subunit of HtrA2 trimer favors the consequent binding of others. Interestingly, upon pre-incubation of HtrA2 with HAX1, the catalytic efficiency ($k_{cat}/K_{0.5}$) increased by approximately 3.2 fold thus indicating greater stabilization of the relaxed (active) state of protease upon HAX1 binding [22]. However, the substrate concentration at half maximal velocity ($K_{0.5}$) remained unchanged, even in presence of HAX1 implying the existence of a similar binding pocket.

The activity of HtrA2 was monitored after pre-incubation with HAX1 and the Vmax was found to be altered without significantly altering the apparent K_m (with L2 specificity pocket mostly unaltered) and hence follow the 'V system' of allosteric modulation. In this system, both the relaxed (R) and the tensed (T) states bind the substrate at the active site with similar affinity while the activator at the allosteric site binds the R and T states with different affinity. This differential affinity of the activator towards the binding site along with R state stabilization shifts the equilibrium towards R state thus positively influencing its turnover rate and hence catalytic efficiency which has been observed in case of HtrA2 in the presence of HAX1. Thus, HAX1 possibly acts as an activator to allosterically modulate HtrA2 to form a catalytically active enzyme, which then cleaves β-casein.

This observation suggests interaction of HAX1 with HtrA2 brings about rearrangement around the active site of the enzyme by positively influencing its activity thus behaving as an allosteric regulator. The activation assay shows 3.2 fold increase in the activity of HtrA2 and 1.5 fold increase in N-SPD activity (Table 5.3, Figure 5.21b) in the presence

of HAX1. The cooperativity is also altered for N-SPD from ~1.3 in the absence of HAX1 to 1.9 in its presence. The significant increase in the activity for HtrA2 in the presence of HAX1 proves that the latter might be an activator of HtrA2. This is a first such report in the context of these two crucial apoptotic proteins.

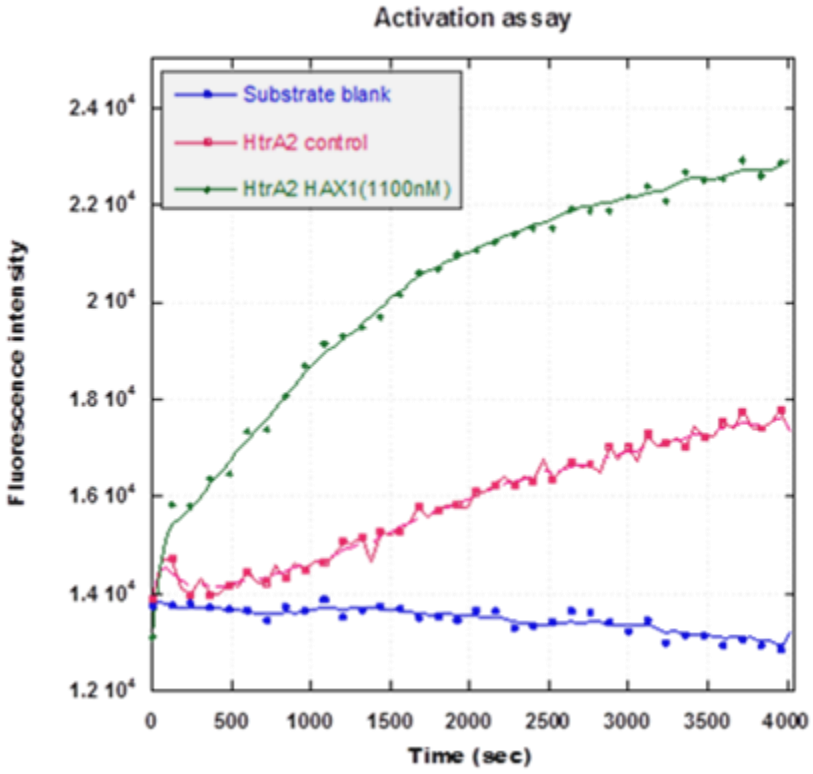

Figure 5.20. Representative graph for the β-casein assay showing the saturating concentration of HAX1 for HtrA2 activity. Based on the studies on initial velocity of HtrA2 in the presence and absence of HAX1, it was observed the saturating concentration of HAX1 for activation of HtrA2 was found to be 1.1μM.

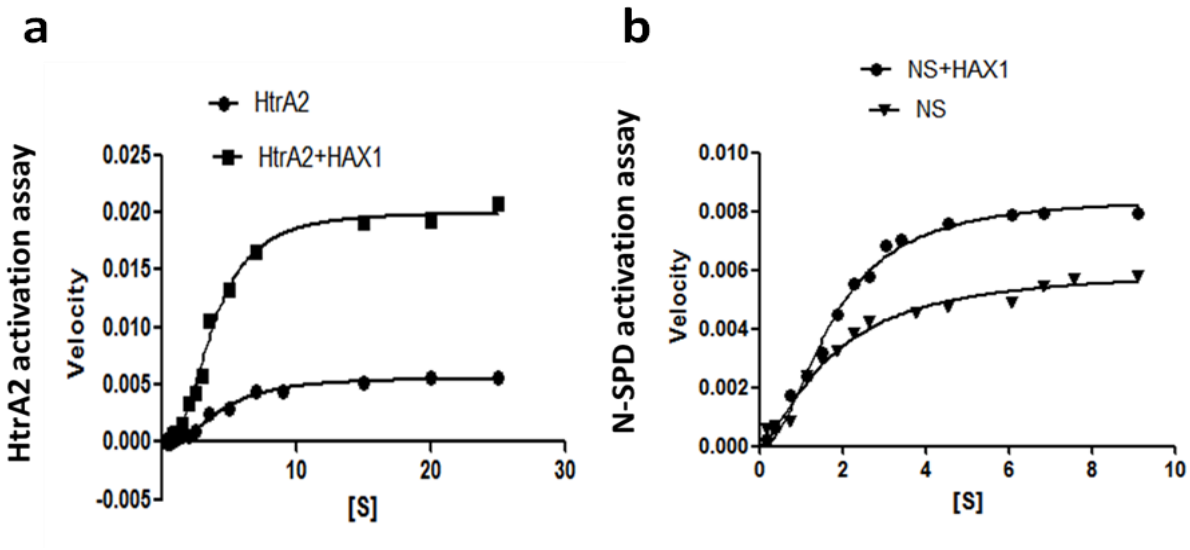

Figure 5.21. HtrA2 activation assay. a. Representation of the kinetics of HtrA2 activity in the presence and absence of HAX1. b. Representation of the kinetics of N-SPD (HtrA2) activity in the presence and absence of HAX1. The data is fit of to the Hill form of the Michaelis-Menten equation: velocity = $V_{max}/(1+(K_m/ [substrate])^n$.

	With HAX1		W/O HAX1	
	HtrA2	N-SPD	HtrA2	N-SPD
Vmax	0.01985 ± 0.0007	0.01341± 0.0031	0.0056 ± 0.000197	0.008278 ±0.0008
Cooperativity	2.418 ± 0.2859	1.926± 0.1003	2.414 ± 0.258	1.352± 0.3942

Table 5.3. Kinetic parameters for HtrA2 in the presence and absence of HAX1. V_{max} $(Ms^{-1})* 10^{-7}$.

5.5.2 Effect of HtrA2 on HAX1 - *in vitro* cleavage assay

With an aim to understand whether HAX1 is only an interacting partner cum activator of HtrA2 or a substrate as well, both were incubated at different temperatures and concentrations. The observations so made clearly show that there was no cleavage of HAX1 by HtrA2 and therefore the latter might not be a substrate of HtrA2 as observed in some studies.

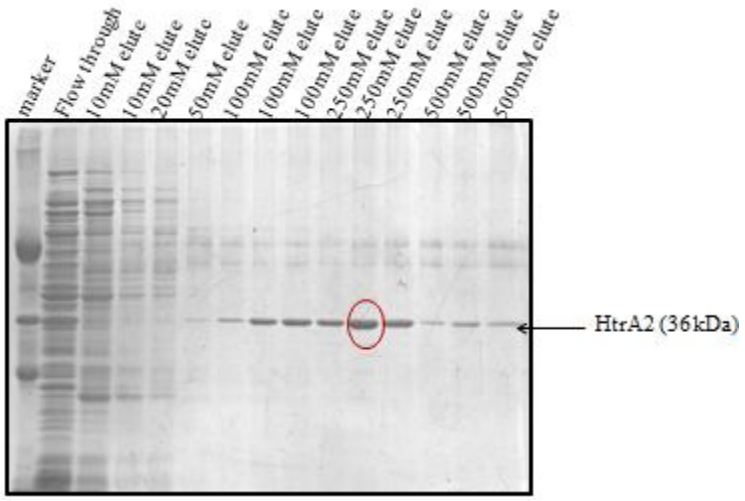

Figure 5.22. SDS-PAGE gel representing purification of HtrA2-WT using Ni-IDA affinity chromatography. The different elutions for purification of HtrA2-WT for assays have been indicated.

His-tagged HtrA2 protein (36 kDa) was purified using Ni-IDA column. On analyzing the eluted fractions on SDS-PAGE post purification, the pure fractions were used for further cleavage assays (Figure 5.22). Similarly the fraction with least impurities and having highest amount of MBP-HAX1 obtained through first step of purification using amylose resin was subjected to TEV cleavage. The TEV cleaved protein was injected into the FPLC column (Superdex 200) to obtain purified HAX1 protein. Fractions were collected

at appropriate elution volume and analysed on SDS-PAGE. The fractions with higher HAX1 concentration were pooled and used for cleavage assays with different concentrations of HtrA2 as well as different temperatures.

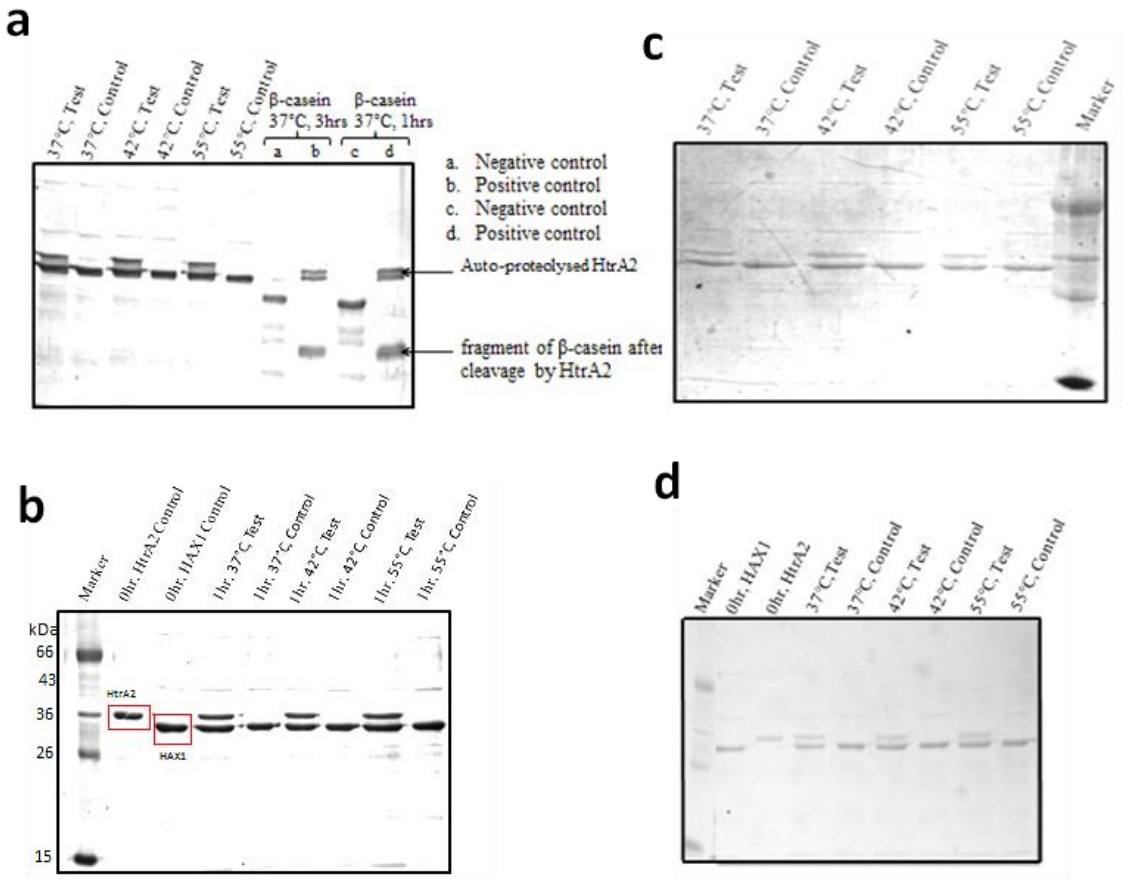

Figure 5.23. Representative SDS gels for cleavage assay. HAX1 was incubated with HtrA2 at different temperatures, at different concentrations and monitored after 1 and 3 hrs (a, b) and overnight (c, d) incubations. There was no cleavage of HAX1 by HtrA2 observed for any of these parameters.

No cleavage of HAX1 by HtrA2 was observed, for incubation at different time points at any of the 3 different temperatures (37°C, 42°C and 55°C). β-casein, a known substrate of HtrA2 was used as a control. In the β-casein positive control (β-casein + HtrA2), cleavage of β-casein is observed, indicating that HtrA2 is active. Cleavage of HAX1 by HtrA2 was not observed for 5, 7 and 8 hours of incubation time, at any of the three temperatures (37°C, 42°C and 55°C). HtrA2 shows maximal activity at 55°C. Thus a cleavage assay was set at 55°C for various time intervals. On analyzing the samples on SDS-PAGE, has been observed that HAX1 is not cleaved by HtrA2 at any of the time intervals. Also, there is no cleavage of HAX1 by HtrA2 for overnight incubation at the three temperatures used for the assay (Figure 5.23).

5.5.3. Probing the possibility of adapter proteins in HtrA2-HAX1 mediated apoptosis

Based on literature, two proteins PARL (Presinilins associated rhomboid like protein) and XIAP can be the probable partners of HtrA2 and HAX1. These proteins have been cloned, expressed and purified for combinational cleavage assays. Understanding the interplay between PARL, HtrA2 and HAX1 that are part of a complex in the mitochondria would usher in fresh perspective on the context dependent maturation of HtrA2 and HAX1 cleavage.

5.5.3.1 GST Pull-down assay

HtrA2 has been reported to interact with XIAP (*6*) and PARL (*8*) respectively under different scenarios. To confirm the direct interaction of HtrA2 with these two interacting partners individually, pull-down assay were done. PARL was cloned in the vector

pGEX2T hence consisted of a GST tag. It was purified by affinity purification using Glutathione Sepharose 4B column. The protein GST-PARL was eluted at reduced glutathione concentration of 30mM.

The Figure 5.25 indicates that HtrA2 interacts with XIAP and PARL directly. Western blotting was done using anti-HtrA2 antibody to confirm the interaction. The western blotting result confirmed the interaction indicating that HtrA2 interacts directly with XIAP and PARL individually (Figure 5.24).

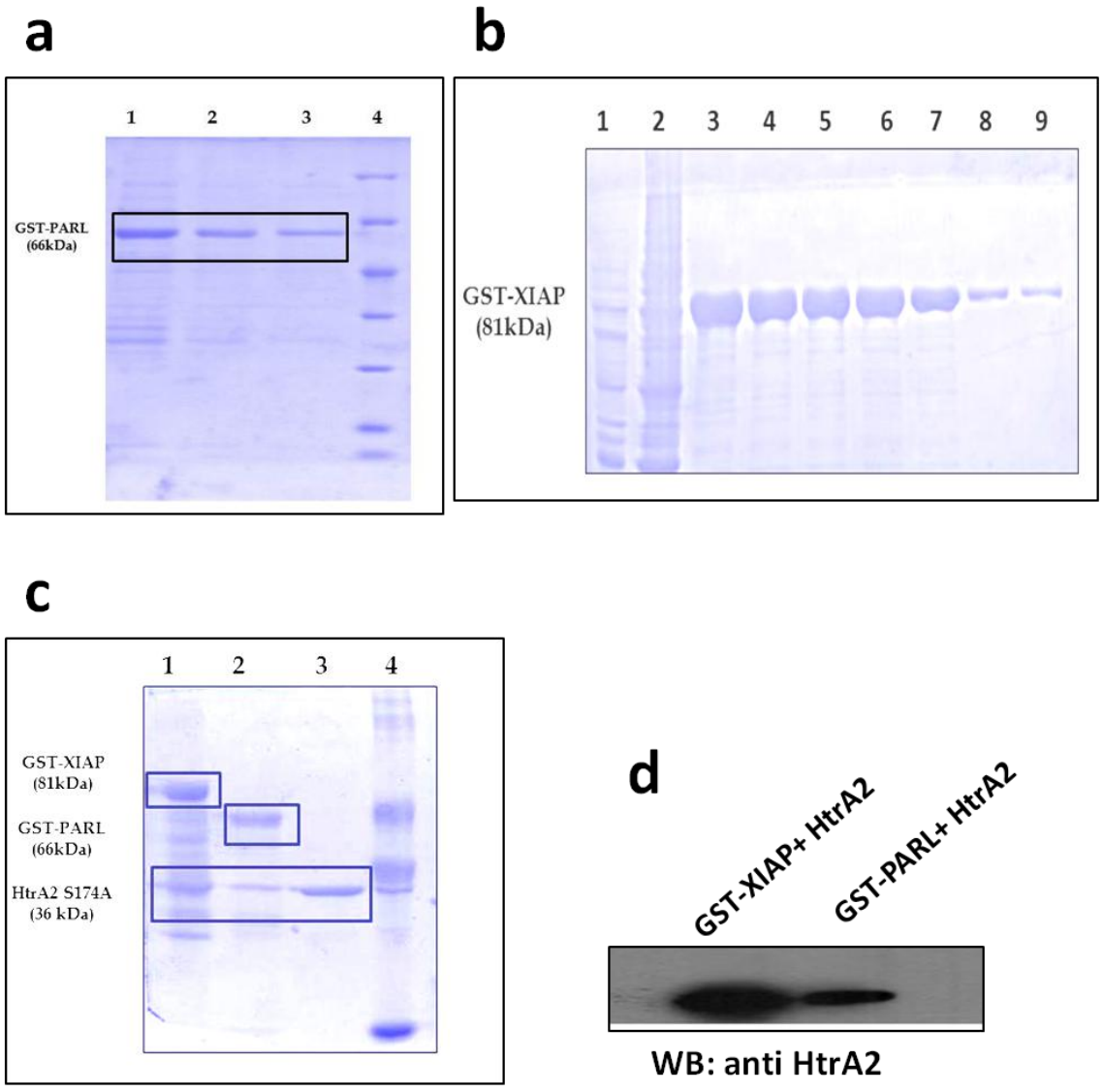

Figure 5.24. Interaction study of HtrA2 with XIAP and PARL. a. Purification of GST-PARL (lanes 1-3) using Glutathione Sepharose 4B column. b. Purification of GST-XIAP using Glutathione Sepharose 4B column (lanes 3-9). c. SDS-PAGE gel representing the pull down assay of HtrA2 with XIAP and PARL. d. Western blot confirmation of the pull down assay clearly shows a direct interaction of HtrA2 with both XIAP and PARL.

5.5.3.2 Cleavage assay in the presence of adaptor proteins

HAX1 was incubated with HtrA2 *in vitro* in the presence of PARL in different combinations. The result for the assay demonstrates that there is no cleavage of any of the three components (Figure 5.25). Similarly the assay for HtrA2 pre-incubated with HAX1 too did not show a significant change in rate of XIAP cleavage (Figure 5.26). These observations need further confirmation through *ex vivo* studies.

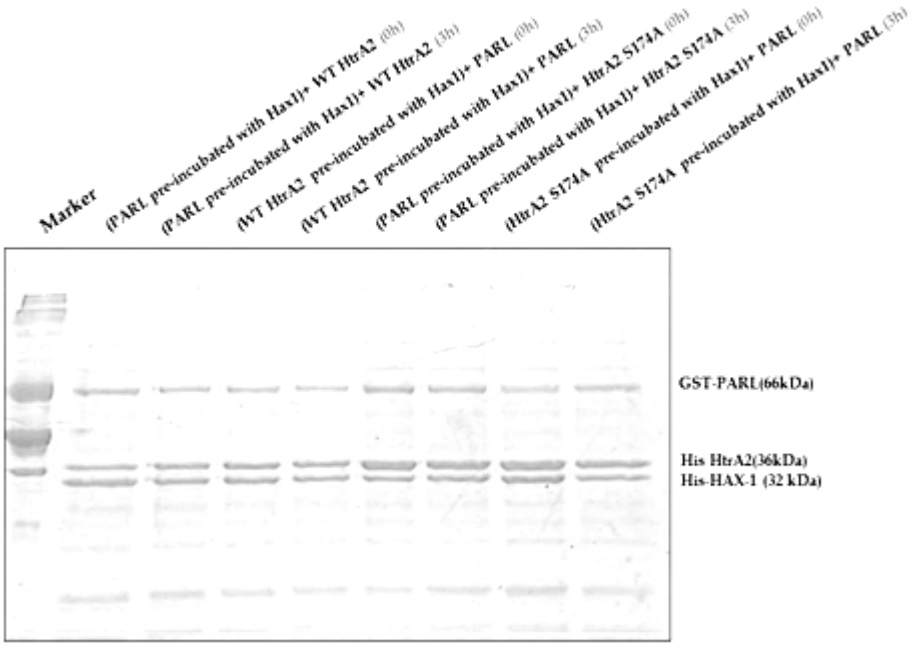

Figure 5.25. Cleavage assay with HtrA2, HAX1 and PARL. The SDS-PAGE gel represents the results of the combination assay of HtrA2 with HAX1 and PARL. Pre-incubations with different combinations have no effect with respect to cleavage of these components.

5.6 Discussion:

The activation assay along with the cleavage assays proves that HAX1 might be an activator of HtrA2 and not a substrate. This changes the equation in the mitochondria and might be significant in understanding of apoptosis in context of these two proteins. Since no HtrA2 mediated cleavage of HAX1 was observed in different conditions, the possibility of mass spectrometric analysis of the cleavage products was ruled out.

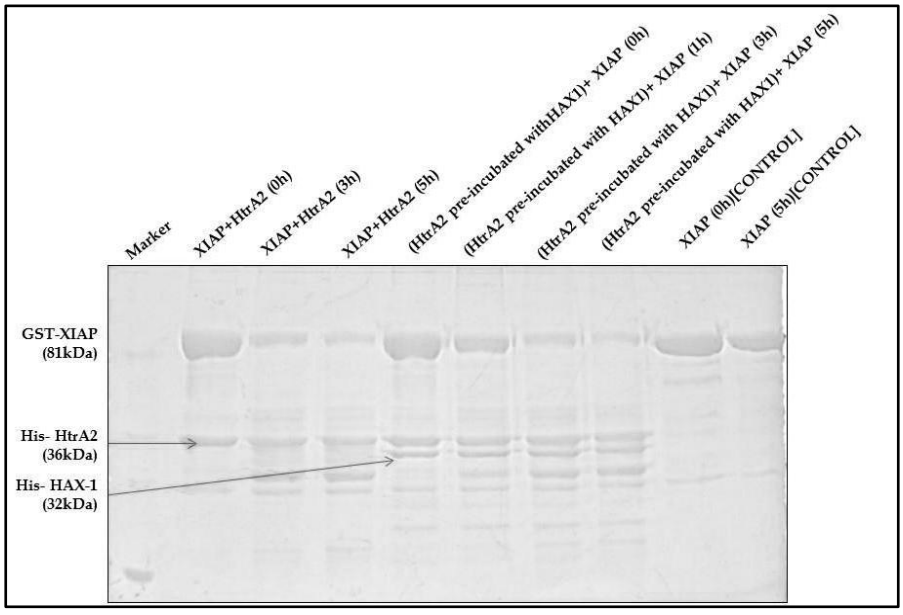

Figure 5.26. Enzyme assay with XIAP. In the gel representing the XIAP cleavage assay no effect was seen on the rate of XIAP cleavage by HtrA2 in the presence of HAX1 upto 5 hrs of incubation.

The complex comprising HtrA2, HAX1 and other adaptor proteins might bring drop in the levels of the anti-apoptotic HAX1. This phenomenon remains largely unexplained and is the major factor for bringing about drop in the mitochondrial membrane potential. The minimal binding region identified by these studies can be an important step forward toward designing peptides for modulation of HtrA2 activity.

The leads obtained from our studies raised very interesting possibilities about the intrinsic mechanism of apoptosis. It was reported by Suzuki, et.al in 2004 that recombinant HtrA2 was observed to catalytically cleave IAPs and to inactivate XIAP *in vitro*, suggesting that the protease activity of HtrA2 might be responsible for its IAP-inhibiting activity. We hypothesized that HtrA2 might cleave other substrates at a higher rate in the presence of its activator HAX1. To test the hypothesis, the three proteins HtrA2, HAX1 and XIAP were incubated together at different combinations *in vitro* and allowed to interact for different time intervals. Though no marked difference was observed in any of these assays more detailed analysis of the stoichiometry might provide better clues on the mechanism. A similar study was also performed for HtrA2 and HAX1 in the presence of PARL with no prominent difference or cleavage. This calls for further investigation in the mechanism of this interaction.

Further investigation in the context of some specific objectives like the role of PTMs, the adapter proteins and pin-pointing the critical residues for interaction will provide us with the complete comprehensive details of the mechanism. This might prove to be of great assistance to investigators intending to manipulate the early stages of apoptosis for curing diseases including cancer and neuro-degenerative diseases.

Chapter 6

PDZome: A PDZ domain database

6.1. Introduction

The concept of domains has been one of the core themes in protein studies. The full-length HtrA2 protein contains the N-terminal mitochondrial targeting sequence (1-40 aa), a transmembrane domain (105-125 aa), followed by a serine protease domain (150-343 aa) with the catalytic triad His198-Asp228-Ser306, and one PDZ [post synaptic density protein (PSD95), Drosophila disc large tumor suppressor (Dlg1), and zonula occludens-1 protein (zo-1)] domain (364-445 aa) at the C-terminal end (Figure 6.1). PDZ is a structural domain of 70-90 amino acid residues. Proteolytic activity of proteases is modulated by the relative orientation of the PDZ domain. In HtrA2, an inactive state the PDZ domain traps the active site of the enzyme as well as its own peptide binding site through non-canonical interactions. Upon ligand binding, the PDZ domain would undergo conformational changes resulting in the formation of a functional and accessible active site. Similarly the PDZ domain has an important role to play in several enzymes across phylogeny and protein-protein interactions in the cellular network.

PDZ helps localization and clustering of membrane receptors by binding primarily to their C-terminus in different pathways that drive life (*50-53*). The specificity of PDZ-domain-based interactions is determined primarily by the sequence of the C-terminus of the proteins they bind, although few exceptions do exist. The only existing database on this domain comprises only about **300 proteins** which was last updated way back in 2004, (*54, 55*) thus creating a need for a database on this domain family that would include the developments of the last decade (Figure 6.1). With cellular PDZ proteins as common targets of pathogenic viruses emerging as an important new theme in virology,

high throughput and wide spectrum studies on this family of proteins is of significant value (*56*).

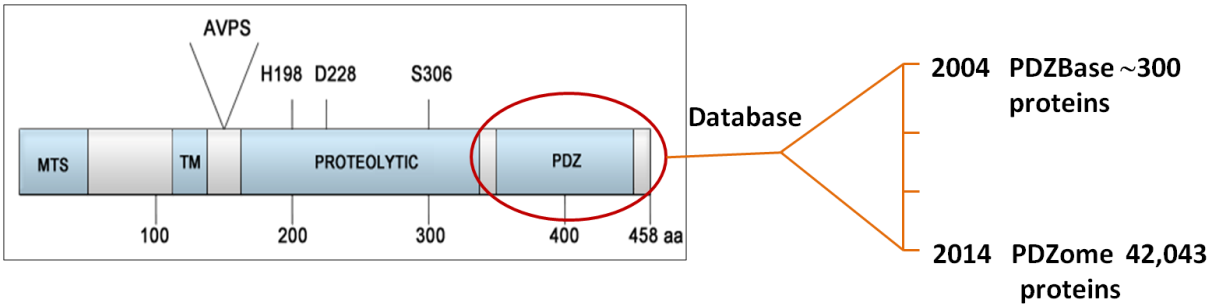

Figure 6.1. HtrA2 domain organization and the PDZ domain databases over the last decade. MTS: mitochondrial targeting signal, TM: transmembrane domain, PROTEOLYTIC: trypsin-like domain, PDZ: PDZ domain, AVPS: amino acids of the IAPs binding motif.

Our database **'PDZ*ome*'** provides information on **42,043** PDZ containing proteins as well as their known and putative interacting partners on one platform. The user-friendly interface can be easily queried with external identifiers for the protein. Here, unique integration of all prominent databases such as NCBI, UniProtKB, Swiss-Prot, PubMed, Protein Data Bank (PDB), Protein Mutant Database, STRING, IntAct, Pfam and KEGG lead to detailed information about PDZ proteins and pathways they are involved in, along with the specific nature of the interaction and the methodology involved (Figure 6.2).

BLAST has been customized for PDZ protein homology search with an additional option of batch downloading the PDZ*ome*. Jmol application is integrated for visualization of protein three-dimensional structure. It enlists all the well established and putative interacting partners thus

providing a comprehensive picture of this domain family. It also includes information on mutations in the PDZ containing proteins, obtained not only from the PMDB (Protein Mutant Database) but also through manual curation from literature.

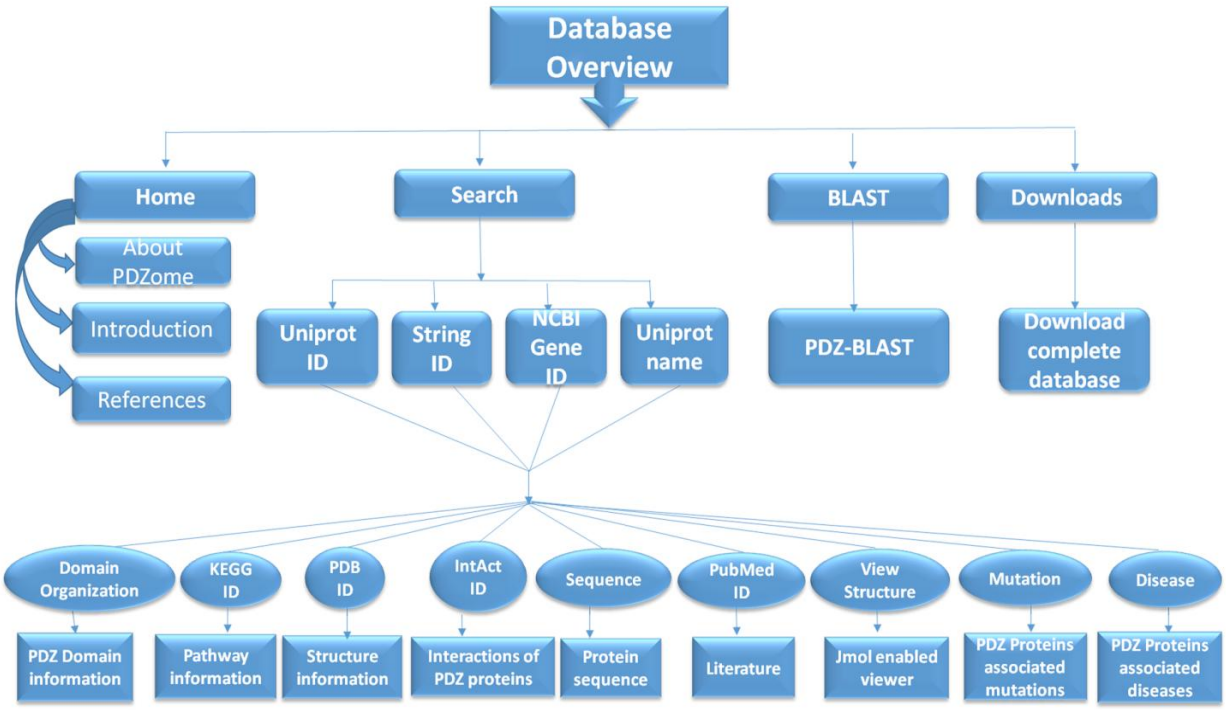

Figure 6.2. Overview of the PDZ*ome* database. PDZ*ome* is an amalgamation of information from all major databases along with manually curated data on available PDZ-containing proteins.

Our manually curated data from PMDB and PubMed on the association of PDZ containing proteins with different pathological conditions significantly enhances the value of the provided information. Lastly, with the amount of data generated in the last decade (Figure 6.4), and its involvement in a myriad of cellular pathways, it is essential

to have updated information exclusively on this very important class of protein-protein interaction domains.

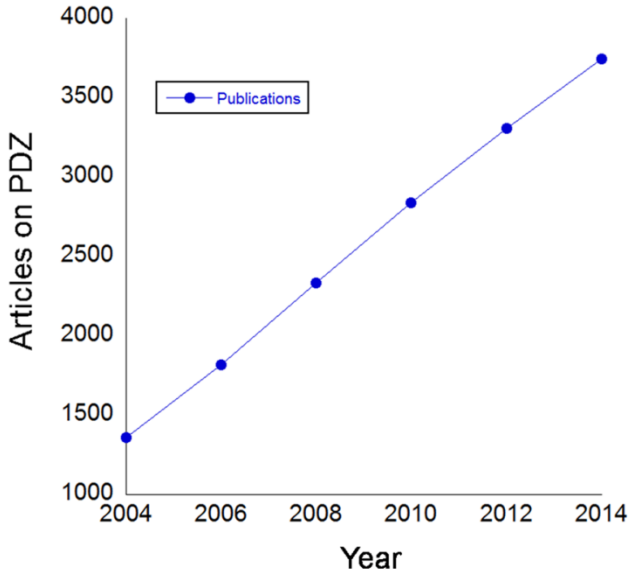

Figure 6.3. Statistical representation of literature on PDZ proteins. Year-wise analysis show a sharp increment in research articles published on PDZ-containing proteins over the last decade.

6.2. Methodology

6.2.1 Software Tools:

MySQL Administrator Tool (Workbench 6.0 CE), SQLyog (32 bit), Eclipse, Apache Tomcat 6, Java.

6.2.2 Data sources:

The PDZ protein data and related information such as sequence, organism information, available structures, localization and related literature were obtained from publicly available Uniprot-KB/Swisprot database (*92*). Uniprot-KB/Swisprot being the largest and up-to-date manually curated database of proteins was the most important data source for

PDZ*ome*. The entire PDZ domain containing data was manually downloaded from Uniprot-KB as flat files and the other related information was extracted out in a CSV (Comma Separated Values) file using Perl regular expressions. This CSV file was further used for the creation of tables in a database using MySQL server. Various information on PDZ*ome* proteins such as their Gene information-Gene IDs (*93*), structural information-PDB IDs (*94*), protein-protein interaction information- STRING IDs (*95*) and Pathway information - KEGG IDs were taken from their respective databases. The number of PDZ domains and its organization has also been included separately. Information on PDZ interacting proteins were obtained from IntAct database (*96*) that is the largest molecular interaction network database which includes all the interacting partners of a protein. In addition, the Jmol application is integrated for visualization of protein three-dimensional structure. Sequences of all PDZ-containing proteins were assimilated to form the source database of PDZ-BLAST (Basic Local alignment Search Tool). The stand-alone BLAST (*97, 98*) feature was downloaded from NCBI offline BLAST executables site (http://blast.ncbi.nlm.nih.gov/Blast.cgi?CMD=Web&PAGE_TYPE=BlastDocs&DOC_TYPE=Download) and integrated in the database employing a Java script.

The results can be generated by a Java script invoked command prompt in the windows where a bat file containing the Blastp command runs generating an output file which is exported to the webserver using JavaScript. For searching and homology scoring functions, default matrices of BLAST (*97, 98*) were used. Importantly PDZ*ome* also includes information on mutations in the PDZ containing proteins, which is obtained not only from the PMDB but also through manual curation from updated literature. The phenotypic implications, if any, associated with each of these mutations have also been

included in the PDZ*ome* output. Extensive manual curation was also performed for obtaining information on the association of PDZ containing proteins with different pathological conditions. PDZ*ome* thus provides crucial information on associated diseases and mutations for PDZ containing proteins. The entire data takes into consideration all PDZ proteins and can be downloaded in '*.csv'* format from download page.

6.2.3 Database Integration:

PDZ*ome* database was developed with Javascript using Eclipse Juno software development environment. For data integration and parsing, programs were written in JavaScript and Perl. These programs were used to search and parse the data on PDZ proteins and their interacting partners from flat files to create output files in MySQL Tables. All MySQL queries to the databases were implemented in a JavaScript page using JDBC connection Java-based data access technology. The database was uploaded on windows based TomCat 6.0 Apache server. The entire data integration server linking was done using Eclipse Juno (Oracle Inc.) Software Development Environment (SDE). Eclipse is a multi-language Integrated Development Environment (IDE) comprising a base workspace and an extensible plug-in system for customizing the environment which is widely used for database and software development. This database has been constructed using various sources of PDZ containing proteins' sequences, and information on their structure and interacting partners. The information so compiled not only includes well established interacting partners but also putative ones that can prove to be useful leads for further investigation by researchers. This wide range of data was

amalgamated together to form a new and comprehensive knowledge-base for PDZ proteins.

6.3 Results and Discussion

6.3.1 Database Availability and Implementation

PDZ*ome* Database is available online through ACTREC Home Page (http://www.actrec.gov.in/) under 'Database & Tools' (http://www.actrec.gov.in:8080/Pdzome1/jsp/index.jsp) and has an easy to browse web interface. End user can retrieve complete information of a particular protein entry using a Uniprot Protein name, Gene IDs, String IDs, KEGG IDs, protein sequence, Pfam ID and PDB IDs. It also includes information on mutations in the PDZ containing proteins, obtained not only from the PMDB (Protein Mutant Database) but also through manual curation from literature as seen in Figure 6.3. Our manually curated data from PMDB and PubMed on the association of PDZ containing proteins with different pathological conditions significantly enhances the value of the provided information. PDZ BLAST is accessible to end user through the hyperlink provided in the main web and the query sequence can be entered either manually by pasting FASTA sequence in respective search box or by uploading a FASTA sequence file. Results can be downloaded in a text file from the BLAST result page. The links provided in the database highly expand the annotations of the PDZ*ome*, and will enable end-user to have access to every bit of required information on a single arena (Figure 6.4).

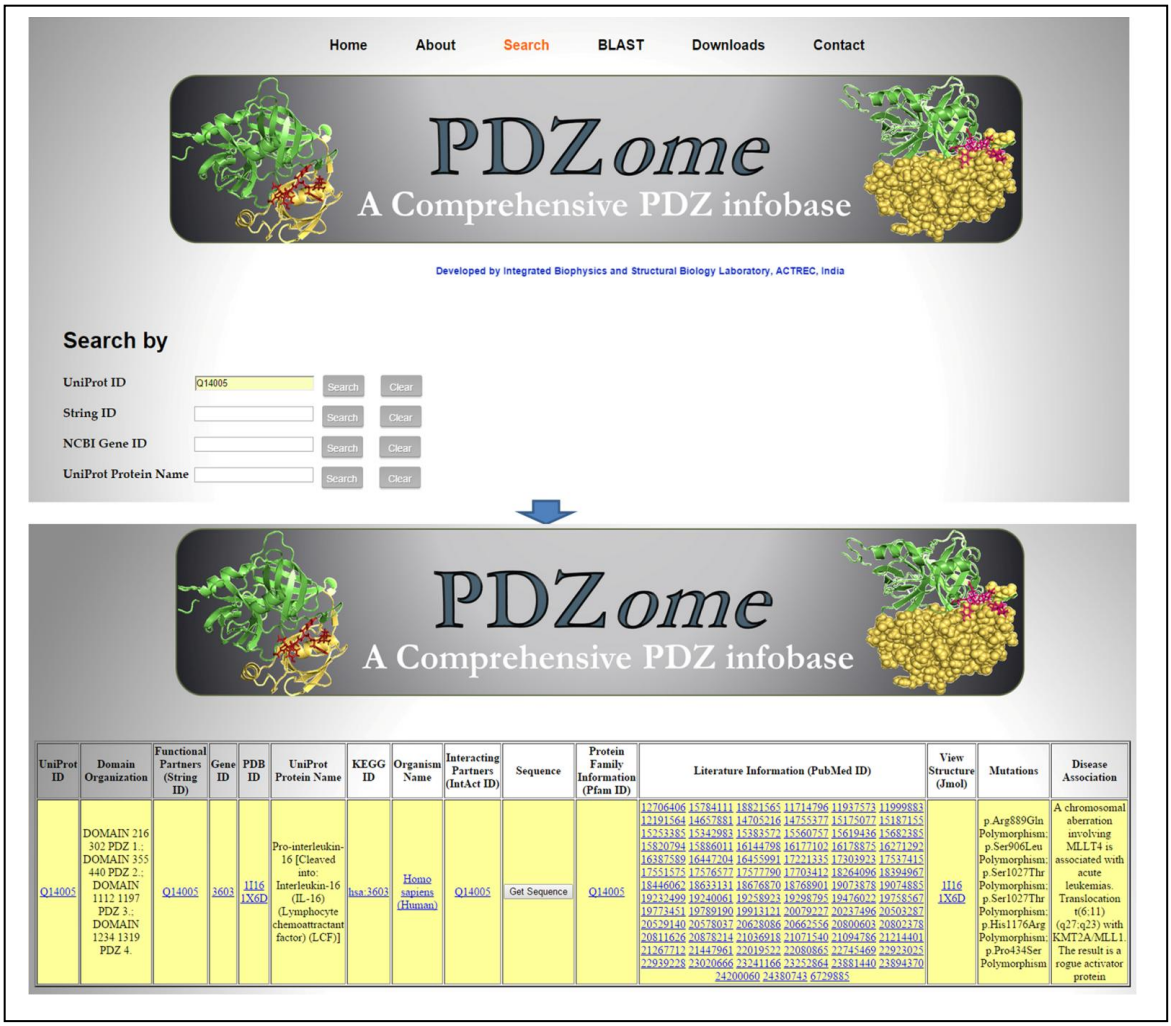

Figure 6.4. The PDZ*ome* graphical user-interface (GUI) and output. The screenshots represent the output generated by the database on being queried for one of the proteins in the search page.

6.3.2 Discussion

A large number of genes have been annotated over the last decade with the exponential increase in the number of depositions in NCBI and other sources. Of these, about 4,00,000 protein sequences have been annotated in UniprotKB. This provides an exciting as well as challenging prospect of studying these newly identified and annotated proteins. Categorizing proteins, though important is a relatively simple job compared to their

structural and functional characterization. With UniProtKB undertaking most of the annotations, and Structural Genomics Consortium carrying out high throughput structure determination (Figure 6.5), new avenues and interesting possibilities in studying important category of proteins such as PDZ are more pronounced than ever thus necessitating the requirement for a dedicated database on this domain.

The existing PDZ domain database, PDZBase currently contains approximately 300 proteins and their interactions (*54*). The information on interacting partners in PDZBase is based on *in vivo* or *in vitro* experiments. However interactions obtained from high throughput methods alone were excluded (*54*). In the current context, where voluminous data is being generated increasingly, this database provides minimal information on PDZ proteins and leads from predicted studies.

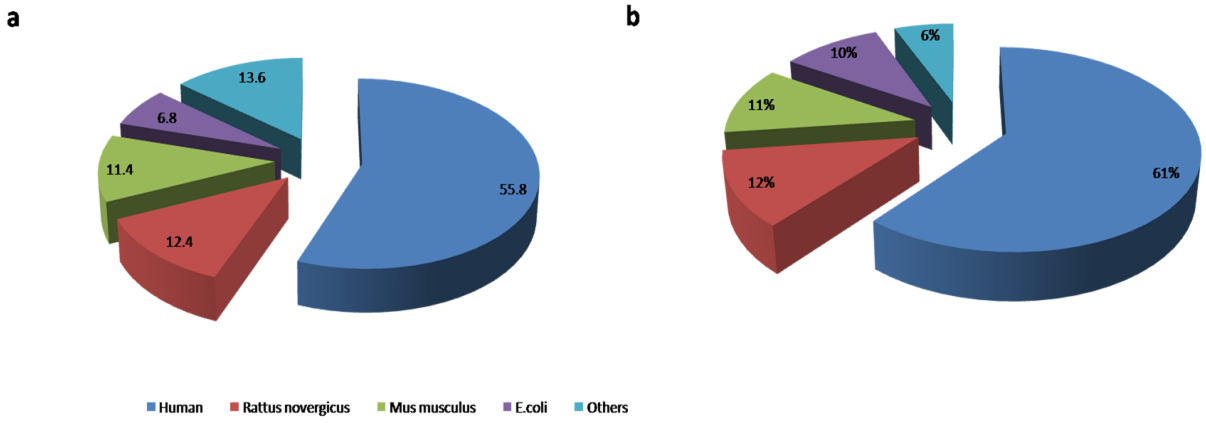

Figure 6.5. Pie chart representation of the structures solved for PDZ proteins. a. A total of 449 structures for the PDZ domains alone are deposited over the years with the distribution in the different organisms mentioned. b. The total deposited structures for proteins comprising one or more PDZ domains are 715, with those for *Homo sapiens* being predominant.

Chapter 7

Conclusions and Future Perspective

7.1 Conclusions

HtrA2 is a pro-apoptotic serine protease that plays a pivotal role in maintaining cellular homeostasis by mediating apoptosis. This multidomain trimeric protease has unique proapoptotic properties as it is associated with both caspase-dependent and independent cellular pathway. One of our aims was to understand the structural dynamics that regulates activation and specificity of HtrA2. Its association with numerous deadly diseases including cancer makes it an important therapeutic target. The model for allosteric regulation that we have deduced might be of great utility for modulating its activity *in vivo*.

HAX1 on the other hand is a ubiquitously expressed anti-apoptotic protein which is predominantly localized to mitochondria. Studies have also established HAX1 to be a binding partner of HtrA2 suggesting an alternate novel apoptotic pathway. Despite this information, the structural details, stoichiometry and mechanism of HtrA2-HAX1 interaction and the subsequent event in the mitochondria are still to be elucidated. Thus, we aimed at structural and functional characterization of HtrA2-HAX1 interaction. The domains and residues at the interface of HtrA2 and HAX1 that might be critical for their interaction were identified by multiple approaches. The protease domain in HtrA2 and not the canonical protein-protein interaction domain PDZ, was involved in the interaction with HAX1. The putative residues thus identified were modified by site-directed mutagenesis to check if there is any abrogation in the interaction due to the mutation. Of all the residues predicted R74 and R76 in HtrA2 and P174 and D176 in HAX1 were identified as critical by pull-down studies and further confirmed by western blotting. One

of the novel findings of this study was that HAX1 is an activator of HtrA2. This might open new avenues of research in context of these proteins.

To functionally characterize the interaction among proteins in a complex, it is essential to study their interaction in the presence of different interacting partners. HtrA2 has been reported to interact with XIAP (*6*) and PARL (*8*) respectively under different scenarios. The HtrA2-HAX1 interaction was studied in the presence of PARL and XIAP respectively. From the preliminary enzyme assay results, it can be observed that the presence of HAX1 does not significantly increase the rate of XIAP degradation by HtrA2. This calls for further studies into this context to get a clearer picture of the mechanism of interaction.

These studies put together could lead a way to elucidate the mechanism ensuing HtrA2-HAX1 interaction. After extensive experimental validation, this information can be utilized for designing small molecule inhibitors and allosteric peptide modulators in therapeutic strategies against cancer and other diseases.

7.2 Future perspective

i. Information obtained on the allosteric modulators of HtrA2 can be utilized for high throughput screening of pharma-grade peptide modulators. These peptides can be checked for their specificity *in vivo* after testing its toxicity *ex vivo*.

ii. The information obtained on the mode of interaction of HtrA2- HAX1 as a result of our studies can be harnessed for generating peptidomimetics.

iii. The studies on the PARL-HtrA2-HAX1 complex can be further understood by detailed *ex vivo* and *in vivo* studies

References

1. Elmore, S. (2007) Apoptosis: a review of programmed cell death, *Toxicologic pathology 35*, 495-516.
2. Fadeel, B., and Orrenius, S. (2005) Apoptosis: a basic biological phenomenon with wide-ranging implications in human disease, *J Intern Med 258*, 479-517.
3. Philchenkov, A. (2004) Caspases: potential targets for regulating cell death, *J Cell Mol Med 8*, 432-444.
4. Cilenti, L., Soundarapandian, M. M., Kyriazis, G. A., Stratico, V., Singh, S., Gupta, S., Bonventre, J. V., Alnemri, E. S., and Zervos, A. S. (2004) Regulation of HAX-1 anti-apoptotic protein by Omi/HtrA2 protease during cell death, *The Journal of biological chemistry 279*, 50295-50301.
5. Trencia, A., Fiory, F., Maitan, M., Vito, P., Barbagallo, A., Perfetti, A., Miele, C., Ungaro, P., Oriente, F., Cilenti, L., Zervos, A., Formisano, P., and Beguinot, F. (2004) Omi/HtrA2 promotes cell death by binding and degrading the anti-apoptotic protein ped/pea-15, *J Biol Chem. 279*, 46566-46572.
6. Suzuki, Y., Takahashi-Niki, K., Akagi, T., Hashikawa, T., and Takahashi, R. (2004) Mitochondrial protease Omi/HtrA2 enhances caspase activation through multiple pathways, *Cell Death Differ 11*, 208-216.
7. Ma, X., Kalakonda, S., Srinivasula, S. M., Reddy, S. P., Platanias, L. C., and Kalvakolanu, D. V. (2007) GRIM-19 associates with the serine protease HtrA2 for promoting cell death, *Oncogene 26*, 4842-4849.
8. Chao, J. R., Parganas, E., Boyd, K., Hong, C. Y., Opferman, J. T., and Ihle, J. N. (2008) Hax1-mediated processing of HtrA2 by Parl allows survival of lymphocytes and neurons, *Nature 452*, 98-102.
9. Martin, T. A., and Jiang, W. G. (2009) Loss of tight junction barrier function and its role in cancer metastasis, *Biochimica et biophysica acta 1788*, 872-891.
10. Sharkey, J., Khong, T., and Spencer, A. (2007) PKC412 demonstrates JNK-dependent activity against human multiple myeloma cells, *Blood 109*, 1712-1719.
11. Poulsom, R., Forbes, S. J., Hodivala-Dilke, K., Ryan, E., Wyles, S., Navaratnarasah, S., Jeffery, R., Hunt, T., Alison, M., Cook, T., Pusey, C., and Wright, N. A. (2001) Bone marrow contributes to renal parenchymal turnover and regeneration, *J Pathol 195*, 229-235.
12. Yamamura, Y., Hua, X., Bergelson, S., and Lodish, H. F. (2000) Critical role of Smads and AP-1 complex in transforming growth factor-beta -dependent apoptosis, *J Biol Chem 275*, 36295-36302.
13. Wong, R. S. (2011) Apoptosis in cancer: from pathogenesis to treatment, *J Exp Clin Cancer Res 30*, 87.
14. Lordan, S., Mackrill, J. J., and O'Brien, N. M. (2008) Involvement of Fas signalling in 7beta-hydroxycholesterol-and cholesterol-5beta,6beta-epoxide-induced apoptosis, *Int J Toxicol 27*, 279-285.
15. Lai, S. K., Wong, C. H., Lee, Y. P., and Li, H. Y. (2011) Caspase-3-mediated degradation of condensin Cap-H regulates mitotic cell death, *Cell Death Differ 18*, 996-1004.
16. Qian, Y., Banerjee, S., Grossman, C. E., Amidon, W., Nagy, G., Barcza, M., Niland, B., Karp, D. R., Middleton, F. A., Banki, K., and Perl, A. (2008) Transaldolase deficiency influences the pentose phosphate pathway, mitochondrial homoeostasis and apoptosis signal processing, *Biochem J 415*, 123-134.

17. Kroemer, G., Galluzzi, L., and Brenner, C. (2007) Mitochondrial membrane permeabilization in cell death, *Physiological reviews 87*, 99-163.
18. Loeder, S., Zenz, T., Schnaiter, A., Mertens, D., Winkler, D., Dohner, H., Debatin, K. M., Stilgenbauer, S., and Fulda, S. (2009) A novel paradigm to trigger apoptosis in chronic lymphocytic leukemia, *Cancer Res 69*, 8977-8986.
19. Chien, J., Campioni, M., Shridhar, V., and Baldi, A. (2009) HtrA serine proteases as potential therapeutic targets in cancer, *Curr Cancer Drug Targets 9*, 451-468.
20. Singh, N., Kuppili, R. R., and Bose, K. (2011) The structural basis of mode of activation and functional diversity: a case study with HtrA family of serine proteases, *Archives of biochemistry and biophysics 516*, 85-96.
21. Hansen, G., and Hilgenfeld, R. (2013) Architecture and regulation of HtrA-family proteins involved in protein quality control and stress response, *Cellular and molecular life sciences : CMLS 70*, 761-775.
22. Zurawa-Janicka, D., Skorko-Glonek, J., and Lipinska, B. (2010) HtrA proteins as targets in therapy of cancer and other diseases, *Expert Opin Ther Targets 14*, 665-679.
23. Zurawa-Janicka, D., Narkiewicz, J., and Lipinska, B. (2007) [Characterization of the HtrA family of proteins], *Postepy Biochem 53*, 27-36.
24. Jones, J. M., Datta, P., Srinivasula, S. M., Ji, W., Gupta, S., Zhang, Z., Davies, E., Hajnoczky, G., Saunders, T. L., Van Keuren, M. L., Fernandes-Alnemri, T., Meisler, M. H., and Alnemri, E. S. (2003) Loss of Omi mitochondrial protease activity causes the neuromuscular disorder of mnd2 mutant mice, *Nature 425*, 721-727.
25. Suzuki, Y., Imai, Y., Nakayama, H., Takahashi, K., Takio, K., and Takahashi, R. (2001) A serine protease, HtrA2, is released from the mitochondria and interacts with XIAP, inducing cell death, *Mol Cell 8*, 613-621.
26. Kadomatsu, T., Mori, M., and Terada, K. (2007) Mitochondrial import of Omi: the definitive role of the putative transmembrane region and multiple processing sites in the amino-terminal segment, *Biochemical and biophysical research communications 361*, 516-521.
27. Li, W., Srinivasula, S. M., Chai, J., Li, P., Wu, J. W., Zhang, Z., Alnemri, E. S., and Shi, Y. (2002) Structural insights into the pro-apoptotic function of mitochondrial serine protease HtrA2/Omi, *Nat Struct Biol 9*, 436-441.
28. Nam, M. K., Seong, Y. M., Park, H. J., Choi, J. Y., Kang, S., and Rhim, H. (2006) The homotrimeric structure of HtrA2 is indispensable for executing its serine protease activity, *Experimental & molecular medicine 38*, 36-43.
29. Vande Walle, L., Lamkanfi, M., and Vandenabeele, P. (2008) The mitochondrial serine protease HtrA2/Omi: an overview, *Cell Death Differ 15*, 453-460.
30. Bejugam, P. R., Kuppili, R. R., Singh, N., Gadewal, N., Chaganti, L. K., Sastry, G. M., and Bose, K. (2013) Allosteric regulation of serine protease HtrA2 through novel non-canonical substrate binding pocket, *PLoS One 8*, e55416.
31. Zurawa-Janicka, D., Jarzab, M., Polit, A., Skorko-Glonek, J., Lesner, A., Gitlin, A., Gieldon, A., Ciarkowski, J., Glaza, P., Lubomska, A., and Lipinska, B. (2013) Temperature-induced changes of HtrA2(Omi) protease activity and structure, *Cell Stress Chaperones 18*, 35-51.
32. Chaganti, L. K., Kuppili, R. R., and Bose, K. (2013) Intricate structural coordination and domain plasticity regulate activity of serine protease HtrA2, *FASEB J 27*, 3054-3066.
33. Marabese, M., Mazzoletti, M., Vikhanskaya, F., and Broggini, M. (2008) HtrA2 enhances the apoptotic functions of p73 on bax, *Cell death and differentiation 15*, 849-858.

34. Liu, J., Xu, J., Wang, G., Yang, M., and Guo, L. (2009) [Study advancement of calpain and apoptosis following cerebral ischemia], *Sheng Wu Yi Xue Gong Cheng Xue Za Zhi 26*, 1150-1153.
35. Chien, Y. C., Huang, Y. J., Hsu, C. S., Chao, J. C., and Liu, J. F. (2009) Maternal lactation characteristics after consumption of an alcoholic soup during the postpartum 'doing-the-month' ritual, *Public Health Nutr 12*, 382-388.
36. Suzuki, Y., Demoliere, C., Kitamura, D., Takeshita, H., Deuschle, U., and Watanabe, T. (1997) HAX-1, a novel intracellular protein, localized on mitochondria, directly associates with HS1, a substrate of Src family tyrosine kinases, *Journal of immunology 158*, 2736-2744.
37. Lees, D. M., Hart, I. R., and Marshall, J. F. (2008) Existence of multiple isoforms of HS1-associated protein X-1 in murine and human tissues, *Journal of molecular biology 379*, 645-655.
38. Fadeel, B., and Grzybowska, E. (2009) HAX-1: a multifunctional protein with emerging roles in human disease, *Biochimica et biophysica acta 1790*, 1139-1148.
39. Kang, Y. J., Jang, M., Park, Y. K., Kang, S., Bae, K. H., Cho, S., Lee, C. K., Park, B. C., Chi, S. W., and Park, S. G. (2010) Molecular interaction between HAX-1 and XIAP inhibits apoptosis, *Biochemical and biophysical research communications 393*, 794-799.
40. Matsuda, G., Nakajima, K., Kawaguchi, Y., Yamanashi, Y., and Hirai, K. (2003) Epstein-Barr virus (EBV) nuclear antigen leader protein (EBNA-LP) forms complexes with a cellular anti-apoptosis protein Bcl-2 or its EBV counterpart BHRF1 through HS1-associated protein X-1, *Microbiology and immunology 47*, 91-99.
41. Rhodes, D. R., Yu, J., Shanker, K., Deshpande, N., Varambally, R., Ghosh, D., Barrette, T., Pandey, A., and Chinnaiyan, A. M. (2004) ONCOMINE: a cancer microarray database and integrated data-mining platform, *Neoplasia 6*, 1-6.
42. Klein, C., Grudzien, M., Appaswamy, G., Germeshausen, M., Sandrock, I., Schaffer, A. A., Rathinam, C., Boztug, K., Schwinzer, B., Rezaei, N., Bohn, G., Melin, M., Carlsson, G., Fadeel, B., Dahl, N., Palmblad, J., Henter, J. I., Zeidler, C., Grimbacher, B., and Welte, K. (2007) HAX1 deficiency causes autosomal recessive severe congenital neutropenia (Kostmann disease), *Nature genetics 39*, 86-92.
43. Yedavalli, V. S., Shih, H. M., Chiang, Y. P., Lu, C. Y., Chang, L. Y., Chen, M. Y., Chuang, C. Y., Dayton, A. I., Jeang, K. T., and Huang, L. M. (2005) Human immunodeficiency virus type 1 Vpr interacts with antiapoptotic mitochondrial protein HAX-1, *J Virol 79*, 13735-13746.
44. Vafiadaki, E., Arvanitis, D. A., Pagakis, S. N., Papalouka, V., Sanoudou, D., Kontrogianni-Konstantopoulos, A., and Kranias, E. G. (2009) The anti-apoptotic protein HAX-1 interacts with SERCA2 and regulates its protein levels to promote cell survival, *Mol Biol Cell 20*, 306-318.
45. Mirmohammadsadegh, A., Tartler, U., Michel, G., Baer, A., Walz, M., Wolf, R., Ruzicka, T., and Hengge, U. R. (2003) HAX-1, identified by differential display reverse transcription polymerase chain reaction, is overexpressed in lesional psoriasis, *The Journal of investigative dermatology 120*, 1045-1051.
46. Jeyaraju, D. V., Cisbani, G., De Brito, O. M., Koonin, E. V., and Pellegrini, L. (2009) Hax1 lacks BH modules and is peripherally associated to heavy membranes: implications for Omi/HtrA2 and PARL activity in the regulation of mitochondrial stress and apoptosis, *Cell Death Differ 16*, 1622-1629.
47. McQuibban, G. A., Saurya, S., and Freeman, M. (2003) Mitochondrial membrane remodelling regulated by a conserved rhomboid protease, *Nature 423*, 537-541.

48. Jeyaraju, D. V., Xu, L., Letellier, M. C., Bandaru, S., Zunino, R., Berg, E. A., McBride, H. M., and Pellegrini, L. (2006) Phosphorylation and cleavage of presenilin-associated rhomboid-like protein (PARL) promotes changes in mitochondrial morphology, *Proc Natl Acad Sci U S A 103*, 18562-18567.
49. Sik, A., Passer, B. J., Koonin, E. V., and Pellegrini, L. (2004) Self-regulated cleavage of the mitochondrial intramembrane-cleaving protease PARL yields Pbeta, a nuclear-targeted peptide, *J Biol Chem 279*, 15323-15329.
50. Boeckmann, B., Bairoch, A., Apweiler, R., Blatter, M. C., Estreicher, A., Gasteiger, E., Martin, M. J., Michoud, K., O'Donovan, C., Phan, I., Pilbout, S., and Schneider, M. (2003) The SWISS-PROT protein knowledgebase and its supplement TrEMBL in 2003, *Nucleic Acids Res 31*, 365-370.
51. Campagne, F., Bettler, E., Vriend, G., and Weinstein, H. (2003) Batch mode generation of residue-based diagrams of proteins, *Bioinformatics 19*, 1854-1855.
52. Dueber, J. E., Yeh, B. J., Chak, K., and Lim, W. A. (2003) Reprogramming control of an allosteric signaling switch through modular recombination, *Science 301*, 1904-1908.
53. Fan, J. S., and Zhang, M. (2002) Signaling complex organization by PDZ domain proteins, *Neurosignals 11*, 315-321.
54. Beuming, T., Skrabanek, L., Niv, M. Y., Mukherjee, P., and Weinstein, H. (2005) PDZBase: a proteinЂ–⌠protein interaction database for PDZ-domains, *Bioinformatics 21*, 827-828.
55. Hung, A. Y., and Sheng, M. (2002) PDZ domains: structural modules for protein complex assembly, *J Biol Chem 277*, 5699-5702.
56. Javier, R. T., and Rice, A. P. (2011) Emerging theme: cellular PDZ proteins as common targets of pathogenic viruses, *J Virol 85*, 11544-11556.
57. Bradford, M. M. (1976) A rapid and sensitive method for the quantitation of microgram quantities of protein utilizing the principle of protein-dye binding, *Anal Biochem 72*, 248-254.
58. Edelhoch, H. (1967) Spectroscopic determination of tryptophan and tyrosine in proteins, *Biochemistry 6*, 1948-1954.
59. Dominguez, C., Boelens, R., and Bonvin, A. M. (2003) HADDOCK: a protein-protein docking approach based on biochemical or biophysical information, *J Am Chem Soc 125*, 1731-1737.
60. Kozakov, D., Beglov, D., Bohnuud, T., Mottarella, S. E., Xia, B., Hall, D. R., and Vajda, S. (2013) How good is automated protein docking?, *Proteins 81*, 2159-2166.
61. Ma, B., Tsai, C., Haliloglu, T., and Nussinov, R. (2011) Dynamic Allostery: Linkers Are Not Merely Flexible, *Structure 19*, 907-917.
62. Jeleń, F., Oleksy, A., Śmietana, K., and Otlewski, J. (2003) PDZ domains □ common players in the cell signaling, *Acta Biochim Pol. 50*, 985-1017.
63. Hung, A., and Morgan, S. (2002) PDZ Domains: Structural Modules for Protein Complex Assembly, *J Biol Chem. 277*, 5699-5702.
64. Li, W., Srinivasula, S., Chai, J., Li, P., Wu, J., Zhang, Z., Alnemri, E., and Shi, Y. (2002) Structural insights into the pro-apoptotic function of mitochondrial serine protease HtrA2/Omi, *Nat. Struct. Biol. 9*, 436-441.
65. Suzuki, Y. T.-N., K., Akagi, T., Hashikawa, T., and Takahashi, R. (2004) Mitochondrial protease Omi/HtrA2 enhances caspase activation through multiple pathways, *Cell Death Differ. 11*, 208-216.
66. Martins, L., Iaccarino, I., Tenev, T., Gschmeissner, S., Totty, N., Lemoine, N., Savopoulos, J., Gray, C., Creasy, C., Dingwall, C., and Downward, J. (2002) The serine protease

Omi/HtrA2 regulates apoptosis by binding XIAP through a reaper-like motif, *J Biol Chem 277*, 439-444.
67. Verhagen, A., Silke, J., Ekert, P., Pakusch, M., Kaufmann, H., Connolly, L., Day, C., Tikoo, A., Burke, R., Wrobel, C., Moritz, R., Simpson, R., and Vaux, D. (2002) HtrA2 promotes cell death through its serine protease activity and its ability to antagonize inhibitor of apoptosis proteins, *J Biol Chem 277*, 445-454.
68. Johnson, F., and Kaplitt, M. (2009) Novel mitochondrial substrates of omi indicate a new regulatory role in neurodegenerative disorders., *PLoS One 4*, e7100.
69. Kooistraa, J., Milojevicb, J., Melacinia, G., and Ortegaa, J. (2009) A new function of human HtrA2 as an amyloid-beta oligomerization inhibitor, *J Alzheimers Dis. 17*, 281-294.
70. Lin, C., Chen, M., Chen, G., Tai, C., and Wu, R. (2011) Novel variant Pro143Ala in HTRA2 contributes to Parkinson's disease by inducing hyperphosphorylation of HTRA2 protein in mitochondria, *Hum Genet. 130*, 817-827.
71. Nam, M., Seong, Y., Park, H., Choi, J., Kang, S., and H., R. (2006) The homotrimeric structure of HtrA2 is indispensable for executing its serine protease activity, *Exp Mol Med. 38*, 36-43.
72. Singh, N., Kuppili, R., and Bose, K. (2011) The structural basis of mode of activation and functional diversity: A case study with HtrA family of serine protease, *Arch Biochem Biophys. 516*, 85-96.
73. Sohn, J., Grant, R., and RT., S. (2010) Allostery is an intrinsic property of the protease domain of DegS: implications for enzyme function and evolution, *J Biol Chem. 285*, 34039-34047.
74. Sherman, W., Day, T., Jacobson, M., Friesner, R., and Farid, R. (2006) Novel procedure for modeling ligand/receptor induced fit effects, *J Med Chem 49*, 534-553.
75. Van Der Spoel, D., Lindahl, E., Hess, B., Groenhof, G., Mark, A., and Berendsen, H. (2005) GROMACS: fast, flexible, and free., *J Comput Chem 26*, 1701-1718.
76. Halgren, T. (2007) New method for fast and accurate binding-site identification and analysis, *69*, 146-148.
77. Ma, S., Song, E., Gao, S., Tian, R., and Gao, Y. (2007) Rapid characterization of the binding property of HtrA2/Omi PDZ domain by validation screening of PDZ ligand library, *Sci China C Life Sci 50*, 412-422.
78. Zhang, Y., Appleton, B., Wu, P., Wiesmann, C., and Sidhu, S. (2007) Structural and functional analysis of the ligand specificity of the HtrA2/Omi PDZ domain, *Protein Sci. 16*, 2454-2471.
79. Bowers, K., Chow, E., Xu, H., Ron, O., Eastwood, M., Gregersen, B., Klepeis, J., Kolossváry, I., Moraes, M., Sacerdoti, F., Salmon, J., Shan, Y., and Shaw, D. (2006) Scalable Algorithms for Molecular Dynamics Simulations on Commodity Clusters, In *Proceedings of the ACM/IEEE Conference on Supercomputing (SC06)*, Florida.
80. Savopoulos, J., Carter, P., Turconi, S., Pettman, G., Karran, E., Gray, C., Ward, R., Jenkins, O., and Creasy, C. (2000) Expression, Purification, and Functional Analysis of the Human Serine Protease HtrA2, *Protein Expr Purif. 19*, 227-234.
81. Ibrahim, A., Mansour, I., Wilson, M., Mokhtar, D., Helal, A., and Al Wakeel, H. (2012) Study of survivin and X-linked inhibitor of apoptosis protein (XIAP) genes in acute myeloid leukemia (AML), *Lab Hematol 18*, 1-10.
82. Nagata, M., Nakayama, H., Tanaka, T., Yoshida, R., Yoshitake, Y., Fukuma, D., Kawahara, K., Nakagawa, Y., Ota, K., Hiraki, A., and .Shinohara, M. (2011) Overexpression of cIAP2

contributes to 5-FU resistance and a poor prognosis in oral squamous cell carcinoma, *Br J Cancer 105*, 1322-1330.
83. Navakanit, R., Graidist, P., Leeanansaksiri, W., and Dechsukum, C. (2007) Growth inhibition of breast cancer cell line MCF-7 by siRNA silencing of Wilms tumor 1 gene, *J Med Assoc Thai 90*, 2416-2421.
84. Sugiyama, H. (1998) Wilms tumor gene (WT1) as a new marker for the detection of minimal residual disease in leukemia, *Leuk Lymphoma. 30*, 55-61.
85. Kraut, J. (1977) Serine proteases: structure and mechanism of catalysis, *Annu Rev Biochem 46*, 331-358.
86. Mazat, J., and Patte, J. (1976) Lysine-sensitive aspartokinase of Escherichia coli K12. Synergy and autosynergy in an allosteric V system, *Biochemistry 15*, 4053-4058.
87. Sohn, J., and Sauer, R. (2009) OMP peptides modulate the activity of DegS protease by differential binding to active and inactive conformations., *Mol Cell 33*, 64-74.
88. Feng, W., Fan, J., Jiang, M., Shi, Y., and Zhang, M. (2002) PDZ7 of glutamate receptor interacting protein binds to its target via a novel hydrophobic surface area, *J Biol Chem 277*, 41140-41146.
89. Christopoulos, A. M., LT., Avlani, V., and Sexton, P. (2004) G protein-coupled receptor allosterism:the promise and the problem(s), In *Biochemical Society*
90. May, L., Leach, K., Sexton, P., and Christopoulos, A. (2007) Allosteric modulation of G protein-coupled receptors, *Annu Rev Pharmacol Toxicol. 47*, 1-51.
91. Berman, H., Westbrook, J., Feng, Z., Gilliland, G., Bhat, T., Weissig, H., Shindyalov, I., and Bourne, P. (2000) The Protein Data Bank., *Nucleic Acids Res. 28*, 235-242.
92. (2012) Reorganizing the protein space at the Universal Protein Resource (UniProt), *Nucleic Acids Res 40*, D71-75.
93. (2015) Database resources of the National Center for Biotechnology Information, *Nucleic Acids Res 43*, D6-D17.
94. Berman, H. M., Westbrook, J., Feng, Z., Gilliland, G., Bhat, T. N., Weissig, H., Shindyalov, I. N., and Bourne, P. E. (2000) The Protein Data Bank, *Nucleic Acids Res 28*, 235-242.
95. Szklarczyk, D., Franceschini, A., Kuhn, M., Simonovic, M., Roth, A., Minguez, P., Doerks, T., Stark, M., Muller, J., Bork, P., Jensen, L. J., and von Mering, C. (2011) The STRING database in 2011: functional interaction networks of proteins, globally integrated and scored, *Nucleic Acids Res 39*, D561-568.
96. Orchard, S., Ammari, M., Aranda, B., Breuza, L., Briganti, L., Broackes-Carter, F., Campbell, N. H., Chavali, G., Chen, C., del-Toro, N., Duesbury, M., Dumousseau, M., Galeota, E., Hinz, U., Iannuccelli, M., Jagannathan, S., Jimenez, R., Khadake, J., Lagreid, A., Licata, L., Lovering, R. C., Meldal, B., Melidoni, A. N., Milagros, M., Peluso, D., Perfetto, L., Porras, P., Raghunath, A., Ricard-Blum, S., Roechert, B., Stutz, A., Tognolli, M., van Roey, K., Cesareni, G., and Hermjakob, H. (2014) The MIntAct project--IntAct as a common curation platform for 11 molecular interaction databases, *Nucleic Acids Res 42*, D358-363.
97. Altschul, S. F., Gish, W., Miller, W., Myers, E. W., and Lipman, D. J. (1990) Basic local alignment search tool, *J Mol Biol 215*, 403-410.
98. Camacho, C., Coulouris, G., Avagyan, V., Ma, N., Papadopoulos, J., Bealer, K., and Madden, T. L. (2009) BLAST+: architecture and applications, *BMC Bioinformatics 10*, 421.

OPEN ACCESS Freely available online

PLOS ONE

Allosteric Regulation of Serine Protease HtrA2 through Novel Non-Canonical Substrate Binding Pocket

Pruthvi Raj Bejugam[1☯], Raja R. Kuppili[1☯], Nitu Singh[1], Nikhil Gadewal[1], Lalith K. Chaganti[1], G. Madhavi Sastry[2], Kakoli Bose[1]*

1 Advanced Centre for Treatment, Research and Education in Cancer (ACTREC), Tata Memorial Centre, Kharghar, Navi Mumbai, India, **2** Schrödinger, Sanali Infopark, Banjara Hills, Hyderabad, India

Abstract

HtrA2, a trimeric proapoptotic serine protease is involved in several diseases including cancer and neurodegenerative disorders. Its unique ability to mediate apoptosis via multiple pathways makes it an important therapeutic target. In HtrA2, C-terminal PDZ domain upon substrate binding regulates its functions through coordinated conformational changes the mechanism of which is yet to be elucidated. Although allostery has been found in some of its homologs, it has not been characterized in HtrA2 so far. Here, with an *in silico* and biochemical approach we have shown that allostery does regulate HtrA2 activity. Our studies identified a novel non-canonical selective binding pocket in HtrA2 which initiates signal propagation to the distal active site through a complex allosteric mechanism. This non-classical binding pocket is unique among HtrA family proteins and thus unfolds a novel mechanism of regulation of HtrA2 activity and hence apoptosis.

Citation: Bejugam PR, Kuppili RR, Singh N, Gadewal N, Chaganti LK, et al. (2013) Allosteric Regulation of Serine Protease HtrA2 through Novel Non-Canonical Substrate Binding Pocket. PLoS ONE 8(2): e55416. doi:10.1371/journal.pone.0055416

Editor: Srinivasa M. Srinivasula, IISER-TVM, India

Received September 6, 2012; **Accepted** December 22, 2012; **Published** February 14, 2013

Funding: The project was funded by a grant provided by Department of Biotechnology (DBT), Govt. of India. The funders had no role in study design, data collection and analysis, decision to publish, or preparation of the manuscript.

Competing Interests: GMS is employed by Schrodinger Inc. This does not alter the authors' adherence to all the PLOS ONE policies on sharing data and materials. The authors declare that they do not have any conflict of interests.

* E-mail: kbose@actrec.gov.in

☯ These authors contributed equally to this work.

Introduction

Multidomain proteins due to their structural complexity require different levels of regulatory mechanisms for executing cellular functions efficiently within a specified time period. Allosteric modulation of conformations is one such mechanism which often helps a protein to regulate a functional behaviour such as for an enzyme to attain an active functional state upon ligand or substrate binding. In allostery, sometimes there are large conformational changes that require significant rotations and translations of individual domains at the timescales of microsecond to millisecond. While in some other cases, minimal structural perturbation helps in propagation of the signal in an energy efficient way to the functional domain where movement is mainly restricted to the side chains, loops and linker regions and which occur within picosecond to nanosecond timescales [1]. PDZ (post-synaptic density-95/discs large/zonula occludens-1) domains that are involved in myriads of protein-protein interactions [2,3] exhibit minimal structural changes during allosteric propagation. These domains have multiple ligand docking sites and are known to possess unique dynamics that regulate conformation of the functional site from a distal region.

HtrA2 (High temperature requirement protease A2), a PDZ bearing protein, is a mitochondrial trimeric pyramidal proapoptotic serine protease with complex domain architecture whose activity is likely regulated by interdomain crosstalk and structural plasticity [4]. Mature HtrA2 comprises 325 amino acids with residues S173, D95 and H65 forming the catalytic triad which is buried 25 Å above the base of the pyramid suggesting requirement of conformational changes for its activation. Apart from PDZ, this multidomain protein has a short N-terminal region, a serine protease domain and a non-conserved flexible linker at the PDZ-protease interface [4]. HtrA2 is involved in both caspase dependent as well as caspase independent apoptotic pathways [5,6,7]. Literature suggests it might have chaperoning functions as well and recently has been found to be associated with several neurodegenerative disorders [8,9,10]. Based on information from literature [4,11], this multitasking ability of HtrA2 can be attributed to its serine protease activity which is intricately coordinated by its unique substrate binding process, complex trimeric structure, interdomain networking and conformational plasticity. However, the unbound inactive form of the crystal structure with partially missing active site loops and flexible PDZ-protease linker has been unable to unambiguously determine the role of dynamics and allostery if any in HtrA2 activation and specificity. Therefore, to understand the molecular details of its mechanism of action, dynamics study at the substrate binding site and active site pocket becomes imperative.

HtrA2 belongs to a serine protease family that is conserved from prokaryotes to humans [12] where allostery is a common mechanism for protease activation in some of its homologs. DegS, a bacterial counterpart of HtrA2, allosterically stabilizes the active site pocket upon substrate binding at the distal PDZ domain [13]. DegP, the most extensively studied protein of the family, has a cage-like hexameric structure whose activation is regulated by allostery and oligomerization. Peptide binding to distal PDZ1

domain leads to rearrangement of the catalytic pocket into enzymatically competent form that readily oligomerizes and renders stability to the active conformation [14].

With an aim at understanding the conformational changes and structural plasticity that govern HtrA2 activity and specificity, we took an *in silico* approach to study the movements of flexible regions of the protein upon ligand binding. The PDZ domain of HtrA2 has a known hydrophobic substrate binding YIGV pocket (similar to GLGF motif) which is deeply embedded within the trimeric protein structure with P225 and V226 from the serine protease domain occupying the groove [4,15]. This structural arrangement makes it impossible for substrate protein to bind without significant conformational changes. Thus, to examine whether allosteric modulation through an alternative site is involved in substrate binding and catalysis of HtrA2, molecular dynamics simulation (MDS) approach with a bound peptide activator was used to look into the structural rearrangements that occur in nanosecond time scale. Although the information usually obtained from MDS is restricted primarily to movements in the accessible and flexible regions of a protein, it nonetheless contributes significantly towards understanding of the overall structural rearrangement and dynamics during its allosteric activation. In our study, we modelled the entire mature protease by filling in the missing regions using Prime 3.0 [16], followed by energy minimization with GRoningen MAchine for Chemical Simulation or GROMACS [17]. Identification of the putative binding site(s) on HtrA2 was done using SiteMap 2.5 [18] and the selective binding pocket (SBP) for the ligand was chosen based on optimum energy parameters. Peptides at SBP were docked from our peptide library that was generated based on available literature reports [19,20,21] and structural complementarities. MDS of the docked structures was done using Desmond 2010 [22] which provided critical information on loop and linker movements in HtrA2. These results combined with mutational and enzymology studies show that upon activator binding at the novel allosteric pocket, SBP, the linker at the PDZ-protease interface and loops L1, LA and LD around the catalytic groove undergo rearrangements in a coordinated manner so as to form an efficient active site pocket. Moreover, the PDZ domains mediate intersubunit interactions which stabilize the oxyanion hole. These observations highlight the importance of allostery which might be an important prerequisite for an active conformation of the trimeric protease.

Results

Identification of Selective Binding Pocket (SBP)

The high resolution crystal structure of HtrA2 [4] (Figure 1a) that lacked flexible loops, linkers and some N-terminal residues was the target protein for our studies. These regions were modelled and energy minimised as described under Methods section. Comparison of refined model with unrefined structure showed significant movements of the loops defining new binding sites on the protein surface. The linker at SPD-PDZ interface moved towards α7 of PDZ domain whereas the linker in the protease domain moved closer to the SPD-PDZ linker so as to form a groove (Figure 1b).

Among the five possible putative binding sites that were identified, Site2 or SBP (Figure 1c) that encompasses the groove generated by SPD-PDZ linker, protease and PDZ domains attained the best score (Table 1). The site score takes into account parameters such as volume, density, solvent exposure, hydrophilic and hydrophobic nature of residues and donor to acceptor ratio and hence is a comprehensive representation of the possibility of it being a binding site.

SBP has optimum volume and contacts available including maximum hydrogen donor and acceptor groups that are crucial for interacting with peptides. The size of the site is very important since the binding peptides have 6–7 residues and the site needs to be large enough to accommodate them. It also has highest hydrophobicity which makes it the best interaction site and hence used in our studies. Although sites 1 and 3 have scores closer to that of SBP, taking into account all the above-mentioned parameters, SBP was chosen for further docking and MDS studies.

Peptide Docking Show Similar Interacting Residues

Here, we have used a holistic approach in designing activator peptides where different techniques were applied in parallel so as to conduct a comprehensive search for a signature pattern that would dock at SBP. In one method, replicas for functional groups were chosen based on sequence and structural complementarities with hydrophobic SBP which were used for generating small molecular fragments. Scores obtained from docking these small molecules (Table S1) provided the framework for designing different combinations of tetrapeptides as shown in Table S2. With leads from literature and *in silico* structure-guided design, Gly and Val residues were added at N- and C-termini respectively of some peptides which subsequently increased the docking scores from −6 to −10 kcal/mol.

Similarly, two peptides previously reported in the literature as well peptides designed from the putative binding sites in pea-15 and Hax-1 also interacted well with SBP. Analysis of docking results with all these different peptides show interaction with similar residues of SBP as observed in ligplot (Figure S1). However, the control peptide KNNPNNAHQN, which has quite a few asparagine residues, is an ideal sequence to act as negative peptide for the pocket due to its stereochemical properties [19], did not bind to SBP demonstrating the specificity of designed peptides.

From the above extensive docking analysis, N216, S217, S219, E292 and E296 in SBP were found to be common for most of the peptide interactions (Figures 2a–b). Of these residues, N216, S217, S219 belong to the linker region while E292 and E296 to the PDZ domain that were either involved in hydrogen bond formation or Van der Waals interaction with the peptides. This result suggests that SBP might be the possible binding site and therefore a prospective putative allosteric site.

The role of some of these important residues in allostery if any and its subsequent effect on catalytic activity and substrate turnover was further probed by enzymology studies as described later in the text.

MDS Analyses of HtrA2 and HtrA2– Peptide Complexes

The peptides GSAWFSF was chosen for MDS studies as it gave the best XP and E-model scores (Table 2). GQYYFV has been reported to be a well known activator of HtrA2 [19] and hence used as another representative peptide for simulation studies. Moreover, the two peptides were chosen such that one is a designed peptide (GQYYFV) while the other is a part of a well-known HtrA2 binding protein Pea-15 (GSAWFSF). In addition to this, GQYYFV with docking score lesser than GSAWFSF was chosen for MDS analysis to understand whether different affinity for the substrate results in similar movements in the protease. MDS analyses of HtrA2-GQYYFV and HtrA2-GSAWFSF complexes demonstrated significant difference in conformation as well as dynamics when compared with unbound HtrA2. Visual inspection of the domain wise movements in peptide bound HtrA2 indicated large fluctuations in hinge/linker region (211–226) as shown in Figures 3a and b. Although these

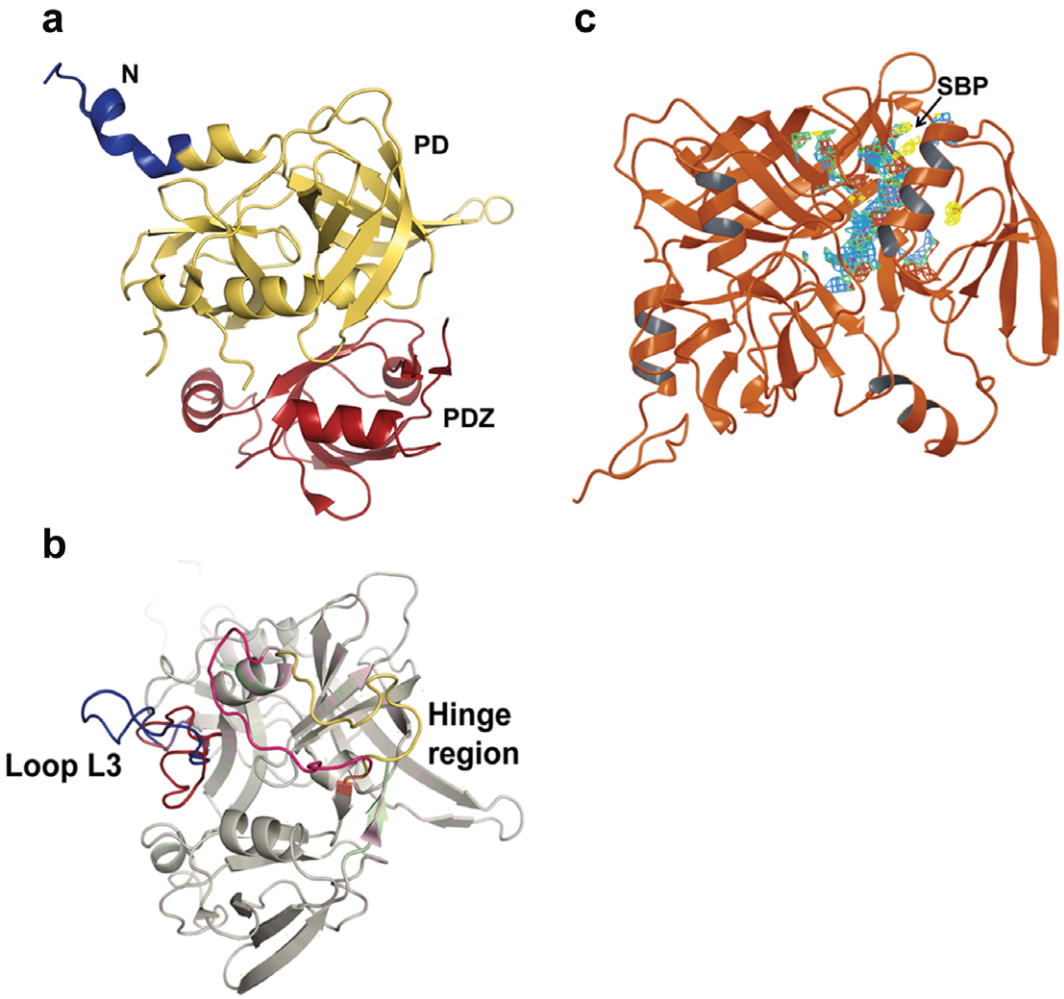

Figure 1. Ribbon model of HtrA2 structures (PDB ID: 1LCY). a. Domain organization of HtrA2 protease which comprises N-terminal region (blue), protease domain denoted as PD (yellow) and PDZ domain (red) at C-terminal end. b. Structural alignment of loop refined (light magenta) and unrefined (light green) structures of HtrA2 protein with modelled N-terminal AVPS, loop L3 (residues 142–162) and hinge region (residues 211–225) built with Prime (Schrödinger 2011). On refinement, loop L3 and hinge region are reorganized so as to define new regions at the protease and PDZ domain interface. c. Selective binding pocket (SBP) on HtrA2. The energy minimised structure of HtrA2 after modelling flexible regions in the protein is represented as a ribbon model. The binding site designated as SBP, selected on the basis of the Sitemap score and residue analyses, is located at the interface of PDZ and protease domain and shown as a multi-coloured mesh.
doi:10.1371/journal.pone.0055416.g001

movements were larger for GSAWFSF than GQYYFV bound complex, the movement pattern remained similar in these two peptides. Enhanced dynamic movement in the former complex could be attributed to the peptide length (heptameric as compared to hexameric in the latter). Domain wise RMSD analysis of these trajectories provided quantitative output of deviations with respect to time. The trajectory graphs (Figures 3c–e) show that along the entire sequence, hinge region (211 −226) has RMSD of 2.5 Å for

Table 1. Putative binding sites in HtrA2 identified by SiteMap tool.

Site Number from SiteMap	Residues present in the site	Site score
Site 2	K214, K215, N216,S217,S219, R226, R227, Y228, I229, G230,V231,M232,M233, L234, T235, L236, S237, S239, I240, E243, H256, K262, I264,Q289, N290, A291,E292, Y295,E 296, R299, S302	1.092716
Site 1	H65, D69, R71, A89, V90, P92, D95,T324	0.957142
Site 3	N48, H65, D169, S173,K191, M232, H261,L265	0.936056
Site 4	V192, F251	0.807891
Site 5	I33,L34,D35,R36,V73,R74	0.673032

doi:10.1371/journal.pone.0055416.t001

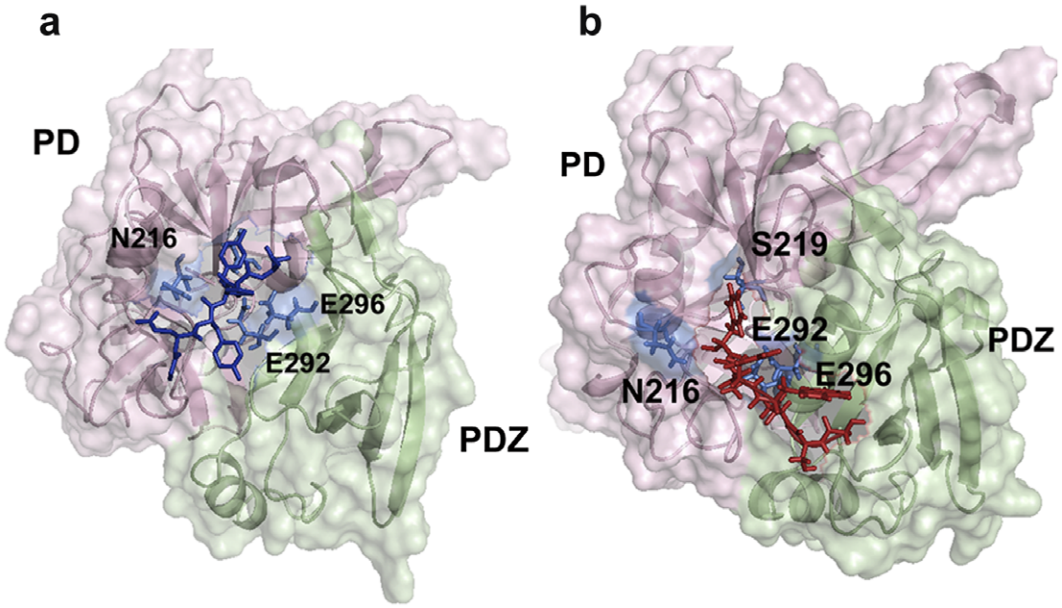

Figure 2. Representative surface structures of peptide activator docked HtrA2. a. Peptide GSAWFSF -HtrA2 complex and b. Peptide GQYYFV-HtrA2 complex. The former peptide represents putative SBP binding peptide in Pea-15 and the latter is a peptide obtained from the literature. The common interacting residues from SBP for both the peptides are labelled and are shown as blue sticks. PD denotes serine protease domain in both the Figures.
doi:10.1371/journal.pone.0055416.g002

the peptide GSAWFSF and 1.5 Å for GQYYFV from the starting unbound form.

The RMSF of these trajectories were comparable with rmsd values showing higher relative fluctuations in and around the hinge region. Representative RMSF plots for GQYYFV and GSAWFSF bound HtrA2 complexes depict these large fluctuations for residues 190–225 as shown in Figures 4b and C respectively. All structural alignment comparisons and relative fluctuation analyses post MDS emphasize distinct significant conformational change in the hinge (211–226) region upon peptide binding. In addition to this, binding of peptides led to dynamic movements in many functionally important regions distal to SBP such as helices α5 and α7 in PDZ domain.

Conformational Transitions in Flexible Regions and at the Active Site

Further detailed analyses of the effect that local subtle structural changes at SBP had on distal regions of the protease especially at the active site and its vicinity revealed the possibility of SBP being a putative allosteric site. Functional active site formation and its accessibility along with a well formed oxyanion hole are important prerequisites for the activity of an enzyme.

Structural comparison of the MD simulated peptide bound structure of HtrA2 with the unbound form show movements in different domains and linker regions. The PDZ-protease linker that covers the peptide binding groove in the PDZ domain moves away from it thus increasing it accessibility. The peptide bound HtrA2 complex show relative movements in the active site triad residues compared to the unbound form. Atomic distance analysis of both the forms revealed that distances between nitrogen (ε) atom of H65 and oxygen (γ) atom of S173 increased in peptide bound complexes while that between nitrogen (δ) atom of H65 and oxygen (δ) of D95 decreased when compared with the unbound HtrA2 structure (Table 3). This pattern being consistent with both the peptides suggests that interaction of peptide activator with SBP leads to opening up of the active site cleft.

Apart from active site triad, changes were also observed in the orientation of mechanistically important L1, LD and LA loops in the peptide bound complex (Figures 4d–e). Their orientations with respect to the active site determine proper oxyanion hole formation, accessibility of the active site, formation of catalytic triad and hence enzyme activity. MDS analyses for these regions showed significant deviations upon peptide binding. Structural alignment of GSAWFSF bound HtrA2 complex with the unbound form demonstrated breaking of Van der Waals contacts between loop LD and β2 strand of protease domain which facilitates LD movement towards α1 of protease domain and bringing P130 of the former in proximity to A25 of the latter. Similarly, S50 in β2 of protease domain establishes interactions with G171 of L1 (oxyanion hole residue) while breaking contacts with A132 of LD loop due to movement or tilt in the L1 loop. As a result of this reorganization, LD which was closer to L1 in the unbound HtrA2 moves sharply away from it upon peptide binding. These positional rearrangements also lead to disruption of interaction between D165 of L1 and G195 of L2 loops. All these movements coordinate to bring LD closer to the proximal region of protease domain thereby opening up the catalytic site. For GQYYFV peptide, movements of all these loops were subtle as compared to that for GSAWFSF except for the LA loop which exhibited larger deviation in the former. The other significant flexible region movement is in loop L3 which, in concert with linker region, assists in accommodating the peptide at SBP.

The relative reorientation of these loops along with catalytic triad residues seems to be assisting formation of a more open structure near the active site. However, loop L2 that harbors the specificity pocket remains mostly unchanged suggesting presence of a well formed binding pocket in the unbound form whose accessibility is limited compared to the substrate bound form. In context with trimeric HtrA2, more open conformation might be

Table 2. Peptide docking of HtrA2 and identification of interacting residues.

Peptides Used in Our study	Interacting Residues		Glide score in Kcal.mole^{-1}
	H bond Interactions	Vdw Interactions	
PEA 15 (GSAWFSF)	Glu 292, Glu 296, Asp 293, Ile 283, Met 287	Gln 286, Ala 297, Ser 222	−10.564
Designed (VKSDSG)	Asn 216, Leu 152,Glu 296, Glu 292	Ala 89, Ile 221, ser 218,	−10.394
Designed (GRTDSV)	Glu 296, Glu 292, Asn 216, Ser 217	Asp 293	−10.037
Designed (GRDTSV)	Ser 219, Glu 292	Ser 239,Gln 286	−9.57
Designed (GRDTYV)	Asp 293, Asn 216, Ser 217, Ser 219	Glu 296, Arg 299,	−9.54
Phosphatase (PAEWTRY)	Asp 117, Ala 149, Arg 150, Lys 215, Gln 146	Pro 148, Leu 152, Lys 214, Gln 156, Val 159, Ser 239	−9.481
HAX-1 (TKPDIGV)	Glu 292, Glu 296, Ser 219, Ile 221, Arg 299	Asn 216, Ser 222	−8.486
Connexin (ARKSEWV)	Asp 293/426, Asn 290/423, Gln 156/289	Glu 292, Pro 155, Gln 289, Met 287, His 256, Glu 255, pro 238	−8.165
Presenilin (AFHQFYI)	Leu 152, Asn 216, Ser 217, Glu 292, Glu 296	Pro 155, Arg 211, ser 218, Ser 219	−8.063
IL-EBF (AGYTGFV)	Asn 216, Ser 217, Glu 292, Arg 150/, Leu 152	Ser 219, Gly 153, pro 155	−7.903
Yes Protein (ESFLTWL)	Asn 216, Leu 152, Glu 296, Asp 293, Gln 289, Ser 237	Gln 156, Pro 238, Pro 155, Ser 218, Glu 292, Gln 286	−7.722
Cathepsin SVSSIFV	Glu 296, Asn 216, Ile 283/416,	Glu 292, Leu 152,Gly 153,Ala 297	−7.524
Warts Protein Kinase (NRDLVYV)	Lys 214, Lys215, Ala 149,Glu 207, Arg150, Gln 146	Leu 152, Gln 156, Val 159	−7.321
GQYYFV[6]	Glu 292, Glu 296, Asn 216, Ile 221,Leu 152	Ser 219,Gly 153, Arg 299	−7.163
GGIRRV[6]	Glu 292, Glu 296, Asn 216,Ser 217, Ser 219	Arg 211, Gly 153	−6.785
Tuberin (EDFTEFV)	Arg 211, Asn 216, Ser 219	Ala 89, Ile 221, ser 218, Arg 299, Glu 296, Glu 292, Gly 153	−1.883
Control Peptide (KNNPNNAHQN)		**Did not dock with HtrA2**	

The possible residues which are involved in hydrogen bonding and Vander Waal's interactions along with Glide scores are mentioned.
doi:10.1371/journal.pone.0055416.t002

significant as it enhances the accessibility of the substrate and thereby might contribute positively toward the rate of enzyme catalysis.

Influence of SBP on HtrA2 Activity and Role of PDZ Domain

To determine whether critical SBP residues (N216, S219, E292 and E296) are important for mediating allosteric propagation in HtrA2, site directed mutagenesis to alanine were done. Mutation of a conserved YIGV residue (G230A) was also done to understand the role of canonical YIGV groove in this complex signal propagation pathway. Moreover, since the protein is found to be active in its trimeric form [4] and also that SBP encompasses a major part of PDZ, we used trimeric and monomeric HtrA2 variants, N-SPD and F16D respectively to understand the role of PDZ in intra and inter-molecular cross-talk.

To negate the role of overall conformational changes if any due to these mutations, MDS and secondary structural analyses were done on the mutant proteins. Similar active site conformations were observed in both the wildtype and mutants. Moreover, the overall secondary structure and thermal stability remained unperturbed due to the mutations (data not shown). Enzymology studies with different SBP mutants were done using β-casein, a well-established generic substrate of serine proteases [23]. β-casein has a putative SBP binding site (GPFPIIV) which has been found to interact with the similar residues at SBP by our docking studies (Table 2) and hence expected to mimic the allosteric modulation mediated by SBP binding if any**.** The kinetic parameters for wild type, N-SPD domain, F16D and other mutants were determined using fluorescent β-casein (Figure 5). The catalytic efficiency (k_{cat}/K_m) for the double mutant N216A/S219A and single mutant E292A showed ~2.4 fold decrease in enzyme activity as compared to wild type whereas enzymatic parameters remained mostly unchanged for E296A. K_m values for the mutants were not significantly higher compared to the wild type, suggesting that the specificity pocket might be mostly intact with some subtle alterations. However, there was a marked decrease in V_{max} and in substrate turnover (k_{cat}) rates for N216A/S219A and E292A suggesting presence of a malformed oxyanion hole in the SBP mutants. These results demonstrate that N216/S219 and E292 of SBP are important for mediating allosteric activation of HtrA2 upon activator binding. This is strengthened by the observation that SBP mutants did not interact with the activating peptides as seen by isothermal calorimetric studies and a representative figure is shown in the supplementary material (Figure S3). In addition, the ligplot of the peptide showing the detailed interaction with HtrA2 is also depicted in figure S1.

In our in silico studies, YIGV has been found to be a part of the greater SBP mesh (Table 1) and since docking with small molecular fragments (~35–100 Da) showed direct binding with YIGV residues (Table S1), we wanted to understand the effect of YIGV mutation on HtrA2 activity as well. Enzymology studies with G230A demonstrated increase in K_m value compared to the wild type highlighting the involvement of YIGV in this intricate allosteric mechanism. Protein turnover rate was also much lower in G230A as compared to the wild type reiterating the importance of oxyanion hole formation upon activator binding at SBP. Thus,

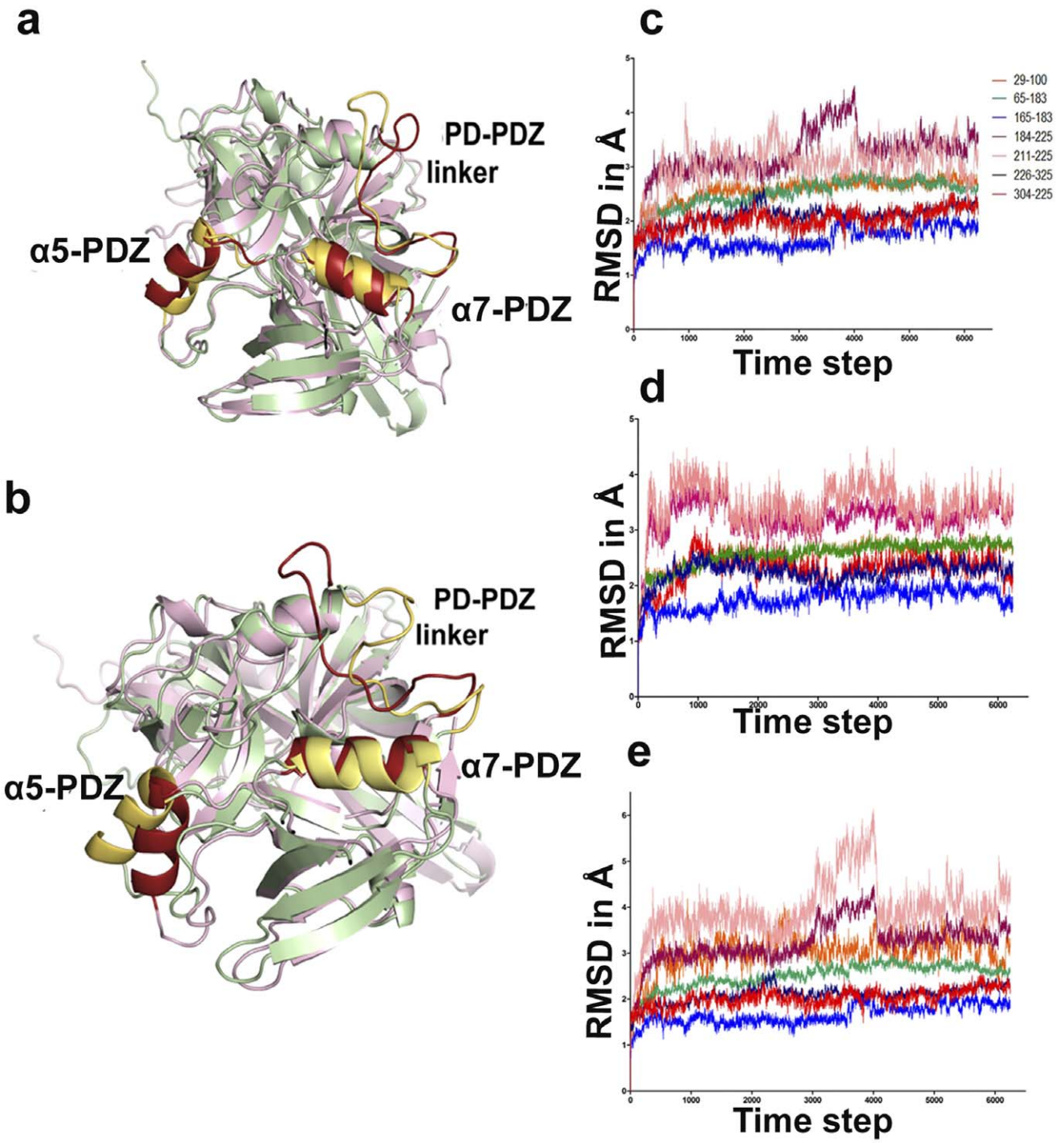

Figure 3. Domain wise conformational changes induced on peptide binding at SBP. a. The structural alignment of minimum energy structure of the peptide bound GQYYFV-HtrA2 complex (light pink) and unbound structure (green) displays orientation of the movement of the hinge region and the α-helices of PDZ. b. The structural alignment of GSAWFSF-HtrA2 complex (light pink) and unbound structure (green). Graphical representations of the RMSD for the 30 ns MDS trajectory of the following: c. HtrA2–GQYYFV complex. d. unbound HtrA2 (negative control). e. HtrA2–GSAWFSF complex. The stretch of residues selected for each set of RMSD calculations are shown on the right of panel c.
doi:10.1371/journal.pone.0055416.g003

inaccessibility of the canonical PDZ binding pocket YIGV, in the trimeric protease structure might have adjured presence of exposed SBP which is dynamically coupled to YIGV groove for efficient allosteric signal propagation to the distal active site. Direct binding of small molecules at YIGV supports this hypothesis as they could be accommodated in the classical binding groove without requirement of any initial conformational change as it might be with the larger peptide activators.

Interestingly, although catalytic efficiency for N-SPD has been found to be 3.4 fold less as compared to the wildtype, its K_m value suggests slight increase in substrate affinity for the enzyme (Table 4). This increase in substrate affinity might be due to

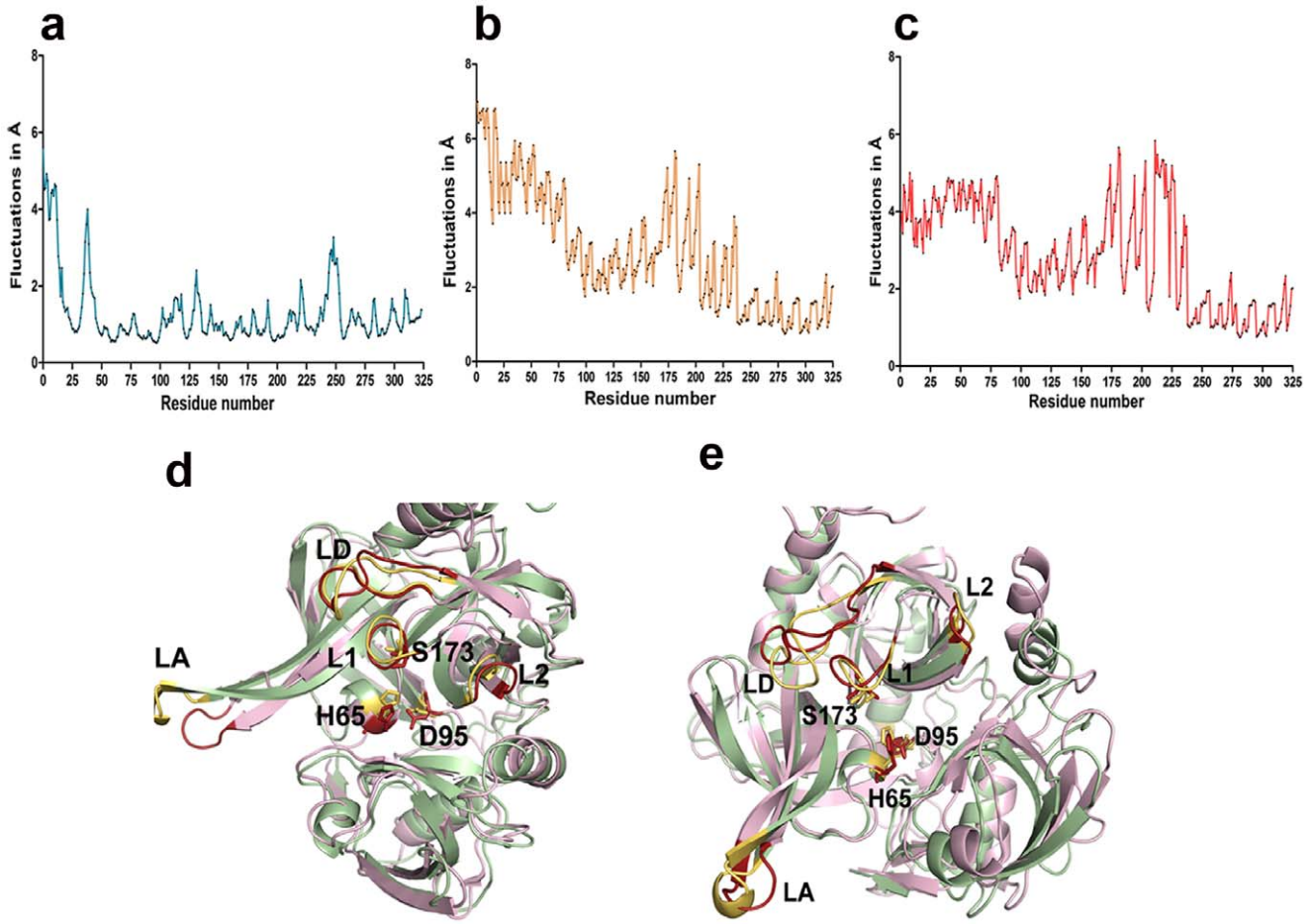

Figure 4. Graphical representation of root mean square fluctuation (RMSF) and loop movements upon peptide binding. a. MD simulation trajectory for unbound HtrA2. b. RMSF graph for GQYYFV bound HtrA2. c. RMSF graph for GSAWFSF bound HtrA2. d. Comparison of fluctuations in loops LA, L1, L2 and LD in the GQYYFV peptide bound (pink) and unbound structure (green). The loops in the bound and unbound forms are displayed in red and yellow respectively. e. Comparison of fluctuations in loops LA, L1, L2 and LD in the GSAWFSF peptide bound (pink) and unbound structure (green). The loops in the bound and unbound forms are displayed in red and yellow respectively. The catalytic triad residues are shown in both panels d. and e.
doi:10.1371/journal.pone.0055416.g004

absence of PDZ surrounding the active site region resulting in greater substrate accessibility. However in N-SPD, k_{cat} was found to be 5 fold less than that of wild type highlighting the role of PDZ in initiating conformational changes near the active site pocket as well as in the oxyanion hole so as to increase overall enzyme stability. However, in the full length monomeric mutant of HtrA2 (F16D), there is a two fold increase in K_m with significant decrease in turnover rate and hence catalytic efficiency (Table 4) which emphasizes importance of intermolecular crosstalk between PDZ and protease domains in trimeric HtrA2 structure.

Table 3. Comparison of distances between atoms of the catalytic triad in the peptide bound and unbound forms of HtrA2.

Protein Complex	NE2 (His) – OG (Ser)		ND1 (His) – OD1(Asp)	
	Bound	Unbound	Bound	Unbound
HtrA2 (GSAWFSF)	5.2	4.1	2.6	2.9
HtrA2 (GQYYFV)	5.5	4.1	2.7	2.9

doi:10.1371/journal.pone.0055416.t003

The importance of intermolecular interaction between PDZ* and SPD has also been manifested in our MD studies where structural analyses show binding of peptide activator (GQYYFV) at the SBP alters PDZ orientation and brings α5 helix of PDZ from one subunit in close proximity to the protease domain of the adjacent subunit. The helix moves towards LD loop of the protease domain, thereby shifting the orientation of the phenyl ring of F170 which is a part of oxyanion hole towards H65 of the catalytic triad (Figure 6a) so as to accommodate the loop. These rearrangements result in a more stable and catalytically competent HtrA2 formation with a proper oxyanion hole. Thus the full length trimeric HtrA2 is more active than trimeric N-SPD, where the activation pocket is not stable in absence of PDZ.

Discussion

Our aim was to understand the structural dynamics that regulates activation and specificity of HtrA2. This multidomain trimeric protease has unique proapoptotic properties as it is associated with both caspase-dependent and independent cell

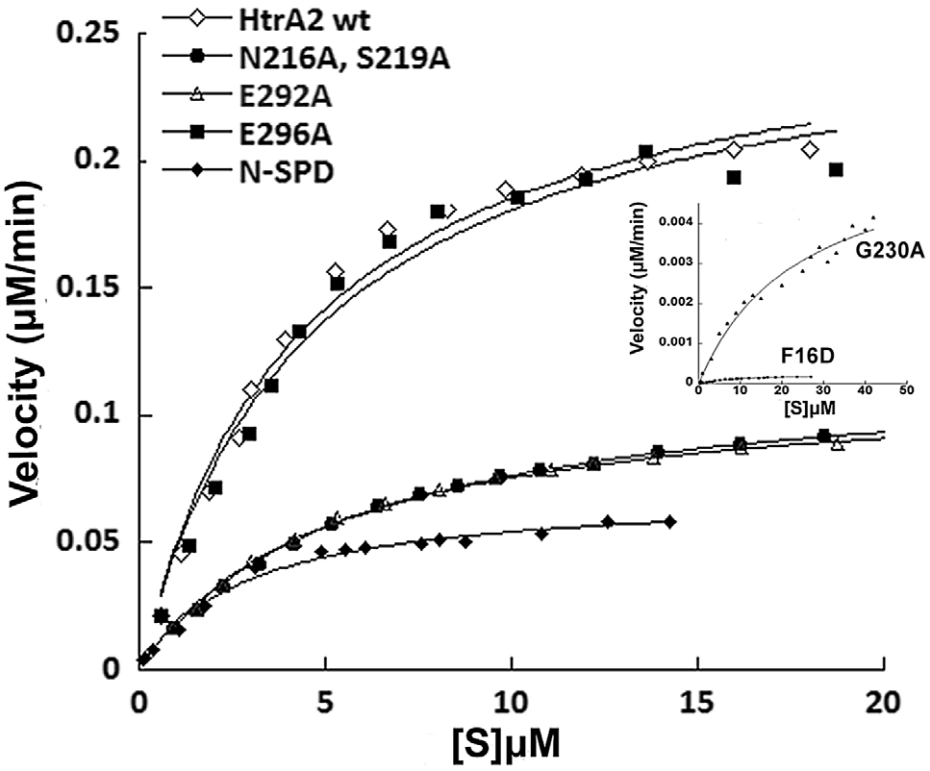

Figure 5. Steady state kinetic parameters of HtrA2. Graph representing relative activity of wild type HtrA2 and its mutants and variants with FITC labelled β-casein as the substrate. The graph for two mutants (F16D and G230A) is shown in inset.
doi:10.1371/journal.pone.0055416.g005

death pathways through its serine protease activity [5,12]. Association of HtrA2 with cancer and neurodegenerative disorders makes it a promising therapeutic target. For example, over-expression of HtrA2 substrates such as IAPs and the Wilms's tumor suppressor protein WT1 in several cancers suggests modulation of HtrA2 protease activity can effectively regulate their relative levels in the cells [24,25,26,27]. Out of several approaches that can be used to regulate HtrA2 activity, allosteric modulation is one of the simplest and most efficient ways. However, modulating HtrA2 functions with desired characteristics for disease intervention will require a detailed understanding of its mode of activation and the underlying conformational plasticity that controls it.

Table 4. Steady state kinetic parameters for HtrA2 wild type, variants and mutants with β-casein as the substrate.

HtrA2 Proteins	K_m (μM)	V_{max} (M/s)	k_{cat} (1/s)	k_{cat}/K_m (1/M.s)
Wild type	4.59	4.083×10^{-9}	0.02041	4.452×10^{3}
N216A, S219A	5.43	1.937×10^{-9}	0.00968	1.788×10^{3}
E292A	5.15	1.903×10^{-9}	0.00951	1.849×10^{3}
E296A	4.68	3.734×10^{-9}	0.01868	3.995×10^{3}
N-SPD	3.02	0.7851×10^{-9}	0.0039	1.29×10^{3}
F16D	9.3	4.08×10^{-12}	0.000025	0.0026×10^{3}
G230A	9.32	1.03×10^{-9}	0.0051	0.54×10^{3}

doi:10.1371/journal.pone.0055416.t004

Peptide design using site complementarity followed by MDS of the docked peptide-macromolecular complex is an extremely useful tool to study subtle conformational changes and protein dynamics. HtrA2 has a complex network of flexible loops surrounding the active site pocket and a linker at the PDZ-protease interface whose relative orientations and crosstalk with different domains might be critical in defining HtrA2 functions. With partially missing loops and the flexible linker region, the solved structure of HtrA2 [4] could not fully explain the dynamics and allostery that regulate its activity and specificity. Here, with an *in silico* and biochemical approach, we have shown that like few other HtrA family proteins, allosteric propagation does regulate HtrA2 activity.

In this study, peptide binding to SBP showed conformational changes in the distal flexible regions of HtrA2 such as the PDZ-protease interface, loops L1, LD and LA that rearrange to form a more catalytically efficient active site thus establishing the role of SBP as an allosteric site in HtrA2. A close look at and around the active site pocket shows that in the bound form, the N atom of Gly (−2 position) faces the oxyanion hole to form an H-bond whereas in the unbound form it flips in the opposite direction to form a malformed oxyanion hole [12,28]. Moreover, keeping in trend with other HtrA proteases, the phenylalanine ring of −3 position moves closer to the imidazole ring of His65 while in the unbound form, it moves outward as observed from Figures 6b–c and Movie S1. All these subtle structural rearrangements along with making and breaking of bonds at sites away from the active site might stabilize the peptide bound form such that it shifts the equilibrium toward catalysis.

Enzymology studies with β-casein that has a putative SBP binding sequence (GPFPIIV) as shown in Table 4 show significant

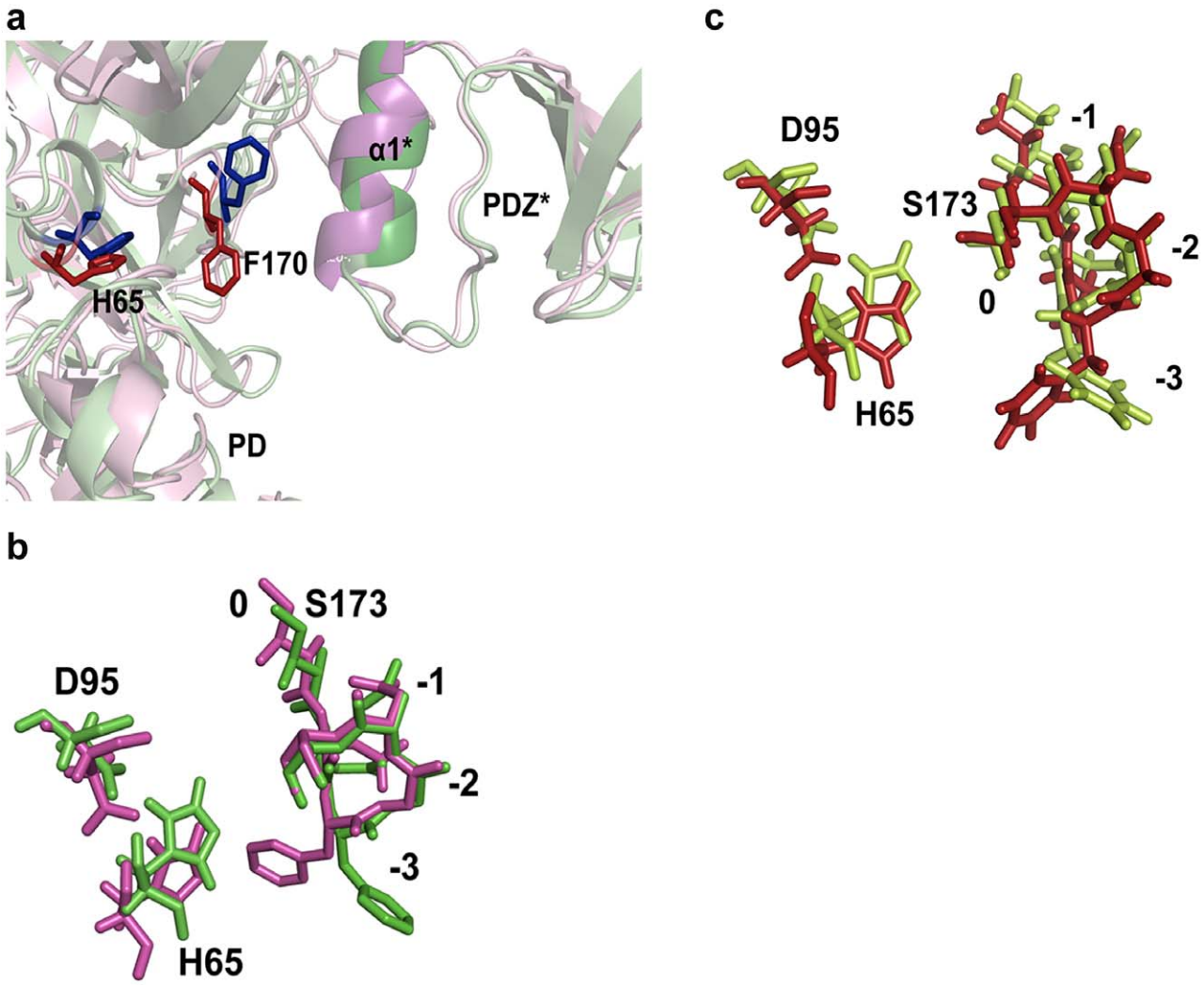

Figure 6. Structural changes at the oxyanion hole and YIGV groove upon peptide binding. a. Overlay of the oxyanion hole and catalytic triad residues represented as sticks for peptide GQYYFV bound (magenta) and unbound (green) structures. PD denotes serine protease domain of HtrA2. b. Overlay of the oxyanion hole and catalytic triad residues represented as sticks for peptide GSAWFSF bound (red) and unbound (limon green) structures. c. Role of PDZ in the formation of proper active site formation. The structural superposition of GQYYFV bound (pink) and unbound (green) structures shows α5 helix of PDZ of one subunit moves towards the LD loop and oxyanion hole of the adjacent subunit. The positions of the residues in the oxyanion hole are denoted as 0, −1, −2 and −3.
doi:10.1371/journal.pone.0055416.g006

decrease in catalytic efficiency in SBP mutants. This observation suggests interaction of substrate protein with SBP brings about rearrangement around the active site of the enzyme by positively influencing its activity thus behaving as an allosteric regulator. The SBP mutants (N216A/S219A and E292A) show apparent decrease in V_{max} without significantly altering the apparent K_m (with L2 specificity pocket mostly unaltered) and hence follow the 'V system' of allosteric modulation [29]. In this system, both the relaxed (R) and the tensed (T) states bind the substrate at the active site with similar affinity while the peptide (activator) at SBP binds the R and T states with different affinity. This differential affinity of the peptide towards SBP along with R state stabilization shifts the equilibrium towards R state thus positively influencing its turnover rate and hence catalytic efficiency which has been observed in case of HtrA2.

In N-SPD, where the PDZ domain is absent, apparent decrease in K_m can be attributed to greater accessibility of the substrate to the active site. However, since the change in binding affinity is not large, the specificity pocket might be mostly unaltered compared to the wild type which is confirmed through our MD studies where the loop L2 remains mostly unaltered. Interestingly, k_{cat} value in N-SPD has been found to decrease significantly which is suggestive of either a malformed oxyanion hole and/or decrease in overall protein stability which might be due to absence of supporting PDZ domain. However, similar studies with F16D (monomeric full length HtrA2 mutant) also show significant decrease in turnover rate and catalytic efficiency which accentuates the importance of intermolecular and not intramolecular PDZ-protease crosstalk in trimeric HtrA2. Our MDS supports this observation by demonstrating that in the peptide bound form of HtrA2, α5* of PDZ* moves towards LD loop of protease domain of adjacent subunit thus pushing phenyl ring of F170 of the oxyanion hole towards H65 of the catalytic triad (Figure 6a). This reorientation in the oxyanion hole makes the protease poised for catalysis as seen in other HtrA family members as well [12] thus significantly enhancing the turnover rate. Therefore, intermolecular crosstalk

stabilizes the active site and makes it catalytically competent establishing the requirement of complex trimeric architecture of the protease.

The GLGF motif (YIGV in HtrA2) is the canonical peptide binding site [2,4] in PDZ domains. However, in HtrA2, it is deeply embedded within a hydrophobic groove where the residues are intertwined with each other through several intramolecular interactions making the site highly inaccessible to the binding of peptide [4]. Thus, peptide binding to YIGV is only possible upon certain structural rearrangements at that site. Given the property of PDZ domains of having multiple docking sites and the fact that HtrA2 requires huge conformational changes for proper active site formation, we hypothesized presence of a relatively exposed pocket where peptide binding occurs prior to interaction with the buried YIGV groove. In our studies, we have found a novel surface exposed region (SBP) around PDZ domain which is easily accessible to the peptide. With an aim at understanding the allosteric mechanism in HtrA2 and whether the binding site is structurally conserved, we did a side-by-side comparison with the peptide-bound PDZ structure of its bacterial counterpart DegS that is known to exhibit allostery [30]. The structural overlay of peptide bound forms of these two proteins show striking structural similarity in the regions of binding (Figure 7a) with the GLGF groove (YIGV in HtrA2 and YIGI in DegS) oriented differently. Since the YIGV motif is buried in HtrA2 structure, its in-accessibility might be the reason for the peptide to initially bind to another relatively accessible region with similar hydrophobic milieu. However, in DegS, the YIGI groove is already exposed to accommodate the peptide easily and hence this kind of initial interaction is not required.

Our MDS studies show that peptide binding at SBP leads to subtle structural changes in the region adjoining YIGV leading to opening up of the pocket. The last β strand of PDZ domain which lies on one side of YIGV groove moves away from it. The YIGV and the loop spanning residues 67–73 move away from each other while the loop comprising residues 263–277 of the β-α-β motif also drifts at an angle away from the YIGV making it more solvent exposed (Figure 7b). Therefore, upon SBP binding, the relative movements of the loops in vicinity of the hydrophobic YIGV pocket might confer it with the kind of exposure that is required for interaction with peptides. These observations along with our enzymology studies with SBP and YIGV mutants, led to defining a model (Figure 8) for allosteric propagation in HtrA2. The model suggests that initial binding of the peptide activator at SBP leads to structural fluctuations which result in subtle rearrangement at and around the YIGV groove (a part of greater SBP mesh as identified by Sitemap) thus exposing it. Opening up of the deeply embedded YIGV pocket makes it accessible to the substrate molecule which consequently leads to allosteric signal propagation at the active site in the serine protease domain.

This alternative non-canonical PDZ binding site though novel in HtrA family of proteins, is not unprecedented in literature. It has been observed that PDZ7 of the scaffold protein Glutamate receptor interacting protein 1 (GRIP1) has an alternative exposed hydrophobic pocket that binds its substrate GRASP-1 since the canonical binding site is deeply embedded within the protein [31]. Overlay of the PDZ from HtrA2 and PDZ7 of GRIP1 show striking structural similarity including the classical peptide binding groove and the novel non-canonical pocket (Figure S2). Thus, in these two proteins, perturbations at the alternative distal binding sites might be coupled dynamically to the classical binding groove by a complex mechanism that includes fast (ps–ns) timescale dynamics which consequently leads to allosteric signal propagation to the active site.

In the recent past, allosteric modulators have evolved into important drug targets due to several advantages they have over

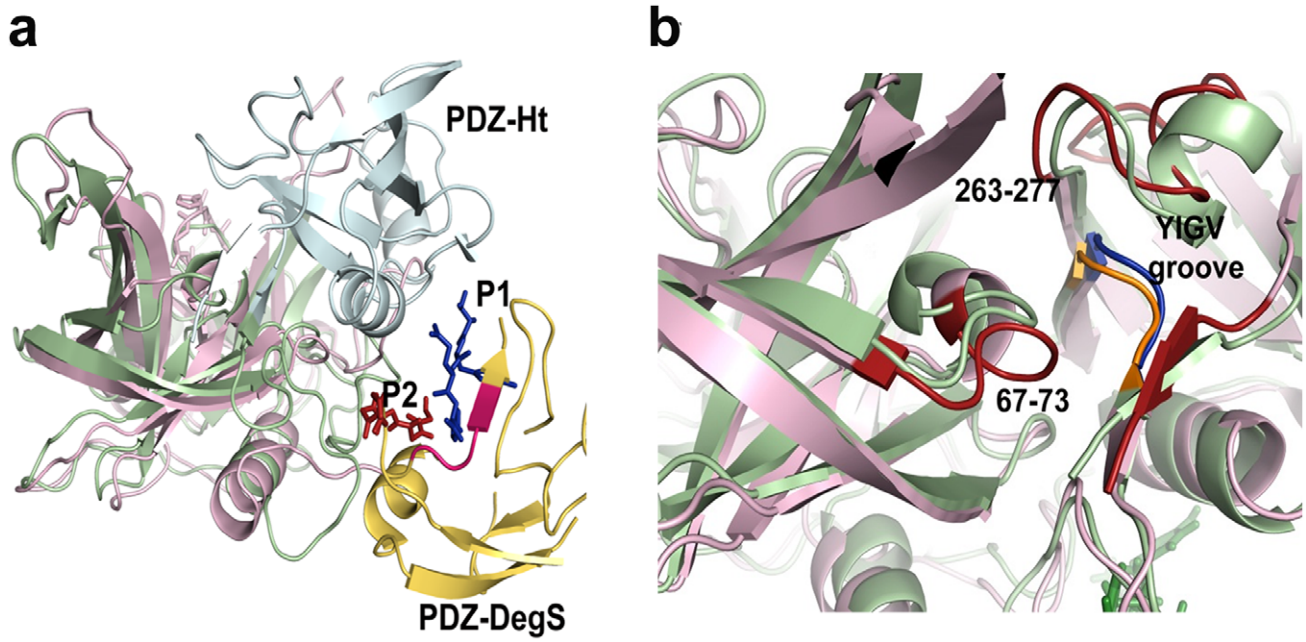

Figure 7. Structural comparison of PDZ domain orientation. a. Structural alignment of *E.coli* DegS (PDB ID: 1SOZ) and the peptide bound HtrA2 showing PDZ domains for both the proteins (represented in blue and yellow respectively) are oriented differently but the peptides, P1 (blue) and P2 (pink) represented as sticks for the respective proteins seem to bind to a structurally similar region. The GLGF substrate binding motif is exposed for DegS while buried for HtrA2 as shown in pink and blue respectively. b. Alignment of the peptide bound (pink) and unbound (green) structures at the region around the YIGV groove shows outward movement of the loops spanning residues 67–73 and 263–277 shown in red for the bound structures which leads to opening up of the YIGV groove.
doi:10.1371/journal.pone.0055416.g007

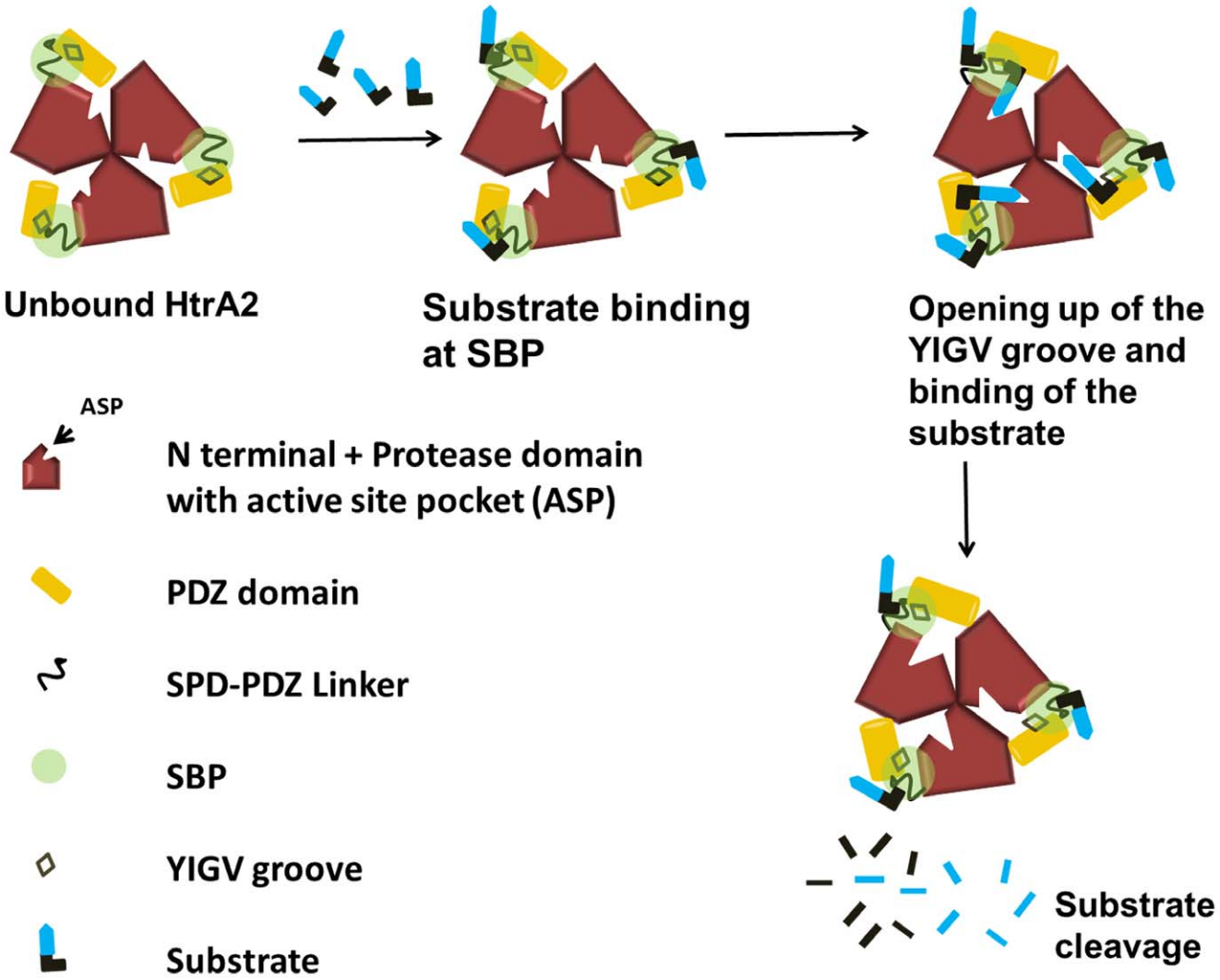

Figure 8. Allosteric model for HtrA2 protease activity. The substrate protein binds to relatively exposed part of SBP due to inaccessibility of the YIGV groove which triggers opening up of the PDZ domain. This reorientation makes the YIGV groove accessible for substrate interaction and the PDZ of a subunit moves closer to the protease domain of the adjacent subunit leading to formation of a proper active site and oxyanion hole. This complex allosteric signal propagation leads to subsequent substrate binding and catalysis at the active site pocket. Thus structural perturbations at these two distant sites (SBP and catalytic pocket) might be dynamically coupled to the canonical peptide binding groove through a complex allosteric mechanism.
doi:10.1371/journal.pone.0055416.g008

orthosteric ligands that include more diversity, less toxicity and absolute subtype selectivity [32,33]. Therefore, designing suitable SBP binding peptides or peptidomimetics of HtrA2 might be an excellent approach to modulate HtrA2 functions for devising therapeutic strategies against various diseases it is associated with.

Materials and Methods

Loop Modeling and Site Prediction

Crystal structure of HtrA2 (PDB ID: 1LCY) [4] obtained from Protein Data Bank [34] has missing N-terminal residues (AVPSP) and two flexible regions (^{211}RGEKKNSSSGISGSQ ^{225} and ^{149}ARDLGLPQT ^{157}). These missing structures were modelled and loops were refined using Prime 3.0 (Schrödinger, LLC, New York, 2011). which was later subjected to molecular dynamics simulation for 5 ns with GROMACS, version 4.5.1 [17] to obtain the lowest energy structure of HtrA2. The binding sites were then predicted using SiteMap 2.5 (Schrödinger, LLC, New York, 2011). Out of 5 pockets predicted, the site that scored the best based on its size, hydrophobic and hydrophilic characters, degree to which ligand might donate or accept hydrogen bonds and exposure to solvent was selected for further analysis. This site selective binding pocket (SBP) encompasses PDZ-protease interface with the involvement of hinge region and a part of PDZ domain (Table 1).

Peptide Designing and Molecular Docking

Based on properties of amino acids lining the binding site, fragment docking (Glide XP, Schrödinger, LLC, New York, 2011) [35] approach was used to dock 20 amino acids and 8 functional group replicas (N-methylacetamide, methanol, phenol, benzene, propane, acetate ion, methylammonium, methylguanidinium) at SBP [36]. Based on properties of the amino acids that form SBP, replicas were chosen and were used for generating fragments in combinations of four as shown in Table S1. Combine Fragment tool (Schrödinger, LLC, New York, 2011) was used to join the

fragments which were docked at SBP with three major filtering options (bond angle deviation 5 degrees, atom-atom distance 1 Å and fragment centroid distance 2.0). The set of replica functional groups that displayed the best docking scores were used to build the peptide. The amino acids Arg, Ser, Gln, Glu, Asp, Asn, Thr, Lys and their positions in tetrapeptide combination were chosen based on the functional groups they resembled. Subsequently all possible peptide combination of these amino acids with respect to their relative positions were generated. The predicted tetrameric peptides (Table S2) were selected and docked again with SBP.

In parallel, another mode of designing was used by identifying signature peptides from literature which bind HtrA2 [19]. Initially two peptides were chosen (GQYYFV and GGIRRV) and based on the sequence similarity and hydrophobicity, stretches of putative binding residues from two known binding partners of HtrA2 were identified (GPFPIIV from C-terminal region of β-casein and GSAWFSF, an internal motif of antiapoptotic Pea-15) [37]. A putative HtrA2 binding pattern was designed based on phage display library [21] which along with the earlier four sequences was used to generate all possible peptide combinations**.** Considering structural complementarity and three dimensional arrangements of amino acids at SBP, Gly and Val residues were added at N- and C-termini of some peptides to increase the stability of the docked complex. A 10 mer peptide having the sequence KNNPNNAHQN that does not match the consensus SBP binding peptide pattern was used as a negative control. These combinations were used for searching all possible sequences of known and potential HtrA2 binding partners [38].

All designed peptides were built *in silico* using BREED (Schrödinger, LLC, New York, 2011) and Combine Fragments tools which were then prepared for docking using LigPrep 2.5 (Schrödinger, LLC, New York, 2011). After ligand preparation, Confgen 2.3 (Schrödinger, LLC, New York, 2011) was used to generate all possible energetically minimum conformers of the designed peptides which were then docked using Glide [39,40].

In the modeled HtrA2 structure, energy minimization was done using Protein Preparation Wizard 2.2 (Epik Version 2.2, Schrödinger, LLC, New York, 2011) after addition of H-atoms. Molecular Docking was initiated by preparing Grid file (input file) which contains receptor (protein structure) and binding site information (Prime output). All three precision methods which include high throughput virtual screening (HTVS), standard precision (SP) and extra precision (XP) [35] of Glide [39,40] were used for docking these peptides on SBP. This series of docking methods were used to filter out energetically less favorable peptide conformers and get a subset of best possible peptides for further studies.

MD Simulation (MDS) and Analysis

After analyzing the docking results, best HtrA2-peptide complexes based on Glide XP score and E-model value were used for Molecular Dynamic Simulation which was performed using Desmond 2010 [22] software package. Optimized Potentials for Liquid Simulations (OPLS) [41] all-atom force field was used to analyze model stability. The protein structures were solvated with Monte Carlo simulated TIP3P [42] water model with a 10 Å buffer space from the protein edges in an orthorhombic box and the system was then neutralized by replacing water molecules with sodium and chloride counter ions. Similarly, unbound HtrA2 system was also developed as a control. Neutralization of systems was done by adding 2 Na^+ ions in unbound HtrA2 and 4 Na^+ ions for peptide bound complexes. The particle-mesh Ewald method (PME) [43] was used to calculate long-range electrostatic interactions with a grid spacing of 0.8 Å. Van der Waals and short range electrostatic interactions were smoothly truncated at 9.0 Å. Nose–Hoover thermostats were utilized to maintain the constant simulation temperature and the Martina–Tobias–Klein method was used to control the pressure [44]. The equations of motion were integrated using the multistep RESPA integrator [45] with an inner time step of 2.0 fs for bonded interactions and non-bonded interactions within the short range cut-off. An outer time step of 6.0 fs was used for non-bonded interactions beyond the cut-off. These periodic boundary conditions were applied throughout the system.

These prepared systems were equilibrated with the default Desmond protocol that comprises a series of restrained minimizations and MDS. Two rounds of steepest descent minimization were performed with a maximum of 2000 steps and a harmonic restraint of 50 kcal/mol/per $Å^2$ on all solute atoms followed by a series of four MDS. The first simulation was run for 12 ps at a temperature of 10 K in the NVT (constant number of particles, volume, and temperature) ensemble with solute heavy atoms restrained with force constant of 50 kcal/mol/$Å^2$. The second simulation was similar to the first except it was run in the NPT (constant number of particles, pressure, and temperature) ensemble. A 24 ps simulation followed with the temperature raised to 300 K in the NPT ensemble and with the force constant retained. The last one was a 24 ps simulation at 300 K in the NPT ensemble with all restraints removed. This default equilibration was followed by a 5000 ps NPT simulation to equilibrate the system. A 30 ns NPT production simulation was then run and coordinates were saved in every 2 ps of time intervals.

The total trajectory of MD simulation was 30 ns. MD Simulation was analyzed using the analytical tools in the Desmond package. In MD quality analysis, potential energy of the protein as well as total energy of the entire system was calculated. The lowest potential energy conformations were then used for comparative analysis of peptide bound and unbound structures. Trajectories of peptide bound complexes and unbound HtrA2 were then compared based on their overall calculated RMSD (root mean square deviation), domain wise RMSD and RMSF (root mean square fluctuation) values and were plotted using GraphPad Prism 5.0 (GraphPad Software, San Diego, CA, USA).

Production of Recombinant HtrA2 Wild Type, its Mutants and Domains

Mature (Δ133 HtrA2) with C-terminal his_6-tag in pET-20b (Addgene, Cambridge, MA) was expressed in *E. coli* strain BL21 (DE3) pLysS. N-SPD, comprising N-terminal and serine protease domains (residues 1–210) of HtrA2 was sub cloned into pMALc5E-TEV using appropriate primers. Point mutations were introduced into pET-20b Δ133 HtrA2 by PCR using primer sets that included mutations for residues N216A, S219A, E292A, E296A and F16D. N-SPD clone and these mutants were confirmed by DNA sequencing. Protein expression was induced by culturing cells at 18°C for 20 h in presence of 0.2 mM isopropyl-1-thio-D-galactopyranoside. Cells were lysed by sonication and the centrifuged supernatants for HtrA2 and its mutants were incubated with pre-equilibrated nickel-IDA beads for 1 h at room temperature. Protein purification was done using Ni-affinity chromatography as described earlier [19]. Eluted protein was further purified using gel permeation chromatography. N-SPD was purified using amylose resin where the bound protein was eluted using 10 mM maltose and was subjected to TEV protease cleavage [46] to remove maltose binding protein (MBP). N-SPD was further separated from MBP by gel filtration using Superdex 75 column. All purified proteins were analyzed by SDS-PAGE for

purity. The fractions with >95% purity were stored in aliquots at −80°C until use.

FITC-β-Casein Cleavage Assay

The proteolytic activity of wild type and the mutants were determined using FITC-labelled β-casein cleavage assay [47]. Fluorescent substrate cleavage was determined by incubating 200 nM of enzymes with increasing concentration (0–25 μM) of β-casein at 37°C in cleavage buffer (20 mM Na_2HPO_4/NaH_2PO_4, pH 8.0, 100 mM NaCl, 0.1 mM DTT). Fluorescence was monitored in a multi-well plate reader (Berthold Technologies) using excitation wavelength of 485 nm and emission at 545 nm. Reaction rates v_0 (μM/min) were determined by linear regression analysis corresponding to the maximum reaction rates for individual assay condition. Assays are representative of at least three independent experiments done in triplicate. The steady-state kinetic parameters were obtained from the reaction rates by fitting data to Michaelis-Menten equation using nonlinear least squares subroutine in KaleidaGraph program (Synergy software).

Supporting Information

Figure S1 Interaction of peptides with HtrA2. a. Ligplot for GSAWFSF with HtrA2 which represents residues involved and the nature of interactions. b. Ligplot for GQYYFV interaction pattern with HtrA2. c. Ligplot for GPFPIIV with HtrA2 which represents residues involved and the nature of interactions. d. Ligplot for SEHRRHFPNCFFV peptide with HtrA2 which represents residues involved and the nature of interactions. The residues of peptides and HtrA2 involved in interaction are shown in blue and red respectively.
(TIF)

Figure S2 Comparison of SBP and allosteric pocket of GRIP-1 protein. Structural overlay of the protein GRIP-1(green) bearing PDB ID 1M5Z and GQYYFV bound HtrA2 (pink) shows striking resemblance of the orientation of buried GLGF motif shown in yellow and blue respectively. The α helix denoted as αB (green) for GRIP-1, known to be involved in formation of allosteric pocket overlays very well with the one involved in SBP formation (orange) in GQYYFV (red sticks) - HtrA2 complex.
(TIF)

Figure S3 ITC studies for activating peptide with HtrA2 and the SBP double mutant. The peptide used was 13mer SEHRRHFPNCFFV, which has similar consensus sequence as defined for PDZ peptide groove binding substrate. The peptide was better in terms of solubility as compared to other activating peptides and binding studies were done using Isothermal titration calorimetry. The titrations were carried out using Micro Cal ITC200 (GE Healthcare) with the calorimetry cell containing 200 μl of wild type or N216A/S219A mutant HtrA2 in 20 mM Na_2HPO_4/NaH_2PO_4 buffer, 100 mM NaCl, pH 7.8. The concentration of protein was in range from 20 to 50 μM and was titrated with 1.5 μl injections of a solution containing 0.4 mM activator peptide reconstituted in the same buffer. To correct the effect of heat of dilution, a blank injection was made under identical conditions. All experiments were performed at 25°C and the data was analyzed using the manufacture provided MicroCal software with the integrated heat peaks fitted to a one site-binding model. Simulated ITC raw data for the protein with the activating peptide is represented in the upper panel and the integrated data in the lower panel. The dissociation constant was calculated to be 7.5 μM for wild type (left panel) and no significant heat change was observed for the SBP double mutant (right panel).
(TIF)

Table S1 Docking analysis of replica fragments with HtrA2. The fragments have been arranged according to their docking scores.
(DOC)

Table S2 Designed peptide fragments. Fragments of peptide combinations generated based on functional group studies have been enlisted.
(DOC)

Movie S1 Orientation of active site triad and oxyanion hole formation during MD simulation of HtrA2-peptide complex. From this visual representation of HtrA2 peptide (GSAWFSF) complex during MD simulation it can be seen that the catalytic triad residues H65, D95, S173 reorient to form an active conformation along with oxyanion hole residues (N172, G171 and F170). All the residues involved are represented as sticks. This movie shows proper active site and oxyanion hole formation.
(AVI)

Author Contributions

Conceived and designed the experiments: KB. Performed the experiments: PRB RRK NG NS LKC. Analyzed the data: KB PRB RRK GMS. Wrote the paper: KB PRB RRK.

References

1. Ma B, Tsai C, Haliloglu T, Nussinov R (2011) Dynamic Allostery: Linkers Are Not Merely Flexible. Structure 19: 907–917.
2. Jeleń F, Oleksy A, Śmietana K, Otlewski J (2003) PDZ domains common players in the cell signaling. Acta Biochim Pol 50: 985–1017.
3. Hung A, Morgan S (2002) PDZ Domains: Structural Modules for Protein Complex Assembly. J Biol Chem 277: 5699–5702.
4. Li W, Srinivasula S, Chai J, Li P, Wu J, et al. (2002) Structural insights into the pro-apoptotic function of mitochondrial serine protease HtrA2/Omi. Nat Struct Biol 9: 436–441.
5. Suzuki Y, Takahashi-Niki K, Akagi T, Hashikawa T, Takahashi R (2004) Mitochondrial protease Omi/HtrA2 enhances caspase activation through multiple pathways. Cell Death Differ 11: 208–216.
6. Martins L, Iaccarino I, Tenev T, Gschmeissner S, Totty N, et al. (2002) The serine protease Omi/HtrA2 regulates apoptosis by binding XIAP through a reaper-like motif. J Biol Chem 277: 439–444.
7. Verhagen A, Silke J, Ekert P, Pakusch M, Kaufmann H, et al. (2002) HtrA2 promotes cell death through its serine protease activity and its ability to antagonize inhibitor of apoptosis proteins. J Biol Chem 277: 445–454.
8. Kooistraa J, Milojevicb J, Melacinia G, Ortegaa J (2009) A new function of human HtrA2 as an amyloid-beta oligomerization inhibitor. J Alzheimers Dis 17: 281–294.
9. Johnson F, Kaplitt M (2009) Novel mitochondrial substrates of omi indicate a new regulatory role in neurodegenerative disorders. PLoS One 4: e7100.
10. Lin C, Chen M, Chen G, Tai C, Wu R (2011) Novel variant Pro143Ala in HTRA2 contributes to Parkinson's disease by inducing hyperphosphorylation of HTRA2 protein in mitochondria. Hum Genet 130: 817–827.
11. Nam M, Seong Y, Park H, Choi J, Kang S, et al. (2006) The homotrimeric structure of HtrA2 is indispensable for executing its serine protease activity. Exp Mol Med 38: 36–43.
12. Singh N, Kuppili R, Bose K (2011) The structural basis of mode of activation and functional diversity: A case study with HtrA family of serine protease. Arch Biochem Biophys 516: 85–96.
13. Sohn J, Grant RA, Sauer RT (2010) Allostery is an intrinsic property of the protease domain of DegS: implications for enzyme function and evolution. J Biol Chem 285: 34039–34047.
14. Merdanovic M, Mamant N, Meltzer M, Poepsel S, Auckenthaler A, et al. (2010) Determinants of structural and functional plasticity of a widely conserved protease chaperone complex. Nat Struct Mol Biol 17: 837–843.
15. Beuming T, Farid R, Sherman W (2009) High-energy water sites determine peptide binding affinity and specificity of PDZ domains. Protein Sci 18: 1609–1619.

16. Sherman W, Day T, Jacobson M, Friesner R, Farid R (2006) Novel procedure for modeling ligand/receptor induced fit effects. J Med Chem 49: 534–553.
17. Van Der Spoel D, Lindahl E, Hess B, Groenhof G, Mark A, et al. (2005) GROMACS: fast, flexible, and free. J Comput Chem 26: 1701–1718.
18. Halgren T (2007) New method for fast and accurate binding-site identification and analysis. 69: 146–148.
19. Martins L, Turk B, Cowling V, Borg A, Jarrell E, et al. (2003) Binding specificity and regulation of the serine protease and PDZ domains of HtrA2/Omi. J Biol Chem 278: 49417–49427.
20. Ma S, Song E, Gao S, Tian R, Gao Y (2007) Rapid characterization of the binding property of HtrA2/Omi PDZ domain by validation screening of PDZ ligand library. Sci China C Life Sci 50: 412–422.
21. Zhang Y, Appleton B, Wu P, Wiesmann C, Sidhu S (2007) Structural and functional analysis of the ligand specificity of the HtrA2/Omi PDZ domain. Protein Sci 16: 2454–2471.
22. Bowers K, Chow E, Xu H, Ron O, Eastwood M, et al. (2006) Scalable Algorithms for Molecular Dynamics Simulations on Commodity Clusters; Florida.
23. Savopoulos J, Carter P, Turconi S, Pettman G, Karran E, et al. (2000) Expression, Purification, and Functional Analysis of the Human Serine Protease HtrA2. Protein Expr Purif 19: 227–234.
24. Ibrahim A, Mansour I, Wilson M, Mokhtar D, Helal A, et al. (2012) Study of survivin and X-linked inhibitor of apoptosis protein (XIAP) genes in acute myeloid leukemia (AML). Lab Hematol 18: 1–10.
25. Nagata M, Nakayama H, Tanaka T, Yoshida R, Yoshitake Y, et al. (2011) Overexpression of cIAP2 contributes to 5-FU resistance and a poor prognosis in oral squamous cell carcinoma. Br J Cancer 105: 1322–1330.
26. Navakanit R, Graidist P, Leeanansaksiri W, Dechsukum C (2007) Growth inhibition of breast cancer cell line MCF-7 by siRNA silencing of Wilms tumor 1 gene. J Med Assoc Thai 90: 2416–2421.
27. Sugiyama H (1998) Wilms tumor gene (WT1) as a new marker for the detection of minimal residual disease in leukemia. Leuk Lymphoma 30: 55–61.
28. Kraut J (1977) Serine proteases: structure and mechanism of catalysis. Annu Rev Biochem 46: 331–358.
29. Mazat J, Patte J (1976) Lysine-sensitive aspartokinase of Escherichia coli K12. Synergy and autosynergy in an allosteric V system. Biochemistry 15: 4053–4058.
30. Sohn J, Sauer R (2009) OMP peptides modulate the activity of DegS protease by differential binding to active and inactive conformations. Mol Cell 33: 64–74.
31. Feng W, Fan J, Jiang M, Shi Y, Zhang M (2002) PDZ7 of glutamate receptor interacting protein binds to its target via a novel hydrophobic surface area. J Biol Chem 277: 41140–41146.
32. Christopoulos A, May LT, Avlani VA, Sexton PM (2004) G protein-coupled receptor allosterism: the promise and the problem(s). Biochem Soc Trans 32: 873–877.
33. May L, Leach K, Sexton P, Christopoulos A (2007) Allosteric modulation of G protein-coupled receptors. Annu Rev Pharmacol Toxicol 47: 1–51.
34. Berman H, Westbrook J, Feng Z, Gilliland G, Bhat T, et al. (2000) The Protein Data Bank. Nucleic Acids Res 28: 235–242.
35. Friesner R, Murphy R, Repasky M, Frye L, Greenwood J, et al. (2006) Extra precision glide: docking and scoring incorporating a model of hydrophobic enclosure for protein-ligand complexes. J Med Chem 49: 6177–6196.
36. Zeng J, Treutlein H (1999) A method for computational combinatorial peptide design of inhibitors of Ras protein. Protein Eng 12: 457–468.
37. Trencia A, Fiory F, Maitan M, Vito P, Barbagallo A, et al. (2004) Omi/HtrA2 promotes cell death by binding and degrading the anti-apoptotic protein ped/pea-15. J Biol Chem 279: 46566–46572.
38. Ma S, Song E, Gao S, Tian R, Gao Y (2007) Rapid characterization of the binding property of HtrA2/Omi PDZ domain by validation screening of PDZ ligand library. Sci China C Life Sci 50: 412–422.
39. Halgren T, Murphy R, Friesner R, Beard H, Frye L, et al. (2004) Glide: a new approach for rapid, accurate docking and scoring. 2. Enrichment factors in database screening. J Med Chem 47: 1750–1759.
40. Friesner R, Banks J, Murphy R, Halgren T, Klicic J, et al. (2004) Glide: a new approach for rapid, accurate docking and scoring. 1. Method and assessment of docking accuracy. J Med Chem 47: 1739–1749.
41. Jorgensen W, Maxwell D, Tirado-Rives J (1996) Development and Testing of the OPLS All-Atom Force Field on Conformational Energetics and Properties of Organic Liquids. J Am Chem Soc 118 11225–11236.
42. Jorgensen W, Chandrasekhar J, Madura J, Impey R, Klein M (1983) Comparison of simple potential functions for simulating liquid water. J Chem Phys 79: 926–935.
43. Darden T, York D, Pedersen L (1993) Particle mesh Ewald: An N-log(N) method for Ewald sums in large systems J Chem Phys 98: 10089–10093.
44. Martyna G, Tobias D, Klein M (1994) Constant pressure molecular dynamics algorithms. J Chem Phys 101: 4177–4189.
45. Humphreys D, Friesner R, Berne B (1994) A Multiple-Time-Step Molecular Dynamics Algorithm for Macromolecules. J Phys Chem 98 6885–6892.
46. Nallamsetty S, Kapust R, Tözsér J, Cherry S, Tropea J, et al. (2004) Efficient site-specific processing of fusion proteins by tobacco vein mottling virus protease in vivo and in vitro. Protein Expr Purif 38: 108–115.
47. Twining S (1984) Fluorescein isothiocyanate-labeled casein assay for proteolytic enzymes. Anal Biochem 143: 30–34.